CONTRIBUTIONS TO GEOID EVALUATIONS AND GPS HEIGHTING

by

Z. Ahmad, B.R. Harvey, A. Kasenda and A.H.W. Kearsley

Editor: A.H.W. Kearsley

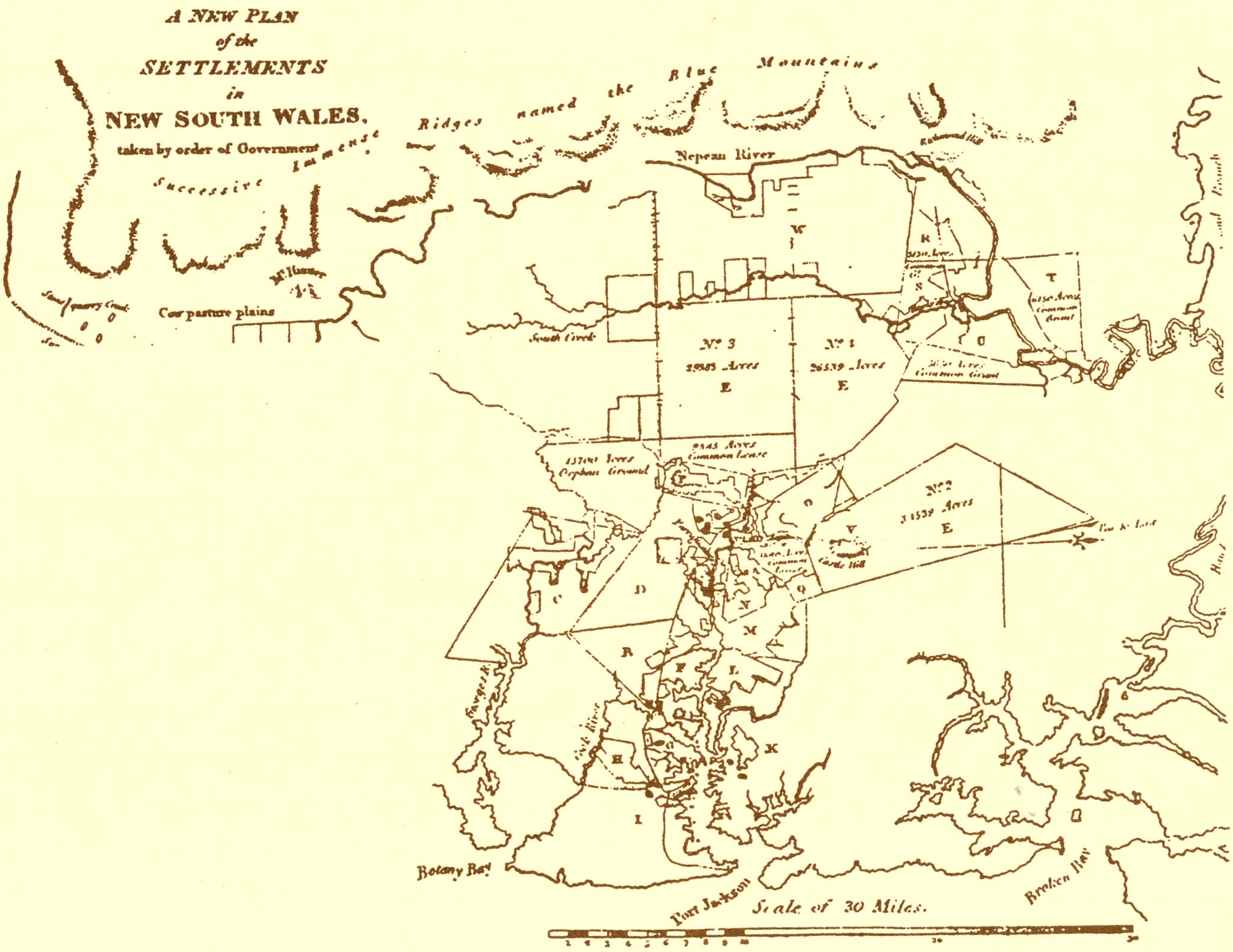

UNISERV S-43, 1993

Reports from

SCHOOL OF SURVEYING

THE UNIVERSITY OF NEW SOUTH WALES KENSINGTON NSW AUSTRALIA 2033

UNISURV REPORT S-43, 1993

CONTRIBUTIONS
TO
GEOID EVALUATIONS
AND
GPS HEIGHTING

A. H. W. Kearsley (Ed.)

Received: June, 1992 to April, 1993

SCHOOL OF SURVEYING
UNIVERSITY OF NEW SOUTH WALES
P.O. BOX 1
KENSINGTON N.S.W. 2033
AUSTRALIA

National Library of Australia

Card No. and ISBN 0 85839 063 9

Contents

List of Tables

List of Figures

A PRELIMINARY GEOID FOR NORTH-WEST IRIAN JAYA
Adolfientje Kasenda and A. H. W. Kearsley **89 - 126**

OPTIMISING GPS, GEOID AND TIDE GAUGE HEIGHTS IN VERTICAL CONTROL NETWORKS

TABLES

FIGURES

SYMBOLS AND DEFINITIONS

$\mathbf{A}$	=	design matrix partial derivatives with respect to the parameters
$\mathbf{b}$	=	vector of functional equations with a priori observations and parameters
$\mathbf{b}_c$	=	vector of constant terms (miscloses) given by the constraint equations at each station calculated from the a priori values of the unknowns
$\mathbf{b}^0$	=	vector of functional equations with observations and approximate values of parameters
c	=	constant
$\mathbf{D}$	=	matrix for the differentiation of the constraint equations with respect to the parameters
$\mathbf{f}_{x_0}$	=	the difference of the approximate value of the parameters from the previous iteration. For the first iteration, it is usually equal to zero
h	=	Ellipsoidal height
H	=	Orthometric height
$\mathbf{J}$	=	a Jacobian matrix
K	=	distance in km
ℓ	=	observation
n	=	total number of observations
N	=	Geoid height.
$\mathbf{N}$	=	normal matrix.
N_L	=	long to medium wavelength component.
N_s	=	short wavelength component.
$\mathbf{P}$	=	inverse of a priori covariance matrix of observations
$\mathbf{P}_x$	=	the inverse of the a priori covariance matrix of the parameters.
$\mathbf{P}_c$	=	the weight matrix of the constraints.
$\mathbf{Q}$	=	a priori variance-covariance (**VCV**) matrix of the observations
r	=	degree of freedom in the adjustment
	=	number of observations minus number of (free) parameters
r'	=	degree of freedom used in the Bayesian Least Squares
	≈	number of observations minus number of parameters without a priori weights
r(i)	=	redundancy number of an individual observation, i
r_{xy}	=	sample correlation coefficient between two random variables x and y
s_{xy}	=	covariance between two random variables x and y
s	=	sample standard deviations
s^2	=	sample variance
u	=	total number of parameters
u'	=	number of parameters with a priori weights
$\mathbf{u}$	=	RHS (right hand side) vector
v	=	residuals.

VF	=	a posteriori variance factor
x	=	parameters
Δh	=	difference in the ellipsoidal height
ΔH	=	the difference in the orthometric height
ΔN	=	the difference in the geoid height
$\Delta x'$	=	correction to the parameters from the unconstrained solution
Δx	=	correction to the parameters from the constrained solution
δh	=	corrections to h
δH	=	corrections to H
δN	=	corrections to N
σ	=	population standard deviation
σ^2	=	population variance

GEOID DETERMINATIONS IN THE PHILIPPINES

A.H.W Kearsley
Z. Ahmad

School of Surveying, University of New South Wales, Australia.

Abstract
The Philippines region is typical of many of the archipelago countries in the Western Pacific, with complex topography and geology because of its proximity to the tectonic plate boundaries. For geoid determinations, the Philippines is further complicated by the shortage of suitable gravity data. The offshore areas are covered by the anomalies predicted from satellite altimetry at 1/8th degree spacing, but the onshore field is, in the main, only sparsely observed, with some of the larger islands having fewer than 20 stations observed in total, and these mainly hugging the coastline. Because of the difficult tectonics, especially in the eastern parts, the prediction of free-air gravity from such a sparsely observed Bouguer field appears almost useless - most of the signal in the free-air field being generated below the geoid. Results from a recent major GPS campaign are used as control to test the various configurations of geoid determination, using OSU86E and OSU89A as reference, both with and without DEM's (to densify the free-air gravity field), and terrain corrections. The results of these tests are presented, and show

i. ΔN comparisons improve to about 6 - 8ppm (rms) from about 8 - 17ppm when the detailed free-air anomaly field is integrated over a cap of about 30 - 80km.

ii. The use of the DEM to supply high frequency data on the anomaly field degrades the solution.

iii. The comparison of N's from the two sources is an efficient means of isolating points with errors in one (or more) of the elements of the height data.

1. INTRODUCTION

The Australian Government, through the Australian International Development Assistance Bureau (AIDAB), contracted SAGRIC International to carry out a first-order geodetic control survey of the Philippines archipelago as a first and fundamental step in the Natural Resources Management and Development Project (NRMDP) - see Larden et al.,(1991) . One part of this project was to recover orthometric heights from the GPS survey used to provide the overall control network. This paper reports upon this aspect of the task - the gravity field and potential model used; the testing of the gravimetric method, and the method used to establish its optimum configuration; problems associated with the control data used to decide this optimum; and, finally, the results obtained for the geoid determination, both in terms of the precision of the geoid differences (slopes) over the control baselines, and of the agreement in the absolute value of N from the gravimetric solution compared with the N values from the conventional terrestrial levelling and from the GPS heighting. These comparisons helped identify control points of dubious quality (although without identifying which component - h, H, or N - is suspect), which would enable their down-weighting in a subsequent simultaneous adjustment for the three height components, which will lead finally to their best possible values.

2. DATA - SUPPLY AND ANALYSIS

2.1 Gravity Data

The gravity data for Philippines region was supplied to the project manager by Jens Pederson of Geotechnical Specialists International Inc., who was consultant geophysicist to the project for this purpose. The data was derived from two main sources as follows.

2.1.1 Altimetrically-derived gravity data

This was comprised of gridded gravity data over the oceans in the region $4^0 \leq \varphi \leq 22^0$, $117^0 \leq \lambda \leq 128^0$. This data was calculated from Geos-3 and Seasat radar altimeter data using collocation by Professor Richard Rapp, Dept. Geodetic Science and Surveying, Ohio State University.

2.1.2 Terrestrially observed gravity, both over land and ocean areas.

This appears to have been compiled from a series of gravimetric campaigns carried out by the Philippines Coast and Geodetic Survey Co., U.S Army Map Service, 1964

(PC&GS) and the F.F. Cruz Co. (F.F.C) between 1961 and 1982. It consists of only 465 observed stations, referenced to the Manila International Air Port Base Station (see Figure 2.1). The density of the points in this data set is small - the average on land areas is about 5 to 10 points per $1^0 \times 1^0$ block.

This data has been augmented with more recent geophysical surveys, notably those which have saturated the region of central southern Luzon, and the east coast of south eastern Luzon. Another 120 points have been included from the gravity profiles across central northern Luzon and eastern Mindanao specifically for this project, to test the Bouguer model for prediction of free air gravity anomalies from heights (see Section 2.1.5). The point data set presented to me contained approximately 17 300 points (most of this data from satellite altimetry in (2.1.1)). After filtering and editing of suspect data (see below), this data set shrank to about 15 800 points.

2.1.3 Problems with the Philippines gravity data.

At an advanced stage of this project, when comparing the ΔN values from the gravimetric solution with those ΔN values found from GPS/Levelling control, it was obvious that some points were not agreeing and it became necessary to re-evaluate the computations. This led to a detailed investigation of the gravity data which revealed the following :

1. The data contains free-air gravity anomalies over land areas which were derived from satellite altimetry measured over the ocean (see Figure 2.2). Such data is highly suspect.

2. There are some **observed** gravity data over ocean areas which conflict

with gravity data derived from the satellite altimetry (also see Figure 2.2).

3. The data file appears to contain large errors in parts. Some values are grossly (> 200 mGal) at odds with the surrounding values.

2.1.4 Marine Data

There were also large discrepancies between the offshore data from shipborne traverses, and the data from the satellite altimetry. Because the former was of unknown quality, and because the altimetry-derived data was at least homogeneous, it was decided to delete all ship-borne gravimetry.

2.1.5 Final Data Set

After this editing, the file contained only 15 800 points. One thousand and five hundred points were deleted because of the problems described above, but at least now we felt we had a relatively trustworthy data set.

The gravity field for the Philippines is shown in Figure 2.3 (Δg generated from OSU89A) and Figure 2.4 (the residual gravity anomaly field). It shows a steep rise in the anomaly field along the east coast and large features in central Luzon and eastern Mindanao. The maximum value for the residual anomaly (>200 mGal) lies in eastern Philippines where φ is approximately 12.5^0. One significant point which follows from this exercise is this. One must be very careful in methods on how the data set is searched for errors. The consultant who supplied SAGRIC with the data was confident that the data he provided was free from outliers. However, the method used to test the data (contouring based upon points selected for their proximity to the grid block centre) was clearly insensitive, and not able to detect such features as the satellite altimetry points over land. The technique used in our testing used contouring over a small area, at a large scale, and involved every point in the data set, so that spurious data was more easily detected. The data points themselves were also plotted, so that the tell-tale pattern of $0.12\,^0$ grid over land revealed the presence of altimetry-derived data there.

2.1.6 Gravity Profiles.

Two gravity profiles were surveyed by the consultant geophysicist in 1990 to allow us to estimate the optimum density of the sub-surface material for the Islands. The first profile was done in eastern Mindanao, in relatively flat terrain (height range about 200m) and running about 25 to 75km inland from, and parallel to the east coast. The second ran from the west coast of northern Luzon, due east for about 70km, then north east for another 100km. The topography here was much more rugged, with the range in height about 1600m. The Bouguer anomalies were obtained using a series of values for sub-surface density (ρ), using the standard technique to establish the optimum value for ρ (Heiskanen and Moritz, 1967, p.284). The profiles which result from these computations, using $\rho = 1.7$ to $\rho = 3.0 gcm^{-3}$, are pictured in Figures 2.5 and 2.6 (profile 1) and Figures 2.7 and 2.8 (profile 2). These results are, to say the least, startling and have far-reaching implications for gravity prediction for this geoid study.

The profiles clearly show that there is no flattening of the profile expected when, using the accepted model for the Bouguer correction, the optimum value of ρ is used. In profile 1, the plots for $\rho = 1.7$ and for $\rho = 3.0$ gcm^{-3} (a wide range in ρ by any standards) are almost identical, and show little correlation with topography. By this I infer that most of the gravity signal (or, more correctly, the variations in the gravity signal) come from mass anomalies beneath the geoid, reflecting no doubt the complex sub-geoid tectonic structures. Similar comments and conclusions can be drawn from profile 2. In this, there may perhaps be some flattening of the profile for the $\rho = 2.7$ gcm^{-3} at the western end of the profile, and certainly there appear to be some correlation with the topography here, but along the eastern half, which shows little topographic relief, the Bouguer anomaly profiles for the extreme values $\rho = 1.7$ and $\rho = 3.0$ gcm^{-3} become almost colinear, and have disturbingly large variations along the profile.

The implications drawn from this study are wide-ranging and profound. It means that

1. it is unlikely that the use of DEM's to recover high-frequency information of the free-air anomaly field from the Bouguer anomalies will be successful. This is unfortunate as there are large gaps in the observed

gravity and a trustworthy method for predicting the gravity anomaly is highly desirable and

2. the terrain-correction term which uses height scaled by one value of density to infer gravity (Moritz, 1980, p. 415) is also unlikely to be accurate since the simple mathematical model upon which it is based is obviously inadequate. Again, this is unfortunate. The Philippines archipelago is characterized by complex geology, including high volcanic mountains rising from coastal plains (Bureau of Mines, Philippines, 1963) and clearly the topographic correction could be significant.

2.2 Geopotential Models for Reference.

I have shown that the optimum geoid solutions result when a best-fitting geopotential model is used as a reference for the gravity field in the geoid solution (Kearsley, 1988). In other words, the smaller the residual gravity field, the more precise the geoid heights derived from it. (The residual gravity field, δg, is the value remaining after the anomaly generated by the geopotential model has been subtracted from the 'observed' gravity anomaly, or $\delta g = \Delta g_{obs} - \Delta g_{model}$).

We conducted a series of tests on the Philippines gravity data to establish which of the models (already narrowed down to OSU86E and OSU89A, Rapp & Cruz,1986; Rapp & Pavlis,1990, resp.) would prove to be best. The sample points per 1^0 block are shown in Figure 2.9. The results of the tests are shown in Figures 2.10 to 2.13 and summarised in Figures 2.14 and 2.15, and Table 2.1.

It appears from these tests that there is little difference between these two models - they both fit the gravity data equally well (or poorly). Given the superiority of OSU89A - its lower order terms are based upon GEMT2 and it contains more recent data in certain parts of the world (but not the Philippines) and because of the more normally distributed differences, it was decided to adopt OSU89A as the reference model. This implies that the geodetic reference model to which the geoid undulations refer is GRS 80 (Rapp & Pavlis, 1989, p. 21896), i.e is based upon an ellipsoid (a=6378 137m,

f^{-1}= 298.257, GM= 3 896 004.36 x $10^8\ m^3s^{-2}$, ω = 7.292115 x 10^{-5} $rads^{-1}$). It should be noted that the authors of this model have already shown it to have problems fitting the terrestrial gravity in the region (ibid,Fig.7), and expected it to have a standard error of just less than 40cm in the Philippines area (ibid, Fig.11).

2.3 Digital Elevation Model.

The digital elevation model (DEM) is expected to play an important part in the computations. Firstly, it will be used to interpolate free-air anomalies from the existing, mostly sparse observed gravity data. Secondly, it will be used to compute the classical terrain correction to the gravity anomaly, to account for the departure of the telluroid from an equipotential surface (see Section 3.3)

The original DEM supplied for our use was a 5' mesh of heights, interpolated from the ETOPO5 world data set which has a 10' density. This was found to be inadequate in the preliminary investigations for heights (Forsberg, 1990), and early in 1990, another DEM was supplied by CERTEZA. This comprised of heights taken from the 1:250,000 topographic maps of the Philippines at 5' intervals. This latter DEM was therefore considered superior to the original in that it did at least have a true sensitivity of 5'. However, its accuracy in many areas, especially in the high mountain country, must still be suspect since the contours on the maps for these areas are only 'guesstimated' (i.e are shown by dashes, not solid lines). It must therefore be expected that the computations which involve the DEM's are unlikely to be anything other than provisional.

2.4 GPS Control

The GPS survey carried out to provide the geodetic control network for the NRMDP occupied 111 stations (see Figure 2.16) whose orthometric heights were established, either because they were tide gauge stations or part of the levelling network for the archipelago. These gave geometric evaluations of the geoid height, and provided control values against which the gravimetric solutions could be tested.

3. GEOID SOLUTIONS

3.1 OSU89A Model-only solution

As shown in Section 2.2 we decided, after testing OSU86E and OSU89A, to use the latter as the reference model for our solutions. Figure 3.1 shows the OSU86E geoid and Figure 3.2 the OSU89A over the Philippines region. Both models show the same distinctive features - the slope along the eastern coast (but most noticeably on the east coast of Mindanao); the deep (46m) trough on the south eastern tip of Mindanao; the plateaus to the west of Mindanao and in central southern Luzon. Nevertheless, the differences between the two models are marked (Figure 3.3), and are greatest on the east coast where the geoid features are changing most quickly. These differences highlight the need to choose the reference model with care (see Section 2.2). The OSU89A model was therefore chosen because of its apparent better fit to anomaly field, and because of the strength of its lower order terms, being based upon GEMT2 (which should mean better long to medium wave length information compared to that provided from OSU86E).

The fit of the geoid differences (ΔN) from this model to the 'control' from GPS, tide gauges and levelling shows that, once doubtful data has been eliminated, the OSU89A model can recover ΔN to an accuracy of 8 to 17 ppm, depending upon the region.

3.2 Preliminary detailed gravimetric geoid

A detailed (0.1^0) geoid was computed in 1988 using a FFT/Stokesian solution, and OSU86E as a reference model (Forsberg,1990). Comparisons along six GEOSAT tracks over ocean areas close to the Philippines (no geometric geoid control was available at the time of this study) show a bias of about -3.2 to -3.5m, with standard deviations of 1.5 to 2.0m, depending upon the solution. Surprisingly, the OSU86E-alone solution gave the best comparisons. Solutions using gravity data, terrain corrected gravity data and DEM's show a degradation from the fit achieved in the model-only solution. Forsberg ascribes this to the DEM being of low accuracy and resolution, as well as the paucity and inaccuracy of the local gravity data.

3.3 Gravimetric solution using Ring Integration

The first phase of the GPS control over Northern Luzon was supplied in mid-1990, which led in turn to the discovery of some problems in the gravity data base (Section 2.1). Geoid heights were recomputed using the edited gravity data using the ring integration (RINT) technique, as in Figure 3.4 (also see Kearsley, 1988). In all, four different data configurations were used, namely

(a) residual gravity $\Delta g'$ (where $\Delta g' = \Delta g_{obs} - \Delta g_{OSU89A}$)

(b) terrain-corrected residual gravity ($\Delta g'$ + TC)

(c) residual gravity, with higher frequency information being inferred from the DEM ($\Delta g'$+DEM)

(d) terrain-corrected residual gravity and DEM ($\Delta g'$+DEM+TC)

(a)The $\Delta g'$ values are found by generating Δg_{OSU89A} from the reference model on a 0.1^0 grid. The model value at the gravity observation station is then interpolated from the nearest grid points, and subtracted from the Δg.

(b) The terrain corrections are evaluated on a 5' grid from the DEM of the same mesh size, using TCFOUR (Forsberg). The terrain correction for a specific gravity station is interpolated from the mesh and then applied to the residual gravity anomaly. Figure 3.5 shows the topography of the Philippines as described by the DEM and demonstrates the high mountain systems in northern Luzon (up to 2400m) and central Mindanao. The resultant terrain correction is shown in Figure 3.6. One notes the obvious correlation of this correction with topography - and the magnitude of the correction (maximum about 14 mGal in northern Luzon).

(c) and (d) The DEM's were used to provide the high-frequency information for the free-air gravity field in areas where observed gravity was sparse. This was done in the usual way, i.e by extracting the Bouguer anomaly field from the free-air gravity, and finding the free-air gravity field at points in the DEM by adding back to the Bouguer anomaly the free-air correction (the height being supplied by the DEM). However, as interpolated at the DEM point, the studies of the gravity profile in Section 2.1.5 show, the 'usual' behaviour of the Bouguer field was **not** obtained. The impact of the DEM's when used to fill in the gaps in observed gravity is described below (Section 3.3.1).

3.3.1 Results of Tests for Optimum Data Type

The four solutions were tested over about 300 baselines in the Luzon area (chosen because of the expected homogeneity in its height datum and, being the most developed of the islands, the relative strength of its levelling network). A comparison of the RINT solutions against the control ΔN, from ring 0 (model only) to ring 10 (a cap size of about 100 km), was made and the differences converted to ppm of the baseline length. The mean and rms of the differences up to ring 5 are listed in Tables 3.1 and 3.2 and plotted in Figures 3.7 and 3.8, respectively. The results show that

(i) there is an improvement in the comparison when local gravity, in any of the four solutions, is integrated and added into the evaluation (cf. Forsberg,1990 which showed a degradation when detailed gravity was included).

(ii) the best solution is obtained when residual gravity **only** is used. The terrain corrected data produces a slightly poorer comparison, but the use of DEM's to interpolate the free-air gravity degrades the comparison significantly.

(iii) the optimum comparison as indicated by the mean and rms for this region comes at ring 3 (a cap of about 30 km radius).

3.3.2 Result of Tests for Optimum Cap Size

Having established that $\Delta g'$ is the optimum data type for this region, it is now necessary to find the optimum cap size for all regions of the Philippines. For this purpose the archipelago was divided into four regions, comprising

(i) Luzon Island to the north,

(ii) Mid-Philippines (the island system between Luzon and Mindanao),

(iii) Mindanao in the south and

(iv) Palawan, the isolated island system to the west.

A separate analysis was done on lines joining tide gauge stations, to try and remove any problems in the control as a result of errors in the heights of stations determined from long lines of conventional levelling.

The surface gravity was integrated out to ring 20 (2^0). The results of the comparison up to ring 10 (1^0 cap size) are presented in Tables 3.3 and 3.4, and illustrated in Figures 3.9 and 3.10. It appears from the analyses that the optimum cap size for integration varies only a little from region to region, as shown in Table 3.5.

The best results for Mindanao, Luzon and Tide Gauges, those data sets with probably the most homogeneous supply of orthometric heights, proved to be around rings 2 and 3 (20 to 30 km radius of integration). This seems a surprisingly small cap of integration, even for a residual gravity field based upon a 360 degree potential model, and may reflect the fairly long lines in the data set as well as the sparse on-land gravity coverage. The small difference between the Luzon results in Figures 3.9 and 3.10, and those in Figures 3.7 and 3.8 result from a slight difference in the ellipsoidal heights used for control in the second analysis. This is not expected to make any material difference to the conclusions in 3.2.1. The Palawan data set is too small to be significant, but shows the tide gauge heights are good in this region. The Mid-Phil region shows up as the 'odd man out', giving best comparisons at ring 8 (cap radius 80 km) and the poorest mean (6.6 ppm) and rms (8.3 ppm) of all the areas. This area was the most difficult to analyse, being made up of many small islands with unconnected or poorly connected height datums, and of some intra-island levelling systems which appeared to be based upon different height datums. This analysis is based upon only 43 lines, selected mainly between tide gauges or over lines between whose terminals levelling appears to have been performed.

3.3.3 Detailed Gravimetric Geoid for the Philippines

As a result of the analyses in Sections 3.3.1 and 3.3.2, the detailed geoid has been computed upon a 0.2^0 grid in each of the four regions used in the analyses, using $\Delta g'$ and the optimum cap size for the region, and the suite of programs shown in Figure 3.11.

It is expected that, for the mean length of the line listed in Table 3.5, the relative precision is that given for the rms of the analysis for the region. It is probable that, for the flatter areas near the west coast or areas of plentiful gravity, the precision will be better than that quoted. For the mountainous regions, and in east coast regions with sparse gravity coverage, the precision and accuracy of N will be considerably worse. These detailed gravimetric geoids for the four areas are shown in Figures 3.12 to 3.16. The 0.2^0 gridded values of N are supplied on the accompanying floppy disks under the filenames North.LST, Mid-Phil.LST, South .LST, South west.LST and West.LST.

A comparison of the absolute gravimetric geoid heights against those from the GPS/levelling were also computed at all 111 points and the results are shown in Figures 3.17 and 3.18. The former shows the differences (contoured in 0.5 m intervals) for all points, and clearly illustrates those points where errors (in at least one of the elements h, H or N) probably exist. These apparent outliers (about 20) were deleted and the map of the differences in N at the remaining 90 points redrawn, producing Figure 3.18.

From this figure we can see the bias and tilt which exists between the independent evaluations of N - these features being largely masked in the first analysis. From the figure we see an apparent tilt of the gravimetric geoid of about 4 m in northern Luzon (this difference rises to over 6m in the mountainous area of central Luzon) to 2m in Mid-Philippines and Palawan Island, rising again to about 4m in Mindanao. In a homogeneous solution for N from both gravimetry and GPS/levelling (as well as, simultaneously, the optimum values of H and h by adjustment of all the observables properly weighted) the tilt and bias between the two solutions will be reconciled, providing final values of the geoid heights.

4. DETAILED ANALYSIS OF GPS AND ORTHOMETRIC HEIGHTS.

4.1 Suspect or problem points

In this section I will describe the three methods used to analyse the data (that is, thecomparisons between the gravimetric and the geometric evaluations of ΔN) in order to isolate those points at which contained possible gross errors of one or more of their elements h, H or N. The formal errors associated with these elements are then summarised, and finally the suspect points, along with their probable errors, are listed.

4.1.1 Comparisons of ΔN across baselines

In this method of analysis, all those lines whose relative errors exceed some prescribed limit (in this case, 10ppm) are listed and the occurrences of control points are found. If for example, the H value of a point is in gross error by 1m, all ΔN values computed for line involving this doubtful point will be in error. By working through the suspect lines list, and eliminating those lines which involve the most commonly occurring points, it is possible to identify those points which are most likely to be in error, and to confirm those points which occur in suspect lines only because they are paired with a suspect point. The result of this analysis is shown in Table 4.1, in column 3, under the heading "Relative (ppm)". This technique identified 34 suspect points, with some (e.g points 25, Bauan and 42, Romblon) being unable to better the 10 ppm for almost all lines involving them.

While this method is felt to be the most sensitive to error in the control data, it does suffer (as do all methods) if there happens to be a change of orthometric height datum across a line. For this reason lines were restricted, where possible, to islands (e.g Luzon, Mindanao) or island groups (Mid-Phil, Palawan). Even so, there were apparent datum changes between some groups of points, both intra-island and inter-island, making it impossible to obtain good line ΔN comparisons between these groups.

4.1.2 Comparisons of N point values

The second technique simply compared the N values, generated gravimetrically using the optimum cap size, with those obtained from the control data (h - H), at common points - see Table 4.2. The differences in N at each point (termed 'diff-N' here to avoid confusion with the ΔN found across a line) are mapped and contoured, and the contour map analysed to detect features which are peculiar. If no errors exist one would expect a smooth, gently sloping surface reflecting the bias and slope differences in the various height datums involved in the data. Any marked departures from this surface show a gross error in one or more of the point elements involved in the analysis.

The contour maps of diff-N are shown in Figures 3.17 to 3.18 showing the comparison with the full data set, and the results of two stages of filtering suspect data. The points identified as suspect in this filtering process are listed in Table 4.1 in the column 4 "Abs. Map". The number in this column shows whether it was deleted in the first (1) or second (2) round filter. It is apparent that there is a high correlation between the points identified as suspect by the relative technique (Section 4.1.1) and this approach, although this method does not identify as many points and is patently not as sensitive to error as the first method.

4.1.3 Geoid Profiling

This technique was developed as an extension of Section 4.1.2, and as a result of its relative insensitivity. In this method, 'diff-N' at control points are compared, as before, but in fairly small regions or across relatively short baselines. The aim is to limit each analysis to points of similar characteristics (e.g region type, height datum) in order to identify those points which are outliers. This usually meant that from as few as 2 points to as many as 8 points could be grouped together for comparison. For each group the mean and standard deviation of the diff-N's were calculated, and the diff-N's plotted, along with the mean - see Figures 4.1 to 4.22 and Tables 4.3 to 4.24. The points which proved suspect from this analysis are noted in Table 4.1, under column 5 "Profile". There is again a high correlation between points identified as suspect both in this technique and the relative technique. The differences are due mainly to the fact that in the first technique relative errors, expressed as ppm of the line length, are used for comparison - not the differences $N_{GPS/Lev} - N_{Grav}$.

4.2 Formal errors associated with height elements

4.2.1 Formal errors in N_{GRAV}

N_{GRAV} is comprised of two parts - the long to medium wavelength component (N_L) which is evaluated in Section 3.1, and the short wavelength component (N_S) found by ring integration of the detailed residual gravity field (N_S). The long wavelength component, N_L was computed using the geopotential model, OSU89A and contribute, to N, a formal error of about 40 cm (see Rapp and Pavlis, 1990, Figure 11). Because of the complex nature of the error contours in this region, the contribution of N_L to ΔN is unclear, but could be as much as 5 to 7 ppm of the length of line. The N_S values, on the other hand, were evaluated up to their optimum cap sizes as discussed in Section 3.3.2. Hence, the formal error in N_S and ΔN_S is a function of the number of rings used in the inner zone evaluation.

The precision of N_S is found by analysing ;

a. the coverage of the gravity data and

b. the 'goodness of representation' of the mean value assumed for a compartment.

The contribution from (a) is based on the density of the gravity data coverage within the area where the control point is positioned, whereas (b) is based on the topographic features of the site and on the type of gravity data (whether gravity is mainly observed terrestrially or deduced from altimetry) surveyed in that area.

From Table 4.1, under the heading 'N $_{(GRAV)}$', the numbers in column 6 describes the category of both the above aspects as described more fully below. The classification in density of the **coverage** of gravity data is divided into 3, i.e

1. Good with dense coverage (equal to or better than 1 per 0.1^0 grid point);

2. Medium coverage (some points sparsely distributed within 0.3^0 cap size);

3. Poor coverage (no points or few (i.e 1 or 2), within 0.3^0 cap size)

The designation of different classes in the '**goodness of representation**' is as shown below.

1. Good. The topographic is benign and gravity are observed terrestrially;

2. Medium. Benign topography (e.g in the ocean area) and gravity are deduced from altimetry;

3. Poor. Difficult topography. Usually in the mountainous areas or near the eastern coast, and suffering from the complex tectonics of that region.

4.2.2 Formal errors in the control - h and H

4.2.2.1 Introduction

Initially the GPS control data supplied to us was that based upon an analysis of the GPS data performed by Dyson. This used one station (Balanacan) to give datum relationships, and carried out the adjustment piecemeal. The first test of ΔN_{GRAV} used the "Dyson" h values for control. A number of these comparisons were poor, and extra information on h and H at non-fitting points was sought, through SAGRIC from Professor Larden. This information is summarised in Table 4.1 under the heading "H,h", columns 8 - 10. It should be noted that this information is incomplete i.e not all control points have been subjected to this scrutiny. In fact, the final adjustment of the GPS control, which was performed by Andrew Jones of the South Australia Lands Dept., used a number of points throughout the region to establish the datum and adjusted the GPS network simultaneously. The difference between h (Dyson) and h (Jones), is illustrated in Figure 4.23. It shows a significant tilt from + 3 to - 1 m, roughly east-west, with the zero line lying on the 121st meridian. (There appears to be an error in h (Jones) and/or (Dyson) at Point 78 which has not been resolved by the time of writing).

This tilt of about 1 m in 2^0 results in a change in Δh (and hence in $\Delta N_{CONTROL}$) of about 4 ppm, and is certainly significant in view of our attempts to achieve a 10 ppm geoid. Because of the more systematic approach to the adjustment, (and on the advice from Professor Larden) the h (Jones) adjustment was accepted and used for the final comparison. However, the disconcerting aspect of this comparison is how much 'h' changed when based upon a different method of determining the height datum i.e how much the absolute, and even the relative, values of h are dependent upon computational approach.

4.2.2.2 **Formal errors in h and Δh**

The formal errors associated with the h output of the Jones adjustment are listed under column 10, Table 4.1. They show, in general, a range of between 0.1 to 0.16 m, with T1 (Basco), T107 (Rio Tuba) and T108 (Balabac), showing much larger errors - 0.38, 0.19 and 0.29 m respectively. This is not surprising as these stations are on isolated islands well separated from the main body of the Philippines.

In general, however, there is little significant variation in the formal errors of h at all the control points after the Jones adjustment, reflecting the homogeneous and well-conditioned nature of the data. In trying to investigate possible reasons why ΔN comparisons contain outliers, we tend therefore not to suspect the 'h' values from the GPS.

Another output from the Jones adjustment was the relative error in the adjusted Δh over lines observed in the GPS survey. These results have been illustrated to show relative errors in Δh for those lines where ΔH was also known i.e over some of those lines which were used in the ΔN comparison. This shows that, although the bulk of lines have relative errors better than 5 ppm, a surprising 7% had relative errors worse than 5 ppm, with one line (28 to 43), having an error of over 14 ppm. Clearly these lines must be treated with caution when comparing the ΔN based upon them with the gravimetric ΔN.

4.2.2.3 Errors in H

The formal errors in H are more difficult to determine, as we did not have access to the levelling data which produced H. What we did obtain were comments on the determination of both h and H from Professor Larden for about 45 points - those points which appeared to be suspect from the initial comparison of ΔN based upon the Dyson adjustment. (These were similar to, but not identical with, the apparent outliers when comparisons of ΔN based upon the Jones adjustment were made. However, lack of time prevented us from obtaining information on any new points). The comments were classified according to the legend below, and summarised in columns 8 to 10 in Table 4.1 (Note that the first and second classification in column 8 refer to H and h respectively).

The legend for comments on possible outliers on H or h is as follows,

Number	Comment
0	Element should be well determined.
1	Element should be well determined, but there may be some problems.
2	Element may be suspect.
3	Element should be down-weighted or excluded from the comparison as value is highly suspect.

4.2.2.4 Formal error in H at tide gauge heights

The last source of information at the control stations is the determination of H from mean sea level observed at tide gauges. The bulk of these were established by Lennon and are the subject of an extensive report by him to the contracting authority SAGRIC (Davill and Lennon, 1990-91).

The comments on the tide gauge observations at stations relevant to these computations are summarised in Tables 4.25 to 4.29. The details which are of interest in this analysis are

1. the duration of time for the observations to establish mean sea level

(column 3) and

2. S_{res}, or the standard error of the residual (i.e the observed data minus the tidal model).

It can be seen that the duration ranges from 45 days (Dipolog, Table 4.30) to 365 days (Legaspi, Table 4.26; San Jose, Table 4.27; Surigao, Table 4.28; Davao, Table 4.29). The S_{res} varies from about 3 cm to 11 cm, although most stations, especially in the central and southern regions , have an error of about 5 cm. These S_{res} values are extracted in mm for Table 4.1, under the heading S(Htg), thus completing the information available to us for analysis of the height control data. Two stations included in this summary, T96 and T101, were not part of Lennon's network or analysis and had only 3 day's tidal observations, and are expected to have an accuracy 3 times that of the other stations. (Larden, personal communication, 13 August, 1991).

4.3 Summary of suspect points

The formal errors in N, h and H at tide gauge points, annotations denoting suspect points i.e points which fail the ΔN comparison test and comments on the 'trustworthiness' of the observations of various components, are all summarised in Table 4.1. This table forms the basis for the discussion of the suspect points.

4.3.1 General Overview

Of the 111 points used in the analysis, 34 points were found to be suspect by the relative method, and many of these were also suspect by one or both of the other two techniques. The suspect points are summarised, along with details, in Table 4.30. If it were possible to identify which of the elements H, h or N of the points in the table were in error, it might be possible to salvage a reasonably good estimate of that element in error (if, indeed, there was only one). To preface this analysis, it is worth making a few general observations.

(i) N : The estimates of the formal error ∂N_s show little variation between points (i.e appears to be insensitive to the nature of the gravity field).

It is also difficult to estimate from ∂N_S the relative error ($\partial\Delta N_S$) over lines. The error in ∂N_L is estimated to be about 40 cm, but again the relative error $\partial\Delta N_L$ is not possible to estimate with certainty. Under these circumstances, it is preferable to use the notation in column 6 as a gauge of the relative accuracy to which N has been evaluated from gravimetry.

(ii) **h** : The estimate of formal errors again appears to vary little between points and certainly appears uncorrelated with the outliers. This parameter is, therefore, not a critical, or sensitive gauge of the veracity of the h values used in the analysis. Probably of more value is the relative error $\partial\Delta h$, illustrated in Figure 4.24 which is only shown over those *levelled* lines which were directly observed in the GPS survey. Particular attention should be paid to the line 28 (Balanacan to the fixed point) to 43 which appears in error by about 14 ppm and line 12 to 15, with an error of about 8 ppm. These errors would surely degrade the integrity of the GPS heights in the vicinity of these lines. Also Jones value of h at point 78 appears to be in gross error (the Figure 4.23). Otherwise, the h element is expected in general to be the most trustworthy of the three parameters; h N and H, determined for each point.

(iii) **H** : The element H is commented upon (if at all) in column 8 and, if a tide gauge in column 9 of Table 4.30. This should provide some feel for the veracity of H. Of all elements, the H value is the most likely to be in error and, as such, is most likely to be suspect.

4.3.2 Possible sources of non-agreement

The suspect points in Table 4.31 are grouped under the suspected element - i.e according to which element h, N or H is expected to be poorly evaluated. Note that these lists are **not** mutually exclusive. For example, it could be that a point occurs in all three categories because **none** of its elements are regarded with confidence.

4.3.2.1 Points with possible problems in h

h is probably the best determined of all the elements. However, as can be seen from Figure 4.24, seven lines which had orthometric height differences determined had relative errors after adjustment of worse than 5 ppm. Not all such (relatively) poor determinations appeared to affect the line comparisons e.g line T5 to 23 has a relative error in Δh of about 7 ppm, yet neither of these points appears in the list of suspect points.

It should be emphasized that not all levelled lines were directly measured by GPS, and that the Δh's over these lines were determined indirectly.

4.3.2.2 Points with possible problems in N

Problems in the coverage and roughness of the gravity field contributed to the identification of points in this category. Not surprisingly, this category contains the largest number of points, as this was the evaluation over which the author had most data and control. It would be wrong, therefore, to infer that the N_{GRAV} element is the weakest of the components in the comparison. Indeed, many points which had apparently poorly determined N values did not appear to be suspect. Nevertheless, this list does give those points whose conditions for N evaluation were far from ideal, and therefore must be treated with caution. This applies in particular to those points in bold type in Table 4.31, which have been evaluated under the worst possible conditions.

Obviously, improvement in the values of N_{GRAV} at these points will only come when the representation of the gravity is improved to give an error of 0.3 mGal for a mean value for the compartments used in the ring integration.

4.3.2.3 Points with possible problems in H

This element is the one most prone to error, the one for which I have least information. The points listed are those assessed as a result of the initial comparison using Dyson's h values. The outliers resulting from this and Jones adjustment are not identical. As a result, the lack of information on H in Table 4.31 may only mean the point was not assessed for problems as it was not in the original list of suspect points.

The 'profile' technique of assessing for outliers may provide some insights into the nature of these errors. For example, points 10 and 13 appear to have similar errors to the neighboring points, but consistent between themselves (Figure 4.5) suggesting that a gross error has occurred in the levelling between 13 and the points south. Point 25 appears to have an error of 2 m in its H value (see Figure 4.4). Before a full and comprehensive survey of all problem points can be carried out, a proper analysis of the levelling network is required to be resolved, if possible,the problems identified in the above comparisons.

4.4 Summary

The above analysis is in no way complete, but it does provide a guide as to which points apparently contain errors, and tries to identify the problem elements.

5. CONCLUSION AND SUMMARY

We have computed a gravimetric geoid for the Philippines using available observed gravity data over land, and altimetrically-derived anomalies at sea; OSU89A, to degree and order 360 as reference model; and ring integration of surface gravity to cap sizes varying between 20 to 80km.

The analysis of gravimetric ΔN's against those provided by GPS and conventional levelling identified a number of doubtful control stations and further, showed that

i. the optimum solutions were obtained using residual gravity only. The use of DEM's to generate terrain corrections, and to provide high frequency information of the free-air gravity field, only degraded the solution casting doubt on the quality of the DEM's and/or the validity of the simple density model to generate the Bouguer field used in the interpolation of the free-air field.

ii. the gravimetric ΔN's agreed with the control with an rms of better than 10ppm, and this occurred in most regions within the surprisingly small integration cap of about 30km.

iii. certain biases exist between the absolute N values from the gravimetry, and those established from the control, notably in Northern Luzon and Central Luzon (4 to 6m). The bias in the centre and the west is much smaller (i.e close to 2m), rising again to 4m in central Mindanao.

Geoid heights have been computed on a 0.2^0 mesh for all the regions of Philippines, using the cap size of the integration found to be optimum for the region. The relative accuracies of the N are expected to be about 6ppm for Luzon and Mindanao, and about 8ppm for the mid-Philippines area. It is not possible to properly estimate the precision in Palawan; the sample of comparisons was too small, but I estimate it to be at least 5ppm.

6. ACKNOWLEDGEMENTS

A number of people have helped in various capacities on the project, including Enrique Macaspac, Philippines National Mapping and Resource Information Authority (NAMRIA) performed the analysis on the gravity profiles in northern Luzon and eastern Mindanao; Robert Holloway, Chris Mazur and Adolfientje Kasenda who helped as research associates; René Forsberg gave invaluable assistance at an early stage of the project, and provided software for the computation of, amongst others, the terrain correction.

7. REFERENCES

Bureau of Mines, Philippines, 1963, Geological Map Series 1:10^6, Edition 1, Reference Numbers NB 50 - 52; NC 50 - 52, ND 51, NE 51, NF 51.

Davill, Paul and Lennon, 1990 to 1991, ' Report to SAGRIC International on Tidal Observations, Phases 1 to 5, NRMDP', National Tidal Facility, School of Earth Sciences, Flinders University (5 Volumes)

Forsberg, René, 1990,' A Preliminary geoid for the Philippines ', *Aust. J. Geod. Photogram. Surv., No 52*, pp1 - 20.

Heiskanen, W. and Moritz, Helmut, 1967, ' *Physical Geodesy* ', Freeman, San Francisco.

Kearsley, A.H.W, 1988, ' Tests on the recovery of precise geoid height differences from gravimetry ', *J.G.R.* , *93*, B6, 6559-6570.

Larden, D.R., Harvey, W.M., Feir, R.B. and Jones, A.C., 1991, ' Preliminary evaluation of the national geodetic differential GPS network of the Philippines.' *Paper 14, Proc., 4th South East Asian Survey Congress, Kuala Lumpur, 3 - 7 June,1991.*

Rapp, Richard H. and Cruz, Jaime Y., 1986, ' Spherical Harmonic Expansions of the Earth's Gravitational Potential to degree 360 using 30' mean anomalies ', Report 376, *Dept. Geod. Science and Surveying, Ohio State University.*

Rapp, Richard H. and Pavlis, Nikolaos K., 1990,' The development and analysis of geopotential coefficient models to spherical harmonic degree 360 ', *J.G.R.*, *95*, B13, pp. 21 885 - 21 911.

U.S Army Map Service, 1964, ' The Philippines Land Gravity Report ',*NSDB Project No. 263 Report. U.S Army Corps of Engineer*

Range in Absolute	Number of Blocks		Range in RMS	Number of Blocks	
Mean	OSU86E	OSU89A		OSU86E	OSU89A
≤ 5	35	41	0 to $\pm$ 30	54	55
5 to 15	41	28	$\pm$ 30 to $\pm$50	32	30
15 to 30	13	22	$\pm$ 50 to $\pm$ 70	11	11
≥ 30	11	11	> $\pm$70	3	4

Table 2.1 : Mean and rms for OSU86E and OSU89A.

	$\Delta g'$	$\Delta g'$ + DEM	$\Delta g'$ + TC	$\Delta g'$+DEM+TC
Ring 0	7.9	7.9	7.9	7.9
Ring 1	6.4	6.7	6.5	6.7
Ring 2	5.5	6.9	5.5	6.9
Ring 3	5.4	7.9	5.4	8.0
Ring 4	5.6	9.1	5.6	9.2
Ring 5	6.0	10.3	6.0	10.4

Table 3.1 : Tests for Optimum Data Type (mean).

	$\Delta g'$	$\Delta g'$ + DEM	$\Delta g'$ + TC	$\Delta g'$+DEM+TC
Ring 0	12.1	12.1	12.1	12.1
Ring 1	8.8	9.7	8.8	9.7
Ring 2	6.7	9.8	6.7	9.9
Ring 3	6.2	11.9	6.3	12.0
Ring 4	6.7	14.0	6.7	14.1
Ring 5	7.3	15.7	7.3	15.8

Table 3.2 : Tests for Optimum Data Type (rms).

	Luzon	Mid-Phil.	Mindanao	Tide Gauge	Palawan
0	7.2	14.1	7.9	4.9	1.2
1	5.7	10.8	5.6	4.1	2.4
2	4.7	8.4	4.8	3.6	2.6
3	4.4	8.0	5.6	3.1	2.9
4	4.5	7.6	6.7	2.9	3.3
5	4.8	7.2	7.3	2.8	3.7
6	5.0	6.9	7.6	2.8	3.9
7	5.1	6.7	7.8	2.9	3.8
8	5.1	6.6	7.9	3.0	3.8
9	5.0	7.1	7.8	3.0	3.8
10	5.0	8.0	7.9	3.1	3.8

Table 3.3 : Results of Tests of Optimum Cap Size (mean).

	Luzon	Mid-Phil	Mindanao	Tide Gauge	Palawan
0	11.2	17.2	11.4	6.5	1.5
1	8.2	13.0	8.0	5.5	3.5
2	6.4	10.7	6.1	4.7	4.2
3	6.1	10.3	7.1	4.1	4.6
4	6.3	10.2	8.5	3.8	5.1
5	6.7	9.5	9.4	3.7	5.5
6	6.8	9.1	9.8	3.7	5.7
7	6.9	8.5	10.1	3.8	5.5
8	6.8	8.3	10.2	4.0	5.2
9	6.6	8.7	10.1	4.1	5.2
10	6.5	9.5	10.2	4.2	5.3

Table 3.4 : Results of Tests of Optimum Cap Size (rms).

Region	Line Details		Optimum Cap Size		Minimum ppm	
	Average Length (km)	No. of lines	Ring #	Radius(km)	Mean	rms
Luzon	313.47	378	3	30	4.4	6.1
Mid-Phil	95.41	43	8	80	6.6	8.3
Mindanao	221.26	252	2	20	4.8	6.1
Palawan	239.72	6	0	0	1.2	1.5
Tide Gauge	608.81	351	5	50	2.8	3.7

Table 3.5 : Summary for Tests of Optimum Cap Size.

Note: Unit for all standard deviations are in mm.

1	2	3	4	5	6	7	8	9	10
CP#	Name	Rel.ppm	Abs.Map	Profile	N(grav)			H,h	
						S(Ns)		S(Htg)	S(h)
T1	Basco				1,2	13		115	377
T2	Claveria				2,3	14		110	166
T3	Palanan				3,3	17		72	174
T4	Baler	x	1	2	3,3	16	1,1	70	139
T5	Real				2,3	15		54	119
6	Sta. Ana				3,2	10			187
7	Pamplona	x			3,2	16			163
8	Vigan			1	2,2	10			155
9	Bangueo				2,3	15			154
10	Tuguegarao	x	1	1	2,2	15	0,0		150
11	Bayombong	x			2,3	14	2,0		143
12	San Fernando	x			2,2	14			147
13	Iragan	x	1		1,1	11			148
14	Caranglan				1,1	12			136
15	Bolinao	x		1	2,2	13			167
16	Tarlac				1,1	9			126
17	Iba	x	1		1,2	10			150
18	Baguio			2	1,2	10			146
19	Cabanatuan				1,1	9	2,0		127
20	Diliman	x			1,1	9			107
21	San Narciso				2,1	10			134
22	Orion				2,1	10			107
23	Famy				1,1	10			106
24	Dasmarinas				1,1	10			105
25	Bauan	x	1	1	2,2	13	3,3		96
26	Edsa Q.C.	x			2,2	13			107
T27	Ambil Is.				2,2	13		50	100
T28	Balanacan				2,2	25		50	fixed
T29	Presentacion				2,2	14		94	117
T30	Ferrol	x	1		2,2	23		50	118
T31	Pula	x	2		2,2	31		60	112
32	Mauban				1,2	10			108
33	Pitogo				2,2	14	2,0		90
34	Daet				1,2	14			115
35	Pasacao				2,2	14			108
36	Tinambac				1,2	14			109
37	Pyanga				3,2	27		35	110
38	Mamburao				3,2	27			100
39	Calapan				3,2	33			94
40	Bongabong	x	1	1	3,3	27	2,0		110
41	Legazpi				2,2	14		76	108
42	Romblon	x	1		3,3	23			109
43	Tiwi				2,3	13			109
44	Puerto Galera				3,2	29	1,1		98
45	Bato				2,2	13			126
46	Vigia	x		1	3,2	32	2,0		119
47	Sorsogon				2,3	14			109
48	Puro	x			3,2	28			112

Table 4.1 : Details of height errors at GPS control stations.

1	2	3	4	5	6	7	8	9	10
CP#	Name	Rel.ppm	Abs.Map	Profile	N(grav)			H.h	
						S(Ns)		S(Htg)	S(h)
49	Libon				2,2	15			110
50	Ibujay				3,2	24			129
51	Mianay				3,2	26	2,0		118
52	Baclayan	x		2	2,2	26	2,0		119
53	Tigbawan	x	1	1	1,2	24			120
T54	Iba				3,2	24		83	120
55	Valladolio				1,2	24			121
56	Kabankalan				1,2	26	0,0		121
T57	Cadiz				1,2	29		69	118
58	Sagay	x	2	1	1,2	28			117
59	Calatrava				2,2	27			118
60	Silay	x			1,2	25	2,0		119
61	Sipalay	x	1	1	3,2	25	2,0		120
62	Bayawan				2,2	26			120
63	Tayasan		2		2,2	27	0,0		119
64	Ormoc			2	2,2	27			118
T65	Palapag				2,3	25		52	120
66	Corte		2		2,2	27	2,0		117
67	Crag		2		2,2	25			118
68	Anda		2		2,2	25			118
69	Tacloban				2,3	27			118
T70	Guiuan	x		2	2,3	24	0,0	34	122
71	Catbalogan	x	2		2,3	27			112
72	Calbayog	x	2		2,3	26			116
73	San Isidro		2	1	3,3	26			117
74	Liloan				2,3	26	2,0		121
75	Jaena				2,3	27			119
T76	Abuyog	x	2	2	2,3	26		94	121
T77	Oslob	x			3,3	27		55	118
78	Catmon	x	1		3,3	28	2,0		116
79	Lambusan	x			3,3	30	0,0		117
80	Bilar			2	2,3	11		45	120
81	Prosperidad				1,1	7			140
82	Tubay				2,2	11			127
83	Bunawan				1,1	7			144
84	Tagum				2,1	8			143
85	Montevista			2	2,1	8			147
T86	Mambajao	x		1	2,3	10		54	121
87	Tubod				2,2	11			131
88	Davao				1,2	10		48	144
T89	Sta. Monica			2	3,3	13		50	142
T90	Gen. Santos				3,2	16		61	147
T91	Mati				2,2	13	0,0	47	147
T92	Palimbang	x	1	1	3,3	12	0,0	65	154
93	Cotabato		2	2	2,3	12			148
94	Macabalan				3,2	12			129
95	Ozamiz				3,2	11			138
T96	Gingoog	x			3,3	12		3s	127

Table 4.1(cont.): Details of height errors at GPS control stations.

1	2	3	4	5	6	7	8	9	10
CP#	Name	Rel.ppm	Abs.Map	Profile	N(grav)		H,h		
						S(Ns)		S(Htg)	S(h)
97	Sta. Filomena				3,2	12			132
98	Penoyak			1	3,2	13	2,0		138
99	Koronadal				1,1	7			148
100	Tacurong				1,1	7			146
T101	Parang	x			3,2	14		3s	147
T102	Liloy	x			3,2	12	0,0	42	149
T103	Dipolog				3,3	11		51	123
T104	Zamboanga				3,2	11		45	159
T105	Pagadian			2	3,2	12		47	137
T106	TayTay				3,2			63	129
T107	Rio Tuba			1	3,2			41	188
108	Balabac				3,2				293
109	P. Princesa				3,2				137
T110	Bongao				3,2	10		54	187
111	Jolo				3,2	11			172

To classify the accuracy and precision of all height elements to be used in the Adjustment process.

1. Relative ppm
   Poor points which are detected from GRAV08 output analysis.
2. Absolute Map
   Contour map of ΔN is plotted and suspect points are filtered out and the effects noted.
   1 - To denote first filter
   2 - 2nd Filter
3. Profile of ΔN
   Control points with common criteria are aggregated into their respective groups and statistically tested by comparing each point against the mean and s of each group.
4. N from Gravimetry
   To classify N's accuracy and precision: by
   a. Coverage
      1 - Good with dense coverage (equal to or better than 1 per 0.1° grid point)
      2 - Medium coverage (some points within 0.3° cap size)
      3 - Poor coverage. no points or few (1 or 2) within 0.3° cap size.
   b. "Goodness of representation"
      1 - Good. Topography benign and gravity observed terrestrially.
      2 - Medium. Topography benign (ocean) and gravity deduced from altimetry.
      3 - Poor. Topography difficult (mountainous/eastern coastal effect)
   S(Ns) : Formal error in Ns from RINT.
5. H, h from comments in letter from Doug Larden.
   0 - Elements well determined.
   1 - Well determined with possible problem
   2 - Suspect
   3 - Down weight or exclude element
   S(Htg) : Standard error in residuals from tide gauge summaries (ex Lennon)
   S(h) : Standard error in adjusted ellipsoidal heights (ex Larden)

Table 4.1(cont.): Details of height errors at GPS control stations.

Control Point	Name	h (Jones)	H (lev.)	N(gps/lev)	N(grav.)	ΔN
T1	Basco	50.074	14.063	36.0110	32.4607	3.5503
T2	Claveria	132.222	92.676	39.5460	34.5788	4.9672
T3	Palanan	48.267	5.698	42.5690	38.3244	4.2446
T4	Baler	49.327	3.493	45.8340	43.9289	1.9051
T5	Real	49.853	1.679	48.1740	45.4525	2.7215
6	Sta. Ana	42.017	1.916	40.1010	35.4256	4.6754
7	Pamplona	49.460	7.539	41.9210	36.1584	5.7626
8	Vigan	45.056	5.778	39.2780	34.8897	4.3883
9	Bangueo	89.911	48.305	41.6060	35.7787	5.8273
10	Tuguegarao	84.575	42.099	42.4760	35.6948	6.7812
11	Bayombong	420.774	373.204	47.5700	42.5527	5.0173
12	San Fernando	84.854	43.285	41.5690	38.6362	2.9328
13	Iragan	125.685	81.013	44.6720	38.3914	6.2806
14	Caranglan	438.656	391.357	47.2990	43.1118	4.1872
15	Bolinao	41.328	1.128	40.2000	37.7306	2.4694
16	Tarlac	86.343	41.530	44.8130	40.8802	3.9328
17	Iba	91.457	47.530	43.9270	39.7351	4.1919
18	Baguio	1289.508	1242.113	47.3950	43.1212	4.2738
19	Cabanatuan	101.903	56.122	45.7810	41.8492	3.9318
20	Diliman	134.095	87.993	46.1020	43.5013	2.6007
21	San Narciso	67.802	22.245	45.5570	42.0275	3.5295
22	Orion	193.796	149.023	44.7730	41.6884	3.0846
23	Famy	55.880	7.543	48.3370	45.4226	2.9144
24	Dasmarinas	239.590	193.320	46.2700	43.6564	2.6136
25	Bauan	392.521	344.072	48.4490	43.3236	5.1254
26	Edsa Q.C.	100.360	54.339	46.0210	43.2137	2.8073
T27	Ambil Is.	119.240	78.548	40.6920	38.8997	1.7923
T28	Balanacan	320.110	268.942	51.1680	49.1273	2.0407
T29	Presentacion	60.230	4.993	55.2370	52.3996	2.8374
T30	Ferrol	75.061	21.018	54.0430	52.7804	1.2626
T31	Pula	76.641	17.983	58.6580	54.9266	3.7314
32	Mauban	51.337	1.232	50.1050	47.1771	2.9279
33	Pitogo	121.336	70.195	51.1410	49.1878	1.9532
34	Daet	56.439	3.114	53.3250	50.3369	2.9881
35	Pasacao	55.771	1.627	54.1440	52.1652	1.9788
36	Tinambac	113.731	58.787	54.9440	51.9173	3.0267
37	Pyanga	278.175	228.712	49.4630	47.2728	2.1902
38	Mamburao	84.427	40.214	44.2130	41.2371	2.9759
39	Calapan	51.409	2.442	48.9670	46.4990	2.4680
40	Bongabong	73.509	23.546	49.9630	50.8427	-0.8797
41	Legazpi	121.006	64.985	56.0210	53.0653	2.9557
42	Romblon	109.277	56.623	52.6540	53.3242	-0.6702
43	Tiwi	163.730	108.686	55.0440	52.3416	2.7024
44	Puerto Galera	98.505	50.559	47.9460	45.1416	2.8044
45	Bato	72.002	17.371	54.6310	51.3820	3.2490
46	Vigia	162.594	103.180	59.4140	57.7645	1.6495
47	Sorsogon	73.144	16.660	56.4840	53.4530	3.0310
48	Puro	209.769	152.541	57.2280	53.7855	3.4425

Table 4.2: Comparison of absolute geoid heights derived (1) gravimetrically and (2) Jones h and levelling.

Control Point	Name	h (gps)	H (lev.)	N(gps/lev.)	N(grav.)	ΔN
49	Libon	107.629	52.040	55.5890	53.3480	2.2410
50	Ibujay	135.138	79.340	55.7980	54.6305	1.1675
51	Mianay	292.491	233.345	59.1460	57.6010	1.5450
52	Baclayan	396.347	334.734	61.6130	59.5119	2.1011
53	Tigbawan	148.538	92.385	56.1530	56.3235	-0.1705
T54	Iba	303.000	246.819	56.1810	55.2666	0.9144
55	Valladolio	65.208	2.493	62.7150	60.2211	2.4939
56	Kabankalan	85.252	21.199	64.0530	61.0786	2.9744
T57	Cadiz	88.979	26.459	62.5200	59.8416	2.6784
58	Sagay	127.663	65.153	62.5100	61.0473	1.4627
59	Calatrava	65.237	2.538	62.6990	60.7940	1.9050
60	Silay	91.516	28.987	62.5290	59.6835	2.8455
61	Sipalay	72.234	10.488	61.7460	56.9469	4.7991
62	Bayawan	87.197	23.133	64.0640	61.3099	2.7541
63	Tayasan	67.333	2.779	64.5540	61.3748	3.1792
64	Ormoc	67.133	1.926	65.2070	62.5558	2.6512
T65	Palapag	71.722	15.609	56.1130	52.9591	3.1539
66	Corte	243.049	176.812	66.2370	65.3528	0.8842
67	Crag	440.761	375.062	65.6990	64.7302	0.9688
68	Anda	186.978	121.461	65.5170	64.1856	1.3314
69	Tacloban	90.392	23.984	66.4080	62.9009	3.5071
T70	Guiuan	68.838	3.484	65.3540	63.6763	1.6777
71	Catbalogan	66.750	2.293	64.4570	60.6595	3.7975
72	Calbayog	64.172	1.609	62.5630	58.9793	3.5837
73	San Isidro	62.767	4.388	58.3790	56.9000	1.4790
74	Liloan	138.600	71.307	67.2930	64.3155	2.9775
75	Jaena	109.917	43.166	66.7510	63.8216	2.9294
T76	Abuyog	68.863	1.559	67.3040	63.6780	3.6260
T77	Oslob	832.802	767.853	64.9490	62.0679	2.8811
78	Catmon	313.234	251.260	61.9740	62.8403	-0.8663
79	Lambusan	182.816	117.953	64.8630	61.7467	3.1163
80	Bilar	163.447	93.995	69.4520	65.7101	3.7419
81	Prosperidad	116.299	44.287	72.0120	68.0594	3.9526
82	Tubay	139.747	67.747	72.0000	67.6191	4.3809
83	Bunawan	109.531	37.579	71.9520	67.8986	4.0534
84	Tagum	103.379	31.878	71.5010	67.3302	4.1708
85	Montevista	168.993	96.549	72.4440	67.8593	4.5847
T86	Mambajao	68.419	1.723	66.6960	64.4522	2.2438
87	Tubod	124.295	52.534	71.7610	67.3753	4.3857
88	Davao	72.132	0.901	71.2310	67.1036	4.1274
T89	Sta. Monica	157.001	88.446	68.5550	63.9034	4.6516
T90	Gen. Santos	114.205	40.334	73.8710	70.2209	3.6501
T91	Mati	72.691	1.889	70.8020	67.1811	3.6209
T92	Palimbang	76.286	2.548	73.7380	72.2997	1.4383
93	Cotabato	134.857	60.621	74.2360	71.3363	2.8997
94	Macabalan	89.796	18.304	71.4920	68.5763	2.9157
95	Ozamiz	72.146	1.422	70.7240	67.5396	3.1844
T96	Gingoog	95.821	26.177	69.6440	66.6802	2.9638

Table 4.2(cont.): Comparison of absolute geoid heights derived (1) gravimetrically and (2) Jones h and levelling.

Control Point	Name	h (gps)	H (lev.)	N(gps/lev.)	N(grav.)	ΔN
97	Sta. Filomena	73.535	1.992	71.5430	68.2527	3.2903
98	Penoyak	86.095	15.036	71.0590	67.6511	3.4079
99	Koronadal	136.589	61.131	75.4580	71.7412	3.7168
100	Tacurong	159.888	84.922	74.9660	71.5461	3.4199
T101	Parang	172.402	97.790	74.6120	70.6327	3.9793
T102	Liloy	68.496	2.929	65.5670	63.7746	1.7924
T103	Dipolog	79.854	12.761	67.0930	64.9746	2.1184
T104	Zamboanga	78.086	8.767	69.3190	67.5205	1.7985
T105	Pagadian	135.573	64.946	70.6270	67.4800	3.1470
T106	TayTay	60.962	10.670	50.2920	50.6047	-0.3127
T107	Rio Tuba	54.081	7.437	46.6440	47.5482	-0.9042
108	Balabac	75.980	30.125	45.8550	45.8999	-0.0448
109	P. Princesa	84.771	34.980	49.7910	50.2531	-0.4621
T110	Bongao	154.342	90.096	64.2460	62.4194	1.8266
111	Jolo	87.389	18.274	69.1150	66.0084	3.1066

Table 4.2(cont.): Comparison of absolute geoid heights derived (1) gravimetrically and (2) Jones h and levelling.

Name	Control Point	N(gps/lev)	N(grav.)	Control Point	ΔN
Basco	T1	36.0110	32.4607	T1	3.5503
Claveria	T2	39.5460	34.5788	T2	4.9672
Sta. Ana	6	40.1010	35.4256	6	4.6754
Pamplona	7	41.9210	36.1584	7	5.7626
				Mean	4.7389
				Std. Dev	0.9159

Table 4.3 : ΔN profile for northern Luzon.

Palanan	T3	42.5690	38.3244	T3	4.2446
Baler	T4	45.8340	43.9289	T4	1.9051
Real	T5	48.1740	45.4525	T5	2.7215
				Mean	2.9571
				Std. Dev	1.1874

Table 4.4 : ΔN profile for eastern Luzon.

Presentacion	T29	55.2370	52.3996	T29	2.8374
Pitogo	33	51.1410	49.1878	33	1.9532
Daet	34	53.3250	50.3369	34	2.9881
Pasacao	35	54.1440	52.1652	35	1.9788
Tinambac	36	54.9440	51.9173	36	3.0267
Legazpi	41	56.0210	53.0653	41	2.9557
Tiwi	43	55.0440	52.3416	43	2.7024
Sorsogon	47	56.4840	53.4530	47	3.0310
Libon	49	55.5890	53.3480	49	2.2410
				Mean	2.6349
				Std. Dev	0.4519

Table 4.5 : ΔN profile for southern Luzon.

Real	T5	48.1740	45.4525	T5	2.7215
Diliman	20	46.1020	43.5013	20	2.6007
Orion	22	44.7730	41.6884	22	3.0846
Famy	23	48.3370	45.4226	23	2.9144
Dasmarinas	24	46.2700	43.6564	24	2.6136
Bauan	25	48.4490	43.3236	25	5.1254
Edsa Q.C.	26	46.0210	43.2137	26	2.8073
Mauban	32	50.1050	47.1771	32	2.9279
				Mean	3.0994
				Std. Dev	0.8351

Table 4.6 : ΔN profile for mid of Luzon.

Bangueo	9	41.6060	35.7787	9	5.8273
Tuguegarao	10	42.4760	35.6948	10	6.7812
Bayombong	11	47.5700	42.5527	11	5.0173
Iragan	13	44.6720	38.3914	13	6.2806
Baguio	18	47.3950	43.1212	18	4.2738
				Mean	5.6360
				Std. Dev	1.0002

Table 4.7 : ΔN profile for central north of Luzon.

Vigan	8	39.2780	34.8897	8	4.3883
San Fernando	12	41.5690	38.6362	12	2.9328
Bolinao	15	40.2000	37.7306	15	2.4694
Iba	17	43.9270	39.7351	17	4.1919
San Narciso	21	45.5570	42.0275	21	3.5295
				Mean	3.5024
				Std. Dev	0.8143

Table 4.8 : ΔN profile for west coast Luzon.

Caranglan	14	47.2990	43.1118	14	4.1872
Tarlac	16	44.8130	40.8802	16	3.9328
Cabanatuan	19	45.7810	41.8492	19	3.9318
				Mean	4.0173
				Std. Dev	0.1472

Table 4.9 : ΔN profile for central Luzon.

Eastern Mindanao

Bilar	80	69.4520	65.7101	80	3.7419
Prosperidad	81	72.0120	68.0594	81	3.9526
Tubay	82	72.0000	67.6191	82	4.3809
Bunawan	83	71.9520	67.8986	83	4.0534
Tagum	84	71.5010	67.3302	84	4.1708
Montevista	85	72.4440	67.8593	85	4.5847
Tubod	87	71.7610	67.3753	87	4.3857
Sta.Monica	89	68.5550	63.9034	89	4.6516
				Mean	4.2402
				Std. Dev	0.3161

Table 4.10 : ΔN profile for eastern Mindanao.

Davao Gulf

Davao	88	71.2310	67.1036	88	4.1274
Gen. Santos	T90	73.8710	70.2209	T90	3.6501
Mati	T91	70.8020	67.1811	T91	3.6209
Palimbang	T92	73.7380	72.2997	T92	1.4383
Cotabato	93	74.2360	71.3363	93	2.8997
Koronadal	99	75.4580	71.7412	99	3.7168
Tacurong	100	74.9660	71.5461	100	3.4199
Parang	T101	74.6120	70.6327	T101	3.9793
				Mean	3.3565
				Std. Dev	0.8586

Table 4.11 : ΔN profile for Davao Gulf.

Moro Gulf

Penoyak	98	71.0590	67.6511	98	3.4079
Liloy	T102	65.5670	63.7746	T102	1.7924
Dipolog	T103	67.0930	64.9746	T103	2.1184
Zamboanga	T104	69.3190	67.5205	T104	1.7985
Pagadian	T105	70.6270	67.4800	T105	3.1470
				Mean	2.4528
				Std. Dev	0.7698

Table 4.12 : ΔN profile for Moro Gulf.

Mindanao northern Coast

Mambajao	T86	66.6960	64.4522	T86	2.2438
Macabalan	94	71.4920	68.5763	94	2.9157
Ozamiz	95	70.7240	67.5396	95	3.1844
Gingoog	T96	69.6440	66.6802	T96	2.9638
Sta. Filomena	97	71.5430	68.2527	97	3.2903
				Mean	2.9196
				Std. Dev	0.4081

Table 4.13 : ΔN profile for Mindanao northern coast.

SW Phil.

Bongao	T110	64.2460	62.4194	T110	1.8266
Jolo	111	69.1150	66.0084	111	3.1066
				Mean	2.4666
				Std. Dev	0.9051

Table 4.14 : ΔN profile for south west Philippines.

Palawan

TayTay	T106	50.29	50.6047	T106	-0.3127
Rio Tuba	T107	46.6440	47.5482	T107	-0.9042
Balabac	108	45.8550	45.8999	108	-0.0449
P. Princesa	109	49.7910	50.2531	109	-0.4621
				Mean	-0.4704
				Std. Dev	0.4297

Table 4.15 : ΔN profile for Palawan.

Island of Panay

Ibujay	50	55.7980	54.6305	50	1.1675
Mianay	51	59.1460	57.6010	51	1.5450
Baclayan	52	61.6130	59.5119	52	2.1011
Tigbawan	53	56.1530	56.3235	53	-0.1705
Iba	T54	56.1810	55.2666	T54	0.9144
				Mean	1.1115
				Std. Dev	0.8445

Table 4.16 : ΔN profile for Island of Panay.

Island of Negros

Valladolio	55	62.7150	60.2211	55	2.4939
Kabankalan	56	64.0530	61.0786	56	2.9744
Cadiz	T57	62.5200	59.8416	T57	2.6784
Sagay	58	62.5100	61.0473	58	1.4627
Calatrava	59	62.6990	60.7940	59	1.9050
Silay	60	62.5290	59.6835	60	2.8455
Sipalay	61	61.7460	56.9469	61	4.7991
Bayawan	62	64.0640	61.3099	62	2.7541
Tayasan	63	64.5540	61.3748	63	3.1792
				Mean	2.7880
				Std. Dev	0.9268

Table 4.17 : ΔN profile for Island of Negros.

Island of Bohol

Corte	66	66.2370	65.3528	66	0.8842
Crag	67	65.6990	64.7302	67	0.9688
Anda	68	65.5170	64.1856	68	1.3314
				Mean	1.0615
				Std. Dev	0.2376

Table 4.18 : ΔN profile for Island of Bohol.

Island of Samar

Palapag	T65	56.1130	52.9591	T65	3.1539
Guiuan	T70	65.3540	63.6763	T70	1.6777
Catbalogan	71	64.4570	60.6595	71	3.7975
Calbayog	72	62.5630	58.9793	72	3.5837
San Isidro	73	58.3790	56.9000	73	1.4790
				Mean	2.7384
				Std. Dev	1.0863

Table 4.19 : ΔN profile for Island of Samar.

Island of Leyte

Ormoc	64	65.2070	62.5558	64	2.6512
Tacloban	69	66.4080	62.9009	69	3.5071
Liloan	74	67.2930	64.3155	74	2.9775
Jaena	75	66.7510	63.8216	75	2.9294
Abuyog	T76	67.3040	63.6780	T76	3.6260
				Mean	3.1383
				Std. Dev	0.4125

Table 4.20 : ΔN profile for Island of Leyte.

Island of Cebu

Oslob	T77	64.9490	62.0679	T77	2.8811
Catmon	78	61.9740	62.8403	78	-0.8663
Lambusan	79	64.8630	61.7467	79	3.1163
				Mean	1.7104
				Std. Dev	2.2345

Table 4.21 : ΔN profile for Island of Cebu.

Island of Tablas

Ferrol	T30	54.0430	52.7804	T30	1.2626
Romblon	42	52.6540	53.3242	42	-0.6702
				Mean	0.2962
				Std. Dev	1.3667

Table 4.22 : ΔN profile for Island of Tablas.

Island of Mindoro

Pyanga	37	49.4630	47.2728	37	2.1902
Mamburao	38	44.2130	41.2371	38	2.9759
Calapan	39	48.9670	46.4990	39	2.4680
Bongabong	40	49.9630	50.8427	40	-0.8797
Puerto Galera	44	47.9460	45.1416	44	2.8044
				Mean	1.9118
				Std. Dev	1.5897

Table 4.23 : ΔN profile for Island of Mindoro.

Island of Masbate

Pula	T31	58.6580	54.9266	T31	3.7314
Vigia	46	59.4140	57.7645	46	1.6495
Puro	48	57.2280	53.7855	48	3.4425
				Mean	2.9411
				Std. Dev	1.1279

Table 4.24 : ΔN profile for Island of Masbate.

PHASE 1

Control Sta. No.	Control Sta. Name	Duration	Corr. Coef.	S res	Max	Min	Range	S obs	Comments
		(days)		(m)				(m)	
1	Basco Batanes	95	0.889	0.115	1.51	0.08	1.43	0.244	Westerly Exposure
2	Claveria Cagayan	92	0.908	0.110	2.04	0.52	1.52	0.261	Westerly Exposure
3	Palanan Isabela	90	0.986	0.072	2.58	0.43	2.15	0.427	Easterly Exposure
4	Baler Aurora	92	0.986	0.070	2.79	0.63	2.10	0.421	Easterly Exposure
5	Real Quezon	96	0.994	0.054	3.00	0.55	2.45	0.504	Easterly Exposure
41	Legaspi	365	0.986	0.076	2.84	0.38	2.46	0.460	Primary Tidal Ref. Station
	Port Irene	349	0.965	0.103	3.18	1.29	1.89	0.393	Primary Tidal Ref. Station

Notes :

1. Two procedures adopted to remove effect of noisy manual tide staff observations.
2. The 'Average Seasonal Variations' for Manila is considered relevant to stations with westerly exposure.
3. The 'Average Seasonal Variations' for Legaspi is considered relevant to stations with easterly exposure.
4. Manila shows a clear non-linearity with a steep rise in sea level.
5. Legaspi shows a more consistent trend.

Table 4.25 : Tide gauge summary Phase 1.

P H A S E 2

Control Sta. No.	Control Sta. Name	Duration (days)	Corr. Coef.	S res (m)	Max	Min	Range	S obs (m)	Comments
27	Ambil Island	76	0.9892	0.050	2.49	0.93	1.56	0.337	See notes
28	Balanacan	93	0.9939	0.050	2.90	0.68	2.22	0.447	See notes
30	Ferrol	76	0.9950	0.050	2.64	0.40	2.24	0.458	See notes
31	Masbate	90	0.9925	0.060	2.73	0.39	2.34	0.491	See notes
29	Presentacion	78	0.9784	0.094	3.10	1.00	2.10	0.452	See notes
37	San Jose	365	0.9960	0.035	2.75	0.66	2.09	0.388	Primary Tidal Ref. System
	Cebu	365	0.9966	0.040	3.15	0.52	2.63	0.490	Primary Tidal Ref. System

Notes:
1. BALANACAN shows some 'spikes' in predicted versus observed.
2. CEBU - the MASBATE section seems to be in error.
3. LEGASPI - the PRESENTACION section seems to be in error.
4. Adopt Manila for Western sections (for seasonal variation).
5. Adopt Legaspi, Tacloban and Cebu for Eastern section (for seasonal variation)
6. Sea level topography of 12cm (August); 2cm (September); -8cm (October)
7. Long period trends: Manila positive, Central Philippines (Tacloban and Cebu) undeterminate.

Table 4.26 : Tide gauge summary Phase 2.

PHASE 3

Control Sta. No.	Control Sta. Name	Duration	Corr. Coef.	S res	Max	Min	Range	S obs	Comments
		(days)		(m)				(m)	
65	Palapag	79	0.9935	0.052	2.63	0.49	2.14	0.455	Indifferent - spikey
76	Abuyog	75	0.9225	0.094	1.98	0.79	1.19	0.244	Good bar bump
57	Cadiz	52	0.9942	0.069	3.34	0.25	3.09	0.640	Indifferent - spikey
54	Antique / 1km	85	0.9843	0.083	2.75	0.33	2.42	0.470	Indifferent - spikey
77	Santander	72	0.9940	0.055	3.90	1.35	2.55	0.506	Better : still anomalies
86	Mambajao	62	0.9918	0.054	2.75	0.66	2.09	0.421	Good
80	Surigao	365	0.9923	0.045	3.45	1.43	2.02	0.363	Primary Tidal Ref. System

Note:
See back of this report for 'Deviation of sea level from 75 to 86 mean sea level.'
16 to 30 cm in Philippines.

Table 4.27 : Tide gauge summary Phase 3.

Control Sta. No.	Control Sta. Name	Duration	Corr. Coef.	S res	Max	Min	Range	S obs	Comments
		(days)		(m)				(m)	
70	Guiuan-East Samar	60	0.9903	0.034	1.68	0.55	1.13	0.242	Good
89	St. Monica	61	0.9930	0.050	2.86	0.75	2.11	0.420	Some small spikes
*	Lianga	62	0.9924	0.051	2.17	0.48	1.69	0.417	Good
91	Mati	59	0.9947	0.047	2.90	0.51	2.39	0.453	Good
90	Makar	61	0.9926	0.061	3.60	1.28	2.32	0.498	Some timing problems
92	Palimbang	61	0.9916	0.065	2.91	0.48	2.43	0.503	Good
88	Davao	365	0.9953	0.048	3.36	0.84	2.52	0.501	Data 1989 analysis
					3.29	0.88	2.41	0.502	Data 1990 analysis
									Primary Tidal Ref. System

Notes:
1. Decadal time variations of oceanic scale appear to be 4/90:-6cm; 5/90: 12cm; 6/90: 5cm.
2. Datum data appear to relate to different epochs.

* Phase 4 Note 3 : No H and h supplied.

Table 4.28 : Tide gauge summary Phase 4.

PHASE 5

Control Sta. No.	Control Sta. Name	Duration (days)	Corr. Coef.	S res (m)	Max	Min	Range	S obs (m)	Comments
102	Liloy	61	0.9952	0.0423	2.50	0.33	2.17	0.4330	Good
103	Dipolog	45	0.9913	0.0510	2.78	0.98	1.80	0.3881	Problems during obs.
104	Zamboanga	62	0.9908	0.0450	3.06	1.52	1.54	0.3328	Good
105	Pagadian	62	0.9966	0.0470	3.58	1.26	2.32	0.5710	Good
106	Taytay	60	0.9892	0.0631	2.43	0.33	2.10	0.4292	Good
107	Rio Tuba	60	0.9948	0.0408	2.28	0.40	1.88	0.4013	Good
110	Bongao	60	0.9921	0.0544	2.61	0.78	1.83	0.4329	Good

Notes:
1. Balabac was used as a tidal analysis reference station for Rio Tuba.
   Data quality for Balabac is generally good.
2. Jolo was used as a tidal analysis reference station for Zamboanga and Bongao.
   Data quality for Jolo is generally good.

Table 4.29 : Tide gauge summary Phase 5.

Note: Unit for all standard deviations are in mm.

1	2	3	4	5	6	7	8	9	10
CP#	Name	Rel.ppm	Abs.Map	Profile	N(grav)			H,h	
						S(Ns)		S(Htg)	S(h)
T4	Baler	x	1	2	3,3	16	1,1	70	139
7	Pamplona	x			3,2	16			163
10	Tuguegarao	x	1	1	2,2	15	0,0		150
11	Bayombong	x			2,3	14	2,0		143
12	San Fernando	x			2,2	14			147
13	Iragan	x	1		1,1	11			148
15	Bolinao	x		1	2,2	13			167
17	Iba	x	1		1,2	10			150
18	Baguio			2	1,2	10			146
20	Diliman	x			1,1	9			107
25	Bauan	x	1	1	2,2	13	3,3		96
26	Edsa Q.C.	x			2,2	13			107
T30	Ferrol	x	1		2,2	23		50	118
T31	Pula	x	2		2,2	31		60	112
40	Bongabong	x	1	1	3,3	27	2,0		110
42	Romblon	x	1		3,3	23			109
46	Vigia	x		1	3,2	32	2,0		119
48	Puro	x			3,2	28			112
52	Baclayan	x		2	2,2	26	2,0		119
53	Tigbawan	x	1	1	1,2	24			120
58	Sagay	x	2	1	1,2	28			117
60	Silay	x			1,2	25	2,0		119
61	Sipalay	x	1	1	3,2	25	2,0		120
63	Tayasan		2		2,2	27	0,0		119
64	Ormoc			2	2,2	27			118
66	Corte		2		2,2	27	2,0		117
67	Crag		2		2,2	25			118
68	Anda		2		2,2	25			118
T70	Guiuan	x		2	2,3	24	0,0	34	122
71•	Catbalogan	x	2		2,3	27			112
72	Calbayog	x	2		2,3	26			116
73	San Isidro		2	1	3,3	26			117
T76	Abuyog	x	2	2	2,3	26		94	121
T77	Oslob	x			3,3	27		55	118
78	Catmon	x	1		3,3	28	2,0		116
79	Lambusan	x			3,3	30	0,0		117
80	Bilar			2	2,3	11		45	120
85	Montevista			2	2,1	8			147
T86	Mambajao	x		1	2,3	10		54	121
T89	Sta. Monica			2	3,3	13		50	142
T92	Palimbang	x	1	1	3,3	12	0,0	65	154
93	Cotabato		2	2	2,3	12			148
T96	Gingoog	x			3,3	12		3s	127
98	Penoyak			1	3,2	13	2,0		138
T101	Parang	x			3,2	14		3s	147
T102	Liloy	x			3,2	12	0,0	42	149
T105	Pagadian			2	3,2	12		47	137
T107	Rio Tuba			1	3,2			41	188

Table 4.30 : Suspect points and their elements.

Element	**Point Numbers**
h	**12, 13, 15, 28, 43,** 85, 78 (in gross error - see Figure 4.23) N.B. Points in **bold** have relative errors worse than 8ppm
N	**T4,** 7, 8, 10, 11, 12, 15, **25**, 26, T30, T31, **40**, **42**, 46, 48, 52, 61, 64, 66, 67, 68, T70, 71, 72, 73, T76, **T77**, **78**, **79**, 80, T86, T89, T92, 93, **T96**, 98, T101,T102, T105, T107 N.B. Points in **bold** have the worst possible scenario for gravimetric evaluation of N
H	11,19,25,33,40,46,51,52,66,67,68,78,98 N.B. Not all suspect points were assessed for possible problems in the levelling used to produce H.

Table 4.31 : Possible problems in the elements of suspect points.

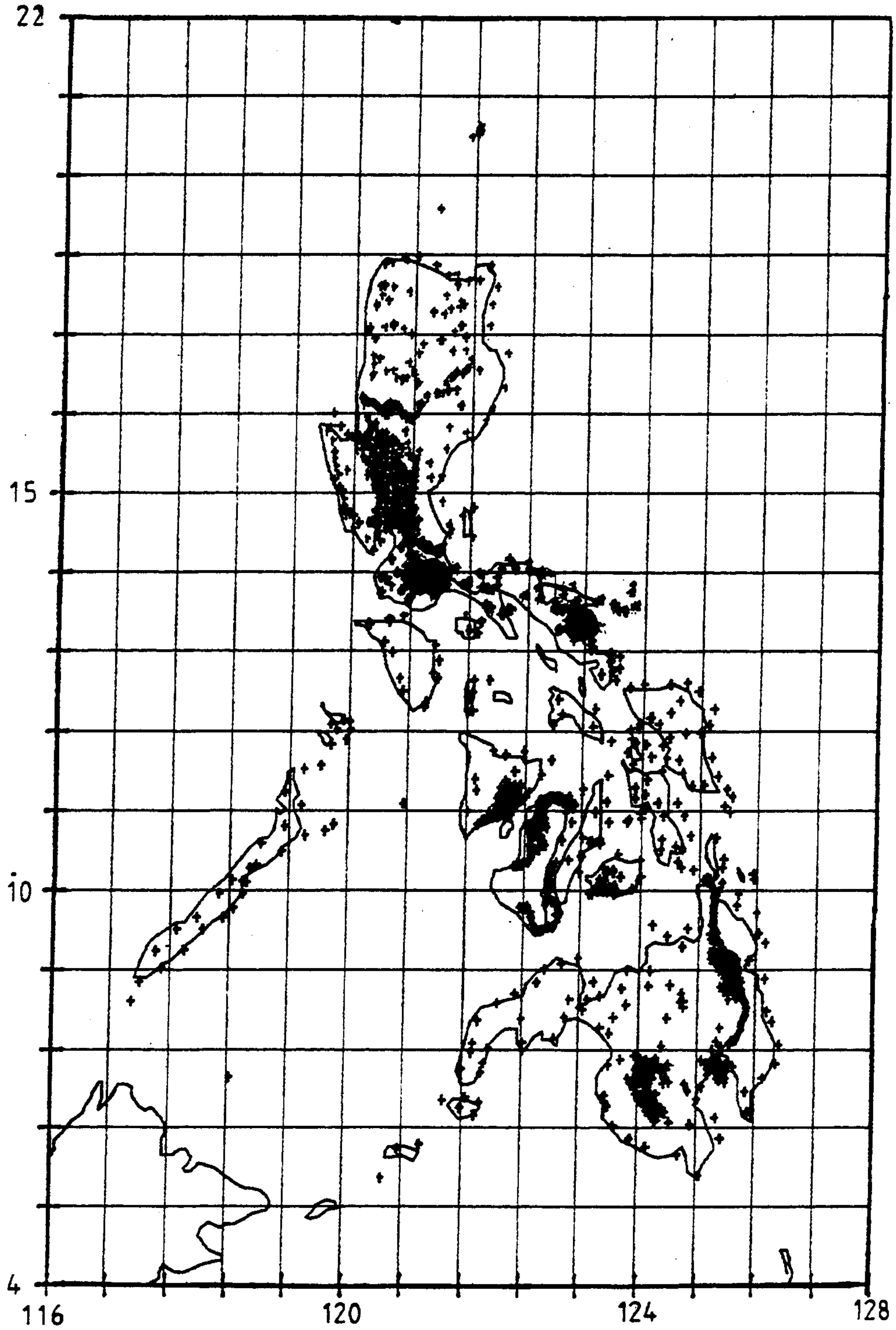

Figure 2.1 : Map of Terrestrially-observed Gravity Data.

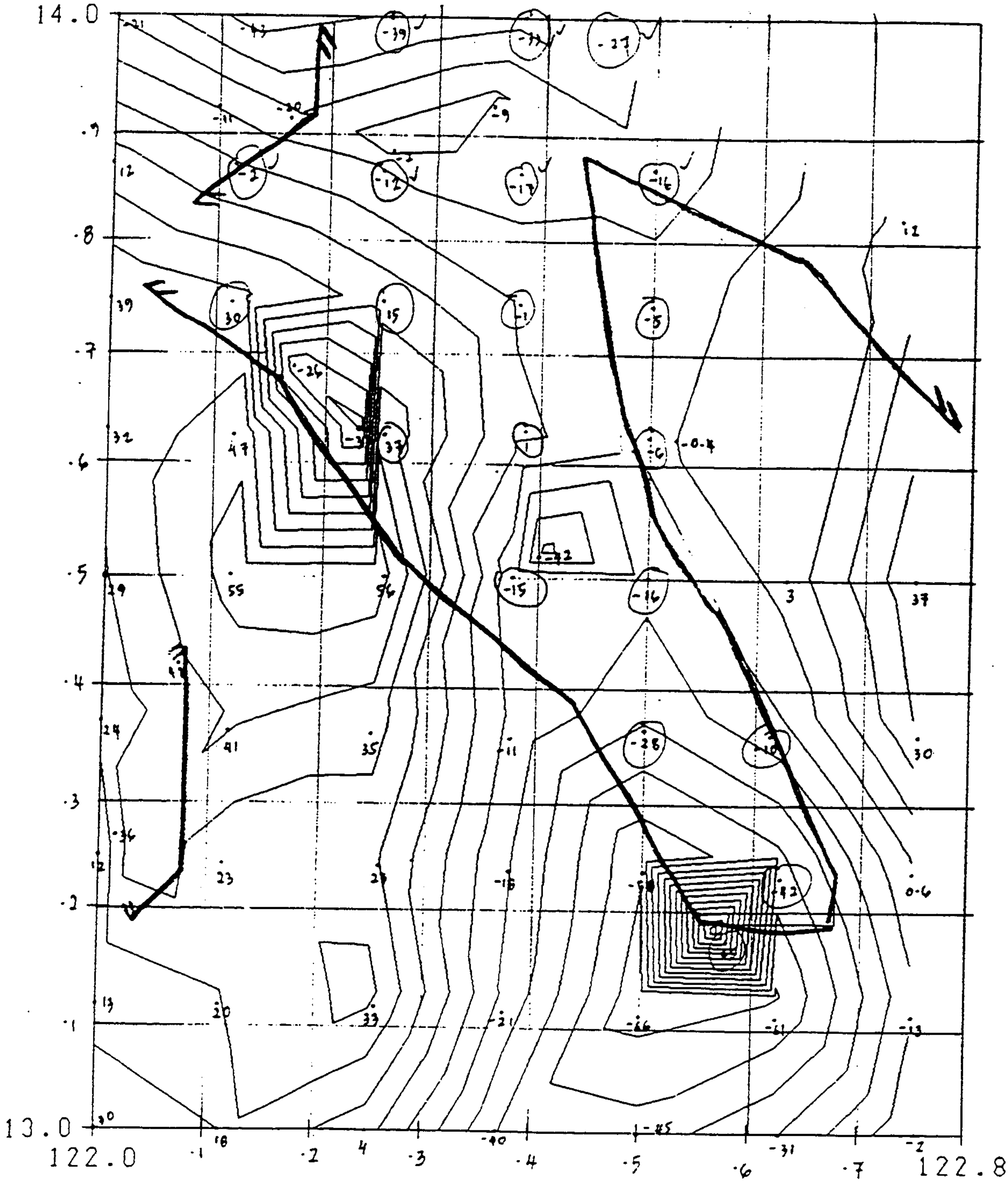

Figure 2.2 : Example of Problems with Gravity Data.

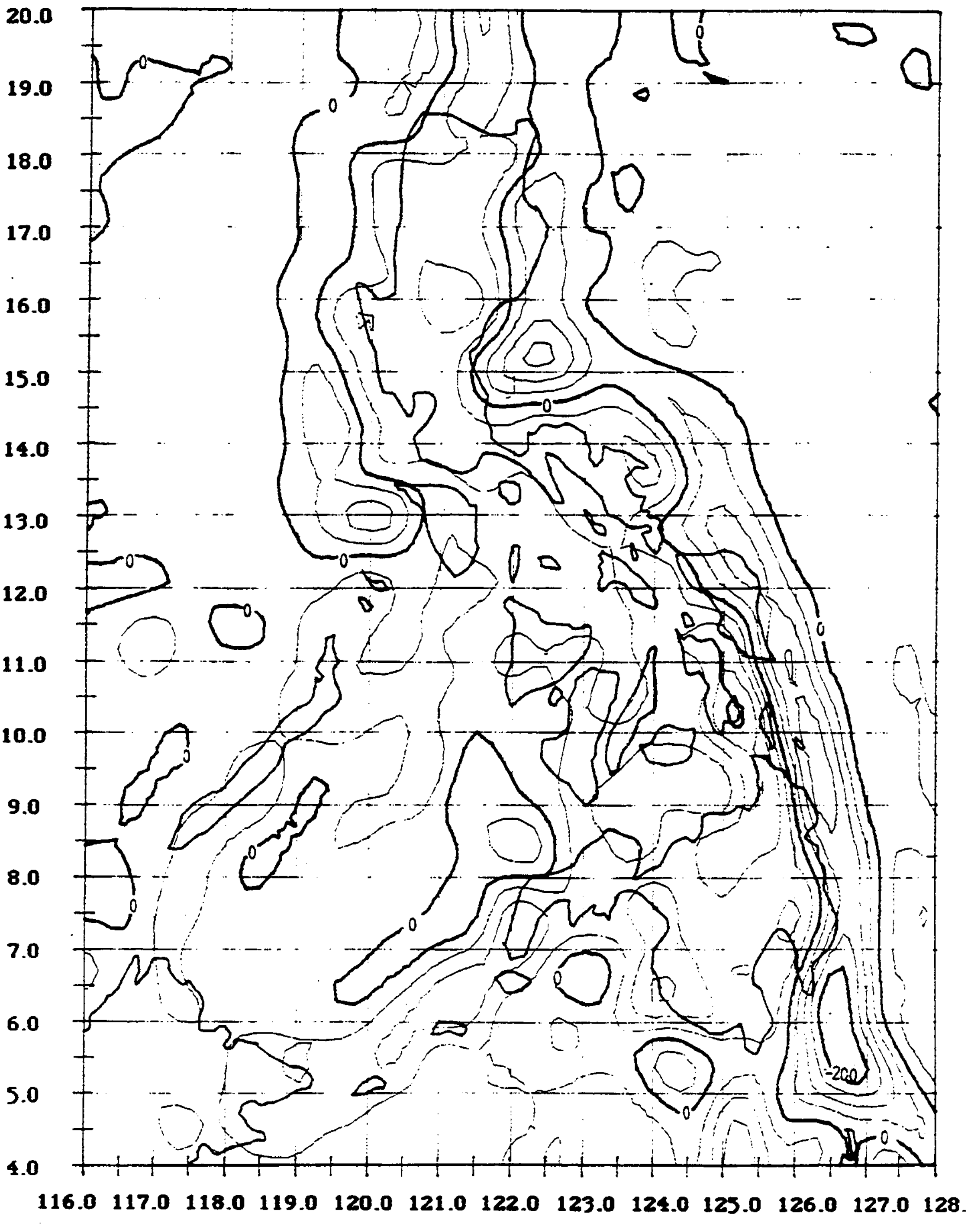

Figure 2.3 : Δg from OSU89A.

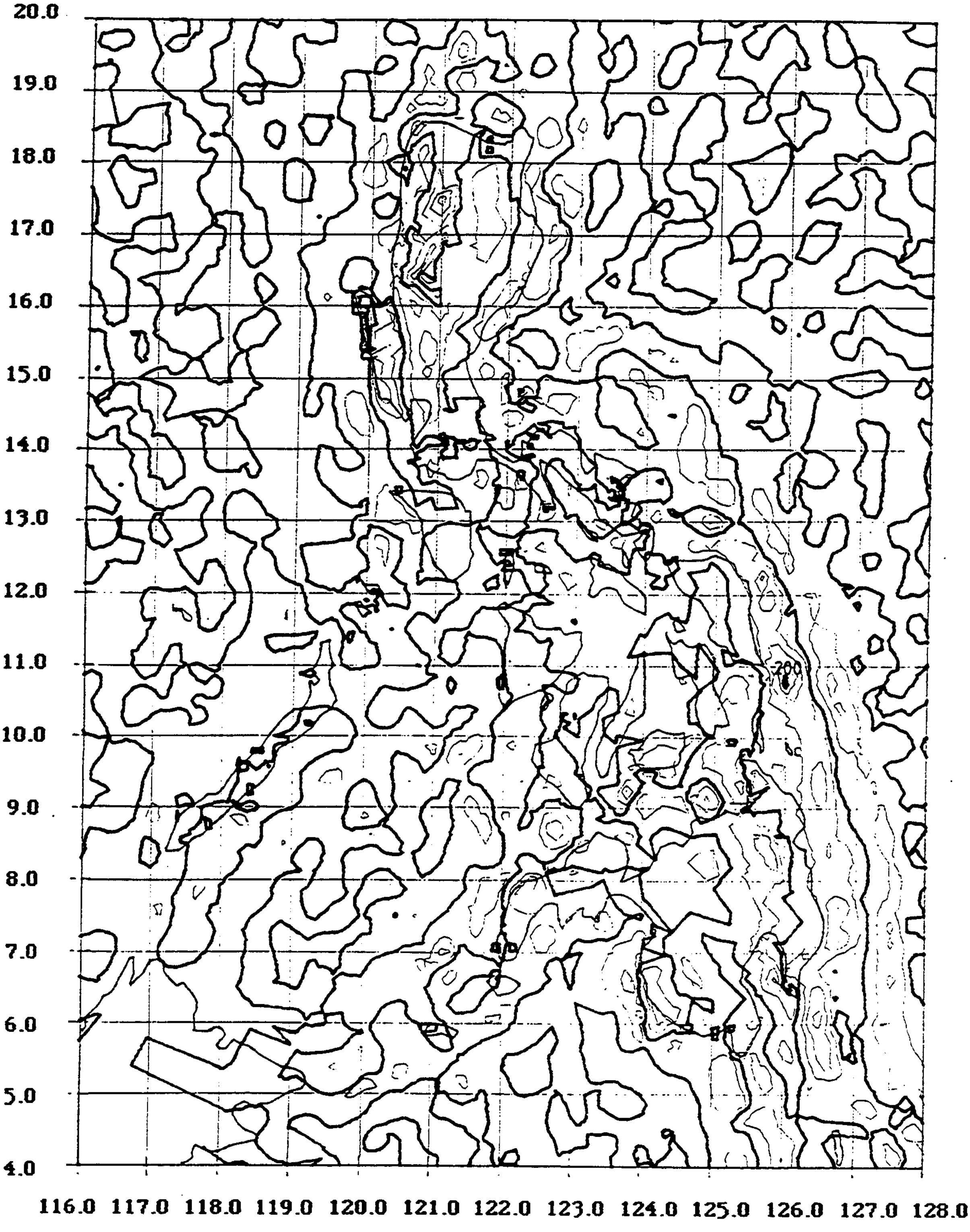

Figure 2.4 : Residual Δg from OSU89A.

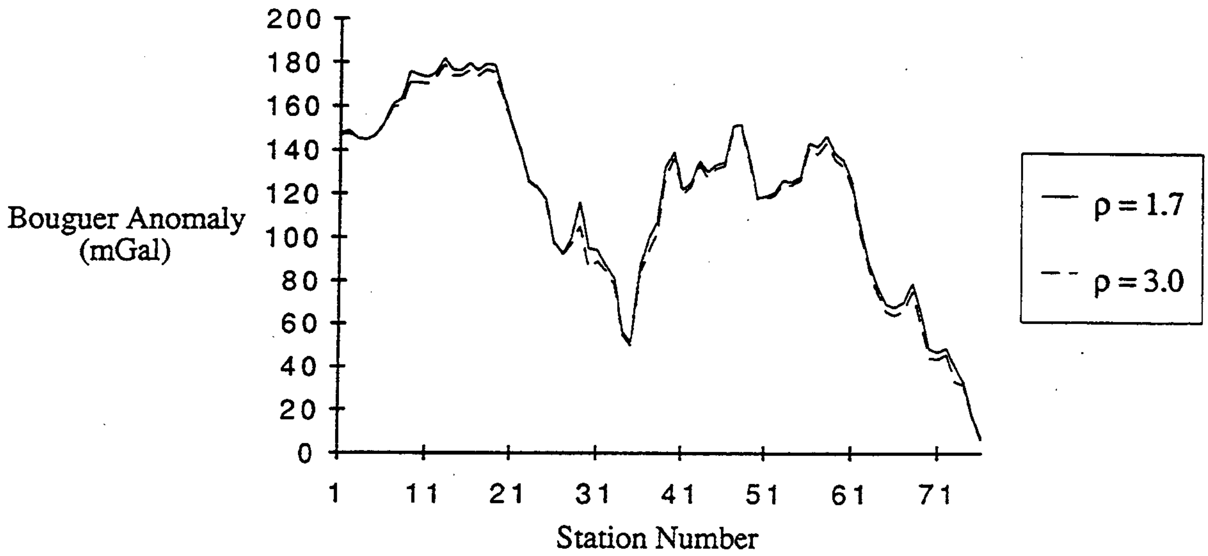

Figure 2.5 : Eastern Mindanao Gravity Profile.

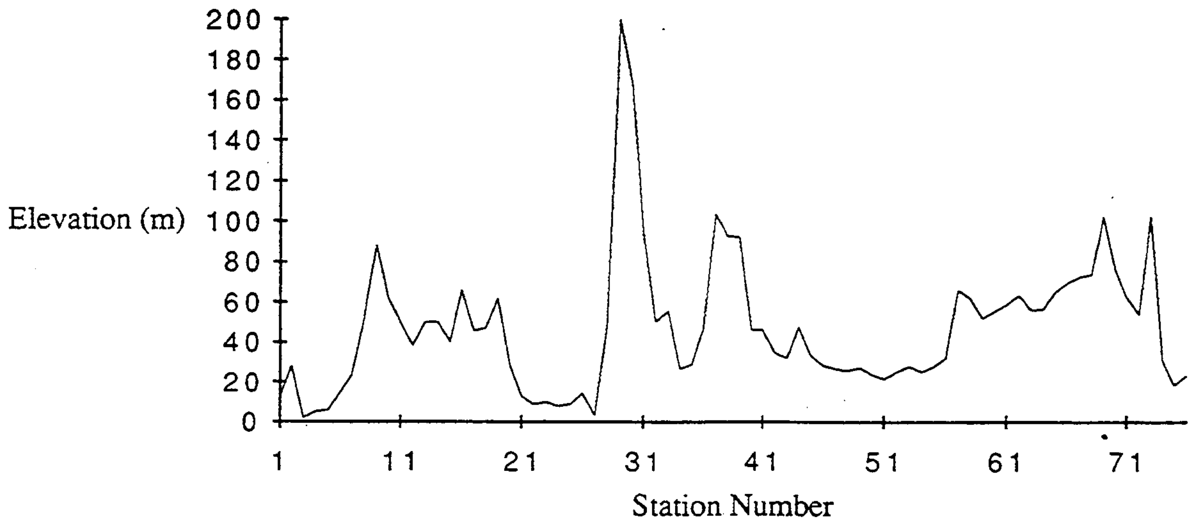

Figure 2.6 : Eastern Mindanao Topographic Profile.

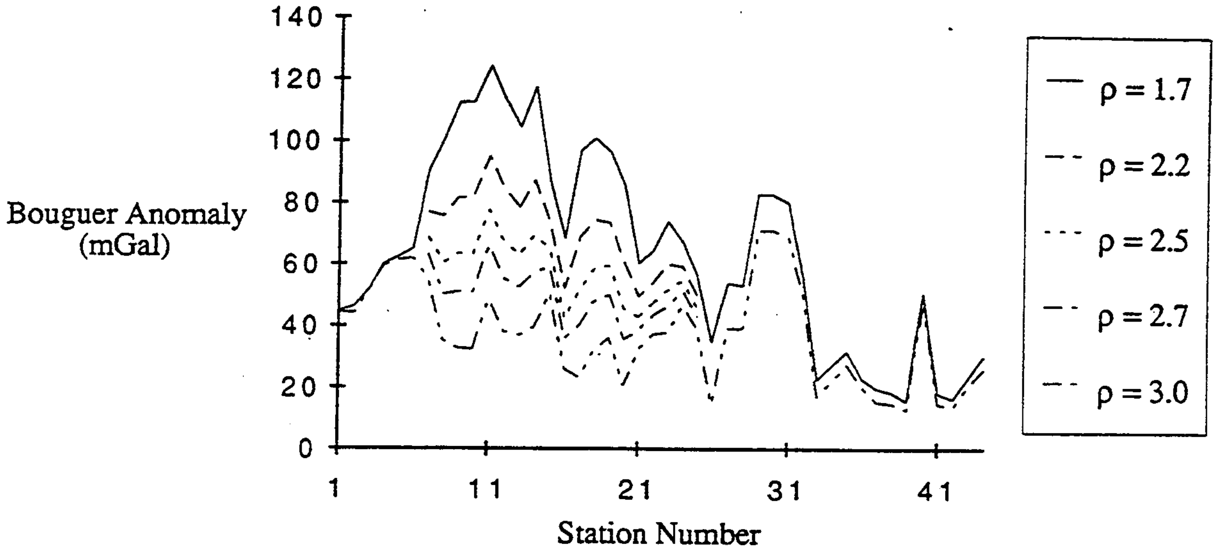

Figure 2.7 : Northern Luzon Gravity Profile.

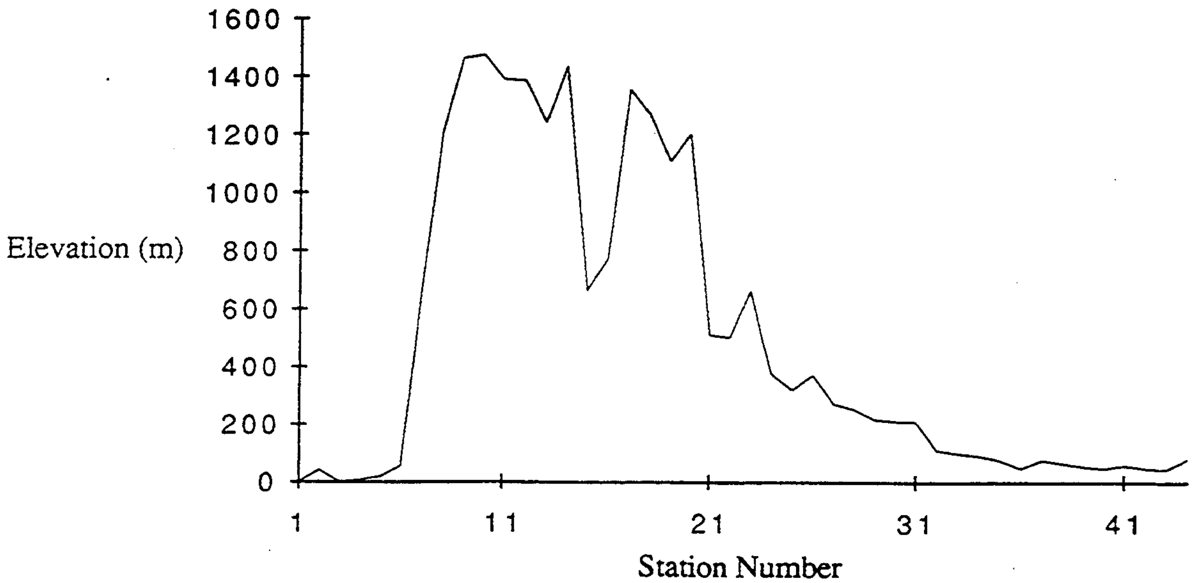

Figure 2.8 : Northern Luzon Topographic Profile.

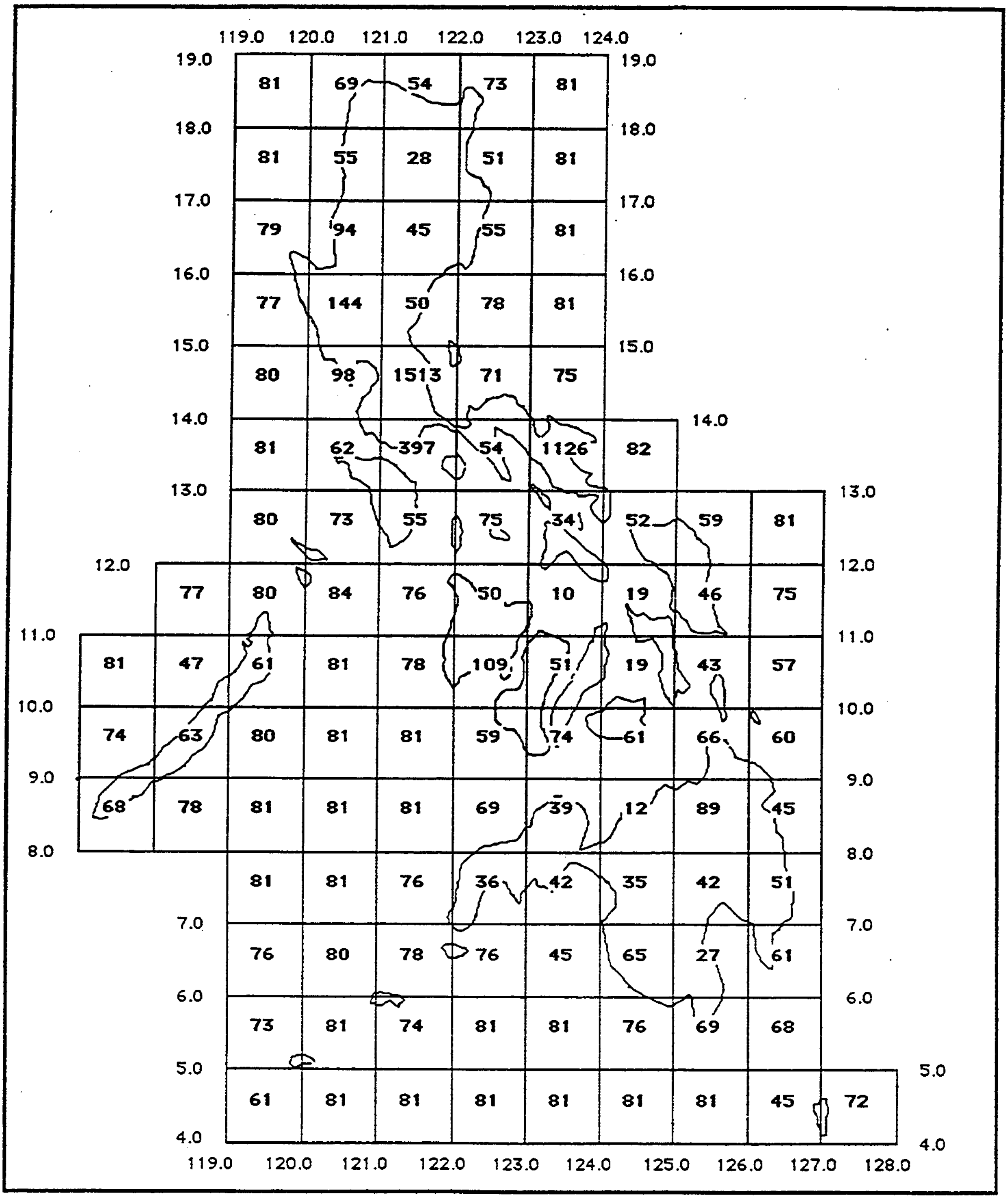

Figure 2.9 : Number of Sample Points in each of 1^0 block.

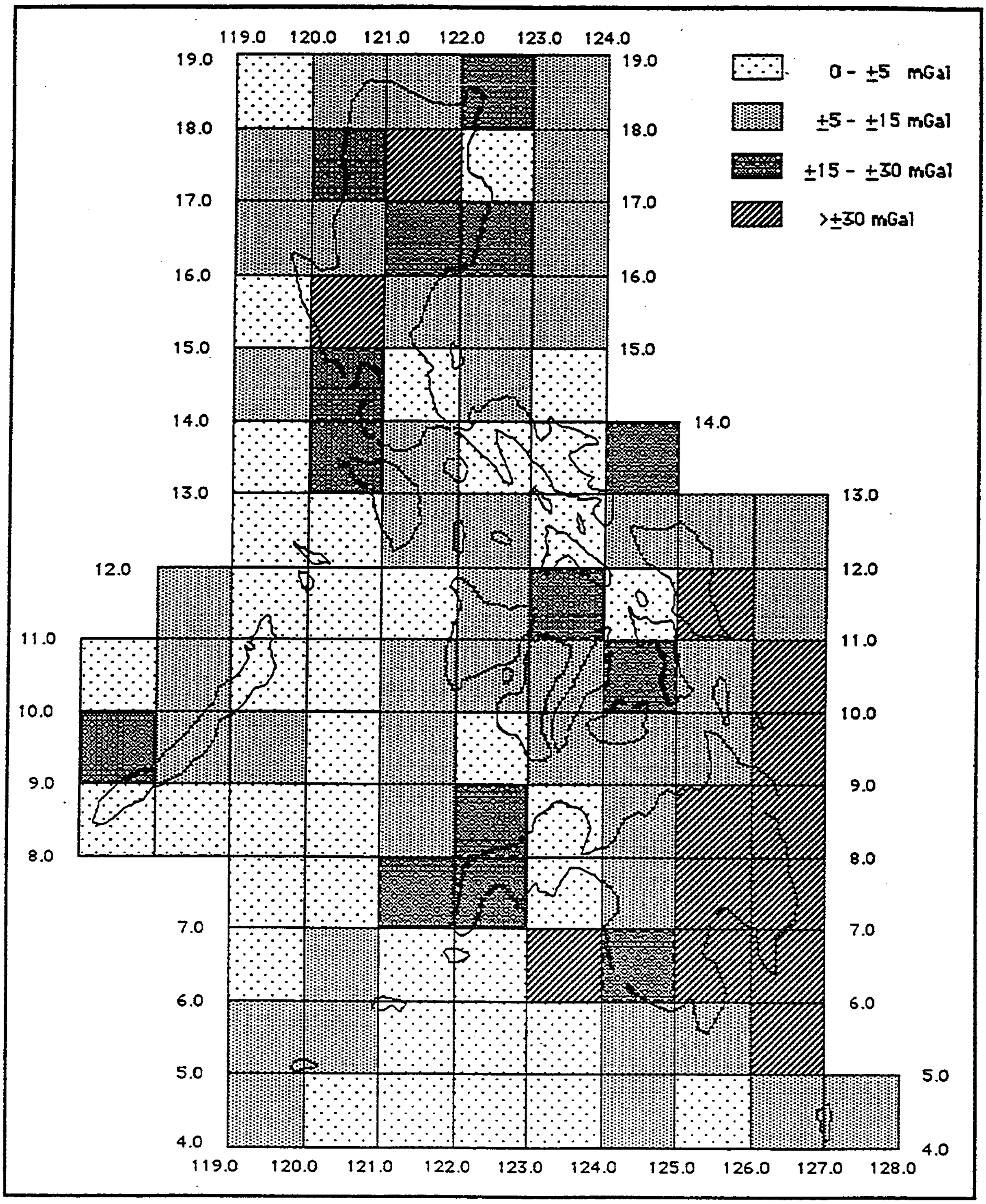

Figure 2.10 : Analysis of OSU86E (mean).

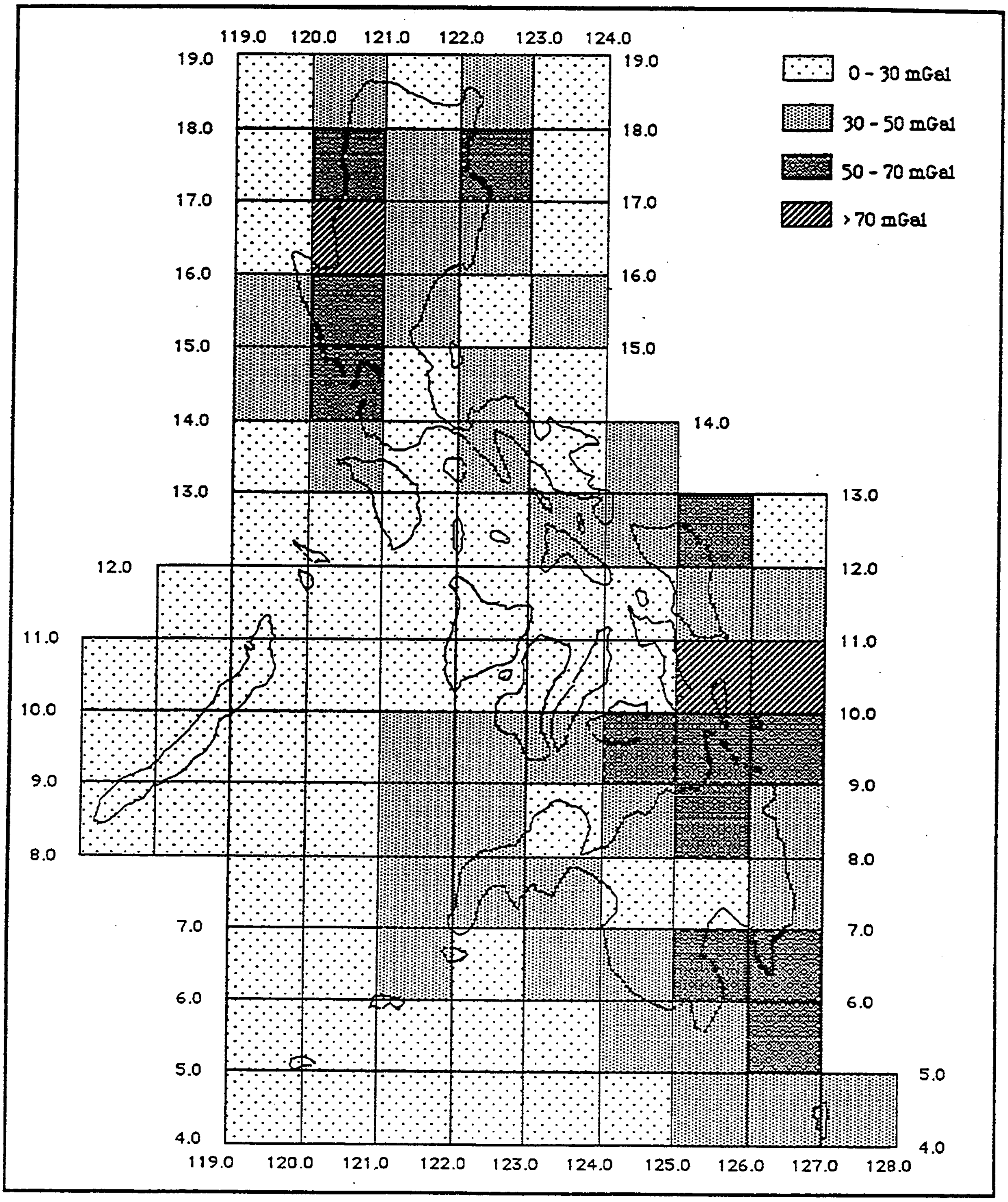

Figure 2.11 : Analysis of OSU86E (rms).

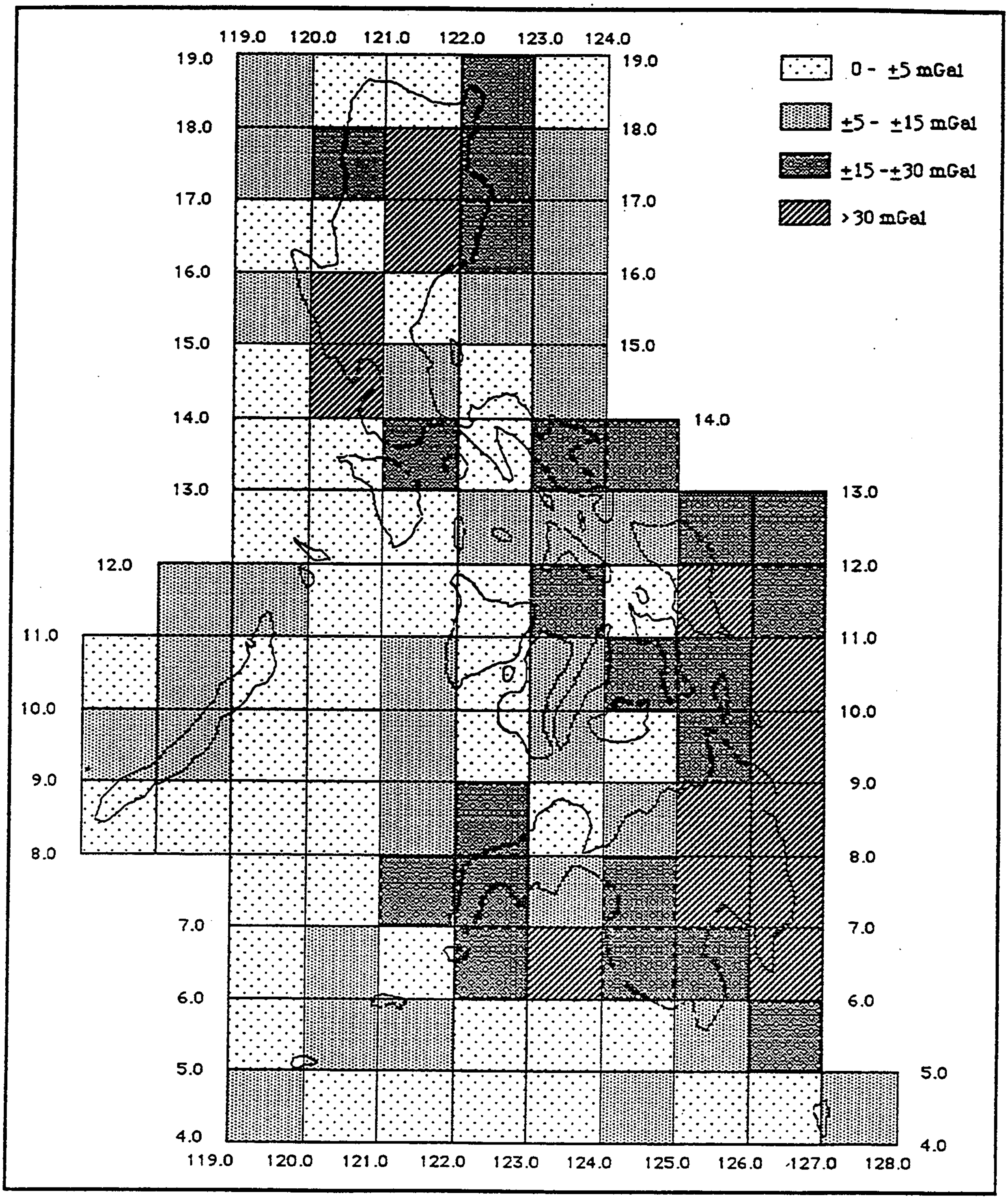

Figure 2.12 : Analysis of OSU89A (mean).

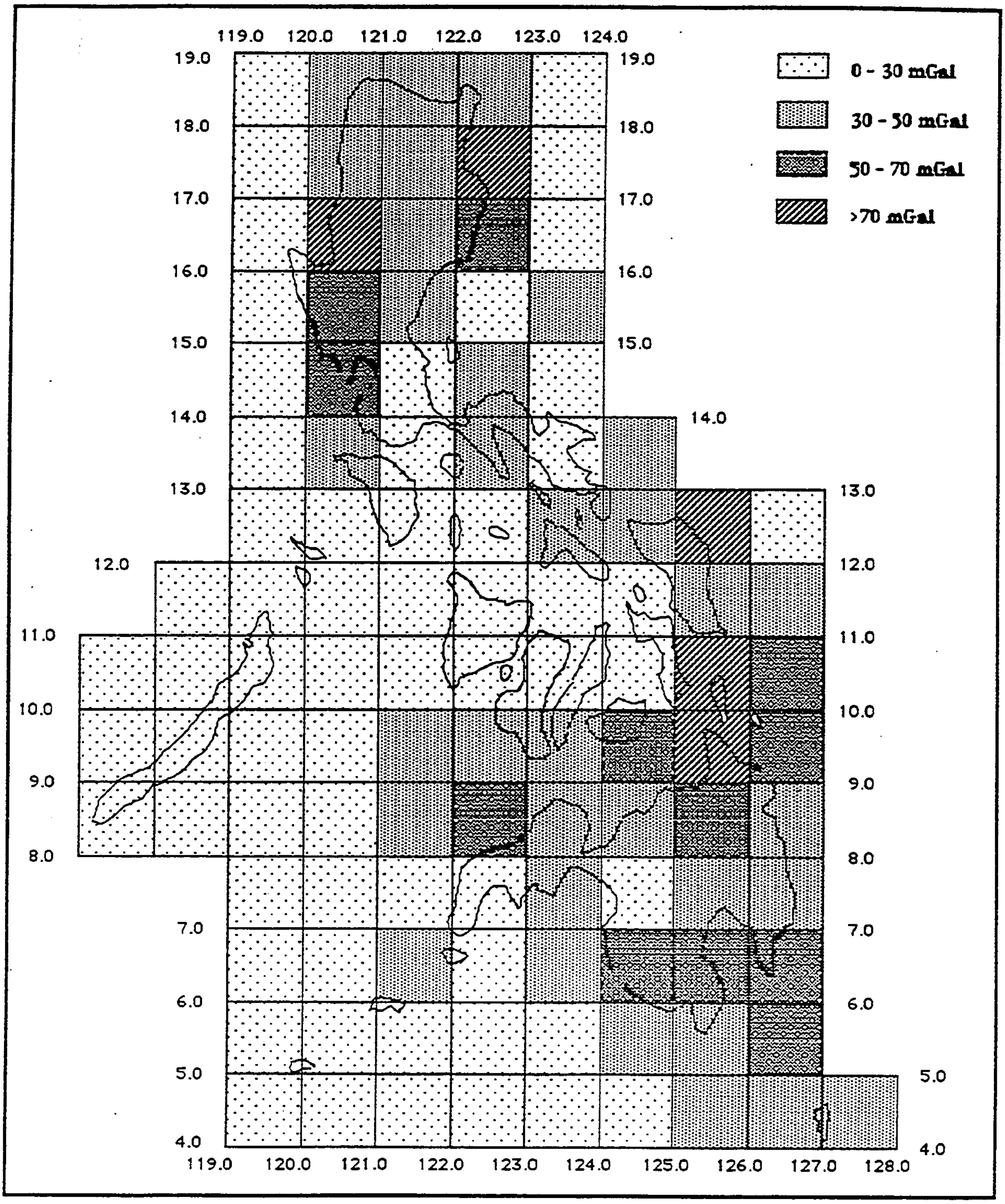

Figure 2.13 : Analysis of OSU89A (rms).

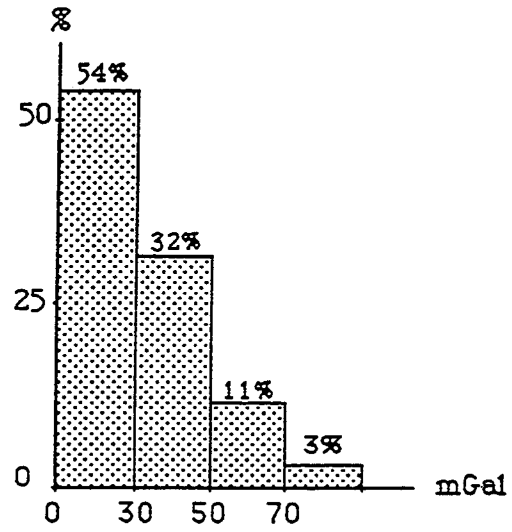

RMS OF OSU86E

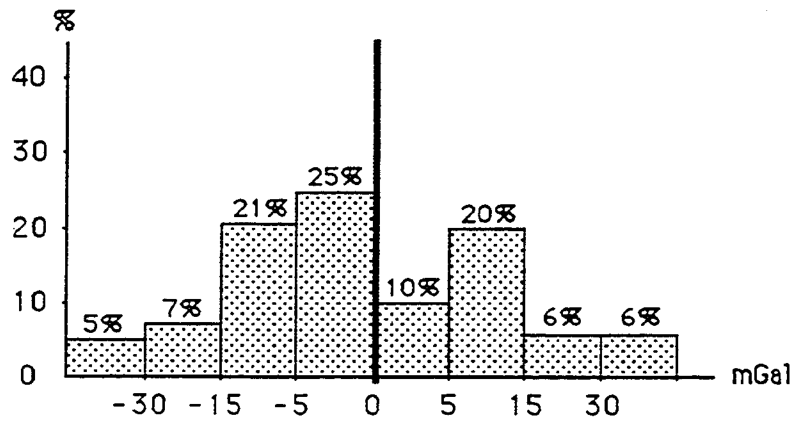

MEAN OF OSU86E

Figure 2.14 : Histogram of mean and rms from OSU86E.

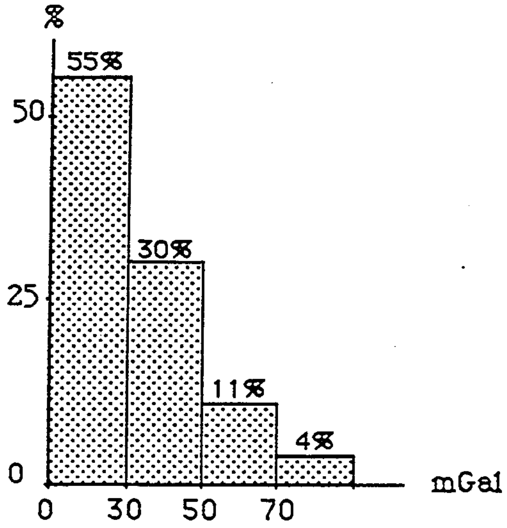

RMS OF OSU89A

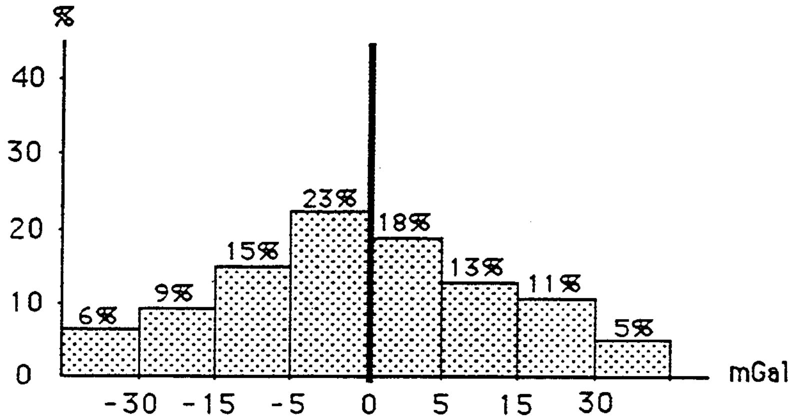

MEAN OF OSU89A

Figure 2.15 : Histogram of mean and rms from OSU89A.

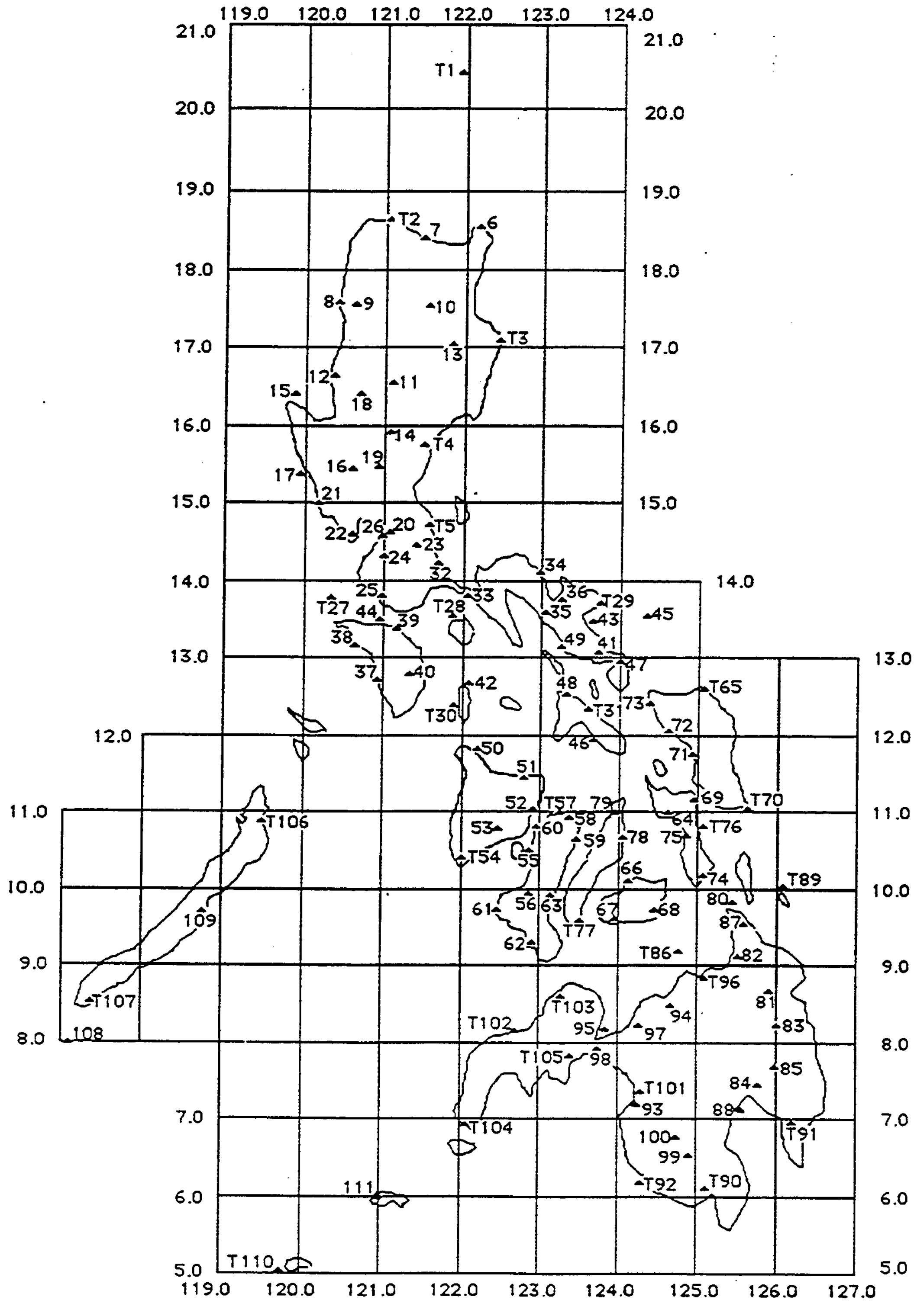

Figure 2.16 : GPS Height Control Points in the Philippines.

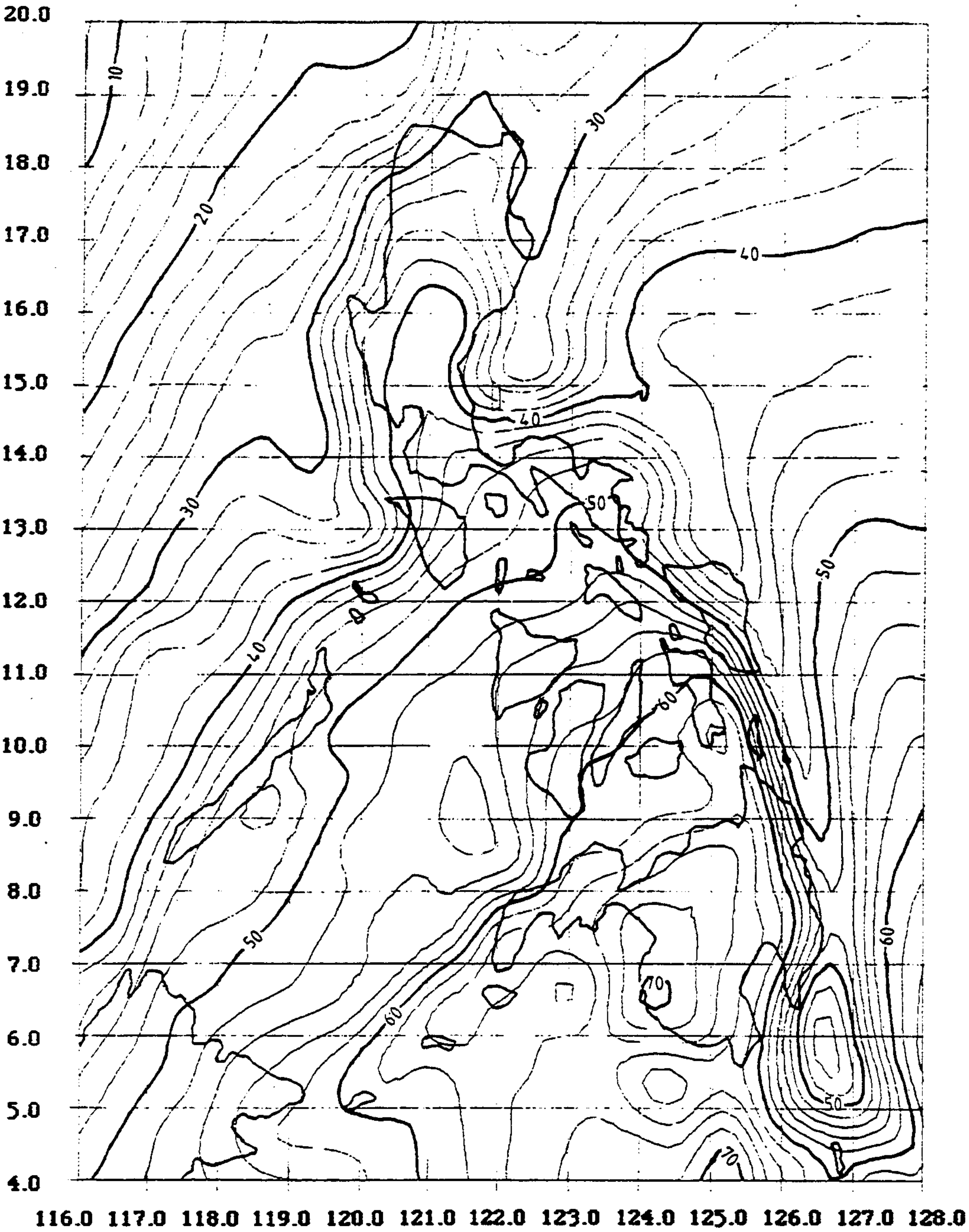

Figure 3.1 : Geoid Map of OSU86E.

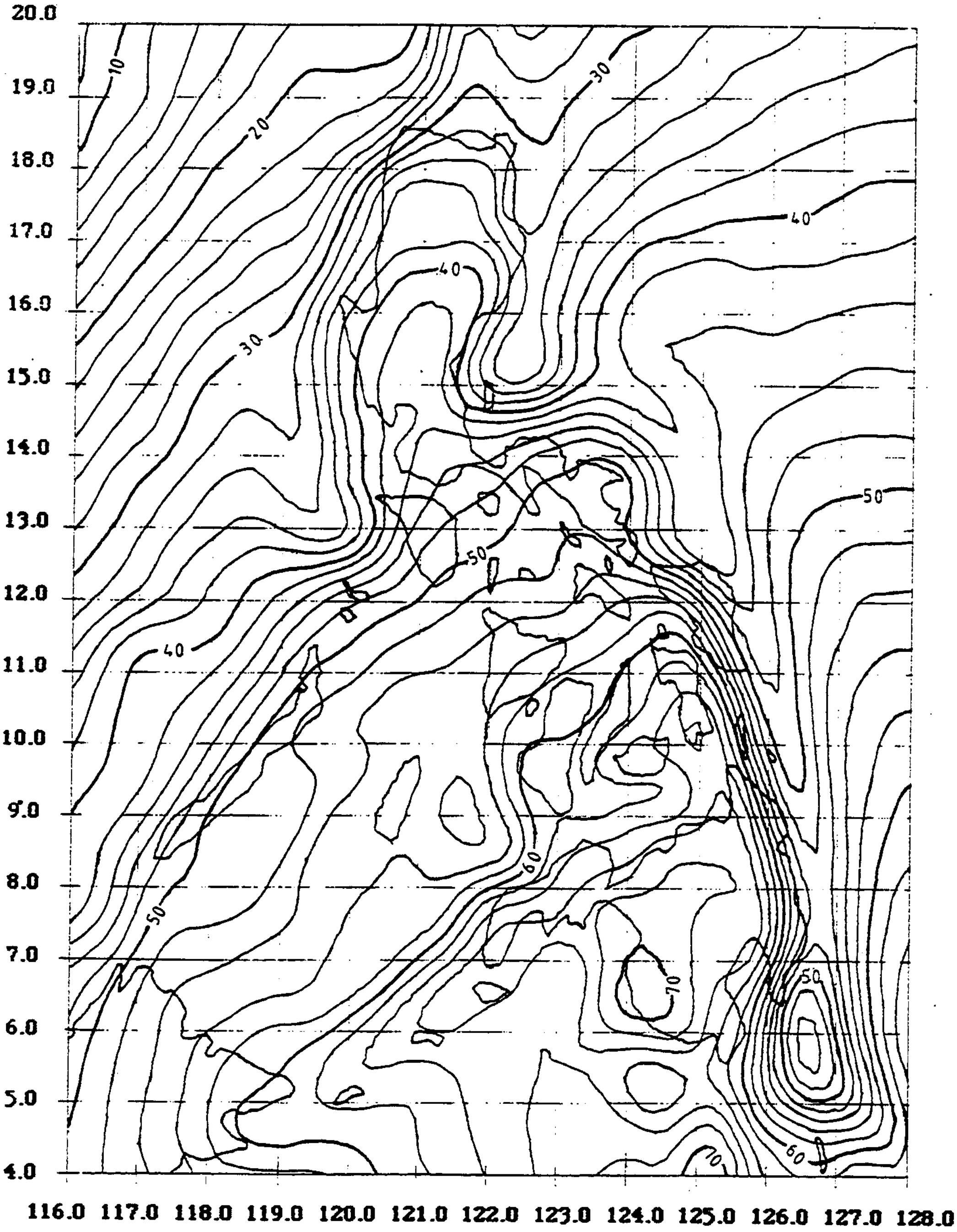

Figure 3.2 : Geoid Map of OSU89A.

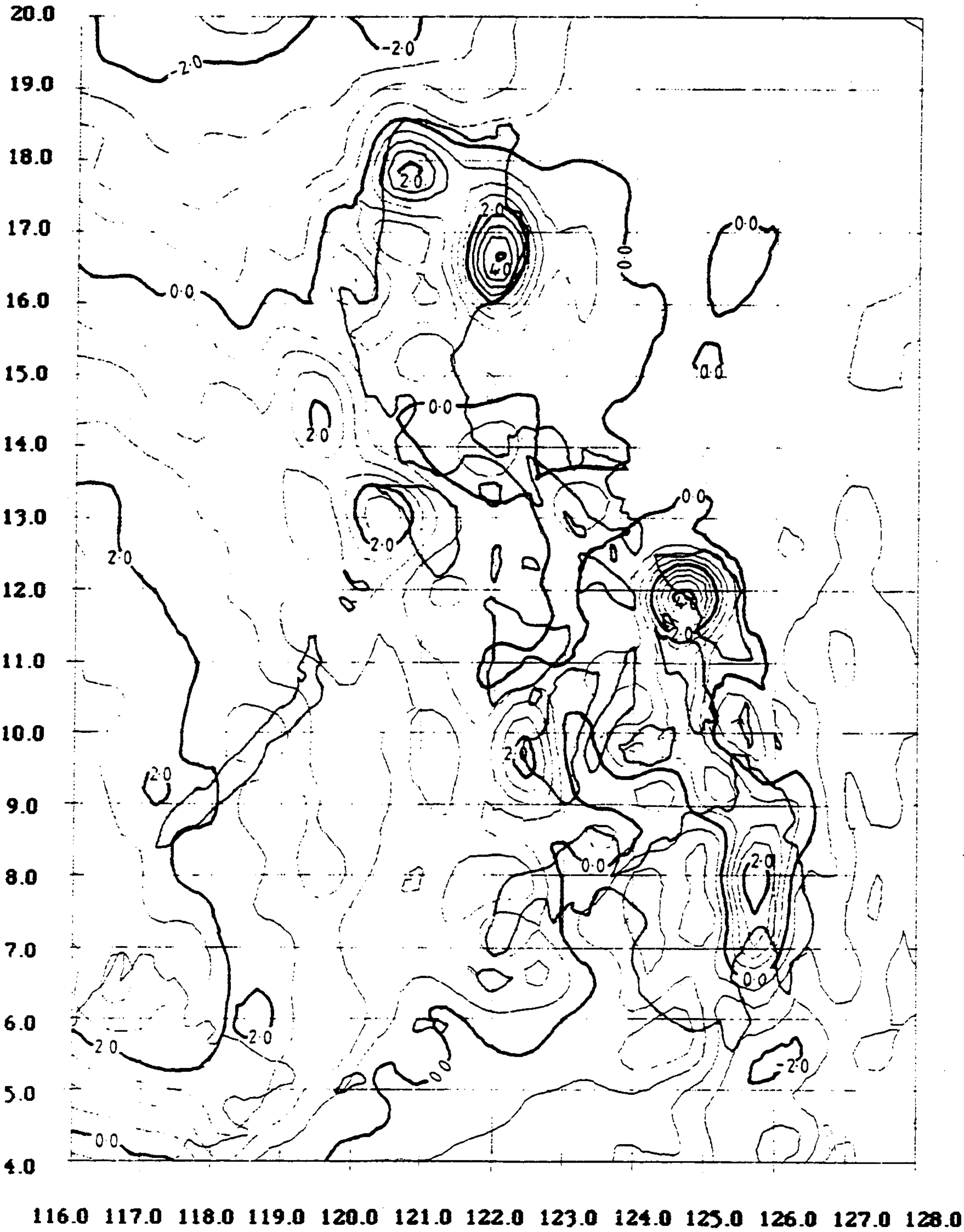

Figure 3.3 : Differences between OSU86E and OSU89A.

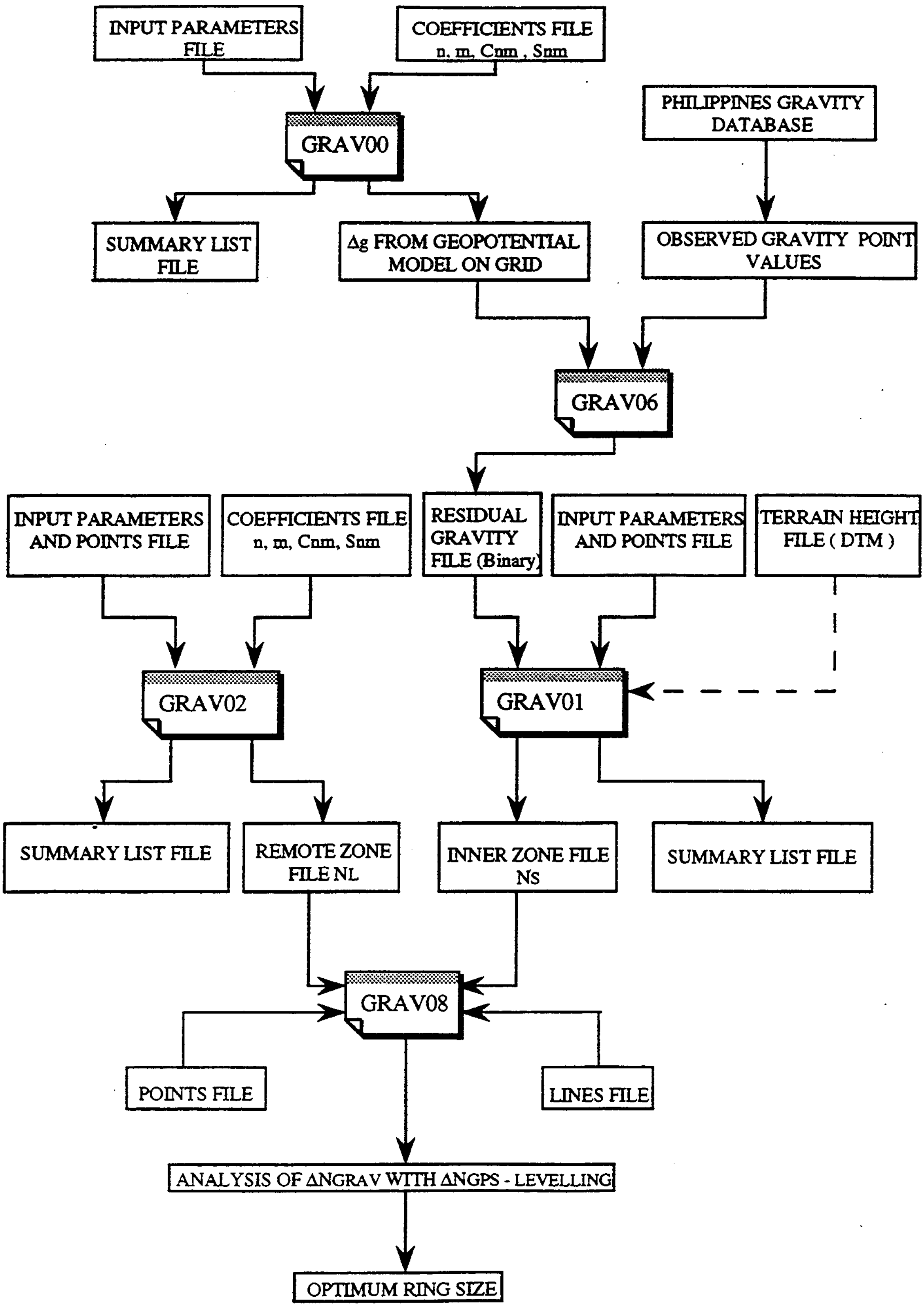

Figure 3.4 : Flowchart of gravity programs.

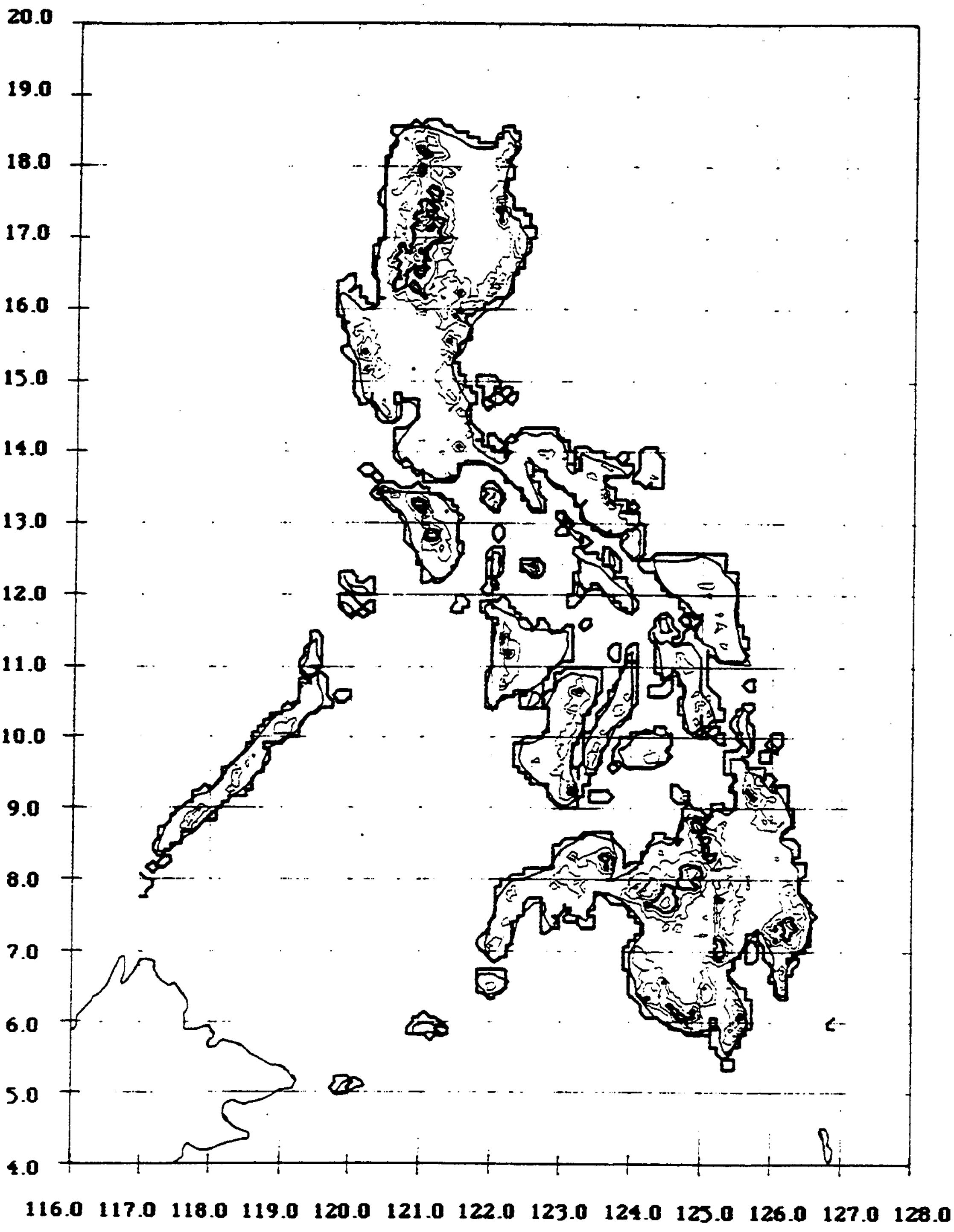

Figure 3.5 : Topography of Philippines using DEM.

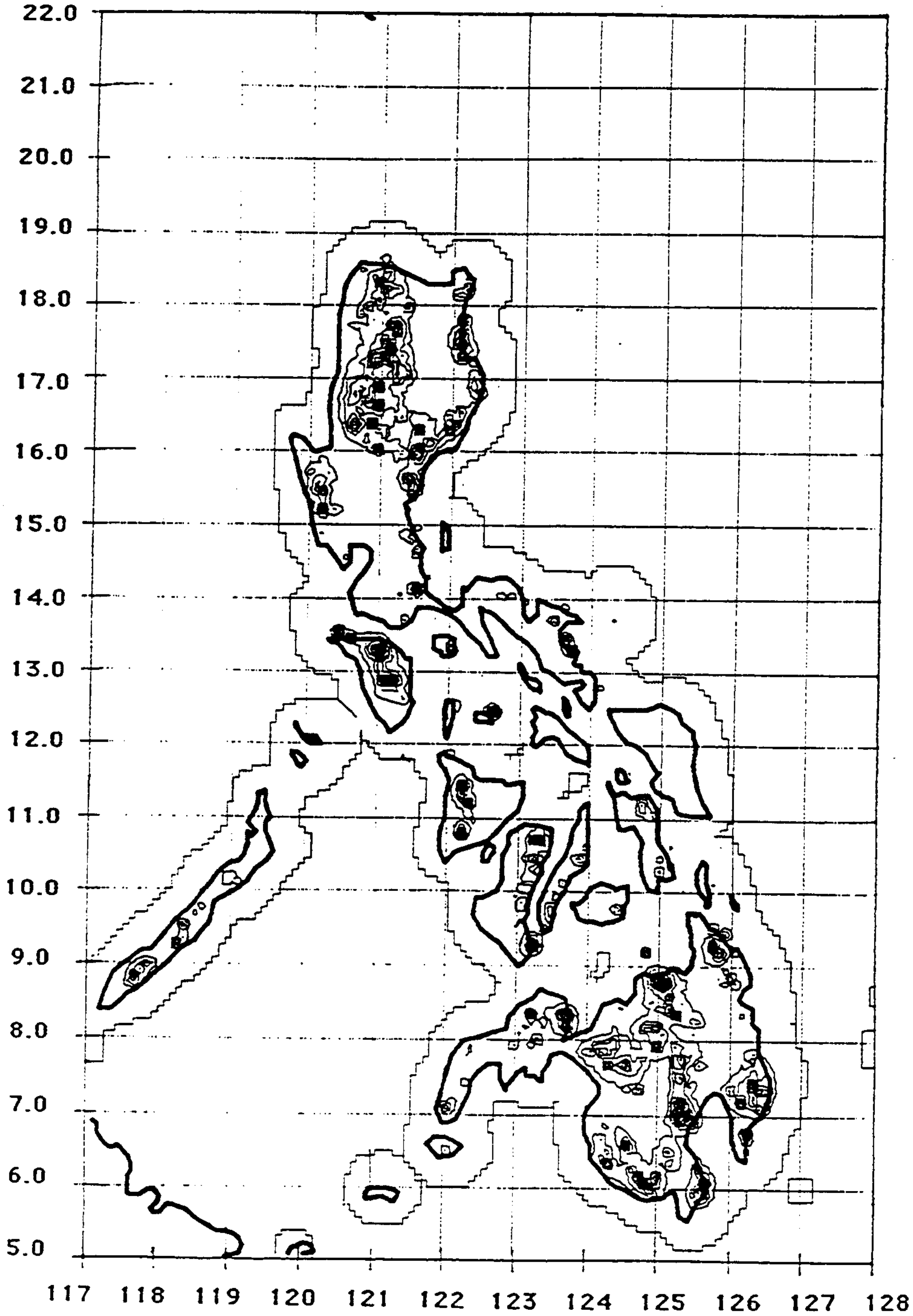

Figure 3.6 : Terrain Correction .

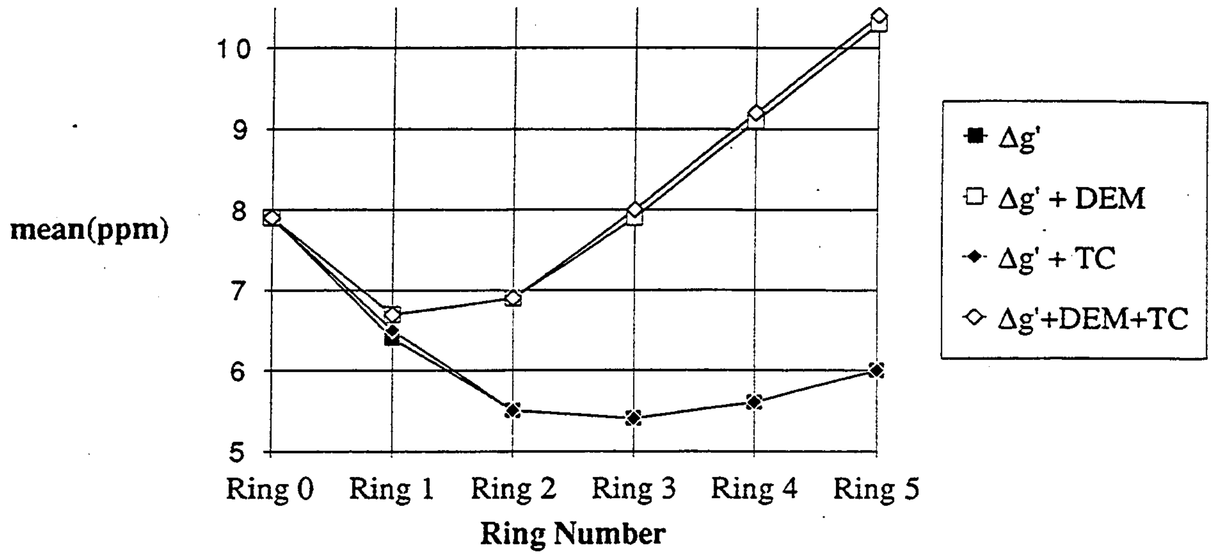

Figure 3.7 : Optimum Data Set - Mean Line Chart.

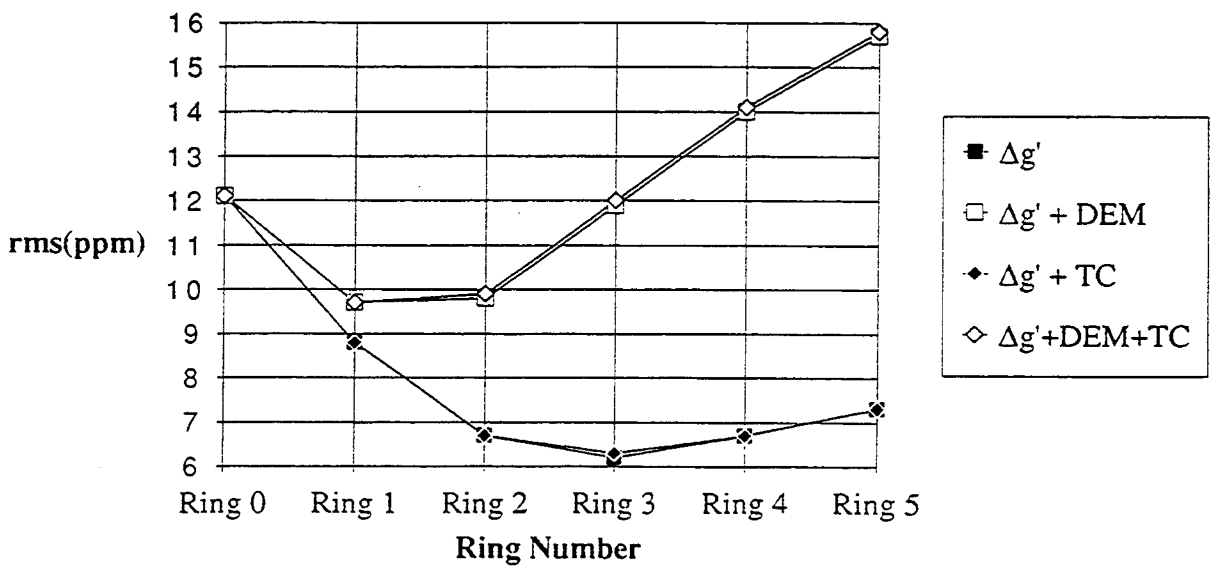

Figure 3.8 : Optimum Data Set - rms Line Chart.

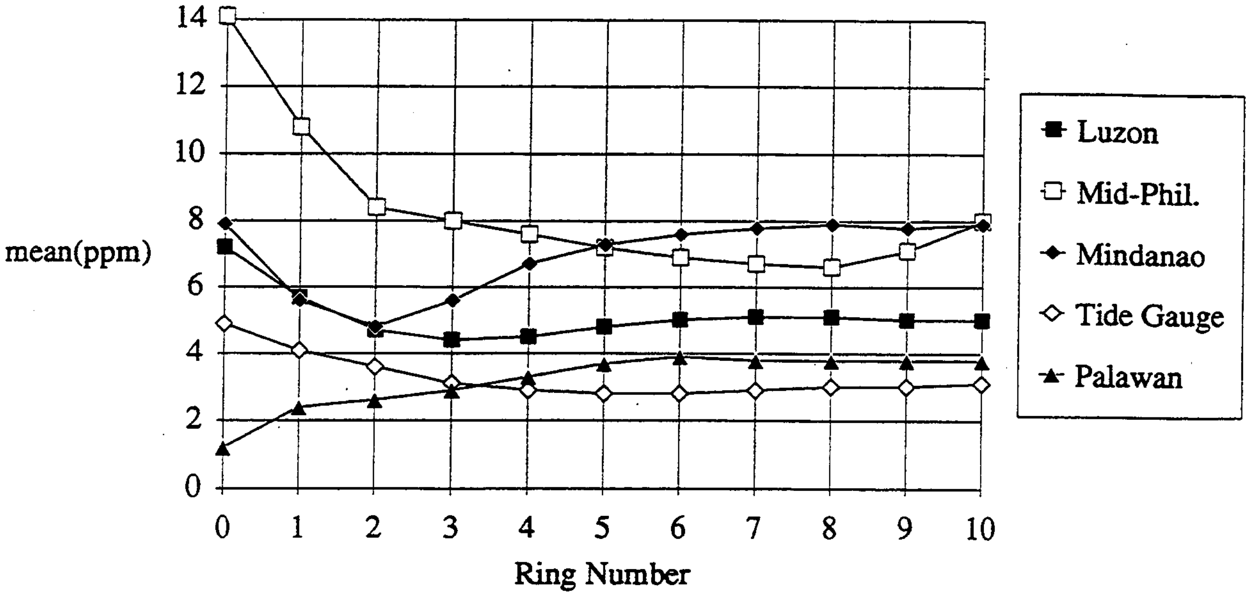

Figure 3.9 : Optimum Cap Size - Mean Line Chart.

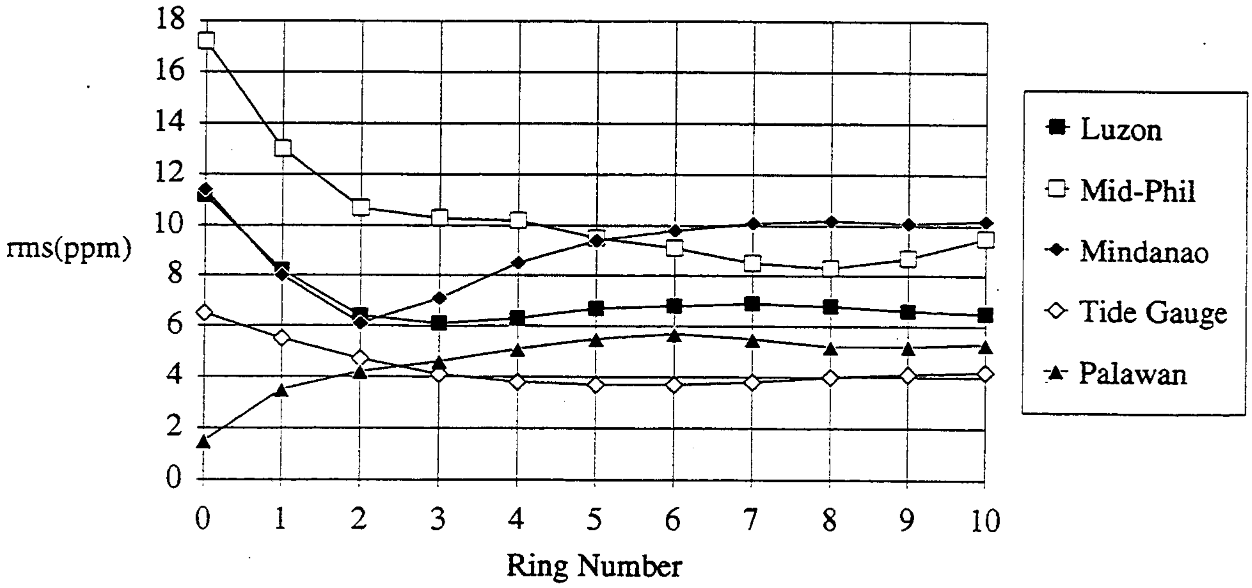

Figure 3.10 : Optimum Cap Size - rms Line Chart.

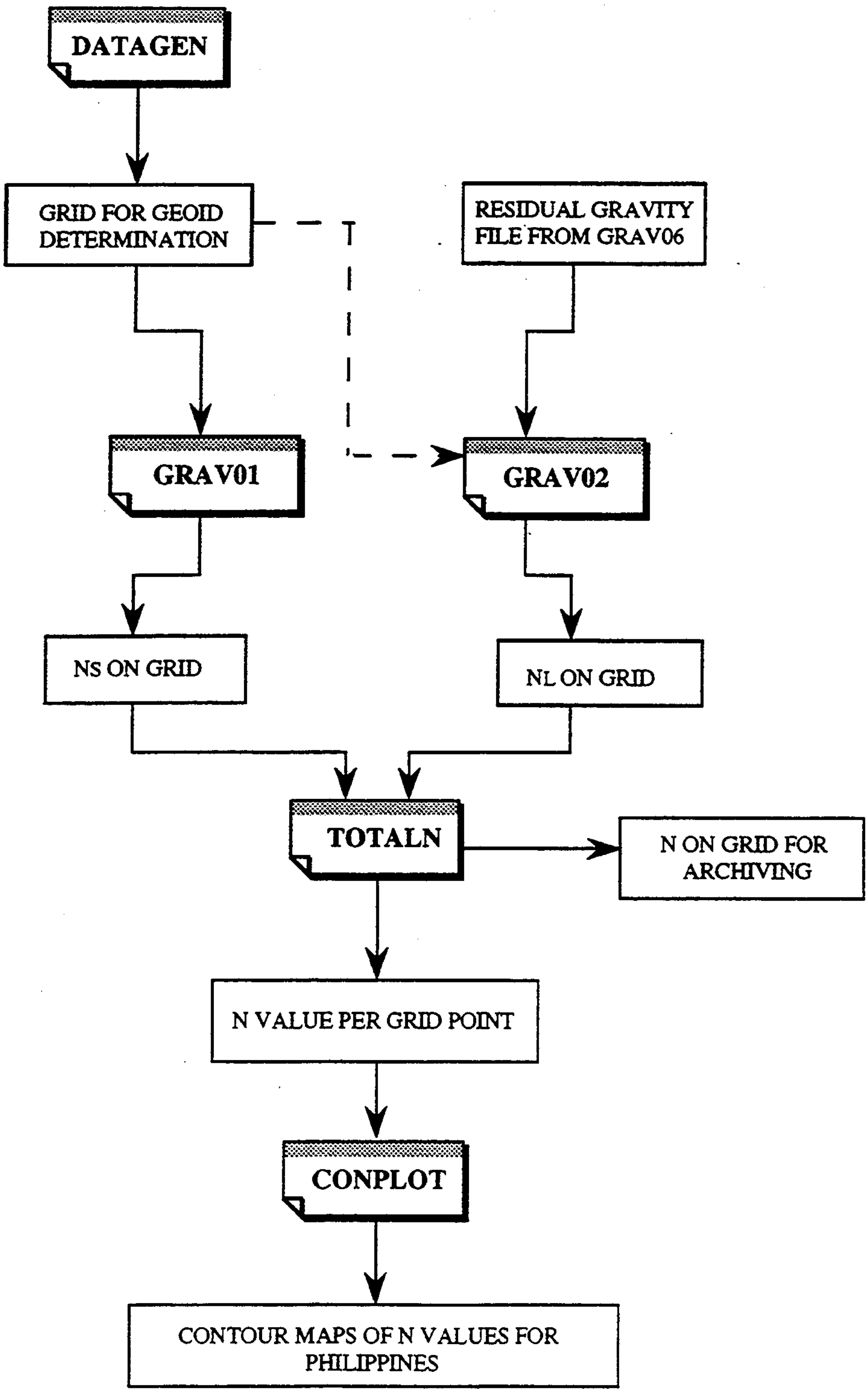

Figure 3.11 : Flowchart for geoid determination on grid.

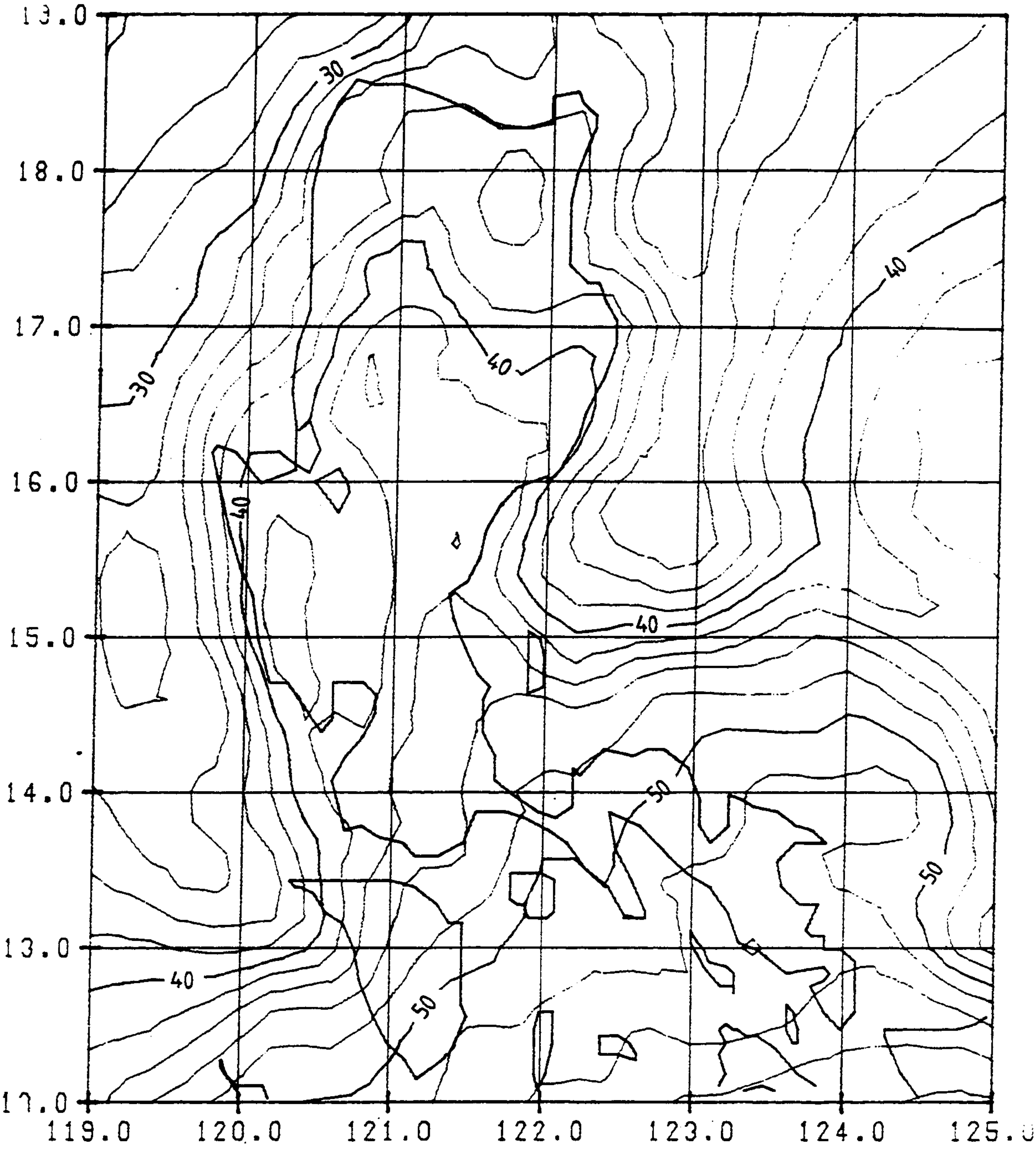

Figure 3.12 : Detailed Geoid of Northern Philippines.

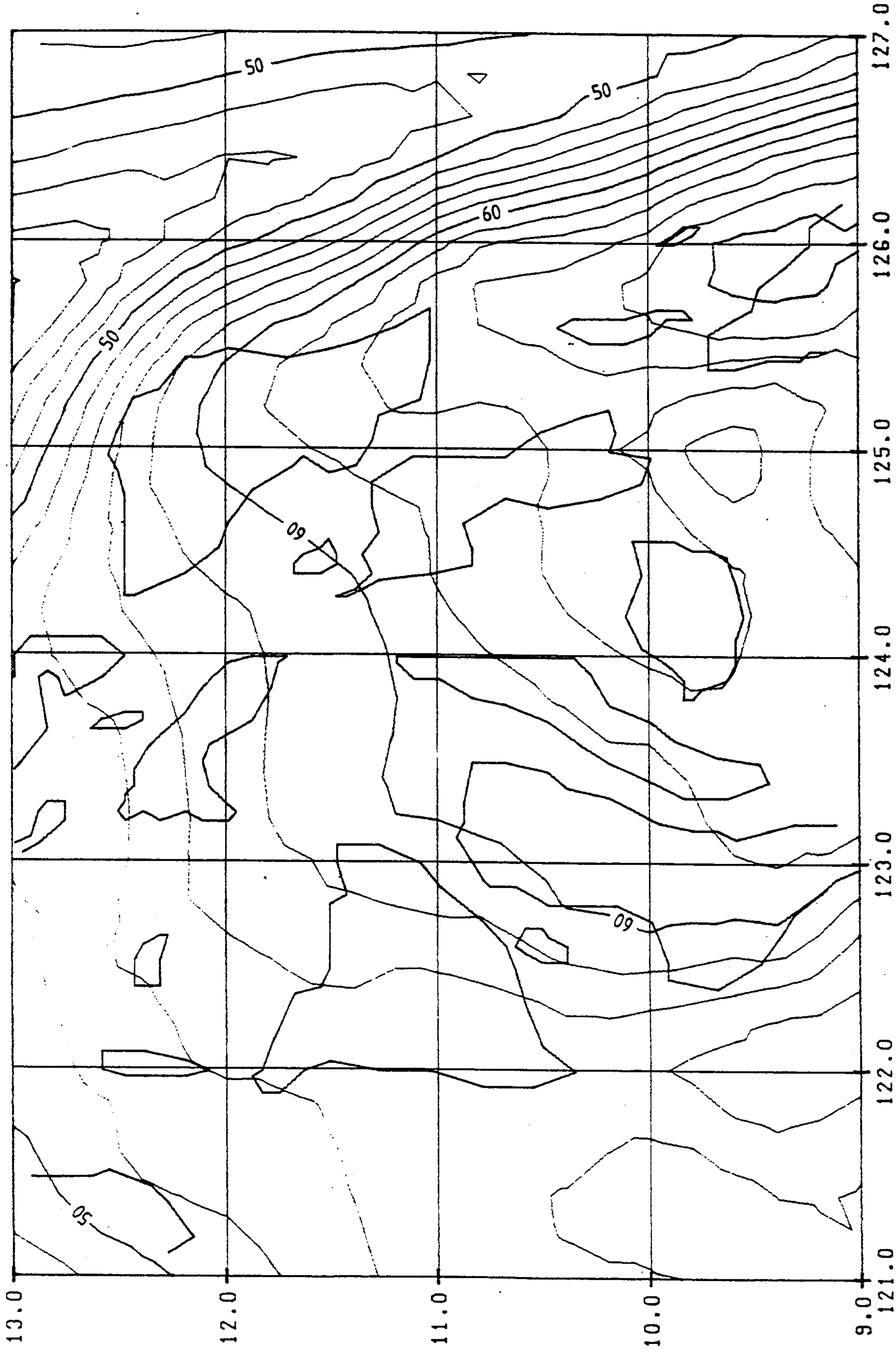

Figure 3.13 : Detailed Geoid of Mid- Philippines.

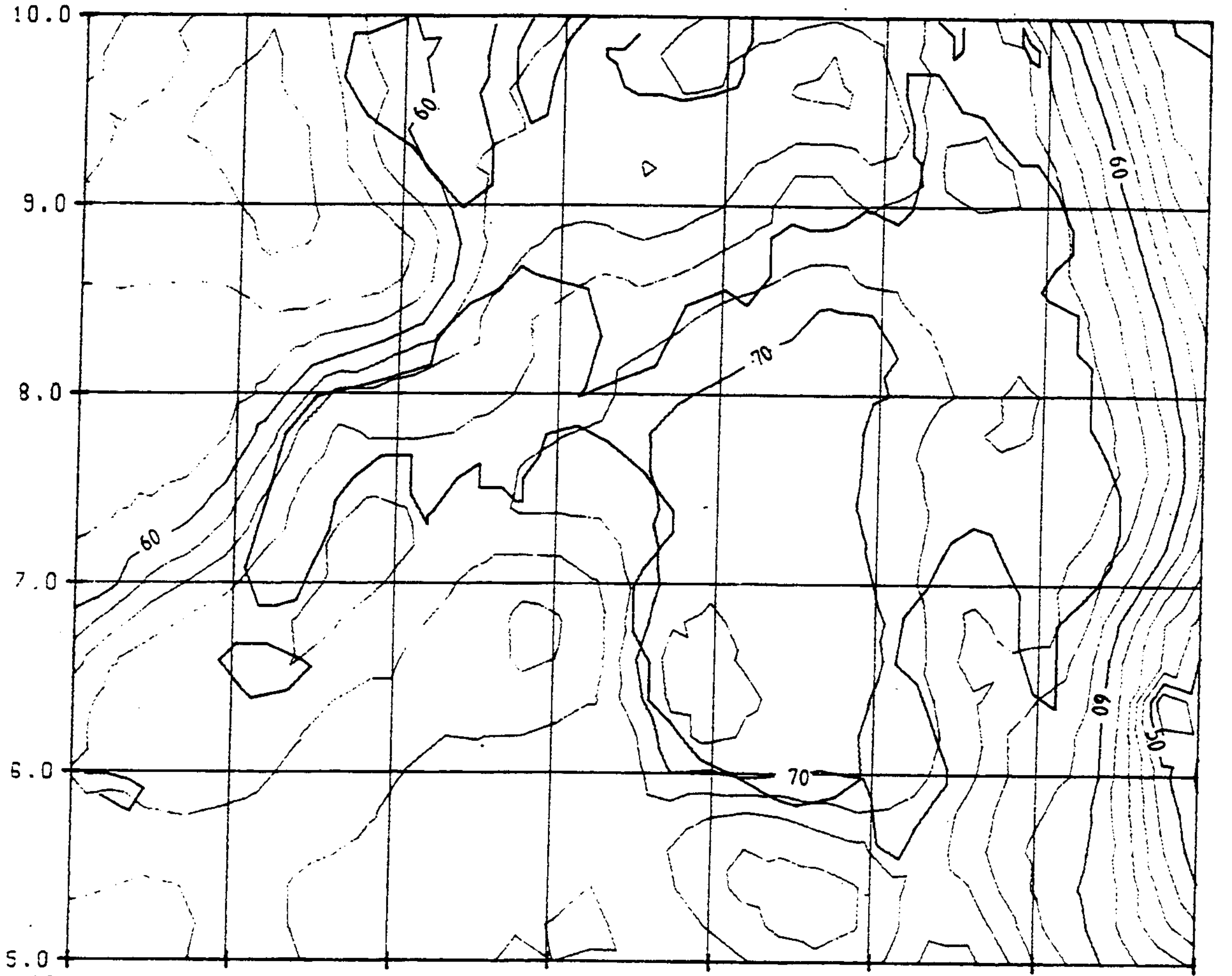

Figure 3.14 : Detailed Geoid of Southern Philippines.

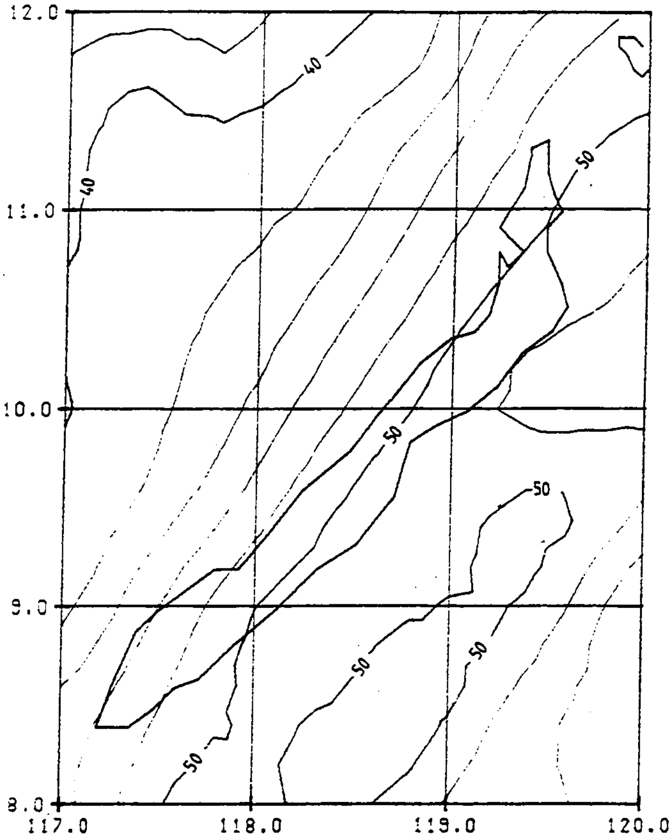

Figure 3.15 : Detailed Geoid of Palawan.

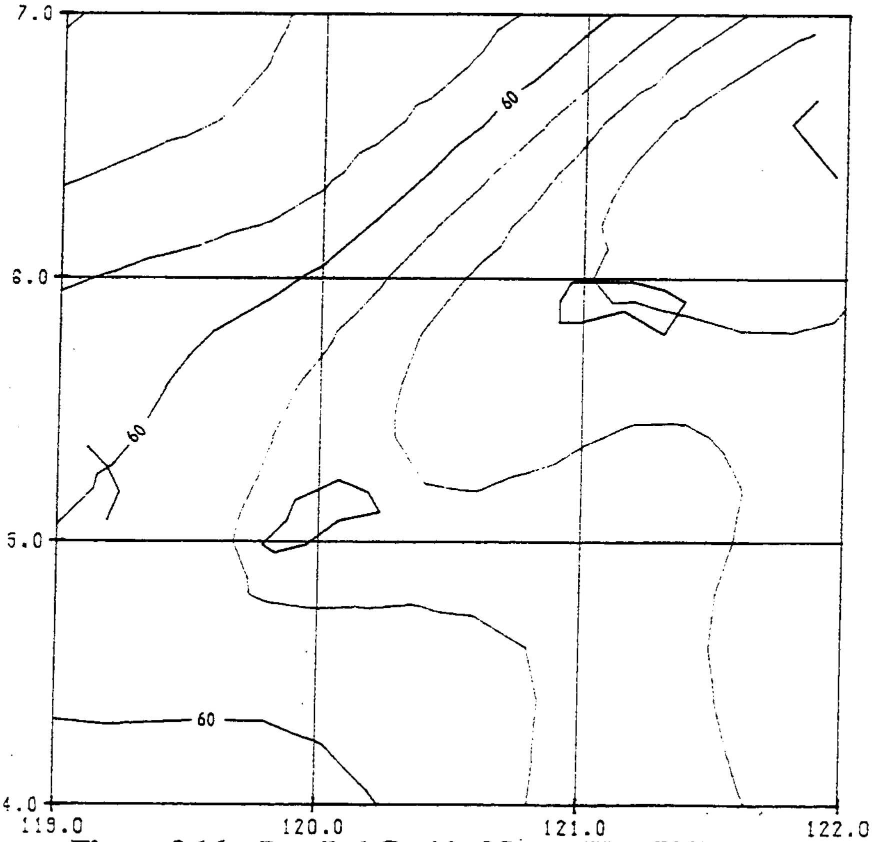

Figure 3.16 : Detailed Geoid of South West Philippines.

Figure 3.17 : N_{Grav} - $N_{GPS/Lev.}$ (including all points).

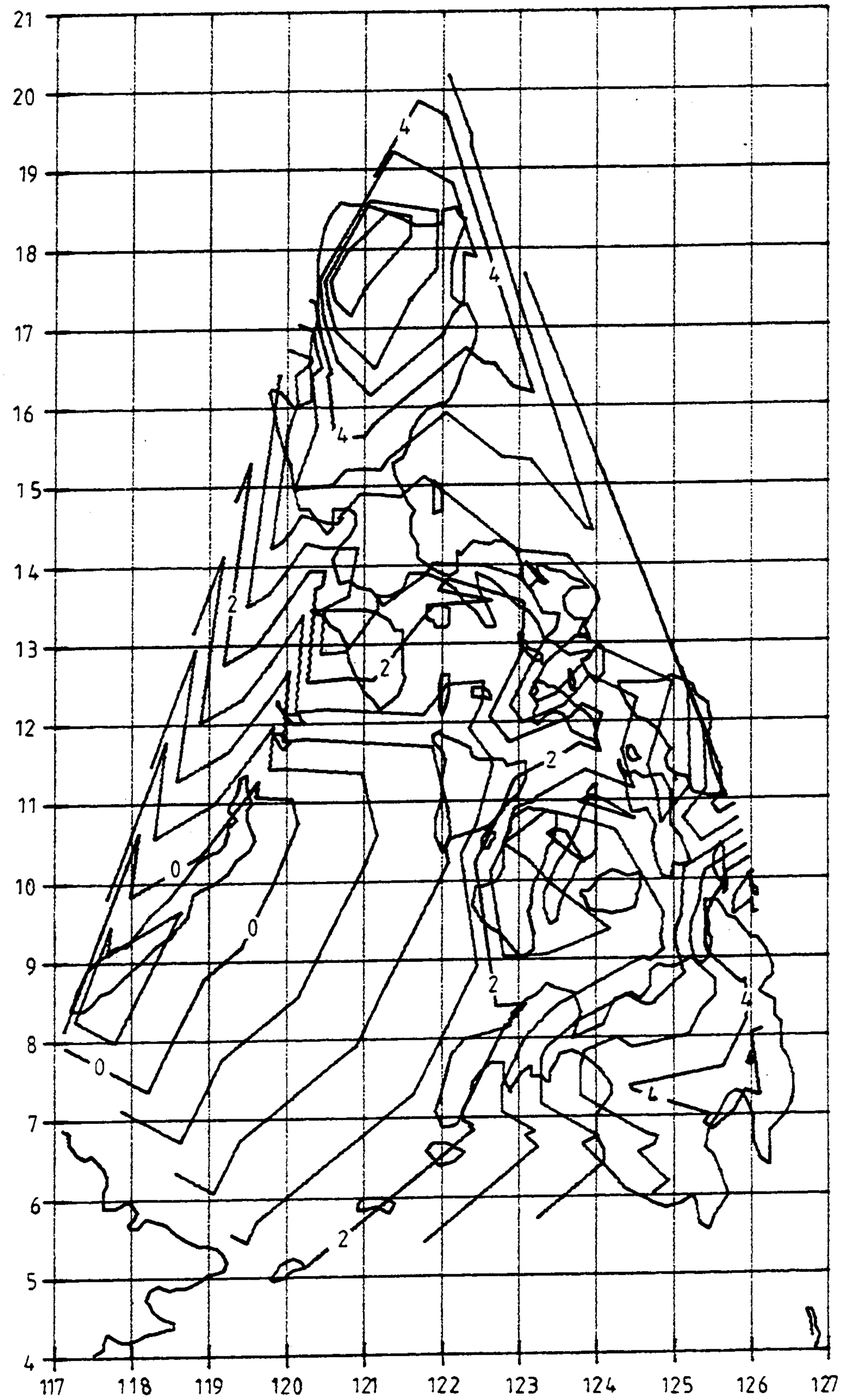

Figure 3.18 : N_{Grav} - $N_{GPS/Lev.}$ (excluding outliers).

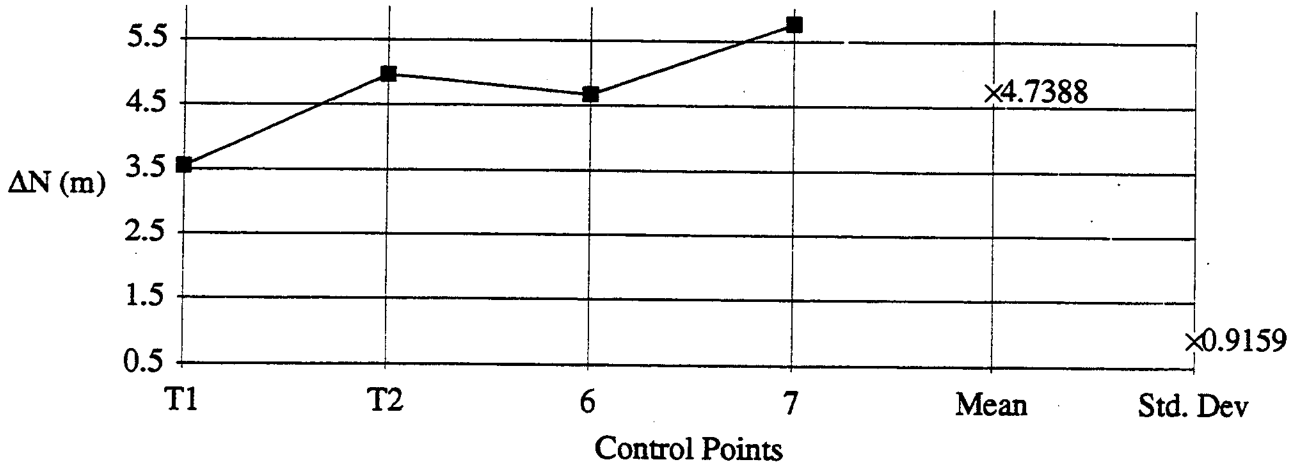

Figure 4.1 : ΔN profile for northern Luzon.

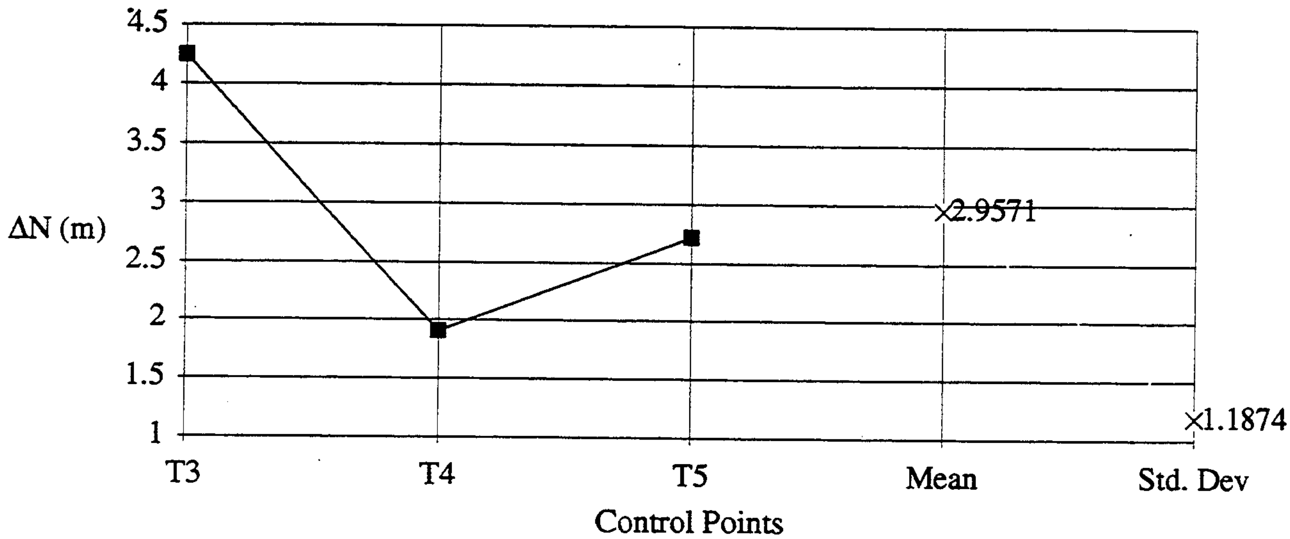

Figure 4.2 : ΔN profile for eastern Luzon.

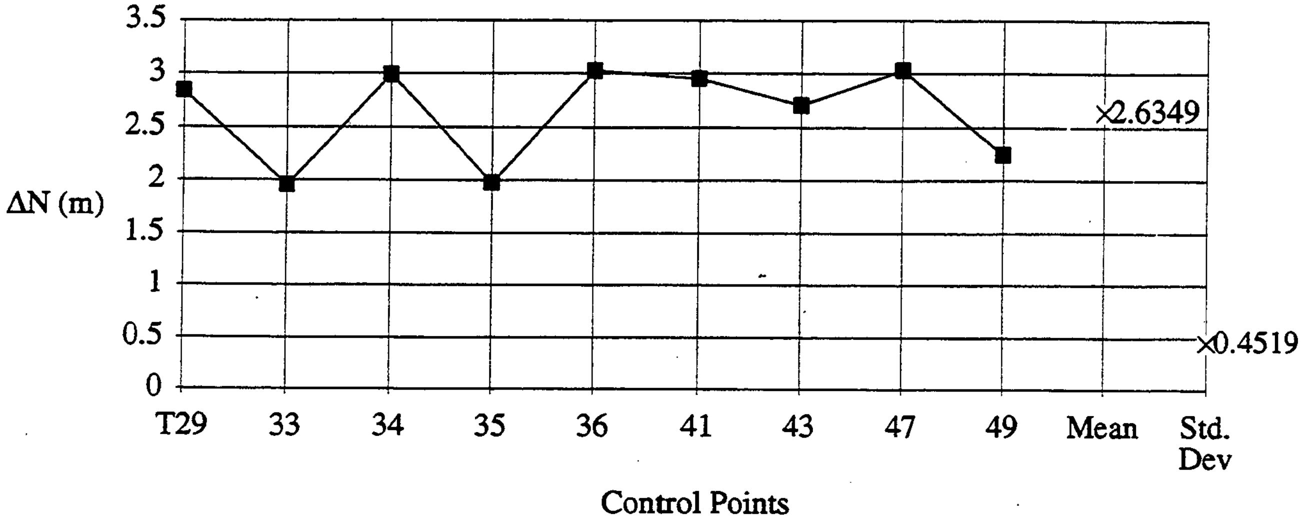

Figure 4.3 : ΔN profile for southern Luzon.

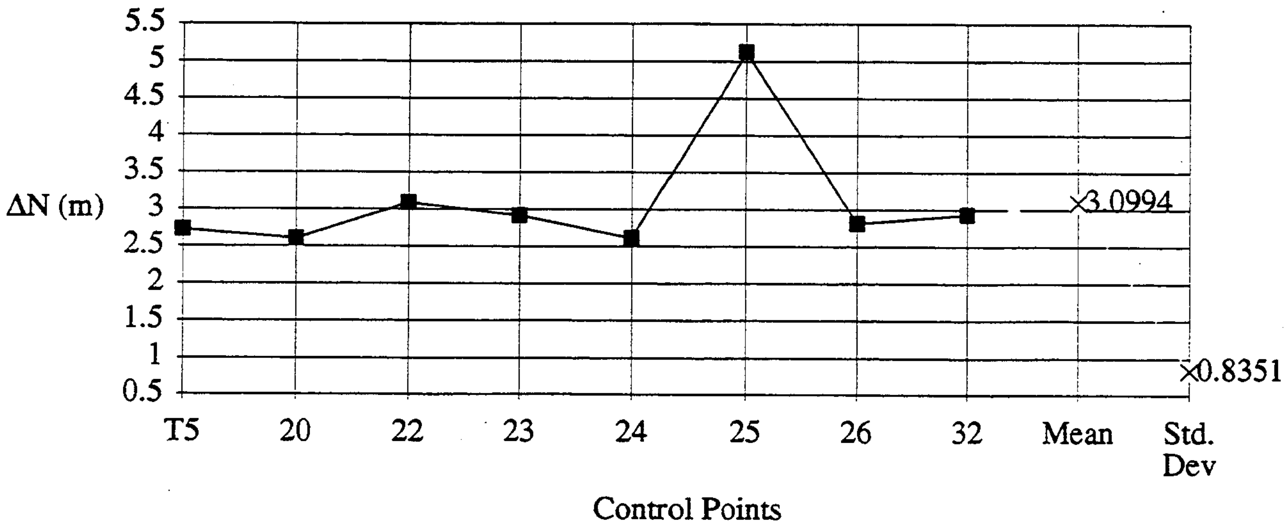

Figure 4.4 : ΔN profile for mid of Luzon.

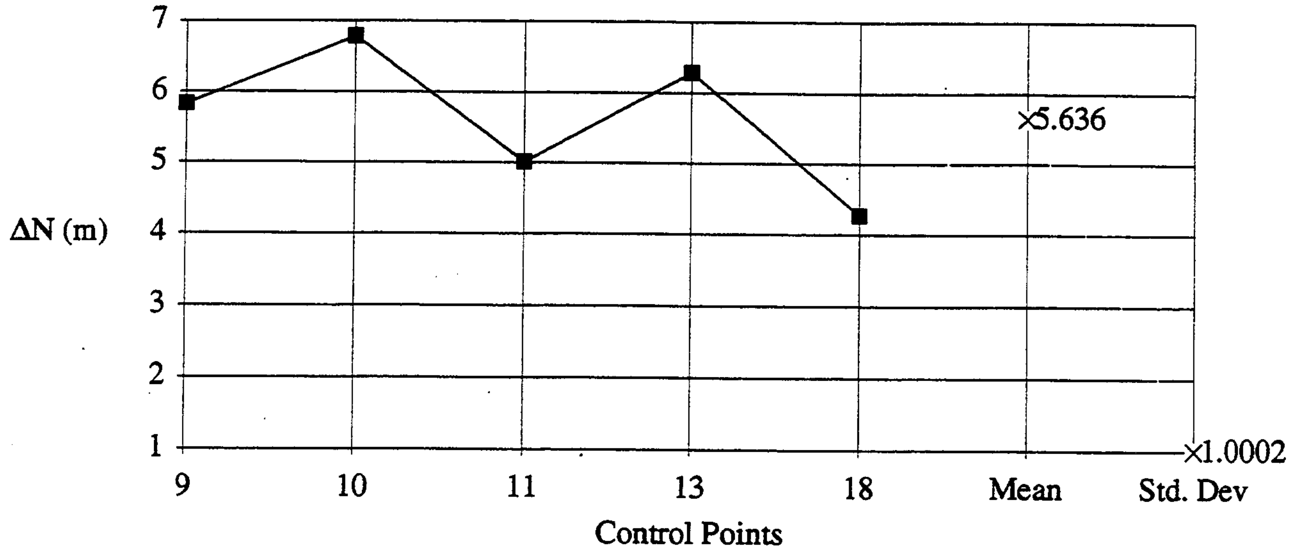

Figure 4.5 : ΔN profile for central north of Luzon.

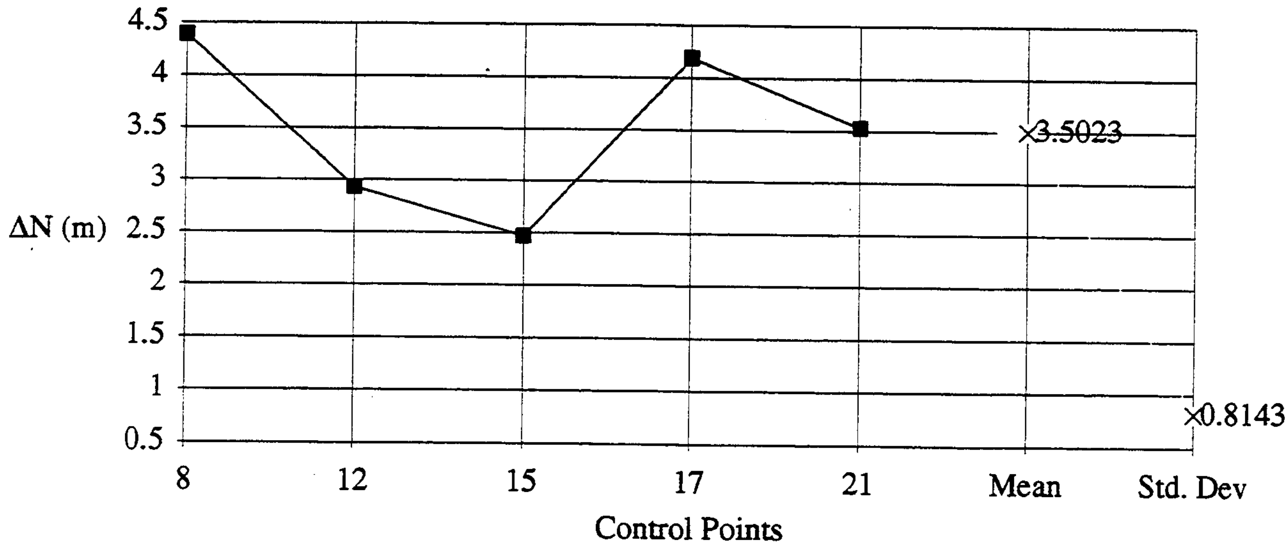

Figure 4.6 : ΔN profile for west coast Luzon.

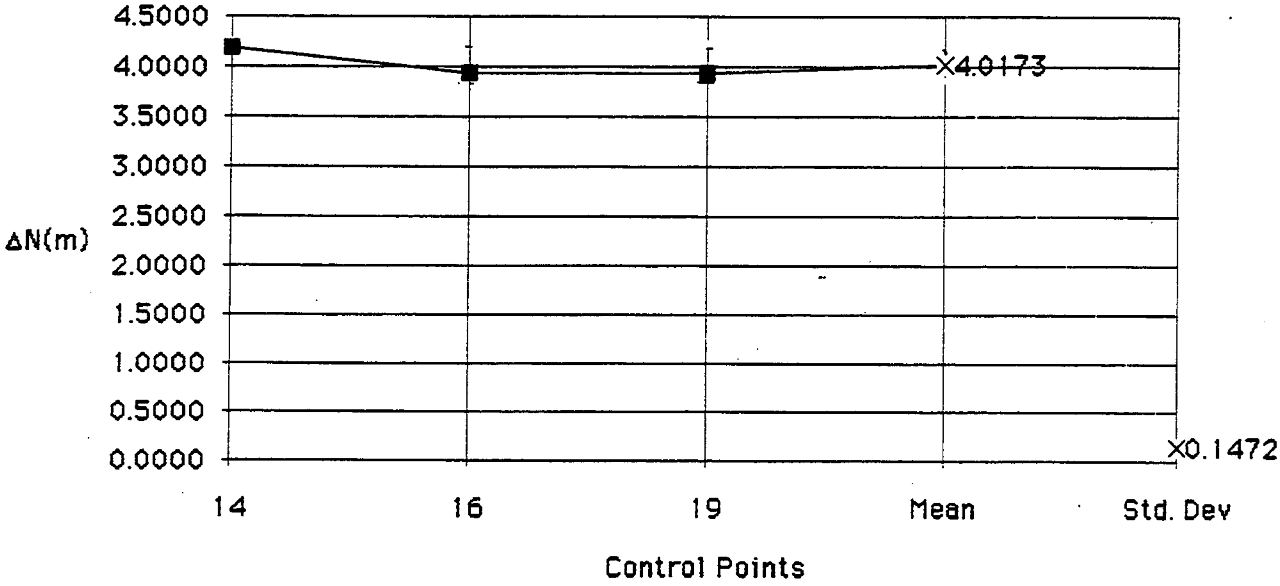

Figure 4.7 : ΔN profile for central Luzon.

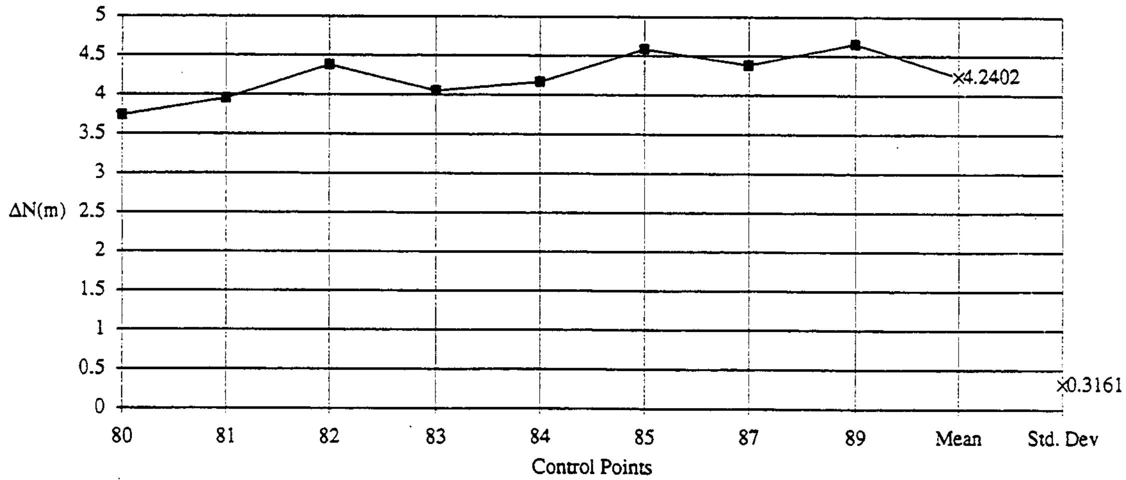

Figure 4.8 : ΔN profile for eastern Mindanao.

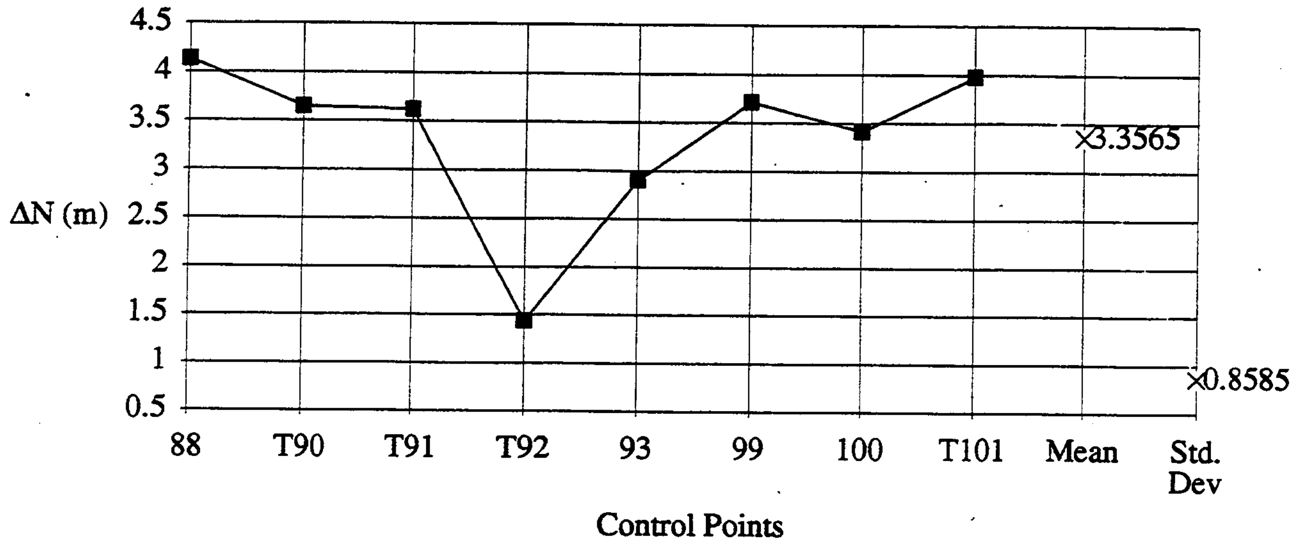

Figure 4.9 : ΔN profile for Davao Gulf.

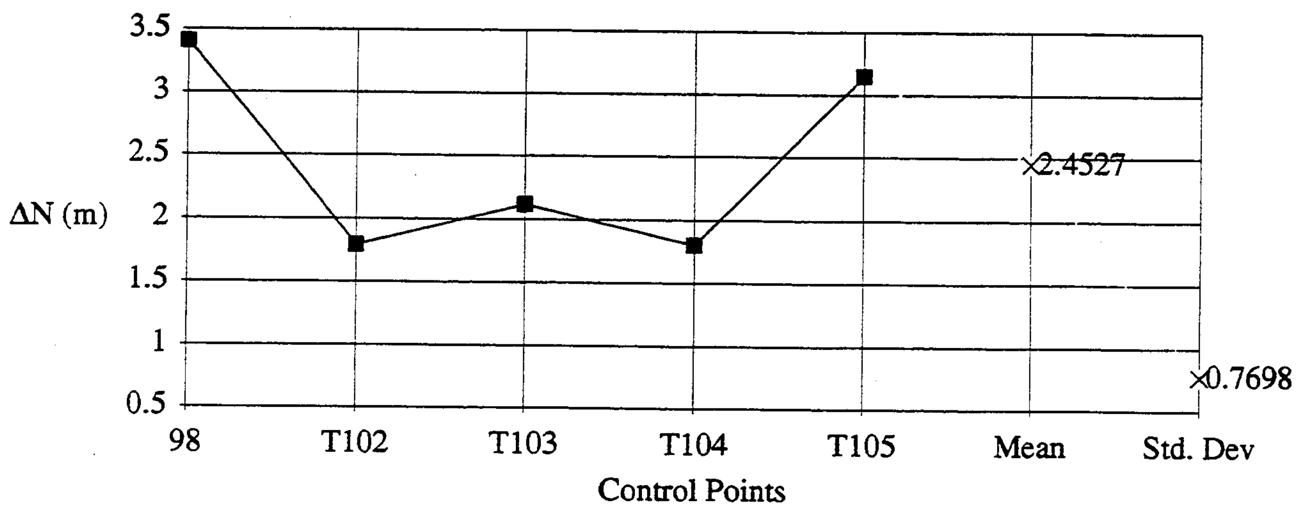

Figure 4.10 : ΔN profile for Moro Gulf.

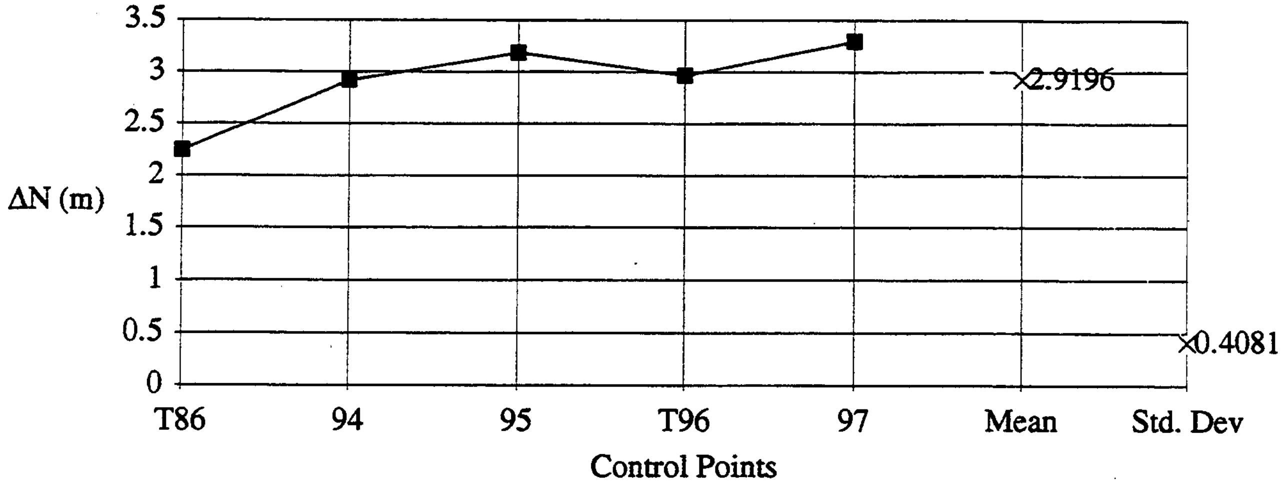

Figure 4.11 : ΔN profile for Mindanao northern coast.

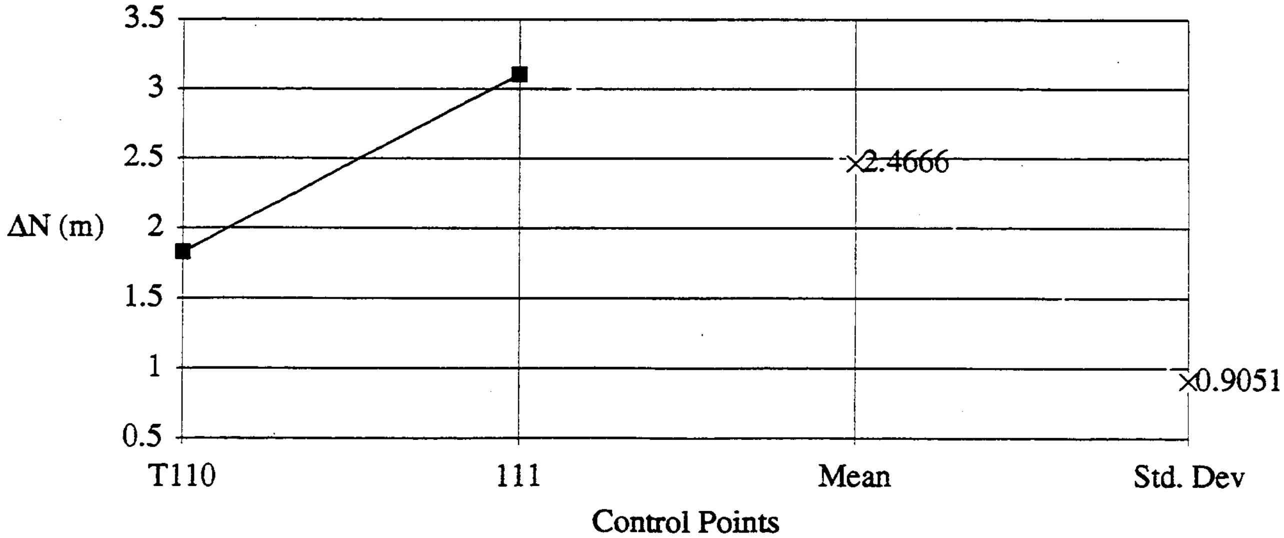

Figure 4.12 : ΔN profile for south west Philippines.

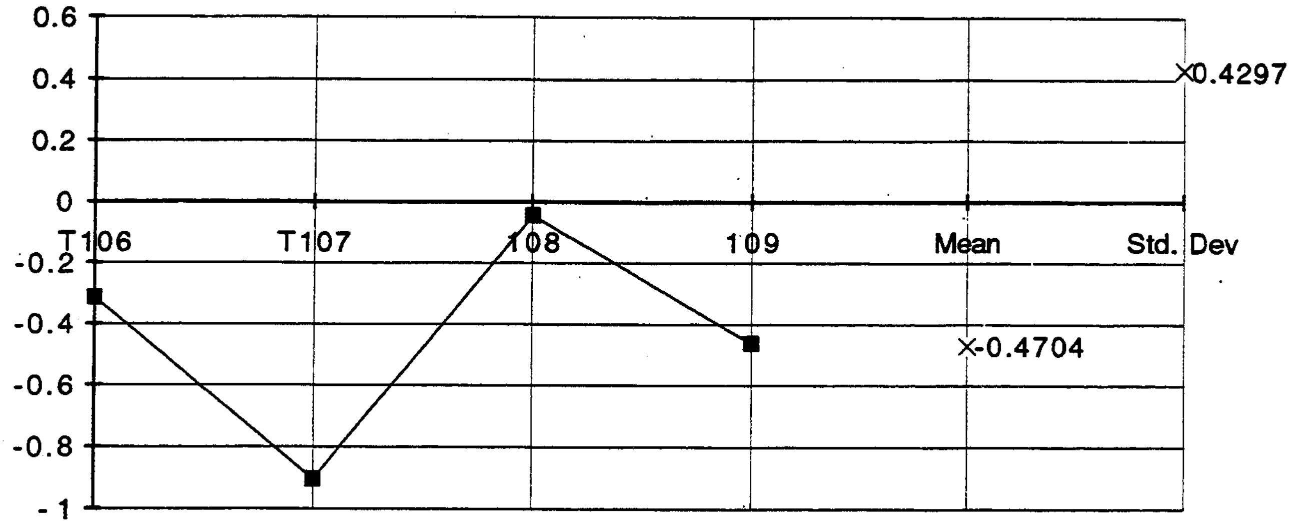

Figure 4.13 : ΔN profile for Palawan.

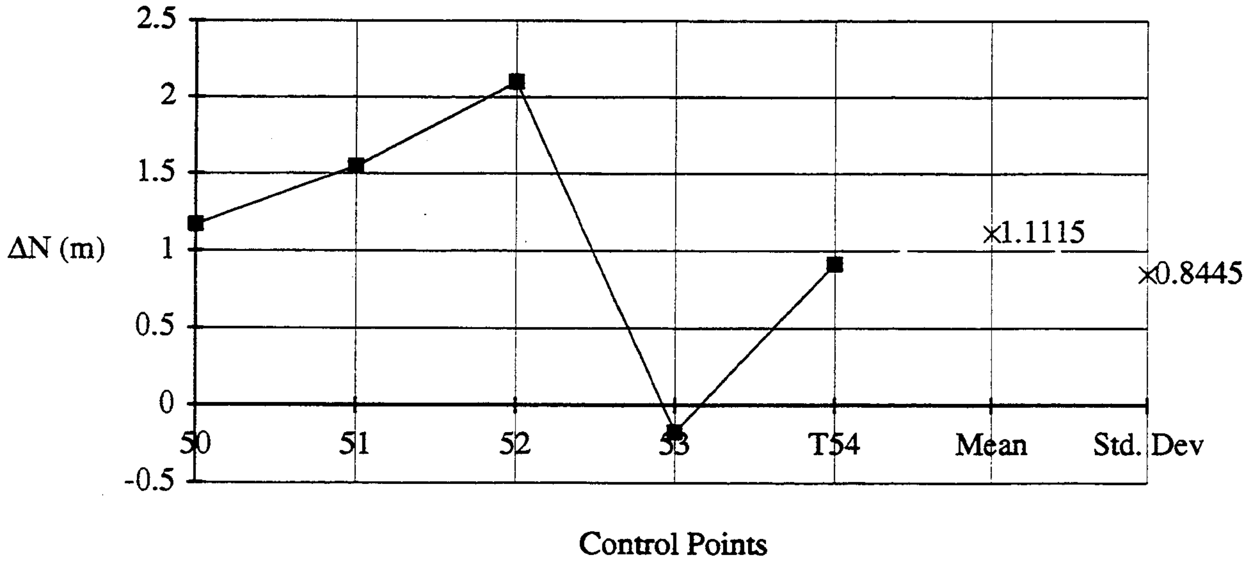

Figure 4.14 : ΔN profile for Island of Panay.

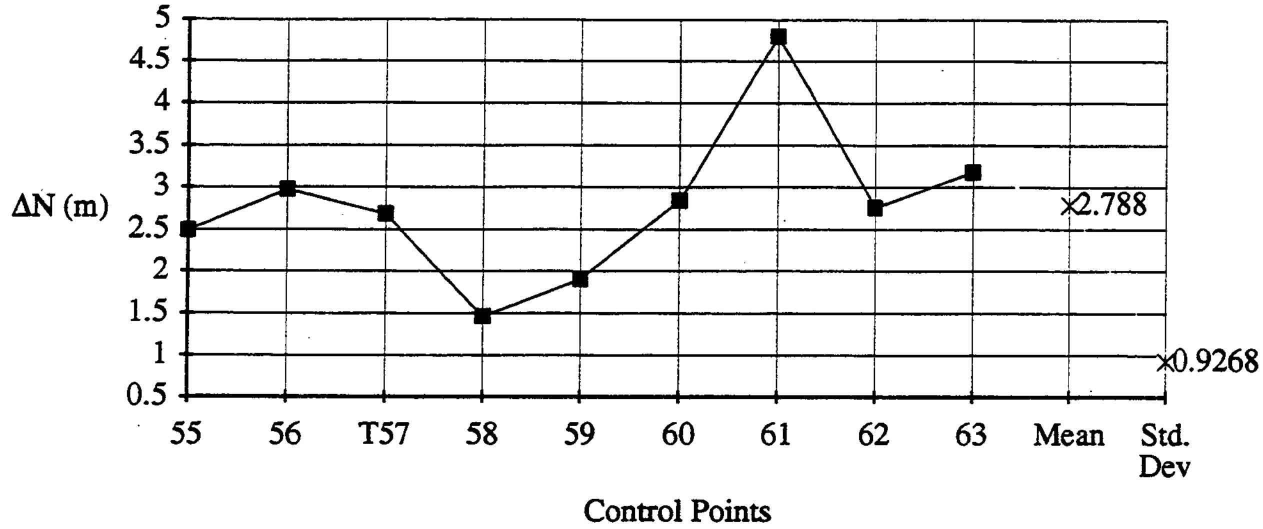

Figure 4.15 : ΔN profile for Island of Negros.

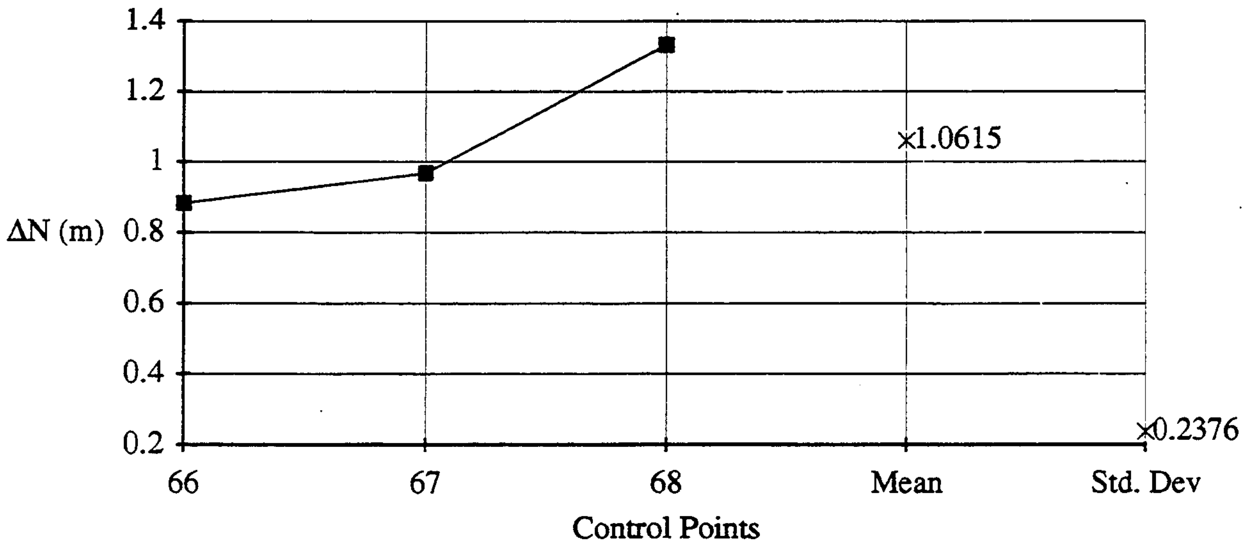

Figure 4.16 : ΔN profile for Island of Bohol.

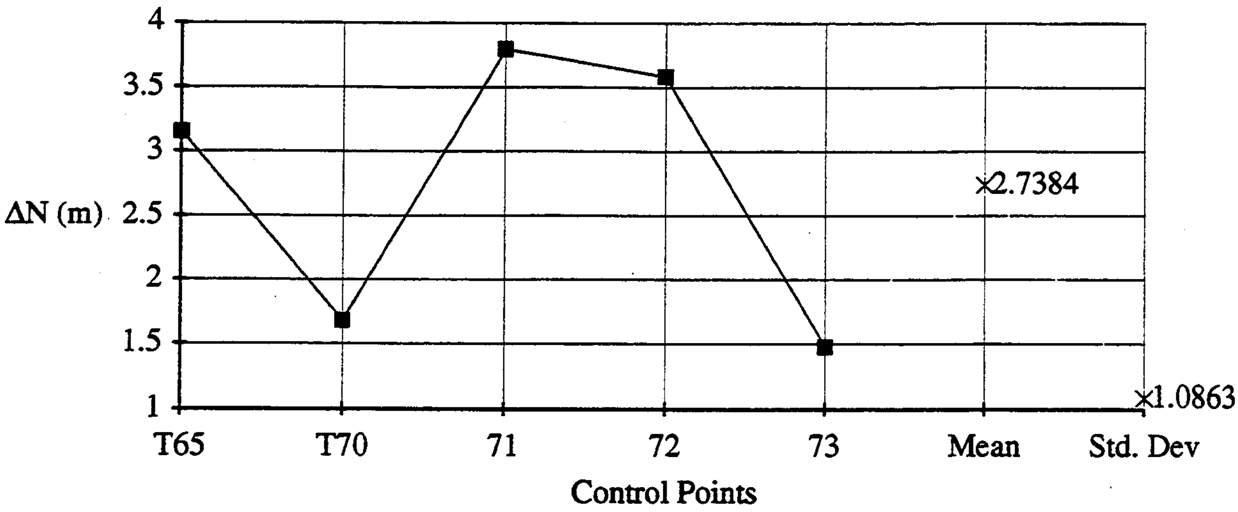

Figure 4.17 : ΔN profile for Island of Samar.

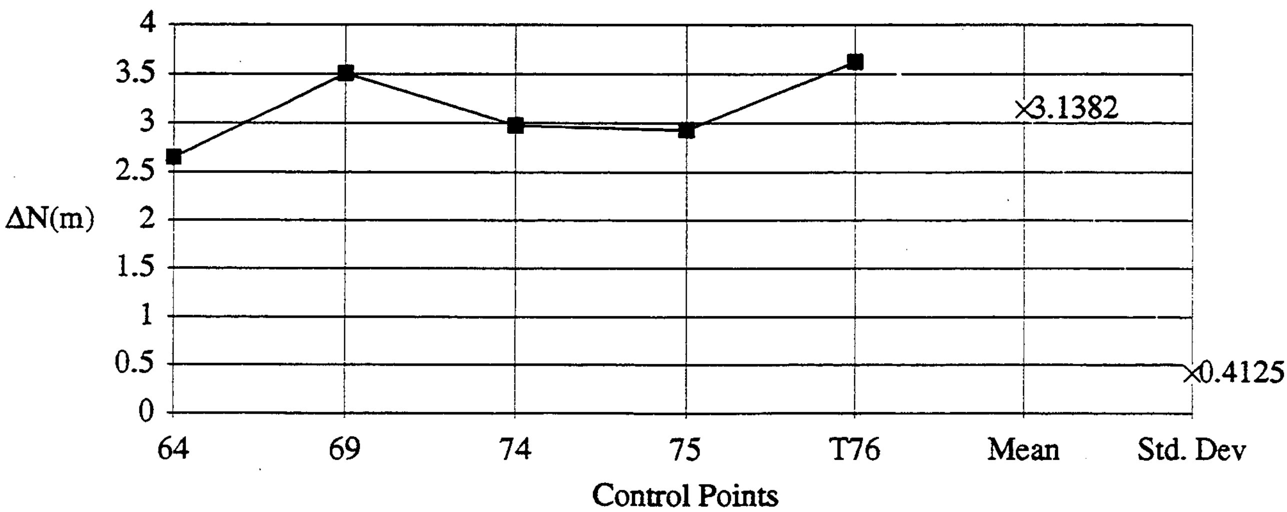

Figure 4.18 : ΔN profile for Island of Leyte.

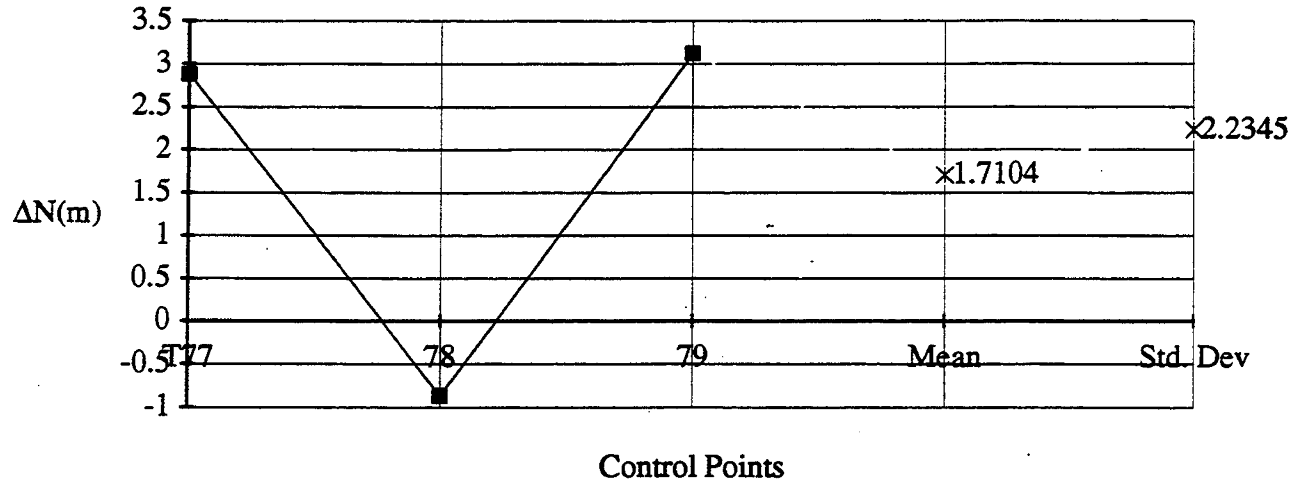

Figure 4.19 : ΔN profile for Island of Cebu.

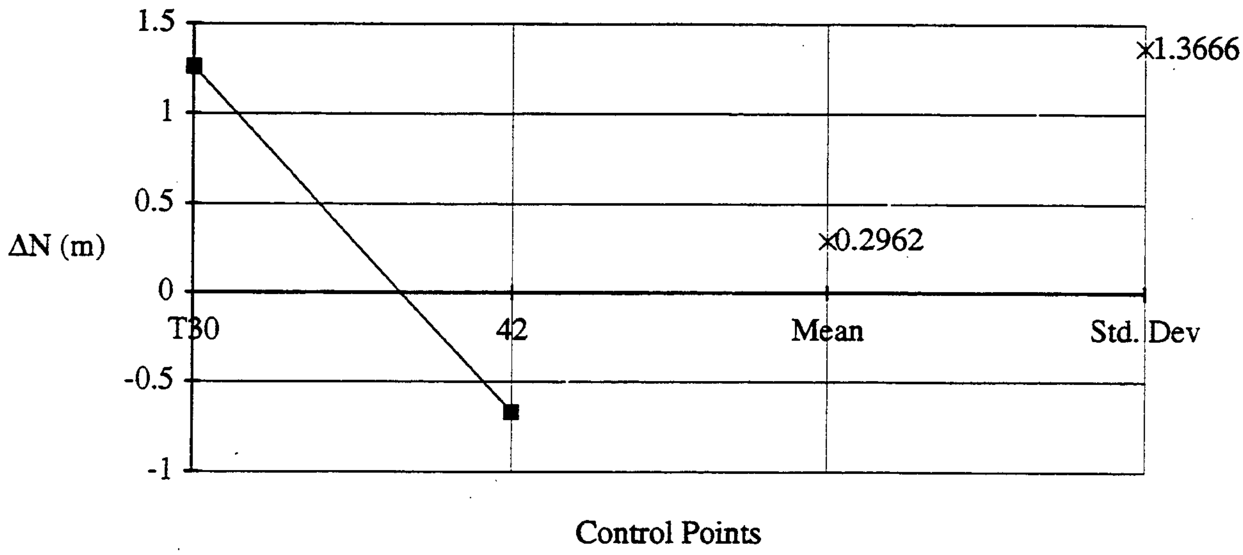

Figure 4.20 : ΔN profile for Island of Tablas.

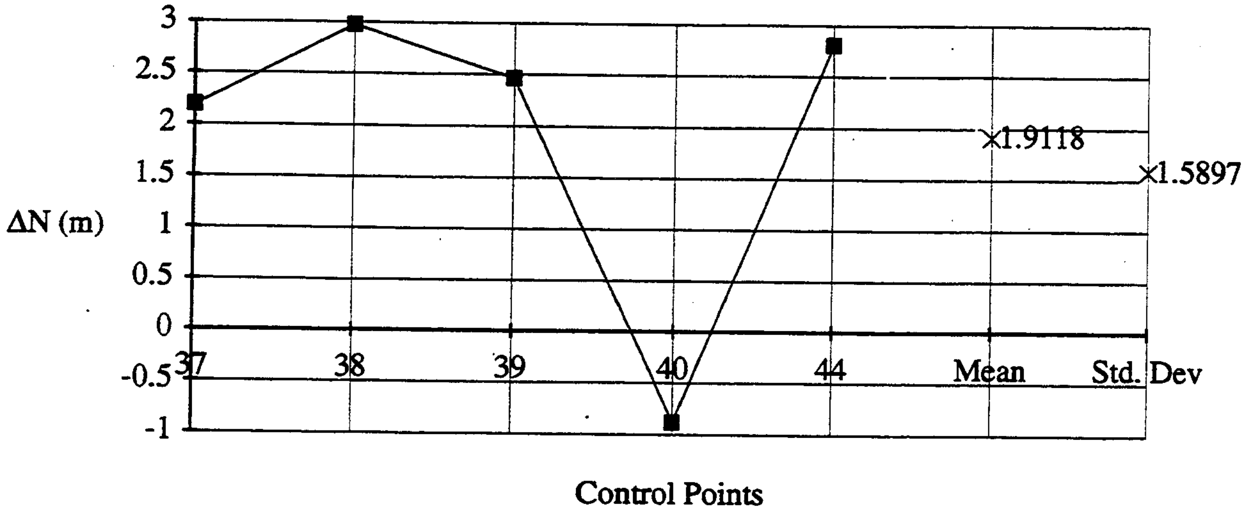

Figure 4.21 : ΔN profile for Island of Mindoro.

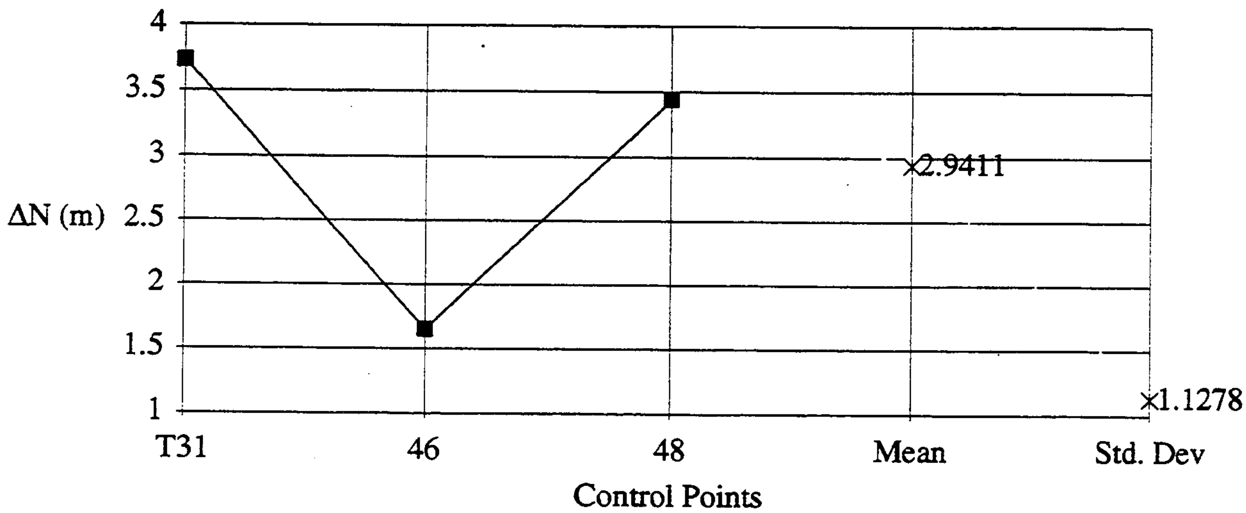

Figure 4.22 : ΔN profile for Island of Masbate.

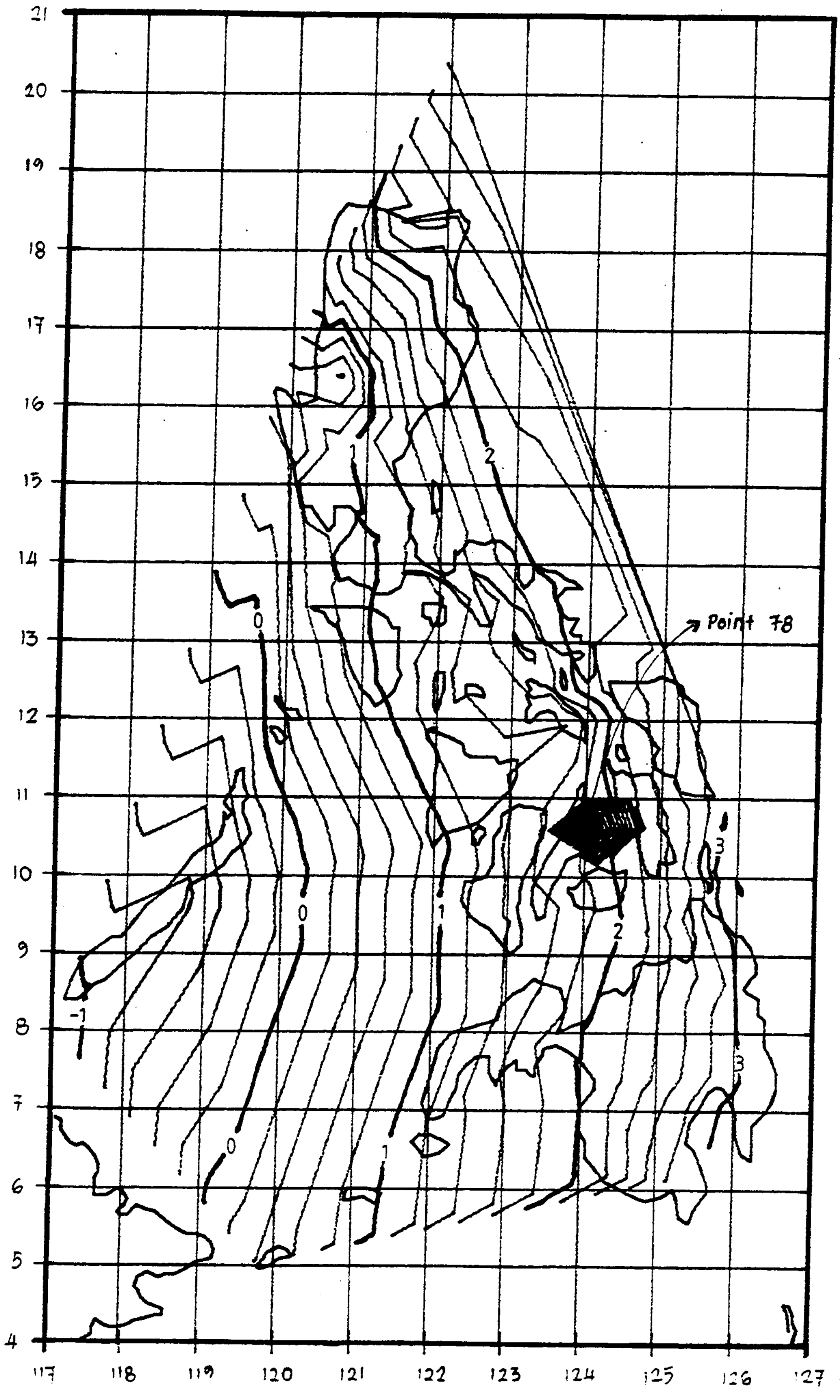

Figure 4.23 : Differences between h (Jones) and (Dyson).

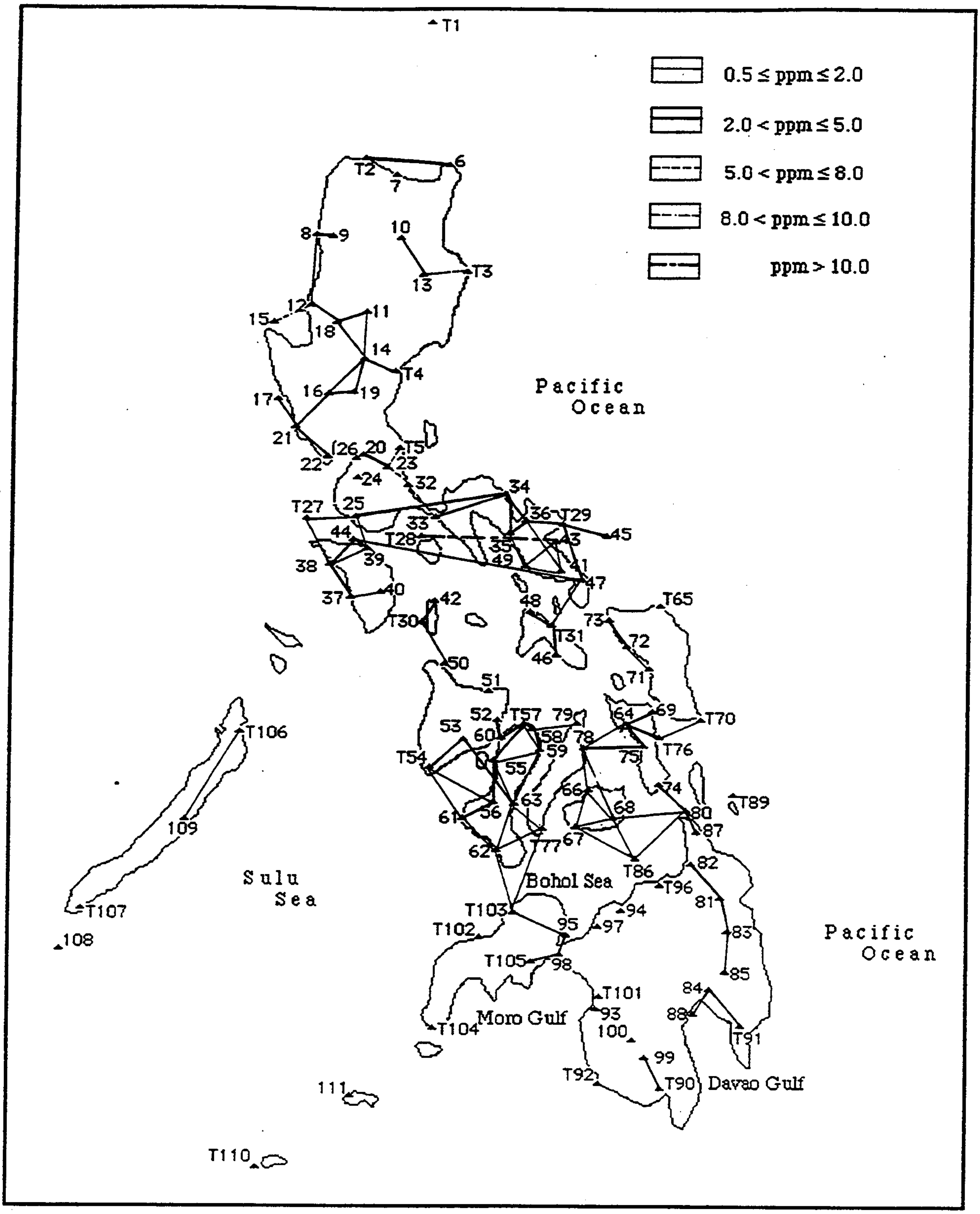

Figure 4.24 : Relative analysis of h from selected GPS control stations.

A PRELIMINARY GEOID

FOR

NORTH-WEST IRIAN JAYA

Aldofientje Kasenda

and

A. H. W.Kearsley

1. INTRODUCTION

1.1. Preamble

The local geoid of the Irian Jaya region has not yet been computed. Consequently, geodetic survey measurements are at present reduced to mean sea level, which is assumed to coincide with the ellipsoidal reference surface. This assumption will cause significant errors in the reduction of geodetic distances, of the order of 7 to 12 ppm, as the geoid in this region lies between 50 and 70m above the GRS'80 ellipsoid.

The region of Irian Jaya is extremely rugged. Its potential for natural resources in hydrocarbons and minerals has, for some time, encouraged survey activities to investigate the geology and the geophysical phenomena. These surveys also undertaken to help define the crustal structure, as Irian Jaya is in a tectonically complex area. For such enterprises, adequate geodetic control is needed to provide the basis for all topographic and geological mapping.

1.2. The Outline Of The Investigation.

The subject area is located between 1^{o} N to 6^{o} S and 129^{o} to 139^{o} East. To properly determine the local geoid undulation gravimetrically, a terrestrial gravity data set, with a spacing of about 10 km and a precision of 1 mGal is required.

Since about 1960, several gravity surveys have been undertaken in Irian Jaya. Until 1963, *Bataafsche Petroleum Maatschappy*, a Dutch company, carried out many gravity surveys aimed at locating structures related to hydrocarbon accumulation. Eight base gravity stations were established during these early surveys. From 1978 to 1981, gravity surveys were done by the Indonesian Geological Research and Development Centre in cooperation with the Bureau of Mineral Resources, Australia, through the Indonesia-Australia Geological Mapping Project, principally for tectonic studies. Around 1330 gravity data points were collected from these various surveys, and these data have been supplied by the Bureau of Mineral Resources, Canberra for this geoid investigation.

In order to find out the optimum computational procedure for the geoid determination, a comparison should be made between the geoid heights calculated from gravity data and the geoid heights derived geometrically by combining Doppler satellite-derived heights and heights from conventional levelling.
As part of the program to establish the National Geodetic Network in Indonesia, *BAKOSURTANAL* (The National Coordination Agency for Surveys and Mapping), from 1979 to 1986, undertook a Doppler satellite-based survey in Irian Jaya. This campaign established 126 control points over both the main island and in the smaller islands of the subject region. These data provided the ellipsoidal heights used for control in this project. The data sets used in this investigation are more fully described in Section 3.

1.3. Methods For Determining The Geoid.

The geoid undulation can be determined by several methods depending upon the location and available data in the subject area. The main techniques use

- terrestrial gravimetry,
- satellite altimetry,
- potential coefficients of the model of the earth's gravity field, or
- a combination of satellite-derived and conventionally measured heights.

(i) Geoid Determination From Gravity Anomalies. (Refer Torge, 1980, Section 5.2; Heiskanen and Moritz, 1967, Section 2.16).

This approach gives the spatial relationship (N) between the geoid ($W=W_0$) and its reference ellipsoid ($U=W_0$), from the force fields on these two surfaces (see Figure 1.1). The fundamental relationship is given by Stokes' integral -

$$N = \frac{R}{4\pi G}\int\int_{\sigma} \Delta g \, S(\psi) \, ds \quad \ldots (1)$$

where,

R is the earth's radius

G is the earth's mean gravity

Δg is the gravity anomaly at the surface element $d\sigma$

$\Delta g = g_p - \gamma_{P_0}$

and the Stokes function is

$$S(\psi) = \operatorname{cosec}(\Psi/2) + 1 - 6\sin(\Psi/2) - 5\cos\psi - 3\cos\psi \ln\{\sin(\Psi/2) + \sin^2(\Psi/2)\} \quad \ldots\ldots (2)$$

and

ψ = angular distance between the point computation and the surface element $d\sigma$, where the surface element of the solid angle can be written as ,

$d\sigma = \sin\psi \; d\psi \, . \, d\alpha$, and

α = azimuth from point of computation to $d\sigma$.

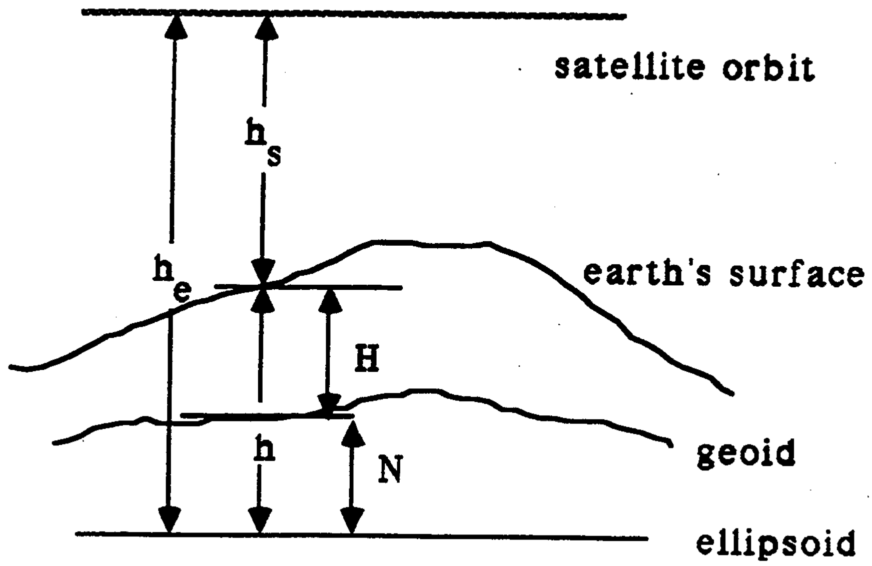

Figure 1-1: The Height Relationships

(ii) **Geoid Determination From Satellite Altimetry.** (Torge 1980, Section 4.4.8)

This technique is applicable over the oceanic areas and uses the range from the satellite to the mean ocean surface, with tidal and other oceanographic influences removed, to determine the height of the quasi-stationary sea surface - see Figure 1.2 and Equation 3. This helps to provide data on the continental geoid both directly - by constraining N values at the coast (e.g. along the coastal reaches of Irian Jaya), and indirectly - by giving data on the geoidal parameters over 70% of the Earth's surface, which is then used as input for the coefficients of the global potential models.

In other words,

$$N = h - h_s - H \qquad \ldots\ldots (3)$$

where,

h = the satellite height above the ellipsoid,
h_s = the satellite height above sea surface, and
H = the orthometric height.

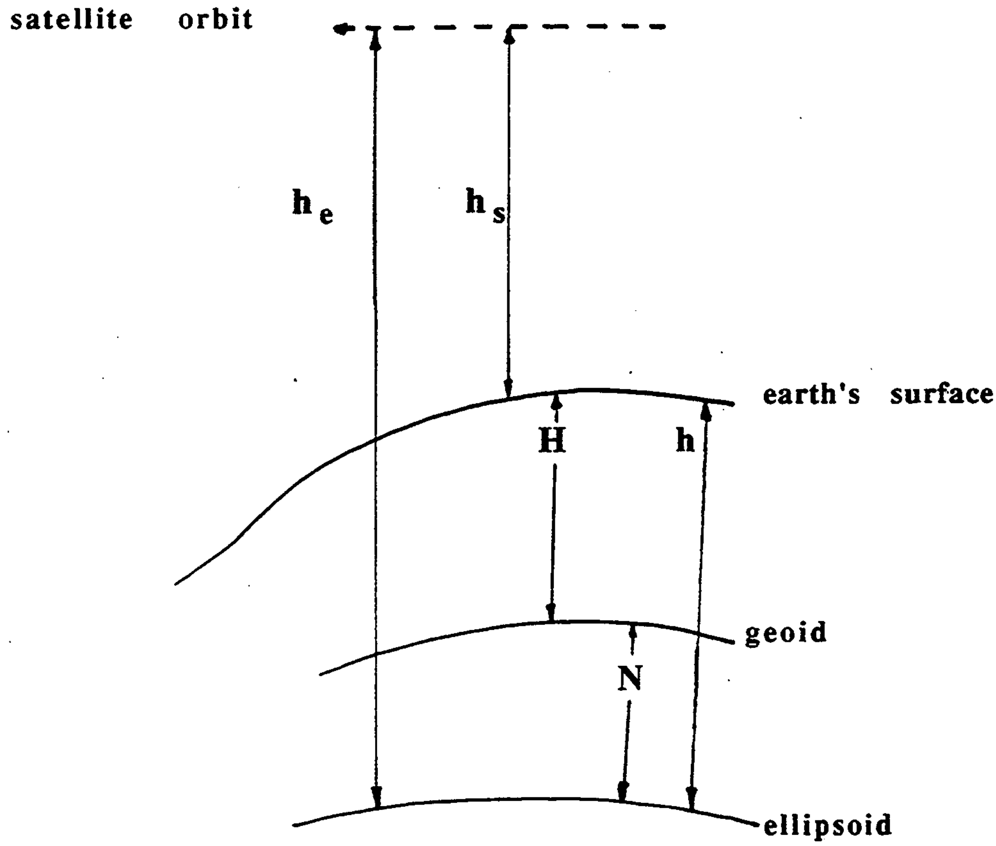

(iii) Geoid Determination From Potential Coefficients.

The geoid height can be expressed by a spherical harmonic expansion, and, providing the coefficients can be properly evaluated, give what is known as a "geopotential model". A variety of such models have been evaluated, which vary depending upon the data used to determine the potential coefficients, the maximum degree and order of the summation, etc. The geoid height is expressed as

$$N = \frac{kM}{\gamma r} \sum_{n=2}^{n_{max}} \left(\frac{a}{r}\right)^n \sum_{m=0}^{n} P_{nm} [\sin \varphi] \left(C_{nm} \cos m\lambda + S_{nm} \sin m\lambda\right) \quad \ldots (4)$$

where,

a is the radius of the equator
r is the geocentric radius to the point of computation
φ, λ is its geocentric latitude, longitude respectively.
k is the gravitational constant
M is the mass of the earth
γ is the normal gravity

P_{nm} is the Legendre polynomial

C_{nm}, S_{nm}, are the fully normalised potential coefficients.

The harmonic coefficients C_{nm} and S_{nm} are determined either by studying the perturbations of satellites in their orbits or by combining these with either derived or observed terrestrial gravimetric data (see Equation 12).

(iv) Geoid undulations from satellite heighting

The undulation of the geoid can be derived from a combination of satellite (e.g. GPS or Doppler) observations and conventional levelling measurements. The geoid height at the point's position can be obtained by subtracting the ellipsoidal height from the orthometric height (see Fig. 1.2), and, based on the assumption of small deflections of the vertical, is simply written as

$$N = h - H \qquad .....(5)$$

where,

h = height above the ellipsoid derived from the satellite position, and
H = orthometric height obtained from levelling or other conventional heighting measurement.

2 THE GRAVIMETRIC GEOID SOLUTION

2.1 Modification of Stokes' integral.

Figure 2-1 shows the behaviour of the Stokes' function (Eq. 1).

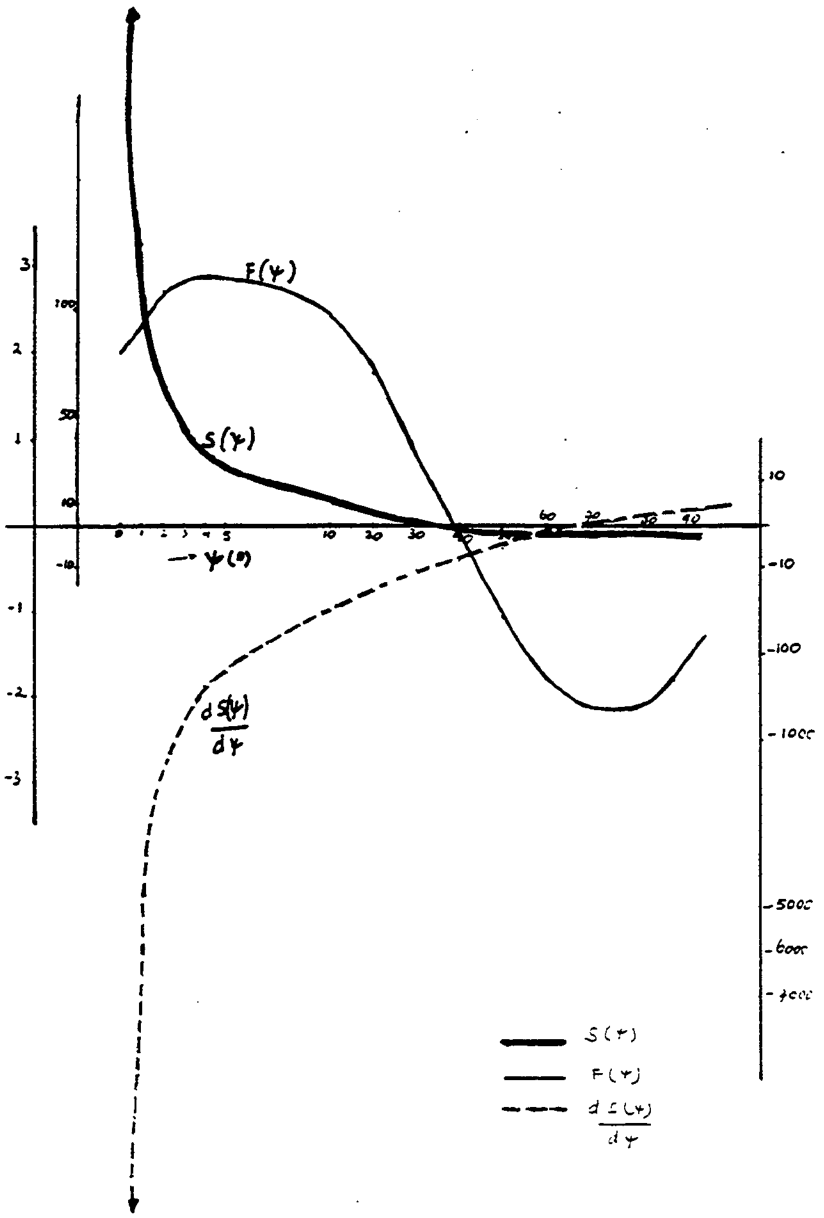

Figure 2-1: The S(ψ) and F(ψ) functions

As the element of areal integration ($d\sigma$) nears the computation point, i.e., as ψ approaches zero, the function $S(\psi)$ goes to infinity In this part of the computation, the Stokes' integral must be treated with caution. The Stokes' integral can be modified by replacing $S(\psi)$ by $F(\psi)$, where

$$F(\psi) = \left(\frac{S(\psi)\sin\psi}{2}\right) \quad \ldots (6)$$

which behaves better i.e, is more stable than $S(\psi)$ as ψ approaches zero (see Figure 2-1). In the approach adopted for this project, $F(\psi)$ is the function applied in evaluating the integral.

By using the polar coordinate form of Stokes' integral, i.e. integrating over the surface with respect to ψ and α, the equation of Stokes' formula then is written as (see Eq. 2)

$$N = \frac{R}{2\pi G}\int_{\alpha=0}^{2\pi}\int_{\psi=0}^{\pi} \Delta g \, F(\psi)\, d\psi \, d\alpha \quad \ldots (7)$$

The Stokes' integral requires the gravity anomaly Δg to be known over the whole earth surface. This is impossible to achieve. Also in practice, we try to create a dense gravity distribution around the computation point, to help overcome the instability in the computation mentioned above, and for more distant areas, use block mean gravity data. In this way, the integral is approximated by a summation. The surface elements $d\sigma$ are replaced by small compartments for which the gravity anomalies are represented by the average values of each compartment.

Stokes' integral in the form of summation over discrete data block anomalies, is given in Heiskanen & Moritz, (1967) as

$$N = \frac{R}{4\pi G}\sum_k \Delta g_k \, S(\psi)\, d\sigma = \sum_k C_k \overline{\Delta g_k} \quad \ldots (8)$$

where,

$\overline{\Delta g_k}$ is the mean gravity anomaly of each compartment.

C_k is the coefficient related to the block q_k.

It is neither feasible nor necessary to integrate over the whole surface. It is only necessary to integrate over a certain spherical cap (eg. up to a radius ψ_o), to determine the contribution to N of the short wavelength features of the gravity field. A high-resolution geopotential model is used to evaluate the medium to long wavelength contribution of the gravity field to N.

To summarise, the geoid undulation is obtained by :

$$N = N_l + N_s \quad \ldots\ldots (9)$$

where,

N_l is generated from the medium to long wavelength features of the gravity field from the geopotential model of the earth (see 1.12 and Section 2.3 below), and

N_s is the short wavelength feature computed by using the Ring Integration method described below.

2.2 N_s from the Ring Integration Method.

The technique used for computing the N_s component of the geoid by applying Stokes' integral is called the Ring Integration method and is fully developed in Kearsley (1985). In this method, the surface is subdivided into compartments formed by concentric rings and radial lines centered on the point of computation P (see Figure 2-2). The integration is then calculated in terms of the summation

$$N_s = C_n \sum_{h=1}^{H} \sum_{i=1}^{I} \Delta g_{h,i} \quad \ldots (10)$$

where

C_N = contribution of Δg to N from each compartment (for this project, 0.3 mm/mGal)

h = counter for the azimuth component

i = counter for the radius component, and

$\Delta g_{h,i}$ = mean gravity anomaly for compartment h,i.

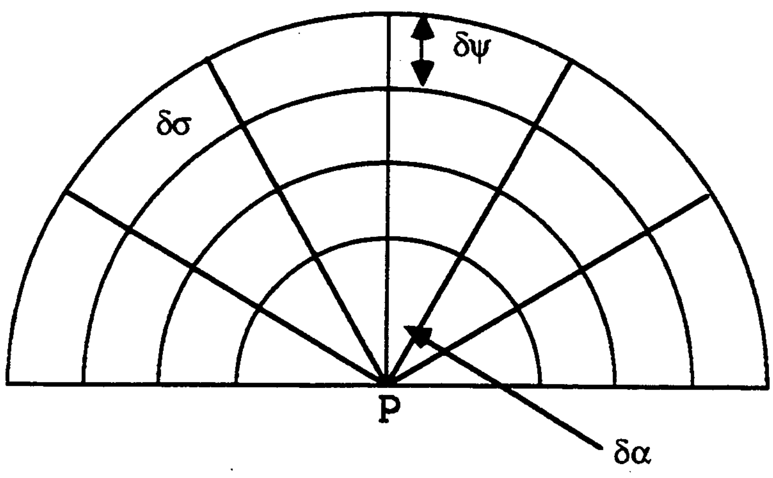

Figure 2-2 The concentric ring compartments

The contribution of N_s computed by the Ring integration method is done by using the UNSW computer program called GRAVO1.

2.3 N_l from the Geopotential Model.

In order to obtain the N_l value, the geopotential coefficients (C_{nm} and S_{nm}) have to be evaluated. Various researchers have estimated these coefficients from the analysis of the terrestrial gravity data over both land and oceans, and from the satellite altimeter data over the oceans have resulted in many different models. At the time of writing, the most recent high degree models with a complete harmonic expansion up to degree and order 360, have been developed at the Ohio State University, and are known as OSU89A and OSU89B (Rapp and Pavlis, 1990).

These two models were based on the combination of the GEM-T2 satellite potential model and global mean gravity anomalies. The GEM-T2 gravitational model was based on observations of 31 satellites and utilized laser tracking data, Doppler data and optical data. The sources of the gravity anomalies were from satellite altimeter data and terrestrial observations to provide the OSU89A model. Because the computation of the coefficients requires global data, for the areas where there was no terrestrial measurements and a lack of altimeter data, the gravity anomalies were derived from a combination of low-degree potential coefficient from satellite models augmented, in the case of OSU89B, by high frequency information implied by the topography and its isostatic compensation (Rapp and Pavlis, 1990).

The gravity data estimated from satellite altimeter data covering the ocean areas was comprised of 143,356 30' mean anomalies. The gravity data from terrestrial measurements, also 30' mean anomalies, consisted of 66 990 points.

If the gravity anomaly is represented as Δg^c (i.e., after some systematic corrections), the relation between the gravity anomaly and the geopotential coefficients is written as

$$\Delta g^c(r,\phi,\lambda) = \frac{GM}{r^2}\sum_{n=2}^{\infty}[n-1]\left(\frac{a}{r}\right)^n \sum_{m=-n}^{n} C^s_{nm} Y_{nm}(\phi,\lambda) \quad \ldots \ (11)$$

with,

$$Y_{nm}(\varphi,\lambda) = P_{nm} \cos\theta \ \cos m\lambda \quad \text{for} \quad m > 0$$

$$Y_{nm}(\varphi,\lambda) = P_{nm} \cos\theta \ \sin m\lambda \quad \text{for} \quad m < 0$$

Based on the equation above, and following Rapp & Pavlis (1990, eq. 20), the fundamental mathematical model for calculating the coefficients from the complete set of discrete area mean values of gravity anomalies is formulated as follows.

$$\overline{C_{nm}}^{s} = \frac{1}{4\pi r\gamma}\sum_{i=0}^{n-1} r_i^E \sum_{k=0}^{s} \frac{L_{nmk}}{S_{n-2,m}^{b/E}} \cdot \frac{\overline{IP}^{i}_{n-2k,m}}{(n-2k-1)\, q^{i}_{n-2k}} \cdot \sum_{j=0}^{2n-1} \overline{\Delta g_{ij}}^{E} \begin{Bmatrix} IC \\ IS \end{Bmatrix}^{j}_{m} \quad \ldots \quad (12)$$

where

$\overline{\Delta g_{ij}}^{E}$ = the discrete mean gravity anomaly value over an equiangular block on the reference ellipsoid.

$\overline{C_{nm}}^{s}$ = the fully normalized spherical geopotential coefficients

$$\gamma = \frac{GM}{r^2}$$

$$\overline{IP}^{i}_{n,m} = \int_{\delta_i}^{\delta_{i+1}} P_{nm}(\cos\delta)\sin\delta\, d\delta\,, \quad \text{and}$$

$$\begin{Bmatrix} IC \\ IS \end{Bmatrix}^{j}_{m} = \int_{\lambda_j}^{\lambda_{j+1}} \begin{Bmatrix} \cos m\lambda \\ \sin m\lambda \end{Bmatrix} d\lambda$$

The equations above were used in the harmonics analysis of an adjusted set of gravity anomalies to provide estimations of C^{s}_{nm}. From these, the coefficient for models OSU89A and OSU89B have been produced.

For this project, OSU89A is adopted as the reference model for the geoid computation of the Irian Jaya region. The N_l component is computed using the program GRAV02 at UNSW.

3 DATA SETS AND COMPUTATION TECHNIQUES

3.1 The available data sets.

For computing the short wavelength component of the geoid, gravity anomalies over the whole cap of radius ψ_0 are required. Control data values are needed for testing the gravimetric geoid heights. Below we describe the data sets used for the project, and outline the techniques used to process these data.

3.1.1 Gravity data set.

Only about 30% of Irian Jaya has been covered by the gravity survey done for the geophysical exploration and the geological interpretation.This data is comprised of about 1330 gravity points. The distribution of these points is irregular, mostly concentrated in the two areas bounded by 129.5° to 134.5° E and 0.0° to -2.5° S, and between 133.5° to 137.0° E and -2.5° to -5.0° S (see Figure 3-1). The rest of the land is poorly covered, and in some parts no data exists at all. The distribution of the number of observed gravity points per 1° block is shown in Figure 3-2.

All the observed gravity values were tied to the existing IGSN'71 base station network in Indonesia. Data reduction was done using the GRS'67 formula and the Bouguer correction was made with an assumed density of 2.67 gr/cc (Almond et.al., 1988).

A strong network of gravity base stations is yet to be established in Irian Jaya. One of the eight old base stations established from the early survey was reoccupied in this survey. This was in turn tied to the IGSN'71 base station in Bandung (DG0 base station). The present value of this Irian Jaya base station is about 3 mGal less than the previous value.

The precision of the later gravity measurements can be inferred from the drift behaviour of the gravimeter used. The later survey involved the La Coste-Romberg type G gravimeters, and over the period of the field measurements the drift varied between 0.04 to a maximum of 0.16 mGal/day. All the gravity readings were adjusted to the local base station which was tied to the IGSN'71 base station. The adjustment of the original data was carried out for two series of data sets. The first data set consisted of 69 loops, with the second having 88 loops of measurements. The standard deviations given by loops closures are, respectively, 0.087 and 0.073 mGal [Untung, 1982].

The original data list supplied by the BMR consisted of the identification number of the point, its position in latitude and longitude, elevation, free-air and Bouguer anomaly and the relative observed gravity values. The Bouguer anomaly in this case is the simple Bouguer anomaly, since the terrain correction has not been applied.

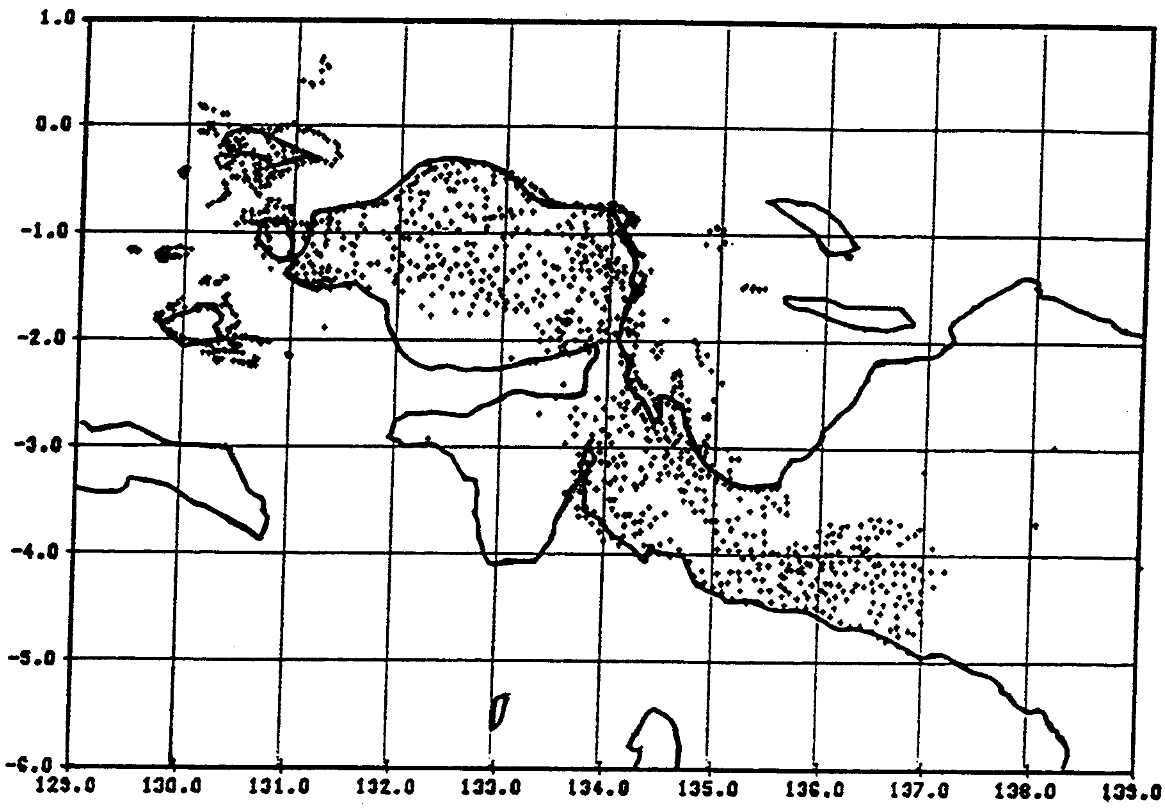

Figure 3-1: The gravity data points distribution

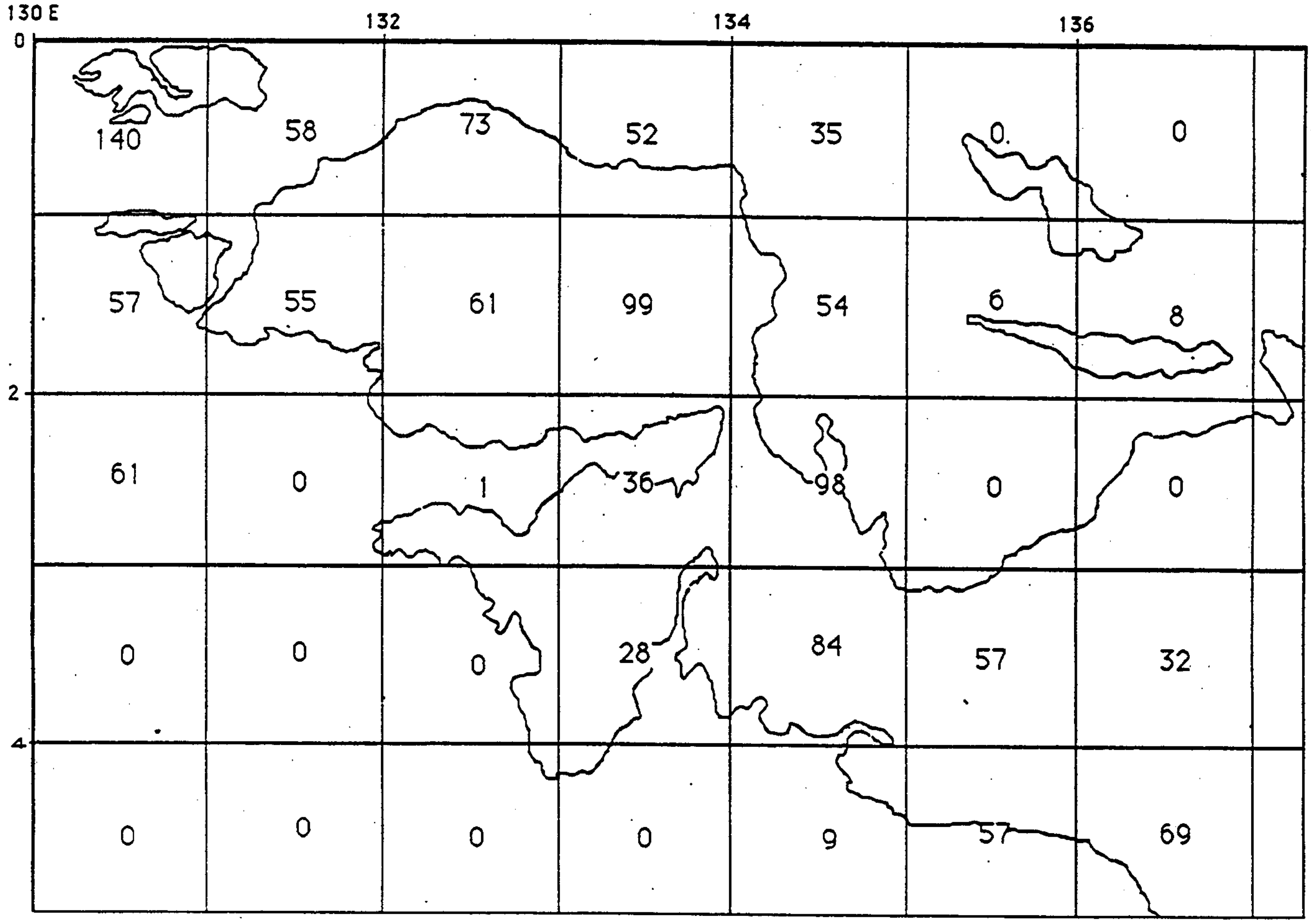

Figure 3-2: Number of gravity stations per 1° block

The free-air anomalies values vary between -84 mGal to 394 mGal. Figure 3-3 shows the contour map of these anomalies with a contour interval of 10 mGal. The Bouguer anomalies values rise from -136 mGal to a high of 172 mGal. The contour map of this anomaly is illustrated with an interval of 25 mGal (Figure 3-4).

The free-air anomaly map shows a high correlation with the topography of the area (see Figure 3-3a), as is expected, whereas the Bouguer anomaly map corresponds with the local structure of the crust underneath the subject region (Figure 3-4a).

In order to identify possible errors in the gravity data, the free-air anomalies were contoured in each 1° block. From this, values which were grossly at odds with the surrounding values were deleted. This brought the final data set, after editing, to 1234 points.

For greatest precision and stability in N_S from the Stokes' integral, the "remove-restore' technique is used in its evaluation. That is, the "observed" free-air gravity anomaly is reduced by the gravity anomaly generated from the geopotential model, and these residual values used in calculating the short wavelength component of the geoid [Kearsley, 1988].

The gravity anomaly generated from OSU89A was obtained by utilizing the computer program called GRAV00 in the UNSW software (discussed in Section 3.2). The output file contained the gravity anomaly values at grid points (the grid spacing we adopted is 0.1°). By interpolating from the grid points the OSU89A value at each gravity point observation was found. The residual anomaly at each point observation is then calculated by :

$$\Delta g_{residual} = \Delta g_{free\text{-}air} - \Delta g_{model},$$

which was obtained by using the program called GRAV06I (see sec. 3.2). This residual gravity data set was then used as the basic data file for calculating the N_S component of the local geoid of this subject area. It is given the descriptive title of *'IRJA89ARES'*.

The minimum value in the IRJA89ARES data set is -166.9 mGal, whereas the maximum is 309.8 mGal. This is still a large variation for a residual gravity data set and is, in fact, only slightly less than the range in the free-air anomaly values. This reflects the fact that OSU89A, having a resolution of about 0.5°, is fairly insensitive to the large changes in the short wavelength features of the gravity field in this region.

These residual anomalies values are illustrated in Figure 3-5 at 25 mGal contour interval.

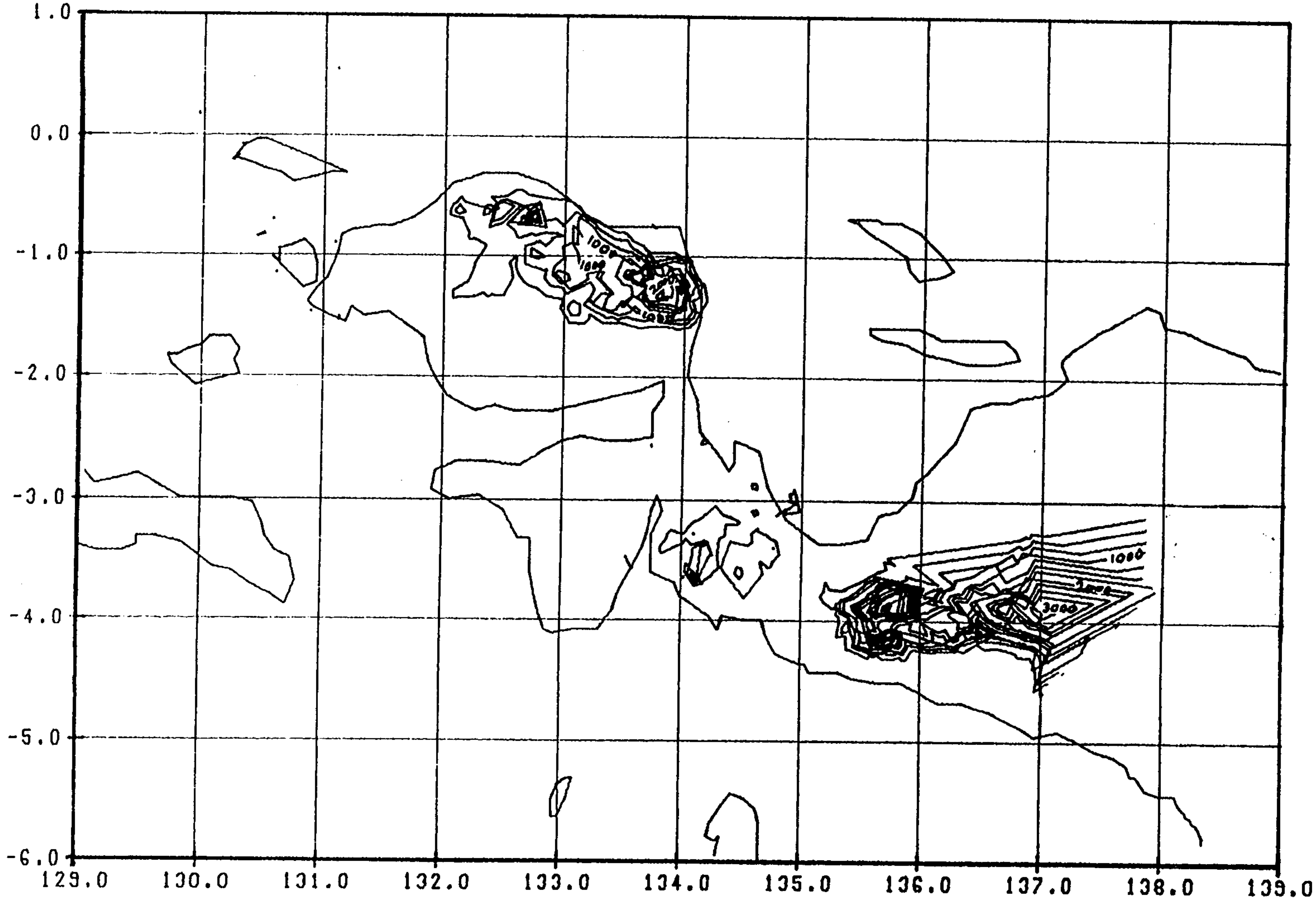

Figure (3-3a)

The topography of Irian Jaya region
based on the Barometric heighting

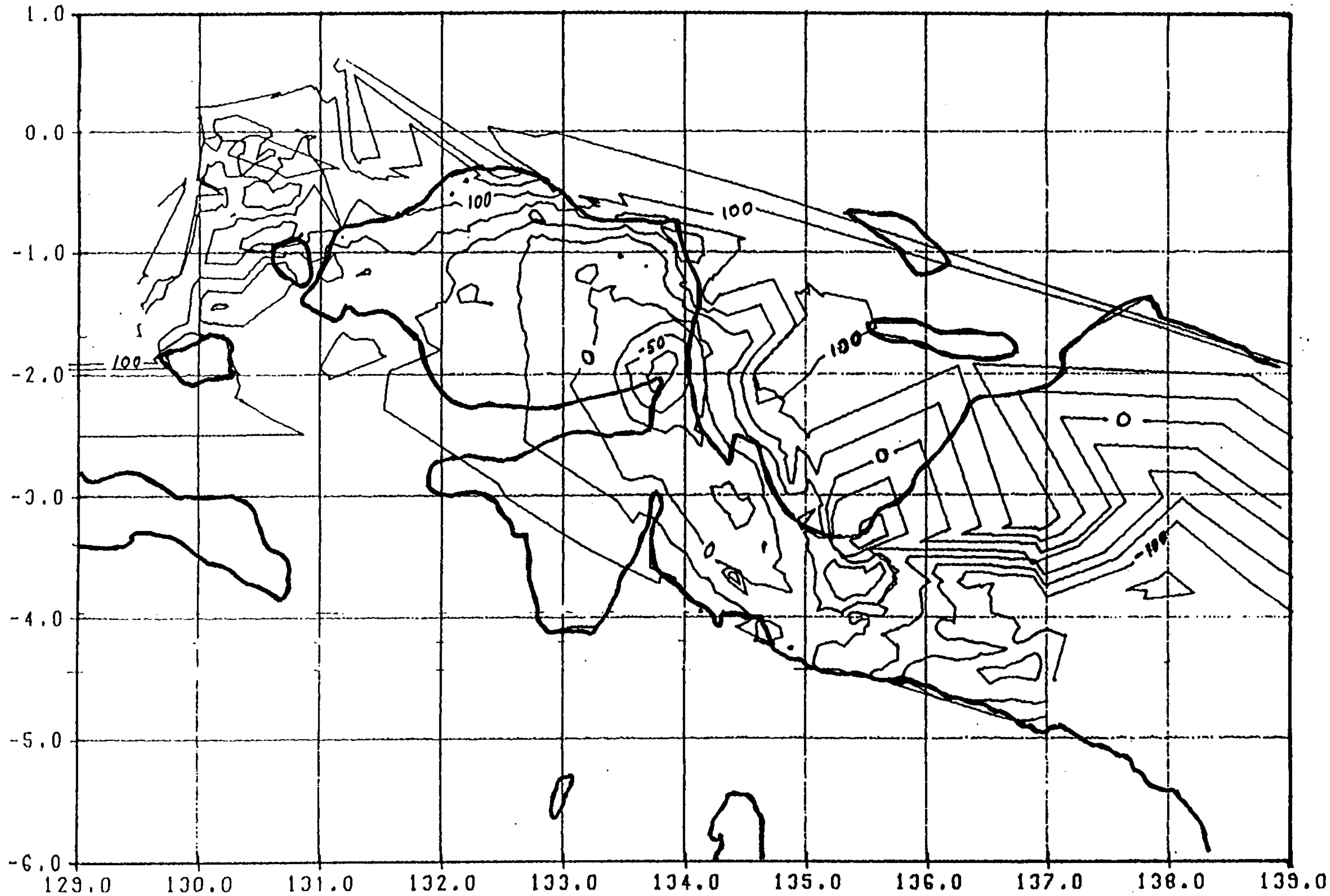

Figure (3-4)

The simple Bouguer anomaly

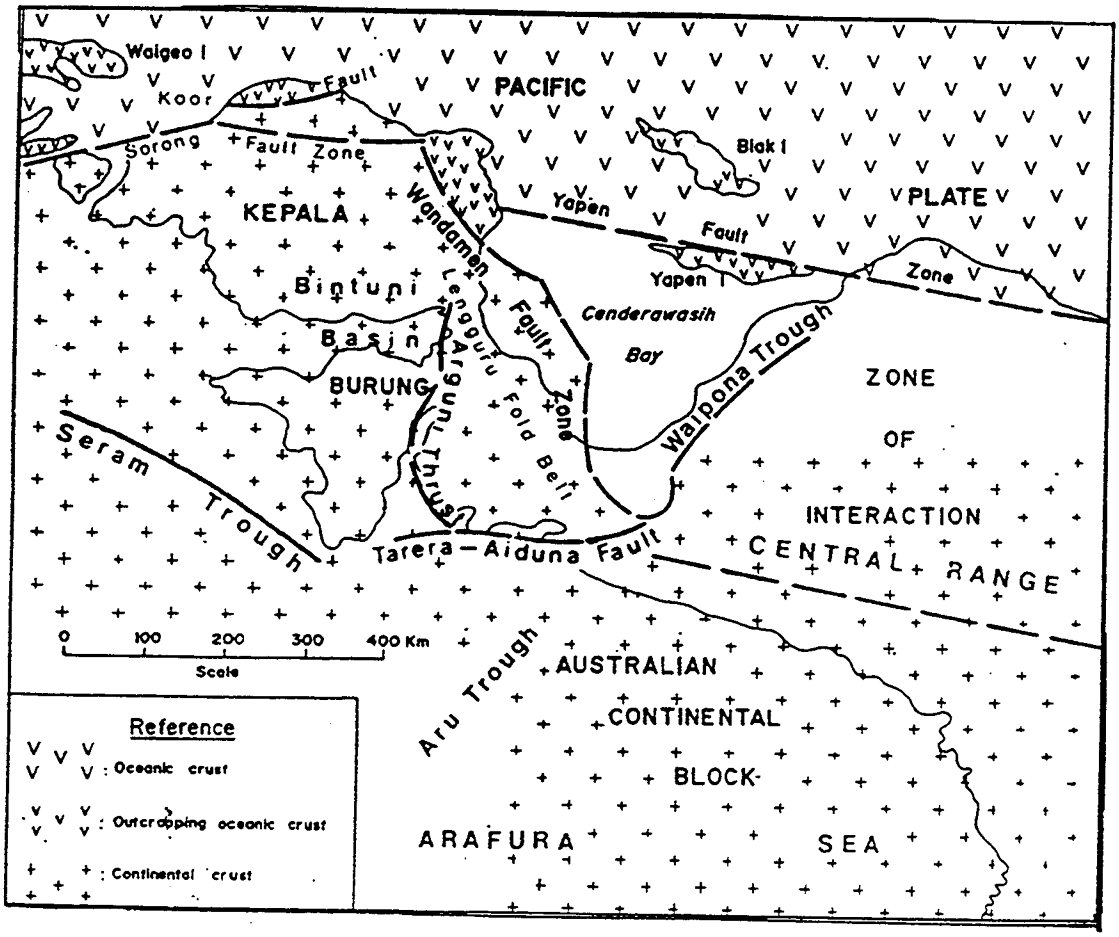

Figure 3.4a: The crustal elements of Irian Jaya
(after Dow, 1982)

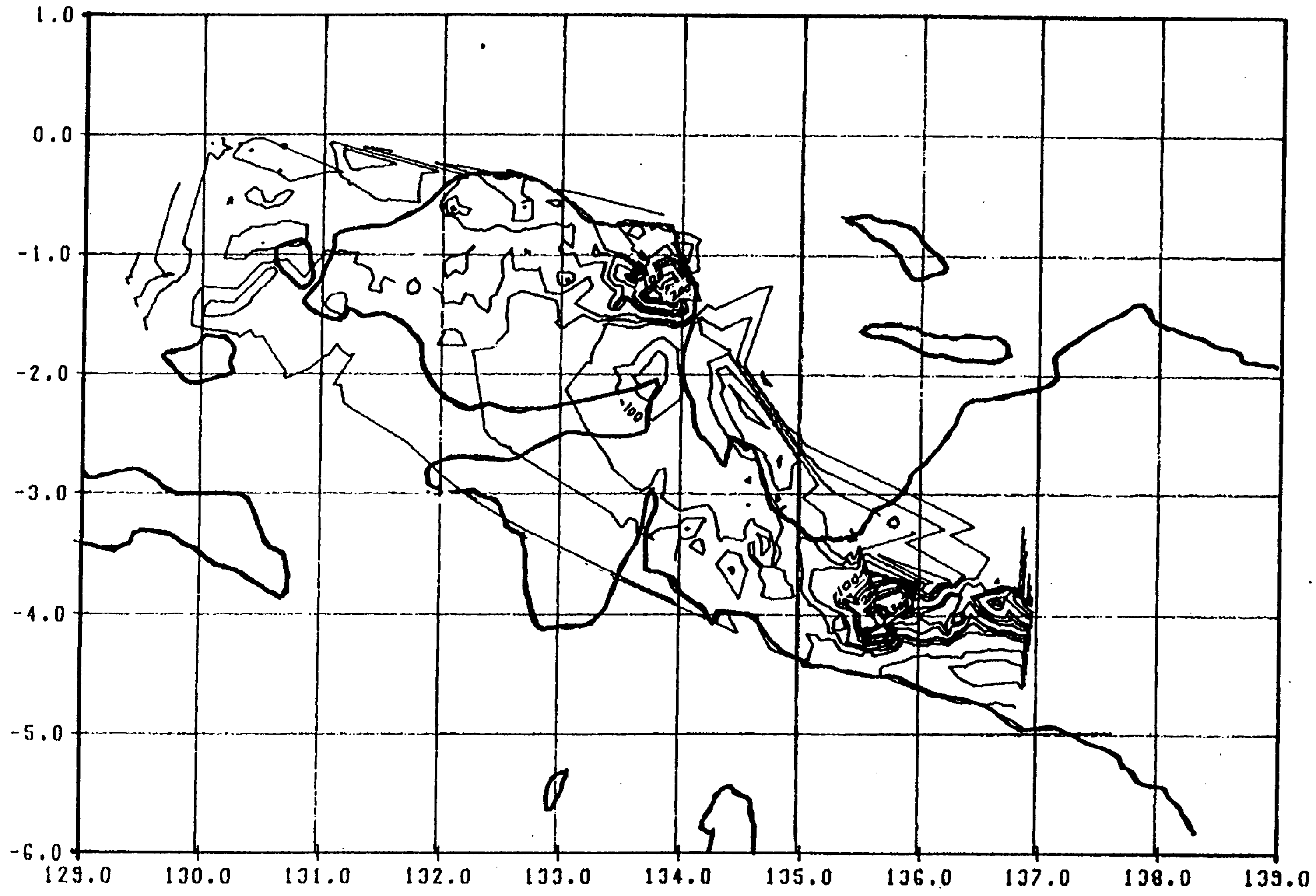

Figure (3-5)

The residual gravity anomaly

The precision of the gravity anomalies

In this investigation, the free-air anomaly has been involved in evaluating the Stokes' integral. The precision of the free-air anomaly depends on the precision of the elevation applied in the observed data reduction. In this case, the barometric levelling was used in measuring the elevation of the gravity point. Theoretically, if the most rigorous barometric technique is used, the degree of accuracy of the barometric heighting is about 2m in both flat and rolling terrain [Krakiwsky, 1982]. In practice, the results that were obtained from the survey over the subject region showed an error ranging from 2 to 10 m [Untung, 1982].

3.1.2. The control data set.

The heights above the ellipsoid can be indirectly determined from Doppler satellite observations. The position of a point in X,Y,Z can be determined by observing and interpreting the signals emitted by satellites in the US Navy Satellite System (NNSS). The X,Y,Z coordinates can then be transformed into geodetic coordinates ϕ,λ,h using the standard relationships (Torge, 1980, p. 52).

To date about 126 Doppler points have been established in Irian Jaya and in some of the smaller islands around it. The field work as well as the coordinate adjustment computations of these control points were done by The Indonesian National Agency for Mapping and Surveying, who has made this data set available.

The relative accuracy of the ellipsoidal height derived from Doppler observations is estimated to be about 1 meter.

The list of the original Doppler-derived positions consists of the identification number of the station, name/location of the station, the position in latitude and longitude, the ellipsoidal and orthometric height. This original data set (in file DOPPLER.DAT) has been reformatted (to file IRDOP.DAT) to enable reading by the UNSW suite of programs used in this project.

In conjunction with the Doppler campaign, Airborne Profile Recording (APR) observations were done by the Cendrawasih Joint Project of the Royal Australia Air Force and The Indonesian Army. From this, the orthometric heights of the control points were obtained. Since neither levelling measurements nor suitable topographic maps of this area are available, the orthometric heights derived from APR are the best (and, in fact, the only) ones available.

APR is a technique of height measurements where a continuous profile of the terrain is measured by radar ranging from an aircraft. The accuracy of the elevation derived from this observation is about 3m to 5m [Krakiwsky, ibid].

The distribution of the Doppler control points is presented in Figure 3-6. If this figure is compared with the the gravity points distribution (Figure 3-1), it is obvious that there is a deficiency of gravity stations around some control points. Ideally, we would like gravity observations here to be uniformly and densely (i.e. 10 km spacing) distributed. For this reason, we limit our comparison to those control points at which the gravity points are well distributed. This matter is discussed further in Section 4.2.

3.2. Computational technique.

The suite of geoid computation programs for the gravimetric solution of N has been developed at School of Surveying, UNSW and the method called *'RINT'* (RIng INTegration) has been applied for this project. The program is written in FORTRAN language and installed on the UNSW's VAX mainframe system.

The software consists of five main programs which are run separately. The simplified flowchart for running the programs used to compute the geoid undulation is described in Figure 3-7. For comparing the resultant gravimetric geoid values with the "control" N values from the combination of Doppler/APR, GRAV08, is used. See Figure 3-8.

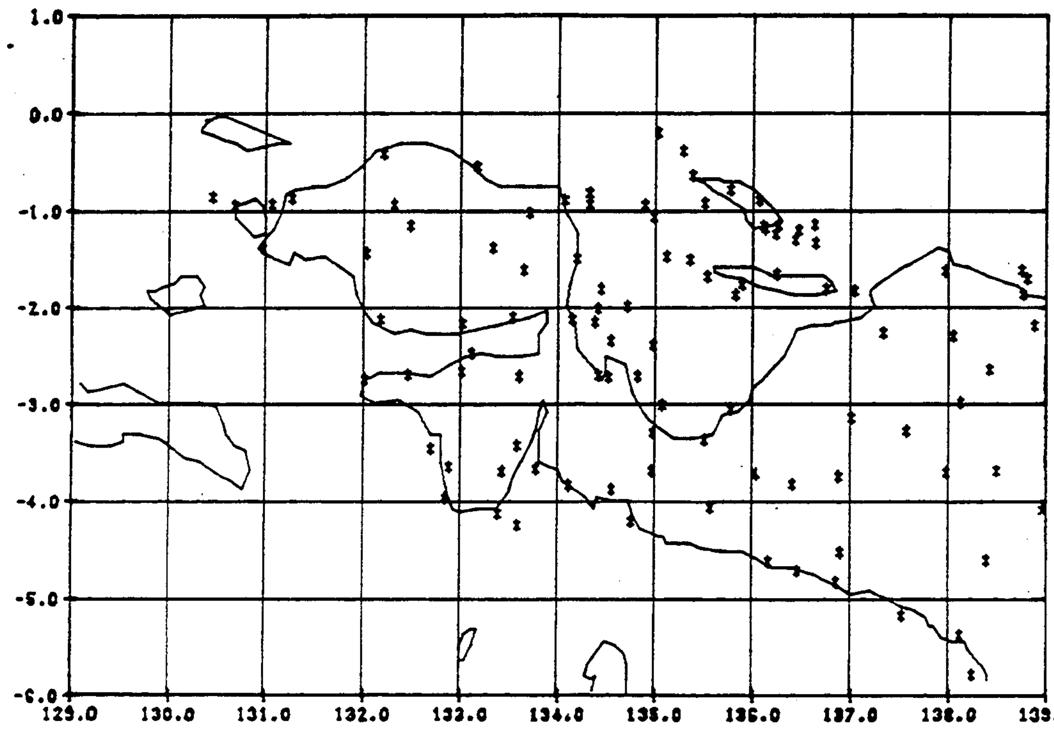

Figure 3-6: The distribution of Doppler control points

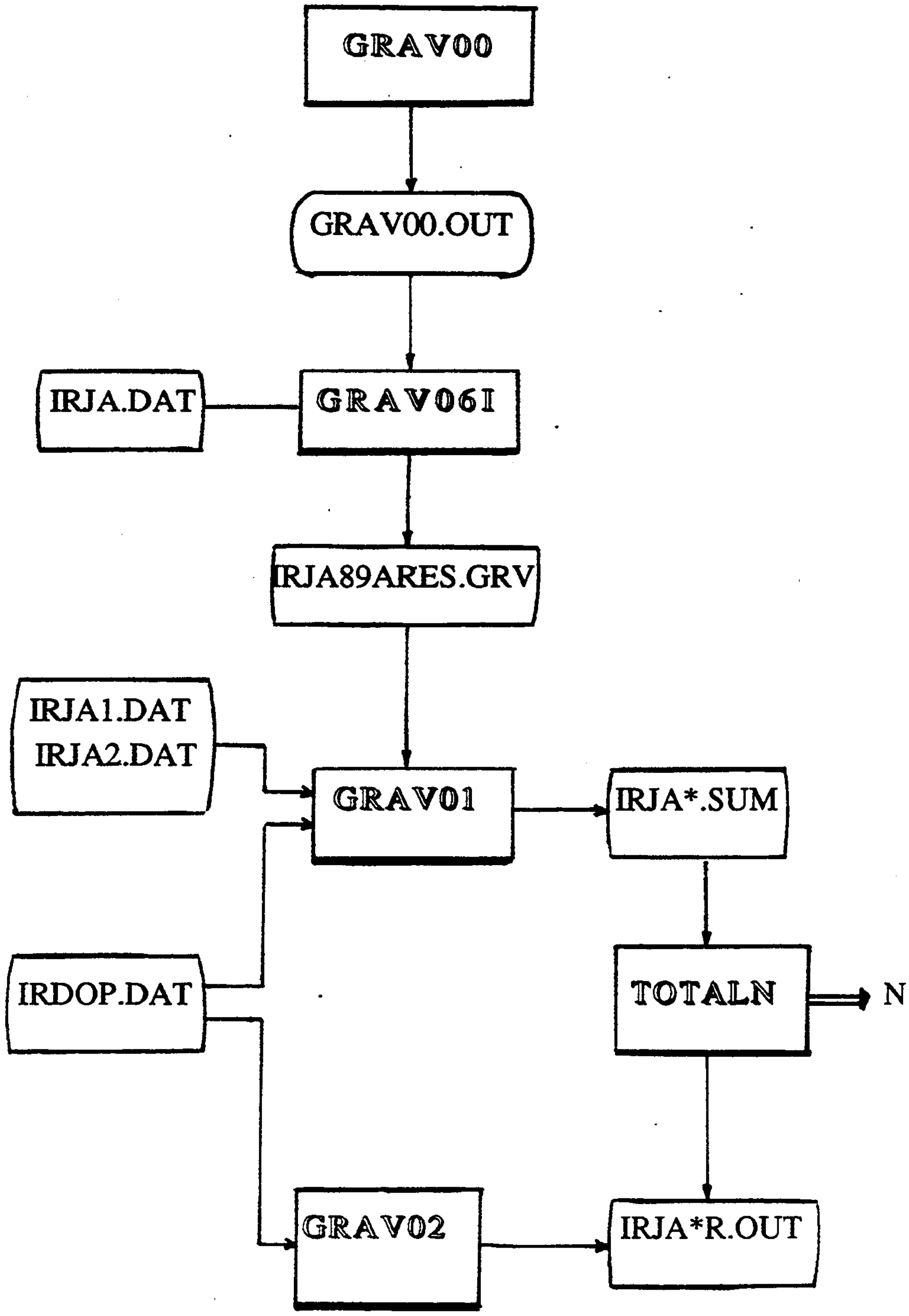

Figure 3-7: Flowchart of programs to evaluate N gravimetrically

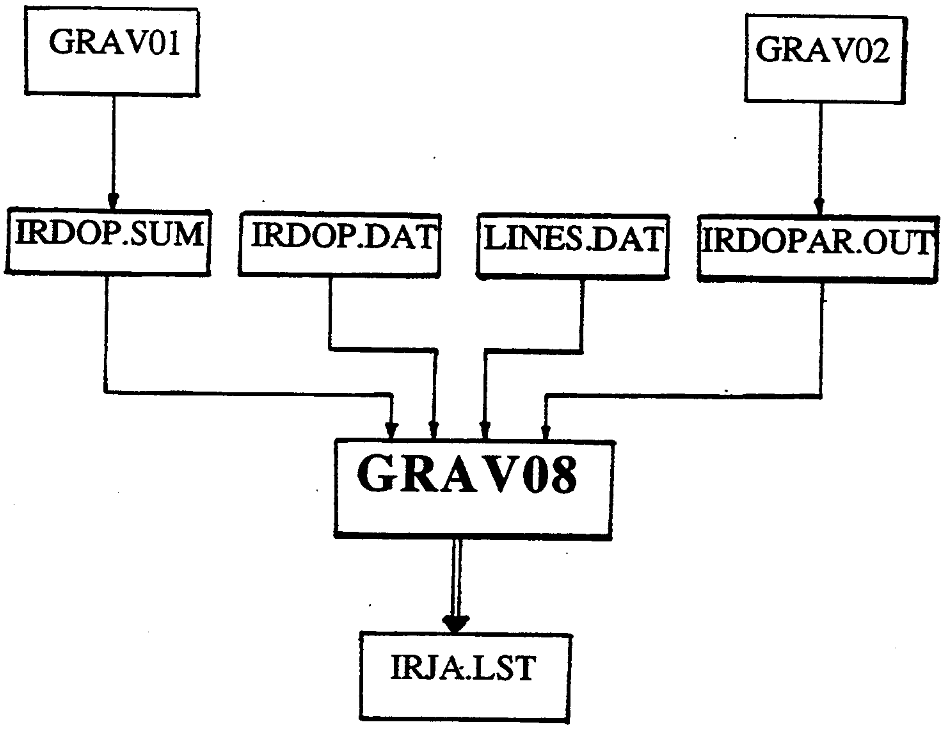

Figure 3-8: Flowchart for comparison of gravimetric N with control

3.3 Evaluation of medium to long wavelength component .

The computation for the medium to long wavelength contribution (N_l) was carried out by running either GRAV00 for gridded data or GRAV02 for points positions. The programs calculate the geoid height using the fully normalized potential coefficient of the spherical harmonic expansion.

To calculate the N_l values over the gridded points, we run the program GRAV00. The input file contains the information about the geopotential model to be used (i.e., OSU89A), maximum degree and order of the geopotential model (e.g., 360), and the geographical limits of the grid with the specified grid spacing. Besides computing the geoid, this program can also compute the gravity anomalies values by specifying a certain parameter in the input data file. The output (results) file is specified as GRAV00.OUT.

If we want to compute the N_l values at a specific point the program GRAV02 is used. Unlike GRAV00, the coordinate of each point must be given in the input data file. Other input parameters are the name of the geopotential model (in this case, OSU89A), the flattening factor of the reference ellipsoid (298.26), and the degree of the harmonic expansion (360). The output result is called by IRJA*.OUT.

3.4 Evaluation of the short wavelength component.

The computation for the short wavelength (N_S) was carried out by running the program GRAV01. This program computes the geoid heights of each point in the network using the residual gravity anomaly data set (Section 3.1.1).

The parameter file is prepared listing the coordinates of the computation points, and the name of the file of residual gravity anomalies (eg. IRJA89ARES).

3.5. The Total Geoid Height.

The total geoid height at each point in the network, as written in Eq. (9), is obviously the sum of those two output files from sections 3.3 and 3.4 respectively. The program TOTALN is used to combine the two components. The results are then plotted to produce the final gravimetric geoid map.

4 COMPARISONS OF GRAVIMETRIC GEOID HEIGHTS WITH DOPPLER/APR GEOID HEIGHTS

The comparison of N values was made at those points of the control network at which both Doppler-derived h and APR-derived H were available, and which had a reasonable density of gravity coverage around them. The way in which the N values are found using satellite-derived heights and orthometric levels is described in Section 1.3(iv), and the data used in this evaluation described in Section 3.1.2.

4.1 The control geoid heights

The geoid undulation at control points located in Irian Jaya region have been calculated using Equation (9) above. Over the whole 126 control data set the geoid heights varies from a minimum value of 59 m in the south-west to a maximum of 71 m in the north-east.

The accuracy of the control geoid heights obviously depends on the accuracy of h and H. The accuracy of the h values derived from Doppler satellite observations depends on many factors related to the field measurements and the data adjustment computation. There is no formal estimate of precision given in the original data set supplied. However, as a guide, the accuracy of the height component of a well-determined Doppler station is approximately about 0.7 m (Rapp, 1984). The relative accuracy along a baseline of 50 km has been estimated to be 0.8 m (Kouba, 1976a). The absolute accuracy of the height of the Doppler station above the ellipsoid computed by using the propagation of variances gave the value about 1.4 m (Kahar, 1981).

The accuracy of the H components as measured by the APR depends on the stability of the isobaric surface during the terrain profiling. The APR use pulsed microwaves having an accuracy of about 3 m (Krakiwsky, 1981).

4.2 Gravimetric geoid computation for control points.

The gravimetric geoid computation for the control points position was done by using the remove-restore technique described in Chapter 3. The N_{Grav} is the combined value of the N_l and N_s (Equations 8 and 10, respectively).

Not all the control points are suitable for the computation of the short wavelength component N_s, as there is insufficient gravity coverage around some of them for a meaningful solution. For calculating the N_s contribution, a dense (10 km) terrestrial gravity net within a radius of cap size ψ_o (in our case, at least 0.5°) around the point computation is desirable. On considering this limitation, we find only 16 out of 126 control points with sufficient gravity data for a proper evaluation. The location of these points is shown in Figure 4-1.

The N_s computation is done by implementing the program called GRAV01 of the *'RINT'* software. The input data file contained the name of the terrestrial data file, the maximum ring size (in this case, 0.5°) and the geographic coordinates of the computation points (the list file of this points called IRDOP.DAT). The terrestrial gravity data used is the residual gravity anomaly data set called IRJA89ARES (see Sec. 3-1).

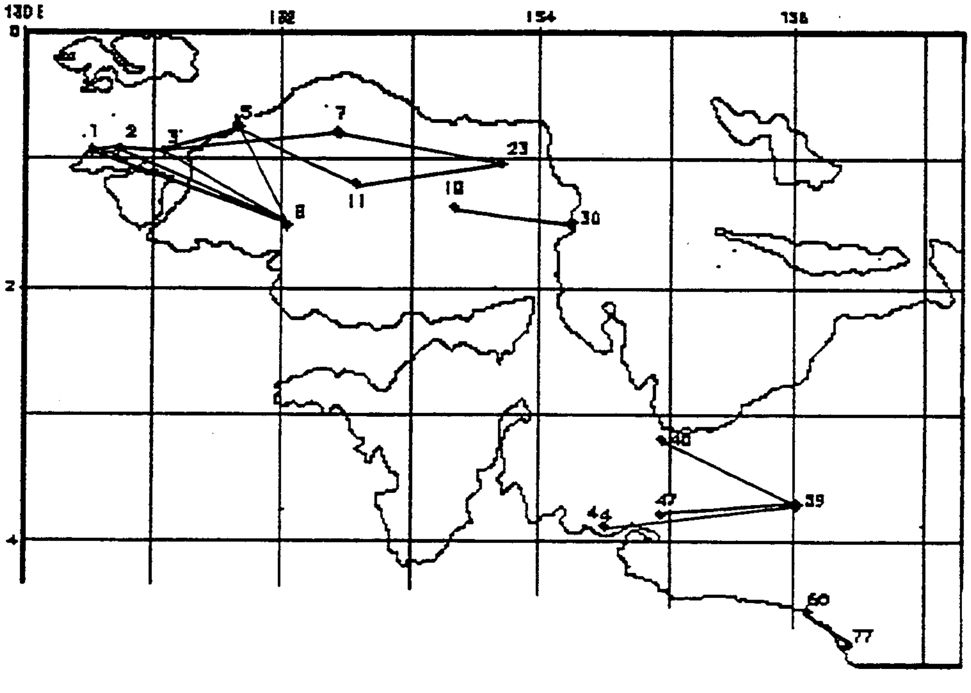

Figure 4-1 : The location of the control points and baselines.

As mentioned.above, the integration of the detailed gravity was computed over a spherical cap size of radius up to 0.5°. The contribution coming from this computation varies between 0.1 m and 7.2 m. This maximum result is large when compared with values obtained from more benign (and better surveyed) areas. This relatively large N_S component mainly comes from the gravity anomaly values close to the computation points. Nevertheless, since the terrestrial gravity data being used in the computation is the residual anomaly referred to OSU89A (Section 3.1.1), the values of N_S obtained are expected to be the best possible under the current conditions.

For the medium to long wavelength contribution (N_l), the calculation was carried out at the 16 selected points by using the program GRAV02.

The input data file prepared consisted of the values for the ellipsoid flattening used, the degree of the harmonic expansion and the same list of the geographic coordinates (IRDOP.DAT) of the computation points used in calculating N_S. The geopotential model was OSU89A, with the complete harmonic expansion of up to degree and order 360.

Those two values are then combined by using program TOTALN. Table 4-1 shows the total gravimetric geoid height value and the geoid height derived from the control at each of the selected control points. The N_{GRAV} values are tabulated from ring 0 to ring 5.

From the 16 control points shown in Table 4-1, 85% improve when the N_S contribution is included in the N_{GRAV} comparison (i.e., $N_{GRAV} - N_{control}$ becomes smaller). The exceptions occur at point numbers 23 and 59, where the deviation increases when N_S is added; by about 2 m for point 23 and 1.6 m for point 59. At this stage we can offer no reason why this occurs.

Table 4-1: Comparison of N_{GRAV} and $N_{control}$

Point #	N Gravimetric (m) Ring 0	3	4	5	N control (m)
1	72.93	73.72	73.62	73.52	67.6
2	72.77	73.13	73.05	72.87	67.4
3	73.98	72.84	72.79	72.67	67.4
5	72.91	72.84	72.78	72.73	67.6
7	74.62	74.34	74.38	74.44	67.7
8	72.60	71.45	71.12	71.12	65.6
11	73.84	73.27	73.03	72.85	67.0
19	72.00	71.73	71.69	71.57	66.5
23	72.50	73.95	74.36	74.54	68.0
30	72.83	71.94	71.72	71.37	66.8
44	67.85	66.10	65.58	65.06	61.0
46	70.49	68.49	67.79	67.01	62.6
47	69.72	67.56	67.03	66.75	61.9
59	69.35	69.80	70.19	71.94	63.1
60	67.16	62.78	61.31	60.00	61.9
77	66.89	62.76	61.40	61.40	62.2

4.3 Comparison N_{GRAV} with $N_{control}$.

The comparison between the control and gravimetric geoid heights was made on the 16 selected control stations. The differences were analysed for N_S contributions of rings 0, 3, 4 and 5 at each point. The mean and the rms values of the deviations were simply calculated by :

$$\overline{\Delta N_R} = \frac{\sum_{i=1}^{n} \Delta N_i}{n} \quad \ldots (13)$$

and

$$\text{rms dev} = \left(\frac{\sum_{i=1}^{n} \left(\Delta N_i^2\right)}{n} \right)^{\frac{1}{2}} \quad \ldots (14)$$

where,

$\Delta N_i = N_{grav} - N_{control}$ at i^{th} point.

ΔN_R is the mean values at certain ring .

n is the numbers of control points in the network.

The result of this comparison is shown below.

Table (4-2): The analysis of the difference between N_{GRAV} and $N_{control}$

# Ring	Mean Deviation	RMS Deviation
0	6.07	6.16
3	5.15	5.41
4	5.04	5.32
5	5.06	5.36

From Table 4-2 above, it can be seen that the mean deviation decreases with an increasing in ring size. The least deviation occurs at ring 4, i.e., the mean deviation between the geoid height from control data and the geoid height from gravity data is 5.04 m. It was expected that this value would decrease at ring 5, where in fact it slightly increases by 2 cm. Since the distribution of the terrestrial gravity data allows integration only up to ring 5, it was not possible to describe the behaviour of the ΔN_R beyond this ring. It could be possible that, for ring sizes greater than 0.5°, the deviation will decrease again to less than the value given at ring 4. Nevertheless, under present conditions, it appears that computing N_s with cap size of 0.4° for N_{GRAV} gives the best agreement with $N_{control}$ over the 16 control points.

4.4 Comparison of Differences in ΔN values along the baselines.

The comparison of ΔN values through the network is now carried out over the selected lines, and related to the line length to find the relative error. The calculation is done between two stations along the line according to the following.

$$\delta N = \Delta N_{control} - \Delta N_{GRAV} \qquad \ldots\ldots (15)$$

where,

$\Delta N_{control}$ is the control geoid difference between the two points.

ΔN_{GRAV} is the gravimetric geoid difference between the two points.

The absolute difference ($|\delta N|$) is divided by the length of the line and expressed in parts per million (ppm). This is then averaged for all lines to get the mean and rms values, thus.

$$m = \frac{\sum_{i=1}^{n} \left|\frac{\delta N_i}{s}\right|}{n} \times 10^6 \quad \ldots \quad (16)$$

and,

$$rms = \frac{\sum_{i=1}^{n} \left(\frac{\delta N_i}{s}\right)^2}{n} \times 10^6 \quad \ldots \quad (17)$$

where,

m is the mean difference in parts per million.
s_i is the length of i^{th} line.
n is the numbers of baselines.

The ppm values are calculated by using program GRAV08. To run this program, a command file with the control points file (IRDOP.DAT), the name of file containing the baselines configuration (LINES.DAT), and the names of the output files of GRAV01 and GRAV02 was prepared. The comparison was done up to the maximum cap size 0.5°. The output file, called IRJA.LST, is then analysed. By including all the possible lines of the 16 selected points in the network, the rms values varied from 11.8 ppm to 30.9 ppm. By omitting the lines of distances greater than 200 km the rms values slightly decreased with the variation between 11.0 ppm to 28.8 ppm.

Because the aim is to compute the best relative geoid over lines of normal geodetic length, the analysis is now limited to lines of less than 200 km. By excluding some short lines which were clearly suspect (i.e, lines whose agreements were worse than 20 ppm), the final configuration of the lines which gives the best values of the comparison is shown in Figure 4-1. Most of the selected lines present in the network happen to lie in the east-west direction and have an average length of about 130 km. The network consists of 17 lines.

The result of this comparison is shown in Table 4-3. From this, the OSU89A model appears to recover the relative geoid at about 10 ppm, where the combined geopotential/terrestrial gravity solution significantly improves the comparison, with the best value (i.e., 5.4 ppm) coming at ring 3. This indicates the best agreement between ΔN_{GRAV} and $\Delta N_{control}$ along the baselines appears when the N (gravimetric) was computed with the optimum cap size of 0.3 degrees. It should be noted that this cap size agrees with the optimum cap size established from an independent study of the Philippines geoid, where GPS and conventional levelling were used to provide control for the geoid solution (see Kearsley and Ahmad, this volume).

Table (4-3): ΔN analysis for various cap size

# Ring	mean ppm	rms ppm
0	9.6	10.1
1	7.2	8.0
2	4.7	5.6
3	4.5	5.4
4	5.6	8.2
5	10.4	12.0

4.5 Discussion Of The Results

The local geoid undulation of the Irian Jaya region has been investigated using the well-known 'remove-restore' technique, as described in the previous chapters. Using the 16 suitable control points, the ΔN_{GRAV} has been tested against the $\Delta N_{control}$ 'values' along the selected baselines.

The result from the comparison shows a good agreement between the two geoid determinations. The rms deviation of 5.4 ppm over the baseline distance of 130 km indicates that the optimum evaluation of the gravimetric geoid fits the control geoid with the relative error of about 0.7 m. This comparison in fact is surprisingly good, given the possible errors in the $N_{control}$ (see sec. 3.2.1).

Obviously, the accuracy of this result depends on the precision in Doppler-derived geoidal height, the orthometric height from the APR observations, the free-air gravity anomalies and the geoid undulation values given by the geopotential coefficient model.

Theoretically, and ideally ,we would like a precise orthometric height accuracy of 0.1m, the accuracy of the Doppler-derived geoidal height will be about 0.33m for precise ephemeris and 0.96 m for broadcast ephemeris. Since the orthometric height here, obtained from the APR measurements, has an accuracy of 2 - 3m, and assuming the precision of the ellipsoidal height derived from Doppler is 1m, the error of the control derived geoidal height is expected to be between 2.2 to 3.3 m.

The error introduced by the gravimetric geoid depends on the precision of both the N_s and the N_l computations. The error in N_l, i.e., the accuracy of the geopotential model OSU89A, is estimated from Rapp's global geoid map [Rapp & Pavlis, 1990] to be about 40 cm over the Irian Jaya region. The precision of the N_s value is mainly dependent on the error of gravity measurements and the elevation used for data reduction. At least for 3 m error in elevation may contribute 1 mGal error in the free-air anomaly values. If this error can be achieved over 0.1° block areas, then the computation of N_s based on the terrestrial data under this ideal condition, gives an accuracy of "better than ±5 cm over 100 km" [Kearsley, 1986].

Clearly, the data used falls well short of the data specifications for high-precision geoid evaluations. The very good results we have achieved may be because the errors that are present in the data, notably the APR and Doppler data, and in the height data used for the gravity stations, are systematic, and tend to cancel over the distances involved in our comparisons.

The comparison of the gravimetric and the control geoid height at each station gives a mean of the absolute difference of 5.04 m (see Table 4-2). This is large, especially when compared with another Doppler-based control/gravimetric undulation comparison made in fairly rugged areas of the USA [Rapp & Wichiencharoen, 1984]. Here the difference of 1.6 m was found over 10 discrete points. After applying a terrain correction, this difference was reduced to 0.1m. The relatively large difference in Irian Jaya probably reflects the comparative weakness in the gravity data from this region used in the solution of the OSU89A coefficients, and the poor quality of the height information used in the gravimetric solution. Because of this poor (or non-existent) height information, no terrain corrections were attempted.

4.6 The Optimum Geoid for Irian Jaya region.

Based on the results given in Sections (4.3) and (4.4), the local gravimetric geoid of the Irian Jaya region was determined. By considering the distribution of the gravity data, the full gravimetric geoid can not be computed for the whole region at this stage. The area is limited by the availability of adequate gravity data, and bounded by latitude 0° to 4° and longitude from 131° to 135°. N values on a grid of 0.2° are generated over this subject area (see Figure 4-2).

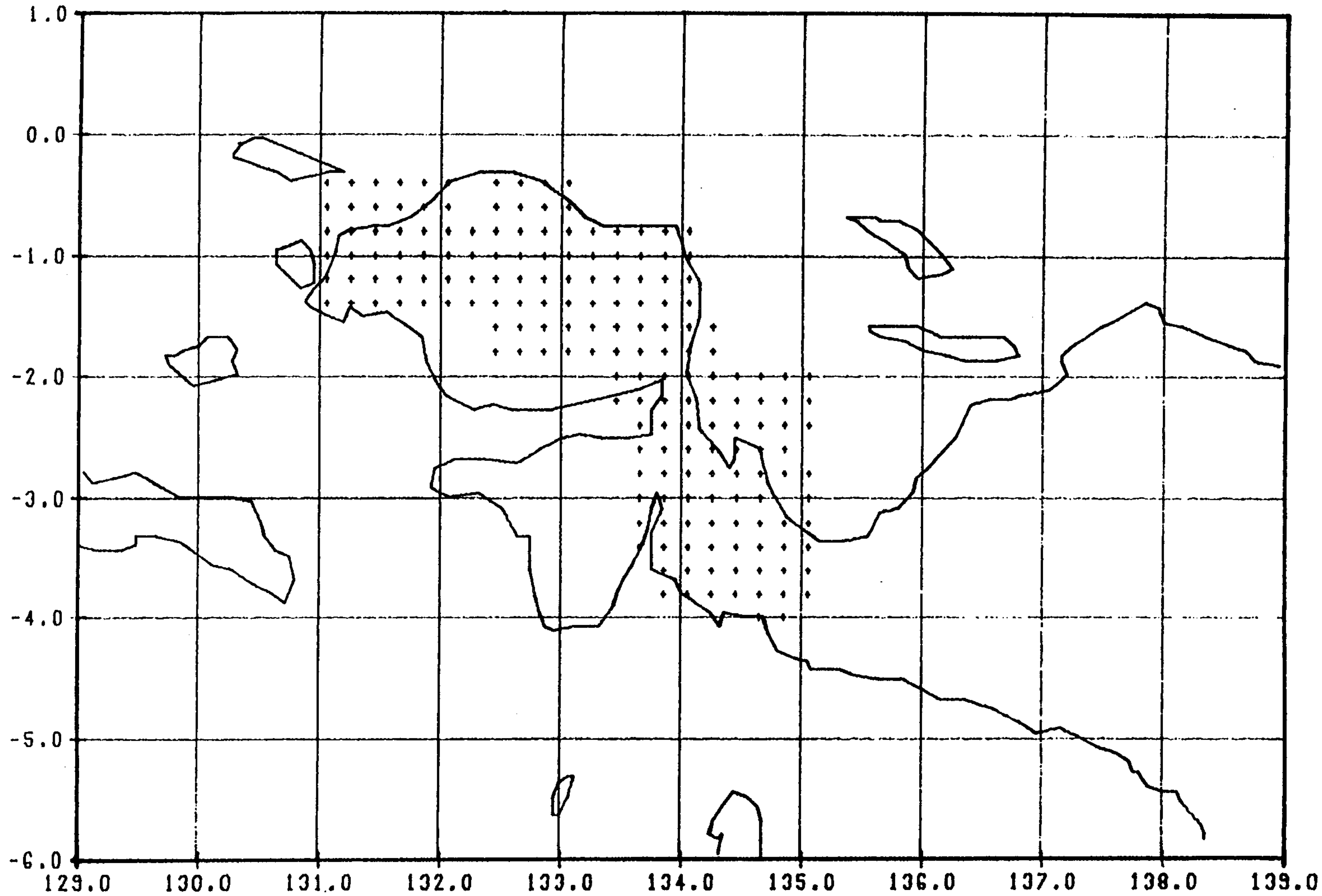

Figure (4-2)

The location of gridded points in used for the test area.

The medium to long wavelength contribution to N are computed over these grid points using program GRAV00, based on OSU89A to degree and order 360. The computation shows the values vary from 51 to 75m. Figure 4-3 shows the contours of these values with 1m contour interval.

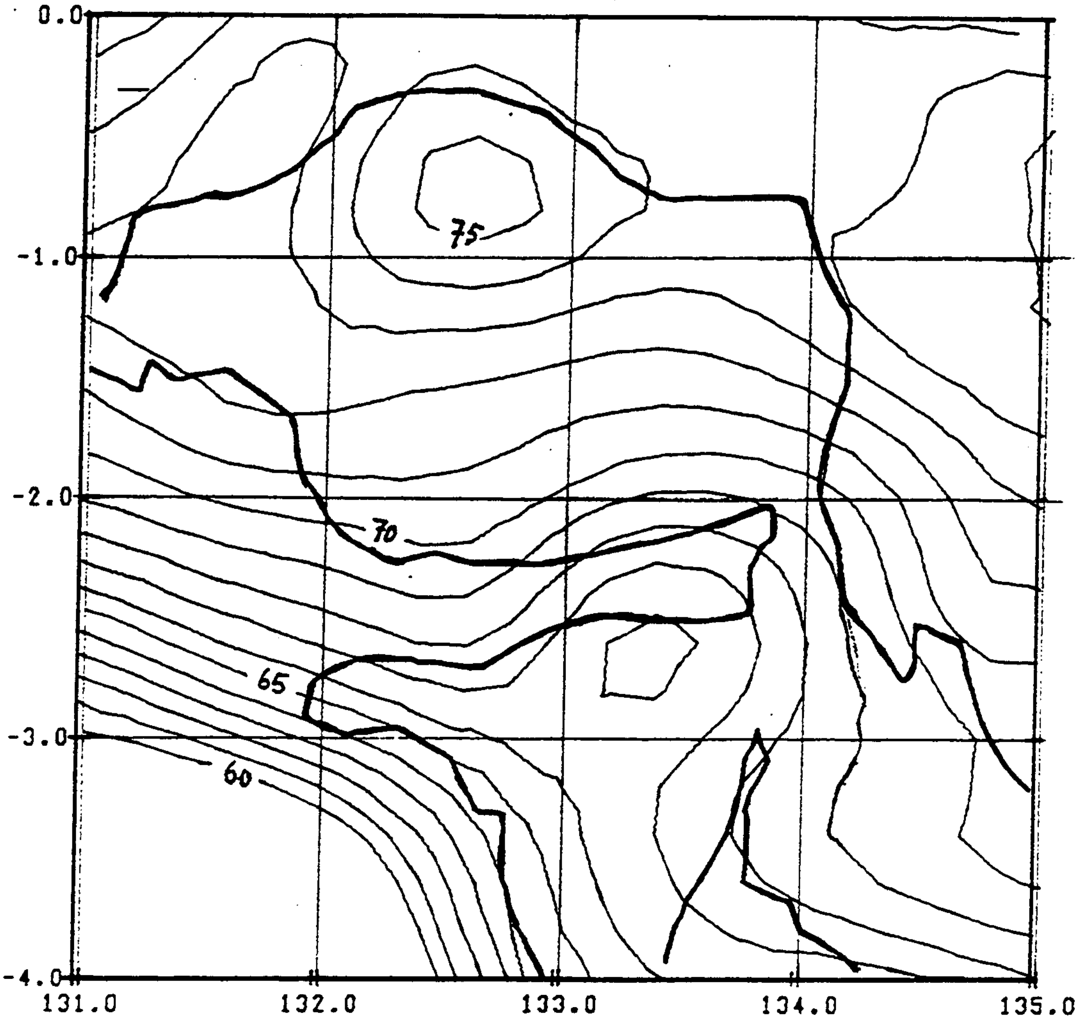

Figure 4-3: The Geoid Map of the Test Area based on N_1 values

The geoid contribution of the short wavelength field was computed by using program GRAV01 over the respective grid points using the residual gravity data set in IRJA89ARES. A cap size of integration up to ring 3 was selected for this computation because it gave the best comparisons with the control for the relative geoid (see Sec. 4.4). The result of this N_S computation gave significant contributions, the largest amount being 6.3 m.

N_S and N_l are then summed at each grid point. These total values were contoured to produced the geoid map (Figure 4-4). We feel that this is the optimum gravimetric geoid solution which can be made under the present conditions, for the Irian Jaya region.

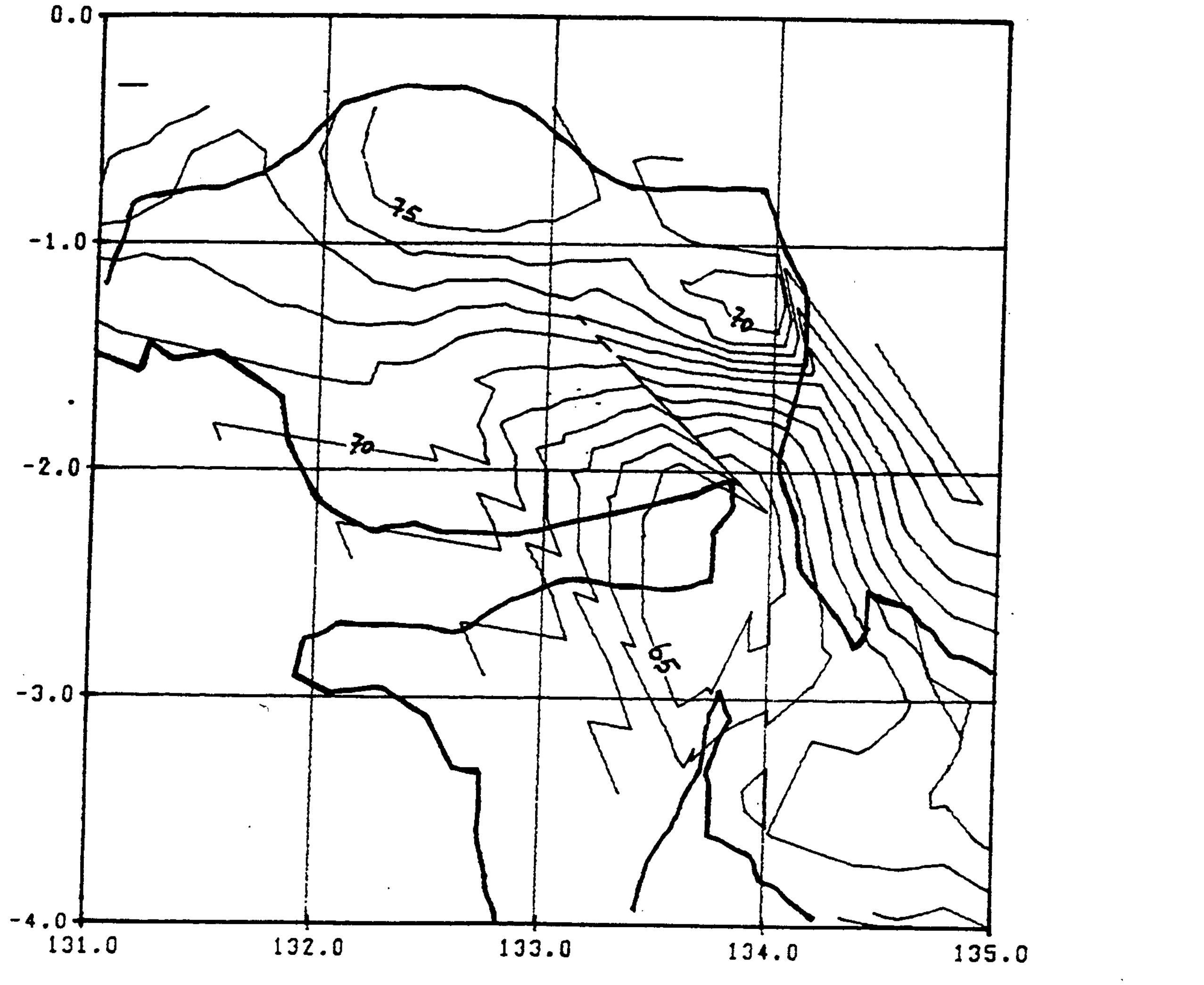

Figure 4-4: The geoid map of the test area based on the total gravimetric geoid solution.

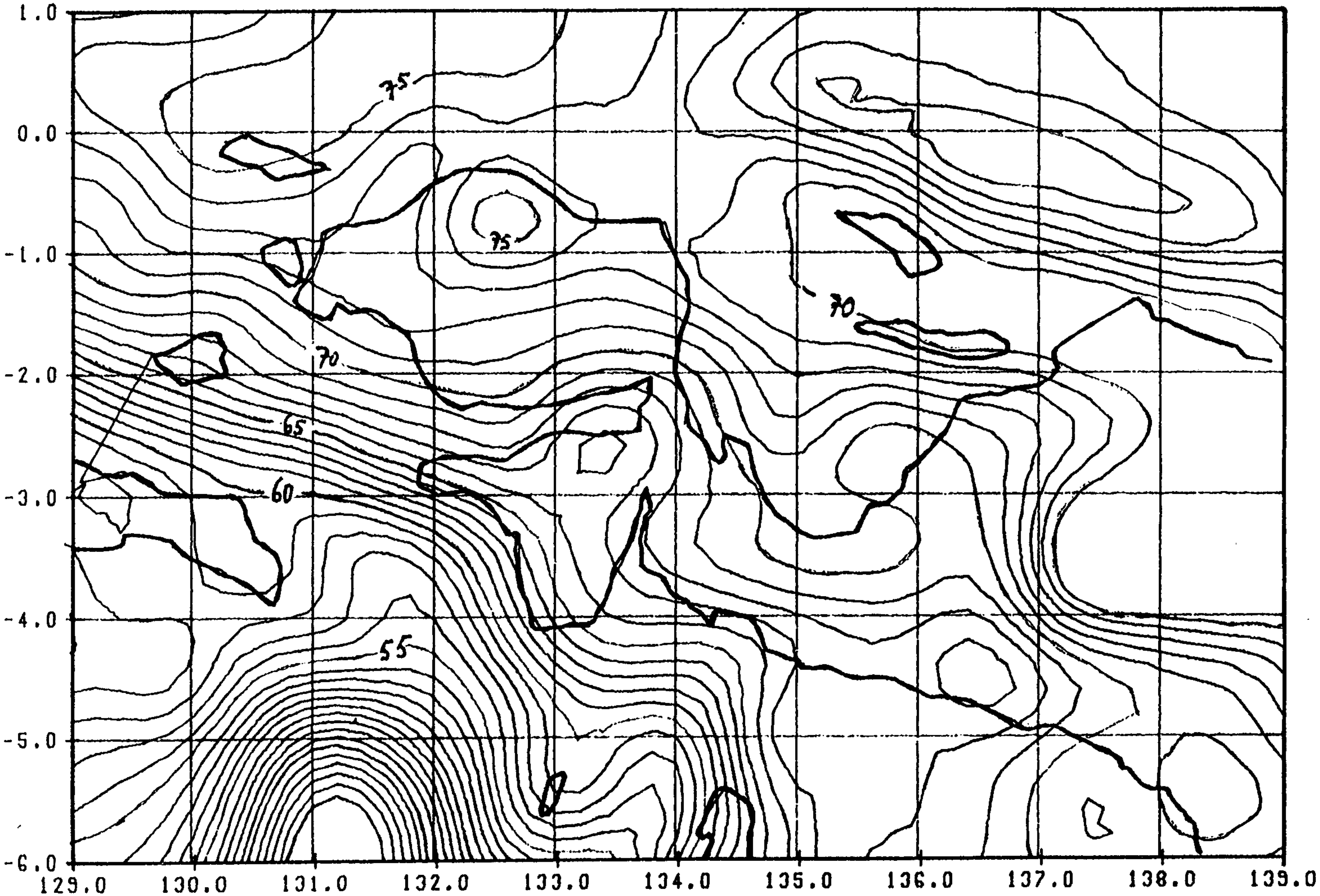

Figure (4-5)

The medium to long wavelength geoid map of Irian Jaya
calculated from the geopotential model OSU89A

5. CONCLUSION

The local gravimetric geoid undulation of the Irian Jaya region has been computed using the 'remove-restore' technique, using the optimum configuration as determined by comparisons with available control.

The OSU89A geopotential model appears to recover the relative geoid at about 10.1 ppm, and the geopotential/terrestrial gravimetric solution significantly improves the comparison with the best ppm value (i.e., 5.4 ppm) occurring at a cap size of integration of $\psi_o = 0.3^\circ$. This cap size agrees with that established from an independent study of the Philippines geoid.

The optimum comparison of 5.4 ppm in fact is better than the value obtained for the Philippines geoid, where GPS and conventional levelling were used to provide the control for the geoid solution. One reason may be that, since terrestrial gravity observations in Irian Jaya region were done for geophysical interpretation, the measurements are fairly closely spaced, even though only about 30% of the land is covered. Thus, the local terrestrial gravity data observed for Irian Jaya may be better (i.e., more recent and more coherent) than that for the Philippines.

The comparison of the absolute geoid heights at the control points showed that the difference decreases when taking into account the N_s contribution for all except two points (i.e., point numbers 29 and 59) where the difference increases significantly. These two exceptions are located in very hilly terrain and have an elevation greater than 1000 m. Since the topographic data of Irian Jaya is not available, no terrain correction has been applied in our calculations. Given the region is topographically rugged, one should incorporate the terrain correction in the geoid calculation. However, experience has shown that, where the digital terrain models are poor, (such as they are here), the application of the terrain correction actually degrades the solution.

Although the comparison of the gravimetric N values with the control N values over selected lines in this region have a relative accuracy of about 5.4 ppm, we are reluctant to claim this relative accuracy for the gravimetric geoid computed for throughout the region, given the large topographic effects which must be present, and the poor quality of the elevation data, and the paucity of gravity data in some parts of the area covered.

Before an improved geoid can be computed for this region, we will need :

(1) An accurate digital elevation model (DEM), preferably at about 1 km grid spacing to maintain the random error in the free-air anomaly at less than 3 mGal over the 0.1° block, especially as the region contains such rugged terrain.

(2). A better overall coverage of gravity observations, possibly in a nominal 10 km spacing for the flat areas and denser over the mountainous region.

(3) Better geometrically determined geoid values of the control points, possibly derived from the combination of GPS/Levelling measurements.

6 REFERENCES

Allman, J.S., (1982). "A geoid for South East Asia and the Pacific". *Aust. J. Geod. Photogram. Surv., 36* , pp. 59-63.

Dow, D.B., and Hartono, U. , (1982). "The nature of the crust underlying Cendrawasih Bay, Irian Jaya" *Geol. Res. and Dev. Centre Bulletin, 6,* pp. 30-36.

Fosberg, R. (1990). " Preliminary Geoid computation in the Philippines area by FFT", *Aust. J. Geod. Photogram. Surv., 52,* pp. 1-20.

Gilliland, J.R., (1989). " A gravimetric geoid of Australia ". *Aust. Surv., 34 (7),* pp. 699-706.

Heiskanen, W. A, and Moritz Helmut, (1967). "*Physical Geodesy*", Freeman & Co., San Francisco.

Kahar, J. , (1981). " *Analysis of Geoid in Indonesian Region* ". Ph.D. thesis, Institute of Technology Bandung, unpublished.

Kearsley, A.H.W., (1976) " The computation of deflections of the vertical from gravity anomalies" *Unisurv. S-15, School of Surveying, Univ. of New South Wales.*

Kearsley, A.H.W., (1985). " Towards the optimum evaluation of the inner zone contribution to geoidal height", *Aust.J. Geod. Photogram. Surv., No.42,* pp. 75-98.

Kearsley, A.H.W., (1986a). " The determination of precise geoid height differences using ring integration" Proc., *IAG Symposium on the Definition of the Geoid,* Florence, Italy, May, 1986.

Kearsley, A.H.W., (1986b) " Data requirements for determining precise relative geoid heights from gravimetry", *J. Geophys. Res., Vol. 91,* No. B9, pp. 9193 - 9201, August 10, 1986.

Kearsley, A.H.W., (1988). " Tests on the recovery of precise geoid height differences from gravimetry". *J. Geophys. Res., Vol. 93,* No. B6, pp. 6559-6570.

Kearsley, A.H.W, (1991). "Geoid determinations in the Philippines"Presented at the XXth IUGG General Assembly, Vienna, August, 1991.

Kouba, J., (1976). " Doppler Levelling". *The Canadian Surveyor , Vol. 30,* No.1. March.

Krakiwsky, E. and Vanicek, P., (1981) "*Geodesy - The Concepts*",.North Holland, Amsterdam.

Marsh, J.G., et. al., (1988). "A new gravitational model for the Earth from satellite tracking data: GEM-T1". *J. Geophys. Res., 93,* pp. 6169-6215.

Marsh, J. G. et al., (1990)," The GEM-T2 gravitational model", *J. Geophys. Res., 95*, No. B13, pp. 22,043 - 22,071.

Rapp, R.H, (1973), " Accuracy of geoid undulation computation" *J. Geophys. Res., 78*, pp. 7589 - 7595.

Rapp, R.H., and Wichiencharoen, C., (1984), " A comparison of satellite Doppler and gravimetric geoid undulations considering terrain-corrected gravity data" *J. Geophys. Res.,89*, No. B2, pp. 1105 - 1111.

Rapp, R. H., and Cruz, J. Y., (1986). " Spherical harmonic expansion of the Earth's gravitational potential to degree 360 using 30' mean anomalies ". *Report No. 376, Dept. Geod. Sci., Ohio State Univ.*, Columbus.

Rapp, R.H., and Pavlis, N.K., (1990) " The developement and analysis of geopotential coefficient models to spherical harmonic degree 360", *J. Geophys. Res., 95*, No. B13, pp. 21,885 - 21,911.

Untung, M. (1982)," Gravity and magnetic study of the Kepala Burung Region, Irian Jaya, Indonesia". Ph.D Thesis, Univ. of New England, unpublished.

OPTIMISING GPS, GEOID AND TIDE GAUGE HEIGHTS IN VERTICAL CONTROL NETWORKS

Z. Ahmad
A.H.W. Kearsley
B.R. Harvey

School of Surveying, University of NSW, P.O. Box 1, Kensington 2033.

ABSTRACT

A method to integrate GPS-derived ellipsoidal heights and gravimetric geoid heights into a levelling network has been developed using a heterogeneous data set and giving due weights to the respective observations, in order to achieve a homogeneous heighting system with optimum values for each of the parameters h, H and N. A variety of numerical methods have been tested, with the Bayesian least squares approach with station constraints proving to be most effective. This approach also allows the incorporation of 'point' height data (e.g. H at tide gauges or h at SLR stations) with their respective accuracies. Results of a number of smaller networks, subsets from surveying networks in New South Wales, South Australia and the Philippines are presented to show the impact on the adjustment when changes are made to the observation precisions and to the point value accuracies, and the way in which the technique is used to identify gross errors or suspect data. From the results of the adjustment, decisions on whether to incorporate GPS into the existing network, to re-level certain parts of the network, or to supply geoid heights with improved accuracies, can then be made.

1 AIMS AND SIGNIFICANCE

We are nowadays presented with a problem of having three different heighting systems, heights which are defined on different refence surfaces and obtained from different sources. Although obtained independently, these heights are geometrically related, and this relationship can be used to solve for a homogeneous and optimum heighting system from a hybrid data set.

The use of heterogeneous height data which include GPS vectors, geodetic levelling and gravity data is certainly not a new era of studies. So far this has only been used to determine the geoid. One approach is to fit a surface of appropriate degree to all geoidal information, in an optimised form (Vanicek and Kleusberg, 1986). Another is the application of integrated geodesy (Eeg and Krarup, 1973), which was put into practise to determine a precise geoid for the Yellowstone-Hebgen Lake region (Milbert and Dewhurst, 1992). However, to gain maximum effect, this approach should use all the originally observed data relevant to the network, e.g. gravity anomalies, levelling observations, GPS observations, with the relevant auto-covariance and cross-covariance functions; this becomes prohibitive for regional or national levelling networks.

Our aim then is to develop and test the numerical methods needed for combining GPS-derived ellipsoidal height (h) and gravimetrically-derived geoid heights (N), into existing levelling (H - orthometric height) networks. In this way, levelling networks can be greatly strengthened without the need to involve the original observations, and optimum estimates of all the parameters involved in the heighting 'equation' - H, h and N - can be found, along with estimates of their precisions. This is especially relevant when national authorities are considering the re-adjustment of their levelling networks to incorporate the results of GPS campaigns and precise geoid evaluations, and to involve tide gauge estimates of mean sea level into the height datum. These results could also be used to analyse the strengths and weaknesses of an existing network, and then to find ways of resolving them. We also, therefore, would like to develop a method which is practically feasible for surveying authorities with limited resources.

2 METHODOLOGY

Classical least squares techniques are used in conventional levelling to adjust discrepancies between repeat measurements of levelling lines, and the misclosures in networks of these lines, in order to find the optimum values of H at the height control points (e.g. Vanicek and Krakiwsky, 1986, pp. 427-436; Bomford, 1980, pp. 226-228; Whalen and Balazs, 1976; Kääriäcnen, 1966). However, these have dealt exclusively with the determination of H from classical levelling. Standard adjustment packages assume N values are errorless, and cannot easily accommodate absolute H value estimates from, for example, tide gauge observations. We want, therefore, to find an approach which uses not only either h or H, but which simultaneously uses and adjusts h, H and N, and at the same time has the flexibility of using information on these heights from other sources.

By introducing the observed Δh (from GPS) and N (from gravimetry) with the appropriate variance-covariances into the existing (ΔH) network; by enforcing the condition of loop closures onto these elements; by invoking the condition which must exist between H, h and N at each control station and by solving the system derived therefrom by constrained least squares, a network of heights which is in effect reinforced, will result. Not only will the technique identify gross errors in the original data (by the introduction of independent measurements), but a homogeneous, compatible and optimal data set for values of h, N and H for a network, is produced.

3 APPROACH TO LEAST SQUARES ADJUSTMENT

3.1 Introduction

The preliminary work requires the development of least squares adjustment to incorporate h, H and N from their various sources, which involves for instance, GPS vectors, geodetic levelling and gravity data. Several methods were developed and tested to achieve this, and these are described in detail in Section 3.4.

The computational methods were carried out using existing programs within the School of Surveying, and other programs developed to accommodate the unique requirement for the adjustment.

3.2 Basis of the Geometric Adjustment

Applying the concept of the geoid, ellipsoid and their relationship (refer to Figure 3.1), the equations below are used as the basis for the adjustment.

$$h_A = H_A + N_A \qquad (3.1)$$

$$h_B = H_B + N_B \qquad (3.2)$$

$$\Delta h_{AB} = h_B - h_A \qquad (3.3)$$

$$\Delta H_{AB} = H_B - H_A \qquad (3.4)$$

$$\Delta N_{AB} = N_B - N_A \qquad (3.5)$$

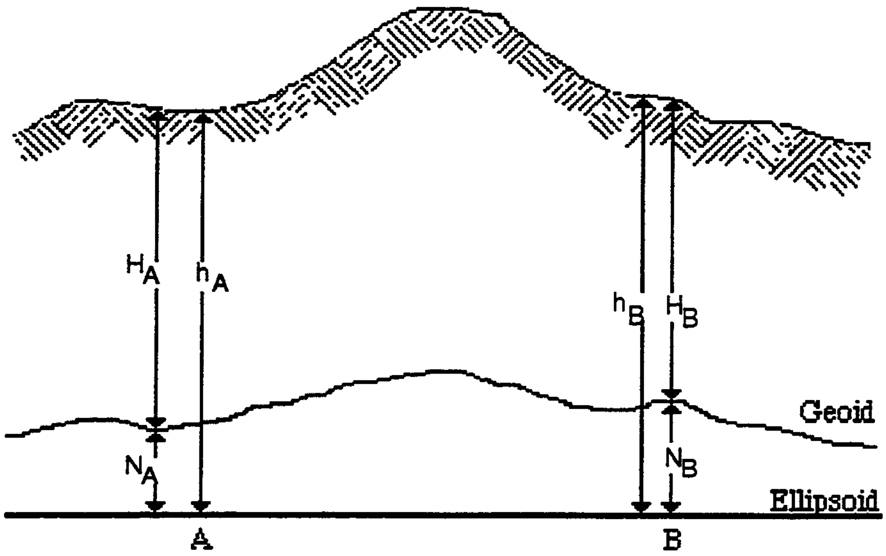

Fig 3.1 : Relationship between Geoid and Ellipsoid

The assumptions made are (refer to Figure 3.2)

a. Levelling gives geometric ΔH without systematic error;

b. N and h refer to the same ellipsoid. Datum shifts or tilts between N and h values are not allowed for;

c. The line normal to the ellipsoid is the same as the line to which H and N is referred i.e the deflection of vertical, ε, is insignificant (< 20 ");

d. All refraction corrections and instrument calibrations have been applied to the data (including height of instrument and error propagation in H).

3.2.1 Basic Equations

The mathematical models relating the observations and parameters are based on geometrical and simple physical laws, as shown above. The general form of a mathematical model in terms of constants c, parameters x and observations ℓ is

$$f(c, x, \ell) = 0$$

However, the explicit reference of any constant value, c, can be omitted since c is part of the function (model) itself. An example of such a constant is Newton's Gravitational constant.

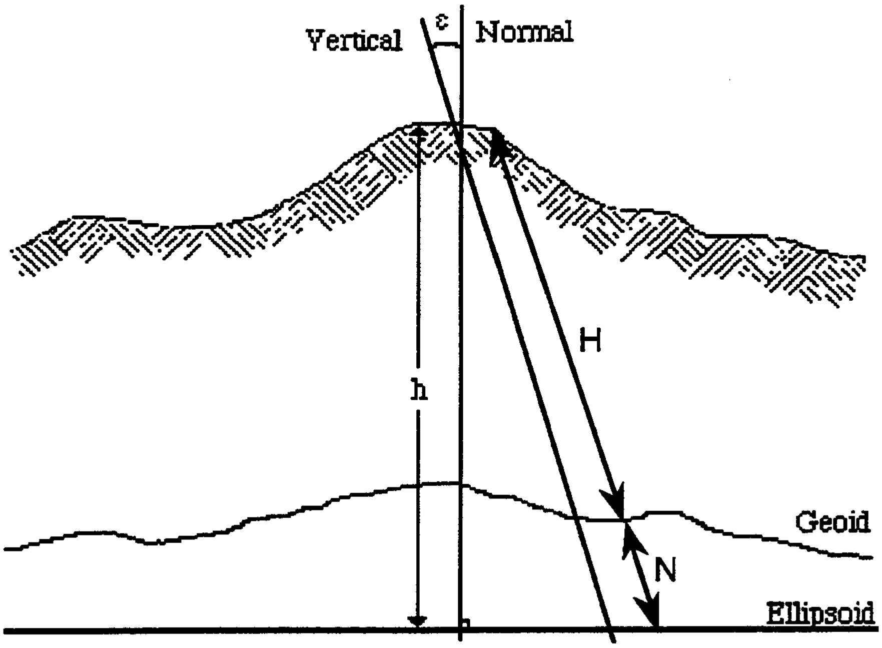

Fig 3.2 : Local relationship of the Geoid and Ellipsoid

For the combination of GPS-derived ellipsoidal height (h), gravimetrically-derived geoid heights (N) and orthometric height (H) from levelling, the model equations for each line (which are also the observations equations) are in the form of (refer to Figure 3.1)

$$h_B - h_A - \Delta h_{AB} = 0 \qquad (3.6)$$

$$H_B - H_A - \Delta H_{AB} = 0 \qquad (3.7)$$

$$N_B - N_A - \Delta N_{AB} = 0 \qquad (3.8)$$

whereas the model equation for each site (or the constraint equation) is given by (refer to Figure 3.2)

$$H_A + N_A - h_A = 0 \qquad (3.9)$$

$$H_B + N_B - h_B = 0 \qquad (3.10)$$

The observations here are constituted by Δh_{AB}, ΔH_{AB}, and ΔN_{AB} and the parameters include h_A, H_A, N_A, h_B, H_B and N_B. However, if the parameters are adjusted in the Bayesian least squares method, then observations of h, H or N can be included with their variance-covariance information.

3.3 Other Considerations

3.3.1 Missing Observations

One aspect to consider is the possibility of a lack in data availability. For some points (e.g. level junction sites) there will be ΔH from tide gauge/levelling observations and presumably N values from gravimetry, but no Δh from GPS. On the other hand, some points will have Δh values from GPS and N values from gravimetry but will lack ΔH from tide gauge/levelling observations. In these cases, two suggestions are offered, namely

a. to leave out some of the model equations and some of the parameters and observations, or

b. to include estimates for the missing observations with large input standard deviation (e.g. $\pm$ 10 m for the a priori ellipsoidal heights).

In the case of the first option, programming will be more difficult whereas the second option will result in having one set of code for all points and all parameters are solved for at each site. For the purpose of practical applications, option (b) is preferable to option (a).

3.3.2 Datum

To avoid rank defect in the normal matrix during the adjustment, some possibilities are to

a. impose a minimum constraint on the parameters by holding any two of the h, H and N fixed for one point. In practice, these elements can be held fixed at the same point, although it is not essential to do so; or

b. apply a free net adjustment by doing a minimum constraint adjustment as above and then transform the results to the mean best fit of the approximate h, H and N of all or of selected points in the network; or

c. over-constrain the network by holding more parameters fixed than the minimum number required to eliminate the rank defect. This is, however, not recommended because it may cause the adjusted observations and parameters to be deformed.

3.3.3 Tide gauges

In the adjustment process for the Australian Height Datum (AHD) 1971, two adjustments were carried out (Roelse, Granger and Graham, 1971, p. 48). The first was a free adjustment with only the Johnston Geodetic Origin held fixed. The second was the 'fixed' adjustment, holding 30 tide gauge stations around the coast fixed to the height of mean sea level (assumed as zero). A similar principle was applied in the general adjustment of the National Geodetic Vertical Datum in North America in 1929 (NGVD 29), where the heights of 26 tidal bench marks referenced to local mean sea level were rigidly constrained to define a reference surface (datum) based on a value of 0.0 m for each local mean sea level (Zilkoski et al, 1991).

A decision needs to be made whether to assume H fixed to zero at tide gauges or to treat the tide gauge information as an observation with an appropriate uncertainty and then to solve for all height elements. We opted for the latter approach, as it is a better reflection of reality. This decision, however, has little effect on the least squares adjustment method that we finally chose.

3.3.4 Programming and Algorithm Aspects

The partial differentials in the **A** matrix consist essentially of +1, 0 and -1. Storing **all** these values for later use in matrix manipulation would result in a much slower process, less accurate values and greater storage problems. To overcome this hurdle, it is possible to write an algorithm which includes equations with the addition and subtraction of relevant terms, or where possible, to form the normal matrix without the need to store either the **A**, **P** or $\mathbf{P}_X$ (used in Bayesian least squares and Combined least squares with weighted parameters). The latter option is the approach taken in our investigation.

Since the normal equation matrix may contain many zero elements (sometimes up to 80% of the full array), it is advisable to arrange the order of the parameters to obtain a 'special' matrix structure. Ideally, we should choose an order that puts all zero elements near each other in groups and all non-zero numbers together in a pattern (i.e not spread randomly within the matrix). One way of achieving this is by applying a 'banded bordered' system or a 'partitioned' system. For further reading, refer to Mikhail (1976). Several other methods are also applicable (Vanicek and Krakiwsky (1986); Bomford (1980) ; Cooper (1987)). For the test triangle in Section 3.4,which is a small data set, bordering and partitioning is not necessary.

3.3.5 Loops and Trivial Observations

If a triangle is observed, the three ΔH will almost certainly be independent in which case all three observations should be used. If the ΔN values are simply differences between the N values at each site, then they are dependant, in which case only two of them and their associated covariances should be used. Alternatively, the N values for all three sites are entered with a covariance matrix instead of the ΔN observations. The Δh observations lie somewhere between these extremes depending on whether all three sites were co-observed and co-adjusted in a full GPS network solution.

3.4 Adjustment methods tested

We tested several approaches to solve the problem. These include the methods of (i) parametric least squares with special equations per line with built-in constraints - method 1; (ii) combined least squares using 5 equations per line - method 2; (iii) combined least squares using 3 equations per line and 1 equation per site - method 3; (iv) parametric least squares using observation equations only - method 4; (v) combined least squares using 3 observation equations and 1 condition equation - method 5; (vi) sequential parametric least squares with constraints equations - method 6; (vii) parametric least squares with constraints equations - method 7; and (viii) Bayesian least squares with constraints equations - method 8. We have not tested either the condition or collocation method.

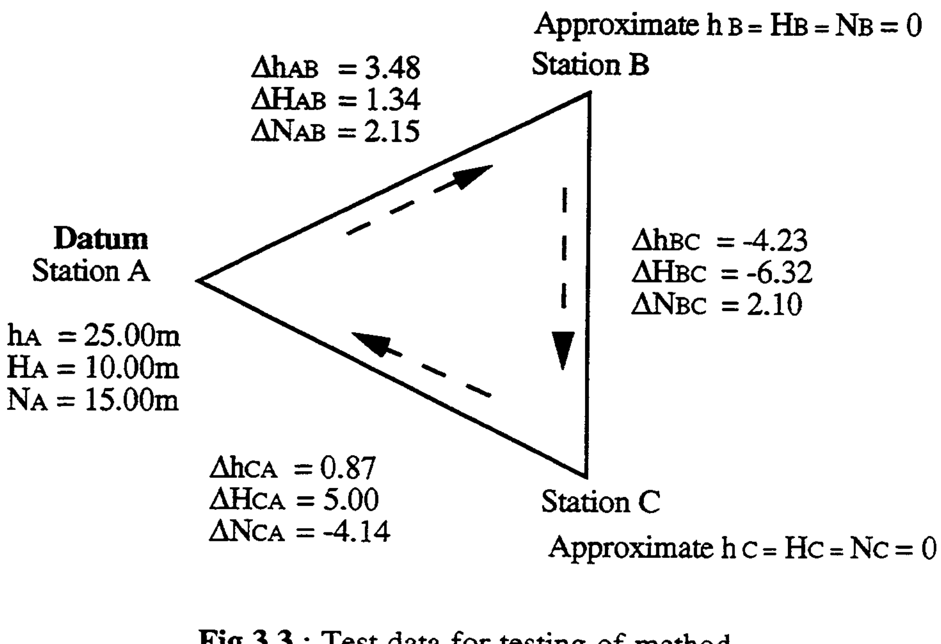

Fig 3.3 : Test data for testing of method.

To test these methods, a test data set was developed as shown in Figure 3.3 below. For this data set, we used a diagonal unit matrix as the variance covariance matrix for observations where the variance of each elements is assumed equal and uncorrelated. If the data is perfect, the sum of the loop closures for all the lines involved will be zero, which is

$$\sum_{i=1}^{n} \left(\Delta N_{ij} - \Delta h_{ij} + \Delta H_{ij}\right) = 0 \ ; \ j = i + 1$$

and the station condition for each station will be zero, given by

$$h_i - H_i - N_i = 0$$

These are the two criteria that we would like to achieve in the adjustment.

3.4.1 Preliminary Methods

Method 1 : Parametric Least Squares - Special equation with built-in constraints.

We attempted this approach so that the height elements are solved both simultaneously and conditionally (constraints applied), in a one step adjustment.

The development of these special equations with built-in constraints are described below. For each line, the model equations used are as outlined in equations (3.6) to (3.10). Substituting equations (3.9) and (3.10) into (3.6), (3.7) and (3.8) we get

$$h_B - H_A - N_A - \Delta h_{AB} = 0 \qquad (3.11)$$
$$h_B - N_B - H_A - \Delta H_{AB} = 0 \qquad (3.12)$$
$$h_B - H_B - h_A + H_A - \Delta N_{AB} = 0 \qquad (3.13)$$

Equations (3.11), (3.12) and (3.13) are used as the model equations per station, totalling up to nine equations altogether, to solve for the test triangle in Figure 3.3.

Method 2 : Combined Least Squares - 5 equations per line.

For each stations (A, B and C) the model equations (3.6) to (3.10) in section 3.2.1 are used, giving a total of fifteen equations, for this test data. Note that the condition equation for each site is repeated twice.

Method 3 : Combined Least Squares - 3 equations per line and 1 equiation per site.

Based on equations (3.6) to (3.9) from Section 3.2.1, that is by imposing three equations per line (equations (3.6), (3.7) and (3.8)) and one equation per site (equation (3.9)), four equations are formed for each station. This gives twelve equations in total. However, since Station A is held fixed, the condition equation at that station is omitted. The number of equations for the analysis of Method 3 is therefore eleven.

Method 4 : Parametric Least Squares - Observation equations only.

The testing of Method 4 involves the observation equations only, namely equations (3.6) to (3.8). The total number of equations therefore is nine, which is made up of three observation equations per station.

Method 5 : Combined Least Squares - 3 observation equation and 1 condition equation per line.

For each station, three observation equations ((3.6) to (3.8)) and one condition equation, which is $\Delta H_{AB} + \Delta N_{AB} - \Delta h_{AB} = 0$, are both imposed. This gives four equations per station, giving a total of twelve equations for this test data.

3.4.2 *Method 6 : Sequential Parametric Least Squares with constraint equations.*

This is a least squares problem which is rigorously and 'sequentially' (in parts) solved. It is achieved by updating the original estimate by a corrective term ($\Delta x - \Delta x'$). $\Delta x'$ is a function of a matrix inverse already computed in the course of obtaining the Δx (Krakiwsky (1982); Kouba (1970)).

This method is approached by first, finding the solutions to x using a parametric least squares (non-constrained) solution and then, by enforcing the constraints which are formulated from any additional information found specifically from the parameters. Such constraints usually reflects some mathematical or physical law associated to the parameters. The two mathematical models are

$$f(x, \ell) = 0 \text{ and } f_c(x) = 0$$

In this case, $f(x, \ell)$ is the model equation and $f_c(x)$ is the constraint equation, and we assume that x can be first solved with $f(x, \ell)$ only, and then further solved by the application of the constraints. The solution from the main model f (which gives an unconstrained solution, $\Delta x'$) is represented by (Vanicek and Krakiwsky (1986); Cross (1983))

$$\Delta x' = -(\mathbf{N})^{-1}\mathbf{u} \tag{3.14}$$

where

$\Delta x'$ = corrections to the parameters from the unconstrained solution,
$\mathbf{N}$ = normal matrix and
$\mathbf{u}$ = RHS (right hand side) vector,
where $\mathbf{N} = \mathbf{A}^T\mathbf{P}\mathbf{A}$
$\mathbf{u} = \mathbf{A}^T\mathbf{P}\mathbf{b}$
$\mathbf{P}$ = weight matrix of the observations.

By using $\mathbf{N}$ and $\Delta x'$ from above, and enforcing the constraints on the model, we get (ibid),

$$\Delta x = \Delta x' - \mathbf{N}^{-1}\mathbf{D}^T (\mathbf{D}\mathbf{N}^{-1}\mathbf{D}^T)^{-1} (\mathbf{b}_c + \mathbf{D}\Delta x') \tag{3.15}$$

where

Δx = correction to the parameters from the constrained solution
$\mathbf{D}$ = matrix for the differentiation of the constraint equations with respect to the parameters $\dfrac{\partial F_c}{\partial x}$ and
$\mathbf{b}_c$ = vector of constant terms (miscloses) given by the constraint equations at each station calculated from the *a priori* values of the unknowns.

The variance-covariance matrix of Δx is given by (ibid)

$$\mathbf{VCV}_{\Delta x} = \mathbf{Q}_{\Delta x} = \mathbf{N}^{-1} - \mathbf{N}^{-1}\mathbf{D}^T (\mathbf{D}\mathbf{N}^{-1}\mathbf{D}^T)^{-1} \mathbf{D}\mathbf{N}^{-1} \tag{3.16}$$

and note that the corrective term (Δx-$\Delta x'$) from equation 3.15, results from the enforced constraints. As a check,

$$\mathbf{Q}_{\Delta x} \cdot \mathbf{D}^T = \mathrm{C} \tag{3.17}$$

From above, $\Delta x'$ and the normal matrix, N both result from the non-constrained solutions, whereas Δx gives the constrained solution of the corrections to the parameters, which means that the total correction to the parameter (or the corrective term) is solved in two steps.

Applying this to a three point levelling problem, the parametric model involves equations (3.6) to (3.8) for each station, giving the total number of nine equations. Since Station A is held fixed, the constraints are imposed only on Stations B and C, as described in equations (3.9) or (3.10), and they are given by f_{c1} (equation 3.18) and f_{c2} (equation 3.19) below.

$$f_{c1}: \quad H_B + N_B - h_B = 0 \tag{3.18}$$

$$f_{c2}: \quad H_C + N_C - h_C = 0 \tag{3.19}$$

3.4.3 Method 7 : 'Unified' Least Squares with constraint equations.

This is based on the unified approach and parameter constraints (Mikhail, 1976, Part III), where all variables involved in the mathematical formulation are treated as observations, such that no distinction is made between the observations and the parameters. Initially, this may be represented by the model $F_c(\ell_c, x) = 0$, where ℓ_c is the observational variable and x is the parameter (ibid). When the unified concept is applied, x will be treated as part of a vector of observable quantities, thus formed as $F_t(\ell_t) = 0$, in which ℓ_t represents the total vector variable (ibid). All 'observations' have *a priori* covariance data.

These following cases demonstrate the practicality of this approach:

1. If an observation (in this case any variable in the model) is given an infinitely large variance ($Q \to \infty$), that is P=0, then it could vary freely in the adjustment, where it will assume the role of a parameter (i.e. free solution of parameters).

2. Conversely, if an observation is given a zero variance (Q=0), or a weight that approaches infinity ($P \to \infty$), then it will not undergo any changes, such that its residual will be zero and consequently will remain as a constant or as a fixed parameter.

When the constraints are introduced, they are viewed as 'conditions' that contain some type of 'observation'. Therefore, under the unified concept, the unknown is regarded as an observed quantity and a weight is given, which is proportional to the reliability of its known value.

Theoretically, the higher the value of its weight, the closer we get to perfect satisfaction of the constraint. For the purpose of this project, this method is tested by using different weights as will be shown later, giving six sets of Δx values.

In our case, all the model equations are linear so the solution (Δx) is obtained from

$$\Delta x = (\mathbf{N} + \mathbf{N_C} + \mathbf{P_X})^{-1} \; (\mathbf{t} + \mathbf{t_C} - \mathbf{P_X} \; \mathbf{f_{X0}}) \tag{3.20}$$

Matrices **N** and **t** are contributions from the observations, where

$\mathbf{N}$ = normal matrix and

$\mathbf{t}$ = $\mathbf{A^T P b^0}$

where $\mathbf{b^0} = - (F(x) - \ell)$

$\mathbf{b^0}$ is the vector of functional equations with observations and approximate values of parameters.

$\mathbf{f_{X0}}$= the difference of the approximate value of the parameters from the previous iteration. For the first iteration, it is usually equal to zero. And

$\mathbf{P_X}$ = the inverse of the a *priori* covariance matrix of the parameters.

Equation 3.21, below, gives the variance-covariance matrix of the parameters

$$\mathbf{VCV_X} = (\mathbf{N} + \mathbf{N_C} + \mathbf{P_X})^{-1} \tag{3.21}$$

where matrices $\mathbf{N_c}$ and $\mathbf{t_c}$ are contributed by the constraints from the observations, namely

$\mathbf{N_c} = \mathbf{D^T} \; \mathbf{P_c} \; \mathbf{D}$

$\mathbf{t_c} = \mathbf{D^T} \; \mathbf{P_c} \; \mathbf{f_c^0}$

where $\mathbf{D} = \dfrac{\partial \mathbf{F_c}}{\partial \mathbf{x}}$

$\mathbf{f_c^0}$ = - $(\mathbf{F_c}\;(\mathbf{x}))$ at approximate value

$\mathbf{P_c}$ = the weight matrix of the constraints

Δx is solved using different weights for $\mathbf{P_X}$ (see Table 3.2). For every condition of $\mathbf{P_X}$, $\mathbf{P_C}$ is an identity matrix, I, and $\mathbf{P_C} = 1000 * I$. The weights used for $\mathbf{P_X}$ are,

1. for free solutions of the parameters, diagonals of $\mathbf{P_X} = 0$ (see Table 3.2, rows 1 and 2);

2. for fixed parameters, diagonal $\mathbf{P_X} \rightarrow \infty$ (corresponding to a diagonal of $\mathbf{Q_X} = 0$), which is achieved by substituting a large number (1000 for instance). (See Table 3.2, rows 3 and 4);

3. for a third case, $\mathbf{Q_X} = 0.1 * I$ (I is an identity matrix) that is $\mathbf{P_X} = 10*I$ (see Table 3.2, rows 5 and 6).

The model equations used are based on equations (3.6) to (3.8). The total number of equations is nine. The constraint equations for a test triangle are as outlined in equations (3.18) and (3.19).

3.4.4 Method 8 : Bayesian Least Squares and Constraints

This method has a twofold solution for solving the parameters; part one uses Bayesian least squares for solutions of the 'unconstrained' parameters and part two imposes some constraints onto the unknowns, subsequently solving for the constrained parameters. It is therefore, in principle, similar to Method 6, but Bayesian least squares is used instead of Parametric least squares. For references, see Harvey (1991), Vanicek and Krakiwsky (1986) and Cross (1983).

Bayesian least squares is applied because it gives the possibilities of using some prior knowledge of the parameters, the standard deviations and perhaps the correlations of the *a priori* estimates of the parameters. This information may be extracted from some independent measurements of the parameters from previous surveys, for example, from the N values from a geoid model.

For testing this method, one extra piece of information is used in the test data - the *a priori* value of one of the parameters (in our example $H_2 = 11.36 \pm 0.02$ m). Applying observed H and σ_H at tide gauge sites, the parameters are then solved using Bayesian least squares.

The solution from the main model *f* (that gives the unconstrained solution, $\Delta x'$) is represented by (Vanicek and Krakiwsky (1986); Cross (1983))

$$\Delta x' = -(\mathbf{N} + \mathbf{P_x})^{-1}\mathbf{u} \tag{3.22}$$

N is the normal matrix and **u** is the RHS (right hand side) vector, where $\mathbf{u} = \mathbf{A}^T\mathbf{P}\mathbf{b}$ and $\mathbf{P_X}$ is the weight matrix of the parameters. For H from levelling, $\mathbf{P_X} = 0$ except for the diagonal terms referring to H at a tide gauge such that

$$P_{ii} = \frac{1}{\sigma^2_{H_i}}$$

for site i. Note that the value of H from the tide gauge is used as the approximate value of H at site i. The parts of $\mathbf{P_X}$ referring to the geoid height (N) and the ellipsoidal height (h) may not be diagonal terms only. In this way, h from GPS and N from the geoid can be entered with their covariance information. Then, the site constraints (N + H - h = 0) are applied at each site using the constrained solutions described in Section 3.4.2 (equation 3.15 to get the constrained solution (Δx) and equation 3.16 for the variance-covariance matrix of Δx).

The model equations are made up of equations (3.6) to (3.8) and the constraints are outlined in equations (3.18) and (3.19). Nine equations are used for stage one and two constraints equations are used in stage two, to solve the triangle in Figure 3.3.

3.5 Discussion of Test Results

The test results have been summarised in Table 3.1 and an extended summary of Method 7 is given in Table 3.2. Methods 2, 3 and 5 are clearly not working because of problems with singularities. Methods 1 and 4 show unacceptably large discrepancies when the check for the adjustment, H-h+N=0, is applied. The errors in the constraints equations from Method 1 are 20 mm to 30 mm for points 2 and 3, respectively and Method 4 gives errors of 6 mm to 14 mm for the same points. We expect, of course, that errors from the constraints for the test triangle to be zero. Method 7 (see Table 3.2), on the other hand, has zero misclose for Px=1000*I. Theoretically, Method 7 and 8 should give the same answers when the same data is used since the only difference between these two methods is that Method 8 uses a sequential adjustment whereas Method 7 has a one step adjustment. Both Methods 6 and 8 have zero errors but Method 8 is superior to Method 6 because it caters for the possibility of treating some of the parameters as 'observations'.

1	2				3	4			5			6	
Method	n	m	u	r	r_i	H_B	h_B	N_B	H_C	h_C	N_C	Check1	Check 2
Parametric	9	9	6	3	$0.2 \leq r_i \leq 0.5$	11.339	28.440	17.131	5.000	24.165	19.187	0.030	0.022
Special Equa. constraints built in													
Combined	9	15	6	9			5 ZERO EIGENVALUES						
5 equa./line													
Combined	9	11	6	5			5 ZERO EIGENVALUES						
3 equa./line + 1 equa./site													
Parametric	9	9	6	3	0.33	11.333	28.440	17.113	5.007	24.170	19.177	0.006	0.014
Observations only													
Combined	9	12	6	6			2 ZERO EIGENVALUES						
3 obs. + 1 condition													
Sequential Parametric	9	9	6	3	$r_i \leq 0.33$	11.331	28.442	17.111	5.002	24.174	19.172	**0.000**	**0.000**
With constraint equation													
Parametric	9	9	6	3			SEE TABLE 3.2						
With constraint equation													
Bayesian Method	9	9	6	3	$r_i \leq 0.33$	6.012	25.783	19.771	2.769	23.058	20.289	**0.000**	**0.000**
With constraint equation													

Comments:

m = no of equations
n = no of observations
u = no of parameters/unknowns
r = degree of freedom
r_i = the redundancy number of the observation, i

Check 1 : $H_B - h_B + N_B$
Check 2 : $H_C - h_C + N_C$

Table 3.1 : Summary of the adjustment methods that are tested

			At Station B			At Station C			Checks	
Row No		Pec	H_B	h_B	N_B	H_C	h_C	N_C	Check 1	Check 2
1	Px = 0	I	11.331	28.442	17.111	5.004	24.173	19.174	0.001	0.004
2		1000* I	11.331	28.442	17.111	5.002	24.175	19.172	**0.000**	**0.000**
3	Px = 1000 * I	I	0.018	0.033	0.015	-0.001	0.020	0.021	**0.000**	**0.000**
4		1000* I	0.018	0.033	0.015	-0.001	0.020	0.021	**0.000**	**0.000**
5	Qx = 0.1 * I	I	1.473	2.884	1.411	0.013	1.899	1.888	0.000	0.001
6	i.e Px = 10 * I	1000* I	1.473	2.884	1.411	0.012	1.899	1.887	**0.000**	**0.000**

Comments:
Check 1 : $H_B - h_B + N_B$
Check 2 : $H_C - h_C + N_C$

Table 3.2 : Summary of the adjustment for method 7

You could therefore, use observed heights at tide gauges, SLR stations and so on. For the practical tests which follow, Method 8 has been adopted as the most flexible and accurate.

3.6 Variance Factors and Statistical Tests

Each method has its own expression for the a posteriori variance factor (VF). If the VF fails the statistical tests, it indicates weaknesses in either the mathematical models, calculations, input variance-covariance data and errors in measurements, or a combination of these. Even if the VF does pass its test, there may still be problems. It is therefore, important to check your work carefully instead of fully relying on the results of the VF test. We present some approximate equations for VF and some other useful tests.

Residuals (v) should be calculated, and their magnitudes inspected. One way to calculate v is to subtract the original observations from equivalent values derived from the final adjusted parameters. In the sequential method 8, two sets of v can be calculated; one set before constraints are applied and the other after applying the constraints. The simple ratio of residual divided by its *a priori* standard deviation should also be calculated and inspected for approximate normal distribution.

The VF is usually calculated from $\mathbf{v}^T\mathbf{P}\mathbf{v}/r$. For the constraint and sequential methods, it is important that v be calculated from the final adjusted parameters. Also, the degrees of freedom, r, vary from method to method. It is generally the number of equations minus the number of unknowns (3 per site). The VF should be close to unity when all input variance-covariance data is reliable (and not subjected to any scale factors).

When Bayesian information is used (e.g. input observations of N or h and tide gauge values of H), then the VF should be calculated as (Harvey, 1987, p. 60-61)

$$\left(\mathbf{v}^T\mathbf{P}\mathbf{v} + \Delta\mathbf{x}^T\,\mathbf{P}_x\,\Delta\mathbf{x}\right) / \; r'$$

where r' is approximately equal to the number of observations (n) minus the number of parameters without a priori weights (u - u', u being the total number of parameters and u' is the number of parameters with a priori weights), given by r' = n - u + u'.

4 BAYESIAN LEAST SQUARES AND CONSTRAINTS: FULL WORKING DETAILS

Because of our preference for Method 8, the working details on the triangle data will be described in full. The test diagram and data used are as outlined in Figure 3.3 but while the approximate values of H = h = N = 0 is assumed at stations B and C, for this method, station B has a priori information about the orthometric height, where $H_B = 11.36 \pm 0.02$ m as discussed in the previous section 3.4.4. Nine observation equations (equations 3.6 to 3.8, composed of three at each station) are formed and at each of stations B and C, one constraints equation (equation 3.9) is imposed. The input standard deviation , $s_{H_B} = \pm\ 0.02$ m here, will contribute to the respective diagonal term of weight matrix of the parameters, $\mathbf{P_X}$ by

$$P_{2,2} = \frac{1}{\sigma^2_{H_B}} = 2500.$$

4.1 Discussion of the Adjustment Results

Initially, the test data have loop miscloses of -0.12 m in the ellipsoidal heights, -0.02 m in the orthometric heights and -0.11 m in the geoid heights. The miscloses in the line elements ($\Delta N_{ij} - \Delta h_{ij} + \Delta H_{ij}$) are -0.01 m in line 1 (from stations A to B); -0.01 m in line 2 (from stations B to C); and 0.01 m in line 3 (from stations C to A).

Tables 4.1(a) and (b) outline the results in the adjustment, showing the corrections to both the parameters and the observations. Since the *a priori* value employed for h_B, N_B, h_C, H_C and N_C equals zero, the corrections applied to the parameters after Bayesian least squares is approximately the observed values. Table 4.1(a) also shows the station misclose (h-H+N) at station B as 0.033 m and station C as 0.027 m after the Bayesian least squares is applied and a zero misclose **after** applying station constraints, as expected. The station miscloses were distributed equally to the three parameters H, h and N as they were given the same weights.

Table 4.1 (b) shows that the line misclose ($-\Delta h - (\Delta H + \Delta N)$)for each line combination (A to B, B to C and C to A) is initially 0.010 m. After introducing the constraints condition into the adjustment, a total correction of the same magnitude but of opposite sign is distributed throughout the observational elements, as shown in column 6 of table 4.1 (b). Looking at Table 4.1 (c) (which shows the loop misclose for each observed ΔH, Δh and ΔN), the original observations give miscloses of 0.02 m, 0.12 m and 0.11 m, for ΔH, Δh and ΔN, respectively. As expected, the total correction applied after the adjustment is the misclose, similar in magnitude but of the reverse sign, namely -0.02 m, -0.12 m and -0.11 m.

Station Number	Parameters	A priori Heights (m)	Δx before constraints	Adjusted Height	Δx after constraints	Adjusted Height (m)
	H_B	11.36	-0.00002	11.360	-0.0111	11.349
B	h_B	0.00	28.440	28.440	0.0111	28.451
	N_B	0.00	17.113	17.113	-0.0111	17.102
			Station misclose =	0.033	-0.033	0.000
	H_C	0.00	5.01999	5.020	-0.00888	5.011
C	h_C	0.00	24.170	24.170	0.00888	24.179
	N_C	0.00	19.177	19.177	-0.00888	19.168
			Station misclose =	0.027	-0.027	0.000

Table 4.1 (a) : Effects of adjustment on parameters.

Station No. AT	Station No. TO	Observational Elements	Observation (m)	Corrected Observations	Corrections (m)
		ΔH	1.34	1.349	0.009
A	B	Δh	3.48	3.451	-0.029
		ΔN	2.15	2.102	-0.048
		Station constraints misclose=	0.010	0.000	-0.010
		ΔH	-6.32	-6.338	-0.018
B	C	Δh	-4.23	-4.272	-0.042
		ΔN	2.10	2.066	-0.034
		Station constraints misclose=	0.010	0.000	-0.010
		ΔH	5.00	4.989	-0.011
C	A	Δh	0.87	0.821	-0.049
		ΔN	-4.14	-4.168	-0.028
		Station constraints misclose=	-0.010	0.000	0.010

Table 4.1 (b) : Effects of adjustment on the observations.

	Misclose (m)	Misclose (after constraints) (m)	Total Corrections (m)
Loop Misclose in $\Delta H = \Delta H_{AB} + \Delta H_{BC} + \Delta H_{CA} =$	0.02	0.00	-0.02
Loop Misclose in $\Delta h = \Delta h_{AB} + \Delta h_{BC} + \Delta h_{CA} =$	0.12	0.00	-0.12
Loop Misclose in $\Delta N = \Delta N_{AB} + \Delta N_{BC} + \Delta N_{CA} =$	0.11	0.00	-0.11

Table 4.1 (c) : Effects of adjustment on the loop misclose.

From the results discussed above, the significant point to note is that we have now achieved both a perfect loop and station close. That is, with this technique, we have satisfied both the network condition (Equations 3.6 to 3.8) and the station condition (Equations 3.9 and 3.10). We prefer this method and will adopt it for further development and testing.

4.2 Software Development

Development of the software involves the automation of matrices by generating $\mathbf{A^TPA} + \mathbf{P_X}$, line by line without the need to store matrices **A**, **P** or $\mathbf{P_X}$ (see Harvey, 1991, p. 155-156), such that the required input consists of the *a priori* values of the parameters and the associated standard deviation, and observational variables, their precisions and information on the line elements details (see Appendix 1). The main program, BAYCON with its suite of subroutines (see Appendices 2 to 4) for computing Bayesian least squares followed by constraints has been implemented on the VAX/VMS computer, written in Fortran 77.

5 PRACTICAL TESTS

5.1 Introduction

We tested the 'Bayesian least squares with constraints' on some small networks. They are (1) part of the 'Operation Longwalk' network in northern South Australia; (2) part of the GPS level run along the tide gauge network on the south-east Australian coast; and (3) part of the GPS/levelling network in south-eastern Luzon, the Philippines. These data sets are purposely chosen to have a range of different qualities and characteristics in them. For example, they range in topography from flat to rugged (the latter with complex tectonics) and incorporate different combinations of the observed parameter types (e.g. tide gauges, SLR-observed height).

Their details are summarised in Tables 5.1 and 5.2. Table 5.1 shows the geographical location of the tested area, the characteristics of its terrain and geoid and the length of lines involved. Table 5.2 summarises the information of the different observation types for height or height differences and the associated precisions. The input data for all cases used in the adjustment and all the results from the adjustment for the tested areas are in Appendices 5 to 10 for the South Australia network, Appendices 11 to 13 for the New South Wales coast network and Appendices 14 to 16 for the south east Luzon network. The input are listed in the beginning of the relevant appendices and followed by listings of the adjustment results. See Appendix 1 for the explanation of codes used in the input data.

	Location		**Characteristics**		**Network Details Line information**			
Area	ϕ (°)	λ (°)	Terrain	Geoid	No.	Shortest Length (km)	Longest Length (km)	Mean (km)
South. Australia	-27.5 to -30.5	134 to 139	Low to flat relief	Smooth or benign	7	180	365	275
NSW Coast.	-34 to -35	151 to 152	Coastal hills	Medium to rough	5	30	146	72
S. E. Luzon	12.5 to 14.0	123 to 124	coastal - tectonically complex	Disturbed	6	50	85	59

Table 5.1 : Details of test networks.

	ΔH		Δh		ΔN		
Area	Class	Precision	Receivers	Precision	Method	Precision	Point Elements
South. Australia	2nd-3rd order	$12\sqrt{k}$ to $8\sqrt{k}$ (mm)	Trimble dual frequency.	1-2.ppm	Detailed gravimetric (RINT)	2 ppm	N/A
NSW Coast	3rd order	$12\sqrt{k}$ to $8\sqrt{k}$	Trimble single freq.	2-3.ppm	ditto	ditto	Tide gauge at Sydney
SE Luzon	3rd order	$12\sqrt{k}$	Trimble dual frequency.	1-2 ppm	ditto	ditto	Tide gauges at 29, 41

Table 5.2 : Details of line elements in test area.

5.1.1 General accuracy requirements of the height elements

As a guide, the accuracy that is specified for the different types of observations are outlined in Table 5.3.

Type of Observations	Obs.. Elem.	Accuracy Requirement or Estimate	References
1. Levelling	ΔH	(K in km)	NMC, 1970, P. 4.
1st Order		Tolerance: 4 √K (mm)	and
2nd Order		" 8 √K (mm)	Mitchell, 1990, p. 36
3rd Order		" 12 √K (mm)	
4th Order		" 18 √K (mm)	
3rd Order (a posteriori σ)		8.1 √K (mm)	Macleod, 1990, p. 41
2. GPS Heighting	Δh	± (10 mm +2 ppm)	Zilkoski and Hothem, (1988)
		With 1σ uncertainty:	
		± (5 mm +(1 to 2)ppm)	
		With improved orbit determination techniques, dual frequency, etc. :	
		± (2 mm+(0.01 to 0.1) ppm)	
		for separations of:	
		5 Km : 0.02 m	Mitchell, (1990,p. 50)
		25 Km : 0.05 m	
		100 Km : 0.20 m	
		500 Km : 1.00 m	
3. Gravimetric Geoid Solution	ΔN	Full Gravimetric : 10 mm + 2 ppm	Zilkoski and Hothem, (1988)
		for separations of:	Mitchell, (1990, p. 50)
		5 Km : 0.02 m	
		25 Km : 0.05 m	
		100 Km : 0.20 m	
		500 Km : 1.00 m	
	ΔN	-from a high order geopotential model (5 ppm)	
		5 Km : 0.025 m	
		25 Km : 0.125 m	
		100 Km : 0.500 m	
		500 Km : 2.500 m	
Interpolated from gridded N		5 to 7 ppm	see Steed, (AUSLIG), Private Communication.
Astro-gravimetric	N	From 1971 Geoid Map of Australia s up to ±1.5 m wrt Johnston Origin	Fryer, 1971, (p. 12)
Gravimetric	N	- From formal error in model, e.g. OSU89B over Australia. ± 24 - 34 cm	Rapp and Pavlis, 1990, p. 21 907
4. Tide Gauge	H	With 1σ uncertainty:	Macleod, 1990, p. 44
Long term 19 years		± 0.03 m	(for Fort Denison.)
Short term - 2 months.		± 0.04 m to ± 0.07 m	Kearsley and Ahmad, (1992, p. 41-45)

Table 5.3 : Specifications for accuracies and precisions of the adjustment data.

5.1.2 Data availability

In the sections which follow, the networks are described, along with the measured line and point elements, and the results are discussed. To provide a basis for this discussion, we need to know how the various lines and point elements (Δh, ΔH, ΔN; h, H and N) were observed (if at all), and give a formal estimate of their precisions. Although the data used in these examples are not the raw 'observed' data, it allows us at least provisionally, to draw some conclusions as to the impact of the error estimates on the adjustment, the means of identifying suspect measurements, and so on.

5.2 Northern South Australia

The means by which the three absolute height elements (h, H and N) were determined from the observed elements (Δh, ΔH and ΔN) are listed in Table 5.2 and their values are shown in Figure 5.1 below.

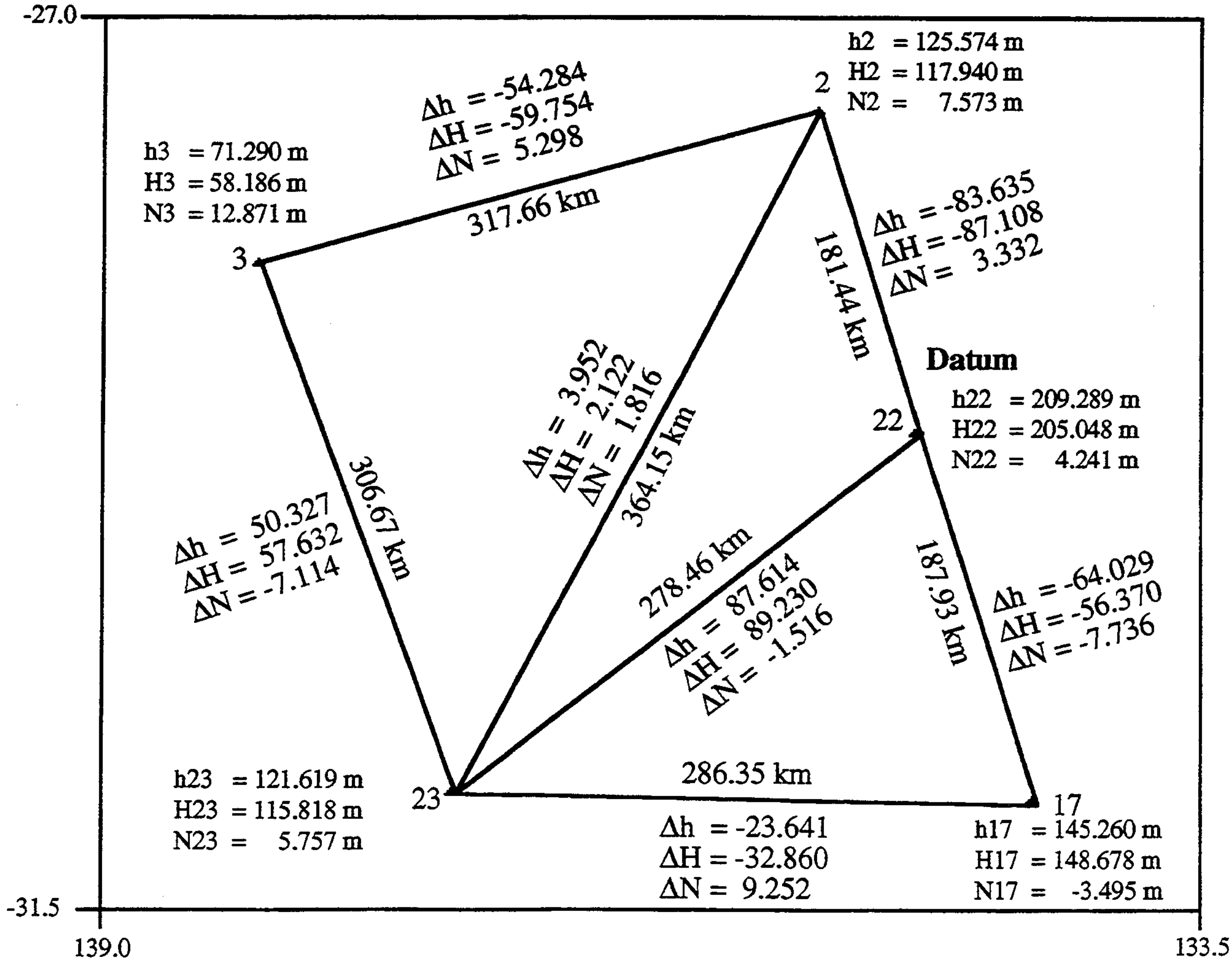

Figure 5.1 : South Australia network diagram.

Values for ΔH, unfortunately, were unavailable, and both ΔH and ΔN were obtained from the point values established for each station, and thus their loop closures are zero. Therefore in this network, although all line elements (ΔH, Δh and ΔN) are assumed to be observed, in fact only Δh_{GPS} were. The precisions for the 'observed' elements were found using the estimators quoted in Table 5.2. Because 7 lines are involved there are 21 parametric equations, with 12 unknowns, before the station constraints are applied, and a further 4 equations after the station are constrained (Station 22 is assumed fixed in all 3 elements).

We adjusted this network under different conditions by varying the accuracies for the parameters and precisions of the observed elements (see Tables 5.4 (a), 5.4 (b)). In each case results were obtained with and without the station constraints ($H + N - h = 0$) being applied. The corrections to each of the parameters after the Bayesian adjustment and after constraints are outlined in Table 5.4 (c).

5.2.1 Effect of station constraints

After stage 1 of the adjustment (i.e. after the adjustment of the network, but before the application of station constraints), the station miscloses ($H + N - h = 0$) range from a large value, e.g. -0.29 m (point 3, Case 1, Appendix 5) to a small -0.09 m (point 23, Case 1, Appendix 5). If the adjustment was assumed complete at this stage then, clearly, quite large discrepancies are left in the heighting system and we would have to consider these results as sub-optimal. For this test data, no corrections are applied to both elements H and N after Bayesian least squares (Table 5.4 (c), columns 3 to 5), which is because the 'observed' elements ΔH and ΔN are extracted from the differences of their absolute values. Applying both the standard adjustment and the station constraints, the total corrections to the parameters are laid out in Table 5.4 (c), varying between 0.003 m (δh, point 23, Case 1) to 0.22 m (δN, point 3, Case 3) reflecting the precisions of the parameters. Obviously the corrections are significant, with the largest changes at each point occurring in h due to the relatively larger error bars of Δh. The next largest corrections are to N, because of the relatively low precision in ΔN over these long lines.

The v/s values were always significantly less than unity, as we expected. The H values, being AHD values, have been subjected to an adjustment already, and one would expect them to be gross-error free. However, even if this expectation is not always realised, both H and ΔH are treated with the smallest error bars, as compared to the elements of h and N. The N values result from a homogeneous gravity data set referred to a global model, and are therefore self-consistent, even though they may contain a systematic error or bias.

In any case, we can see from this example that, by using the station constraints small corrections are applied to produce a result which is more consistent with ***all*** the available data. That is, the network conditions (loop misclose) ***and*** the station condition ($h = H + N$) are satisfied simultaneously, producing, we feel, the best possible values for ***all*** the parameters used in the heighting system.

We also investigated the impact of varying the input standard deviations of the parameters and of the line elements, on the adjusted values. A summary of the input is given in Tables 5.4(a) and 5.4(b). The standard deviation for cases 3 to 6 (see Table 5.4 (b)) are thought to best reflect the actual precisions of the 'observed' elements Δh and ΔH. The input standard deviations of h, H and N are also varied (see Table 5.4(a)). The cases we present here result from various combinations of standard deviations, and we hope that their intercomparisons will provide insights into the sensitivity of the adjustment to the different weightings.

5.2.2 Effect of varying the input standard deviations of the observed line elements

As can be seen from Tables 5.4(a) and 5.4(b), Case 1 and Case 3 have the same standard deviation for their h, H and N parameters, but the $\sigma_{\Delta H}$ for Case 1 is based upon $12\sqrt{K}$ mm while Case 3 is assumed to be $8.1\sqrt{K}$ mm. In Case 3, the total corrections to H have become smaller at the expense of the correction to N and, to a lesser extent, h. For example, (referring to Table 5.4 (c)) for point 2, δH has reduced from 0.005 m (Case 1) to 0.001 m (Case 3), while δh has increased from 0.007 to 0.03 m, and δN from 0.063 to 0.091 m. This simply reflects the relative improvement in the output standard deviation for ΔH (from $12\sqrt{K}$ mm to $8.1\sqrt{K}$), while the standard deviation for Δh has improved less from 2 ppm to 1 ppm and that for ΔN has remained at 2 ppm. The same effect is seen when comparing Case 2 with Case 4.

5.2.3 Effect of varying the input standard deviation of the parameters

We can test this by comparing Case 1 with Case 2, where the line elements standard deviations are unchanged, but the standard deviations of the parameters h and N are changed from 10.0 m (Case 1) to 0.8 m and 0.3 m respectively. From Table 5.4 (c), we see that this results in larger total changes in h and N for Case 2, the magnitude ranging from ± 2 to ± 8 cm (the largest for point 3 - see Fig. 5.1 for possible reason. The height at point 3 is established by only two connections, both of which are relatively long lines of more than 300 km). The standard errors of the adjusted parameters are reduced significantly (see Table 5.4 (a)), as might be expected, as we are now giving the *a priori* parameters for Case 2, smaller standard deviations (from 10 m to 0.8 or 0.3 m, respectively, for h and N).

Similar comments hold when comparing Case 4 with Case 3. These have the same parameter standard deviations as have Cases 2 and 1, respectively, but adopt the new line standard deviations where $s_{\Delta N}$ are deteriorated in most lines, $s_{\Delta H}$ are mostly improved and $s_{\Delta h}$ are mixed. In Case 4 the s_h and s_N are smaller than in Case 3. The corrections to ΔN in Case 4 are smaller than in Case 3, ranging from -0.09 to + 0.10 in case 4, cf. -0.13 to +0.15 in Case 3 (see Appendices 7 and 8, for Cases 3 and 4, respectively). This shows how improved accuracy for N affects the adjusted elements. The corrections to Δh are not reduced in all lines, reflecting the relatively lower accuracy value used for the ellipsoidal heights, compared to the H and N values.

In Case 5 we have varied the standard deviations of each parameter within each type - i.e. the standard deviations of h, H and N are varied between points. Comparing Case 5 with Case 4 however we see that these variations have only a small impact on the adjusted values (up to 1 cm) - see Table 5.4 (c) - reinforcing the conclusion that the adjustment is fairly insensitive to small changes in the standard deviations of the parameters. The largest changes occur in those lines whose elements (i.e. ΔN, ΔH or Δh) are weakest. The standard deviation of the adjusted parameters change by up to 4 cm, reflecting the changes of up to 0.1 m in the *a priori* accuracy values.

Another adjustment was done (Case 6), giving h accuracies of ±10.0 m (cf. ±0.8 m used for Case 4) and leaving the accuracies for H and N at ±0.2 and ±0.3 m respectively as for Case 4. The corrections to the line elements are practically identical with those in Case 4. The main variation occurs in the corrections to h which receive the lion's share of the correction for the station misclose. Such a weighting has the effect of 'floating' the datum for h. The values for H and N, in effect, are used to provide the datum for h, while the observed Δh elements are simultaneously used to control the relative ellipsoidal heights of the points on the network. The accuracies of the adjusted h values are not affected by the *a priori* estimate of accuracy in this comparison.

The same effect is seen by comparing Case 3 with Case 4, which have the same line element precisions, but whose parameter accuracies are varied as for Cases 1 and 2. The corrections to the parameters are smaller in Case 4 cf. Case 3, as are the standard deviations of the adjusted quantities. The corrections to h and N are greater than in the Case 1 vs. Case 2 comparison, reflecting the (relatively) lower precisions of the line elements.

Case	Station#	A priori Values						Total Corrections			Adjusted Values					
		h(m)	Sh(m)	H(m)	SH(m)	N(m)	SN(m)	∂h	∂H	∂N	h(m)	sh(m)	H(m)	SH(m)	N(m)	SN(m)
1	2	125.574	10.00	117.940	0.20	7.573	10.00	0.007	0.005	0.063	125.581	0.23	117.945	0.10	7.636	0.23
	3	71.290	10.00	58.186	0.20	12.871	10.00	-0.082	0.009	0.142	71.208	0.37	58.195	0.13	13.013	0.37
	17	145.260	10.00	148.678	0.20	-3.495	10.00	-0.029	0.004	0.044	145.231	0.24	148.682	0.11	-3.452	0.24
	22	209.289	0.00	205.048	0.00	4.241	0.00	0.000	0.000	0.000	209.289	0.00	205.048	0.00	4.241	0.00
	23	121.619	10.00	115.818	0.20	5.757	10.00	0.003	0.002	0.045	121.622	0.26	115.820	0.10	5.802	0.26
2	2	125.574	0.80	117.940	0.20	7.573	0.30	-0.023	0.010	0.028	125.551	0.18	117.950	0.10	7.601	0.17
	3	71.290	0.80	58.186	0.20	12.871	0.30	-0.154	0.018	0.061	71.136	0.24	58.204	0.13	12.933	0.22
	17	145.260	0.80	148.678	0.20	-3.495	0.30	-0.047	0.007	0.023	145.213	0.19	148.685	0.11	-3.472	0.18
	22	209.289	0.00	205.048	0.00	4.241	0.00	0.000	0.000	0.000	209.289	0.00	205.048	0.00	4.241	0.00
	23	121.619	0.80	115.818	0.20	5.757	0.30	-0.028	0.006	0.010	121.591	0.19	115.824	0.10	5.767	0.18
3	2	125.574	10.00	117.940	0.20	7.573	10.00	0.030	0.001	0.091	125.604	0.28	117.941	0.08	7.664	0.29
	3	71.290	10.00	58.186	0.20	12.871	10.00	-0.003	0.006	0.224	71.287	0.32	58.192	0.10	13.095	0.33
	17	145.260	10.00	148.678	0.20	-3.495	10.00	0.013	0.001	0.089	145.273	0.31	148.679	0.08	-3.406	0.32
	22	209.289	0.00	205.048	0.00	4.241	0.00	0.000	0.000	0.000	209.289	0.00	205.048	0.00	4.241	0.00
	23	121.619	10.00	115.818	0.20	5.757	10.00	0.032	0.000	0.075	121.651	0.25	115.818	0.08	5.832	0.25
4	2	125.574	0.80	117.940	0.20	7.573	0.30	-0.046	0.005	0.011	125.528	0.18	117.945	0.08	7.584	0.18
	3	71.290	0.80	58.186	0.20	12.871	0.30	-0.113	0.016	0.104	71.177	0.20	58.202	0.10	12.975	0.19
	17	145.260	0.80	148.678	0.20	-3.495	0.30	-0.047	0.004	0.026	145.213	0.21	148.682	0.08	-3.469	0.20
	22	209.289	0.00	205.048	0.00	4.241	0.00	0.000	0.000	0.000	209.289	0.00	205.048	0.00	4.241	0.00
	23	121.619	0.80	115.818	0.20	5.757	0.30	-0.034	0.004	0.005	121.585	0.16	115.822	0.07	5.762	0.16
5	2	125.574	0.80	117.940	0.20	7.573	0.30	-0.050	0.006	0.005	125.524	0.18	117.946	0.08	7.578	0.17
	3	71.290	0.70	58.186	0.30	12.871	0.25	-0.124	0.022	0.087	71.166	0.19	58.208	0.11	12.958	0.18
	17	145.260	0.75	148.678	0.40	-3.495	0.20	-0.056	0.006	0.016	145.204	0.17	148.684	0.09	-3.479	0.16
	22	209.289	0.00	205.048	0.00	4.241	0.00	0.000	0.000	0.000	209.289	0.00	205.048	0.00	4.241	0.00
	23	121.619	0.80	115.818	0.25	5.757	0.40	-0.039	0.006	-0.001	121.580	0.16	115.824	0.08	5.756	0.16
6	2	125.574	10.00	117.940	0.20	7.573	0.30	-0.053	0.004	0.005	125.521	0.18	117.944	0.08	7.578	0.18
	3	71.290	10.00	58.186	0.20	12.871	0.30	-0.123	0.015	0.095	71.167	0.20	58.201	0.10	12.966	0.20
	17	145.260	10.00	148.678	0.20	-3.495	0.30	-0.053	0.003	0.021	145.207	0.21	148.681	0.08	-3.474	0.21
	22	209.289	0.00	205.048	0.00	4.241	0.00	0.000	0.000	0.000	209.289	0.00	205.048	0.00	4.241	0.00
	23	121.619	10.00	115.818	0.20	5.757	0.30	-0.040	0.004	0.0004	121.579	0.16	115.822	0.08	5.757	0.16

Table 5.4 (a) : South Australia - Results of adjustment applying various accuracies

Line	At	To	Obs.	Case 1			Case 2			Case 3			Case 4			Case 5			Case 6		
Element			(m)	s	v	v/s	s	v	v/s	s	v	v/s	s	v	v/s	s	v	v/s	s	v	v/s
Δh	2	3	-54.284	0.63	0.09	0.14	0.63	0.13	0.21	0.31	0.03	0.11	0.31	0.07	0.22	0.31	0.07	0.24	0.31	0.07	0.23
ΔH	2	3	-59.754	0.21	0.00	-0.02	0.21	-0.01	-0.04	0.14	-0.01	-0.04	0.14	-0.01	-0.08	0.14	-0.02	-0.11	0.14	-0.01	-0.08
ΔN	2	3	5.298	0.63	-0.08	-0.12	0.63	-0.03	-0.05	0.63	-0.13	-0.21	0.63	-0.09	-0.15	0.63	-0.08	-0.13	0.63	-0.09	-0.14
Δh	3	23	50.327	0.61	-0.09	-0.14	0.61	-0.13	-0.21	0.33	-0.04	-0.11	0.33	-0.08	-0.24	0.33	-0.09	-0.26	0.33	-0.08	-0.26
ΔH	3	23	57.632	0.21	0.01	0.02	0.21	0.01	0.06	0.14	0.01	0.04	0.14	0.01	0.09	0.14	0.02	0.11	0.14	0.01	0.08
ΔN	3	23	-7.114	0.61	0.10	0.16	0.61	0.05	0.08	0.65	0.15	0.23	0.65	0.10	0.15	0.65	0.09	0.14	0.65	0.09	0.15
Δh	17	23	-23.641	0.57	-0.03	-0.06	0.57	-0.02	-0.03	0.35	-0.02	-0.05	0.35	-0.01	-0.04	0.35	-0.02	-0.05	0.35	-0.01	-0.04
ΔH	17	23	-32.86	0.20	0.00	0.01	0.20	0.00	0.01	0.13	0.00	0.00	0.13	0.00	-0.01	0.13	0.00	-0.01	0.13	0.00	0.00
ΔN	17	23	9.252	0.57	0.00	0.00	0.57	0.01	0.02	0.70	0.01	0.02	0.70	0.02	0.03	0.70	0.02	0.02	0.70	0.02	0.03
Δh	22	2	-83.635	0.36	0.07	0.20	0.36	0.10	0.28	0.55	0.05	0.09	0.55	0.13	0.23	0.55	0.13	0.24	0.55	0.13	0.24
ΔH	22	2	-87.108	0.16	-0.01	-0.03	0.16	-0.01	-0.06	0.11	0.00	0.00	0.11	0.00	-0.04	0.11	-0.01	-0.06	0.11	0.00	-0.03
ΔN	22	2	3.332	0.36	-0.06	-0.17	0.36	-0.03	-0.08	1.10	-0.09	-0.08	1.10	-0.01	-0.01	1.10	0.00	0.00	1.10	0.00	0.00
Δh	22	17	-64.029	0.38	0.03	0.08	0.38	0.05	0.12	0.53	-0.01	-0.02	0.53	0.05	0.09	0.53	0.06	0.11	0.53	0.05	0.10
ΔH	22	17	-56.37	0.17	0.00	-0.03	0.17	-0.01	-0.04	0.11	0.00	-0.01	0.11	0.00	-0.03	0.11	-0.01	-0.05	0.11	0.00	-0.03
ΔN	22	17	-7.736	0.38	-0.04	-0.02	0.38	-0.02	-0.06	1.06	-0.09	-0.08	1.06	-0.03	-0.02	1.06	-0.02	-0.01	1.06	-0.02	-0.02
Δh	23	2	3.952	0.73	-0.01	-0.01	0.73	-0.01	-0.01	0.27	0.00	-0.01	0.27	0.01	0.03	0.27	0.01	0.03	0.27	0.01	0.04
ΔH	23	2	2.122	0.23	0.00	-0.01	0.23	0.00	-0.02	0.15	0.00	0.00	0.15	0.00	0.00	0.15	0.00	0.00	0.15	0.00	0.00
ΔN	23	2	1.816	0.73	-0.02	-0.03	0.73	-0.02	-0.03	0.55	-0.02	-0.03	0.55	-0.01	-0.01	0.55	-0.01	-0.01	0.55	0.00	-0.01
Δh	23	22	87.614	0.56	-0.05	-0.10	0.56	-0.08	-0.15	0.36	-0.02	-0.07	0.36	-0.09	-0.25	0.36	-0.09	-0.26	0.36	-0.10	-0.27
ΔH	23	22	89.23	0.20	0.00	0.01	0.20	0.01	0.03	0.13	0.00	0.00	0.13	0.00	0.03	0.13	0.01	0.05	0.13	0.00	0.03
ΔN	23	22	-1.516	0.56	0.04	0.08	0.56	0.01	0.02	0.72	0.08	0.10	0.72	0.01	0.01	0.72	0.00	0.00	0.72	0.00	0.00

Table 5.4 (b) : South Australia - Precision and corrections to the 'observed' elements

Case	Station#	Δx before constraints			Δx after constraints			Total Corrections		
		∂h	∂H	∂N	∂h	∂H	∂N	∂h	∂H	∂N
1	2	0.070	0.000	0.000	-0.063	0.005	0.063	0.007	0.005	0.063
	3	0.059	0.000	0.000	-0.142	0.009	0.142	-0.082	0.009	0.142
	17	0.014	0.000	0.000	-0.044	0.004	0.044	-0.029	0.004	0.044
	22	0.000	0.000	0.000	0.000	0.000	0.000	0.000	0.000	0.000
	23	0.047	0.000	0.000	-0.045	0.002	0.045	0.003	0.002	0.045
2	2	0.060	0.000	0.000	-0.080	0.010	0.028	-0.023	0.010	0.028
	3	0.030	0.000	0.000	-0.190	0.018	0.061	-0.154	0.018	0.061
	17	0.010	0.000	0.000	-0.058	0.007	0.023	-0.047	0.007	0.023
	22	0.000	0.000	0.000	0.000	0.000	0.000	0.000	0.000	0.000
	23	0.030	0.000	0.000	-0.060	0.006	0.010	-0.028	0.006	0.010
3	2	0.050	0.000	0.000	-0.020	0.001	0.091	0.030	0.001	0.091
	3	0.050	0.000	0.000	-0.060	0.006	0.224	-0.010	0.006	0.224
	17	0.040	0.000	0.000	-0.020	0.001	0.089	0.013	0.001	0.089
	22	0.000	0.000	0.000	0.000	0.000	0.000	0.000	0.000	0.000
	23	0.050	0.000	0.000	-0.020	0.000	0.075	0.032	0.000	0.075
4	2	0.040	0.000	0.000	-0.080	0.005	0.011	-0.046	0.005	0.011
	3	0.040	0.000	0.000	-0.150	0.016	0.104	-0.113	0.016	0.104
	17	0.020	0.000	0.000	-0.070	0.004	0.026	-0.047	0.004	0.026
	22	0.000	0.000	0.000	0.000	0.000	0.000	0.000	0.000	0.000
	23	0.040	0.000	0.000	0.070	0.004	0.005	-0.034	0.004	0.005
5	2	0.040	0.000	0.000	-0.090	0.006	0.005	-0.050	0.006	0.005
	3	0.030	0.000	0.000	-0.160	0.022	0.087	-0.124	0.022	0.087
	17	0.020	0.000	0.000	-0.080	0.006	0.016	-0.056	0.006	0.016
	22	0.000	0.000	0.000	0.000	0.000	0.000	0.000	0.000	0.000
	23	0.040	0.000	0.000	-0.070	0.006	-0.001	-0.039	0.006	-0.001
6	2	0.050	0.000	0.000	-0.110	0.004	0.005	-0.053	0.004	0.005
	3	0.050	0.000	0.000	-0.180	0.015	0.095	-0.123	0.015	0.095
	17	0.040	0.000	0.000	-0.090	0.003	0.021	-0.053	0.003	0.021
	22	0.000	0.000	0.000	0.000	0.000	0.000	0.000	0.000	0.000
	23	0.050	0.000	0.000	-0.090	0.004	0.000	-0.040	0.004	0.0004

Table 5.4 (c) : South Australia - Results of adjustment on the corrections to the parameters

5.3 NSW Coast Test Network

The network chosen for this test is shown in Figure 5.2, and its details are summarised in Tables 5.1 and 5.2. It is typical of the levelling network along coastal Australia, with fairly short levelled lines connecting to tide gauge stations of variable quality, across terrain which is fairly hilly, and with geoidal characteristics which are influenced by the coastal effects.

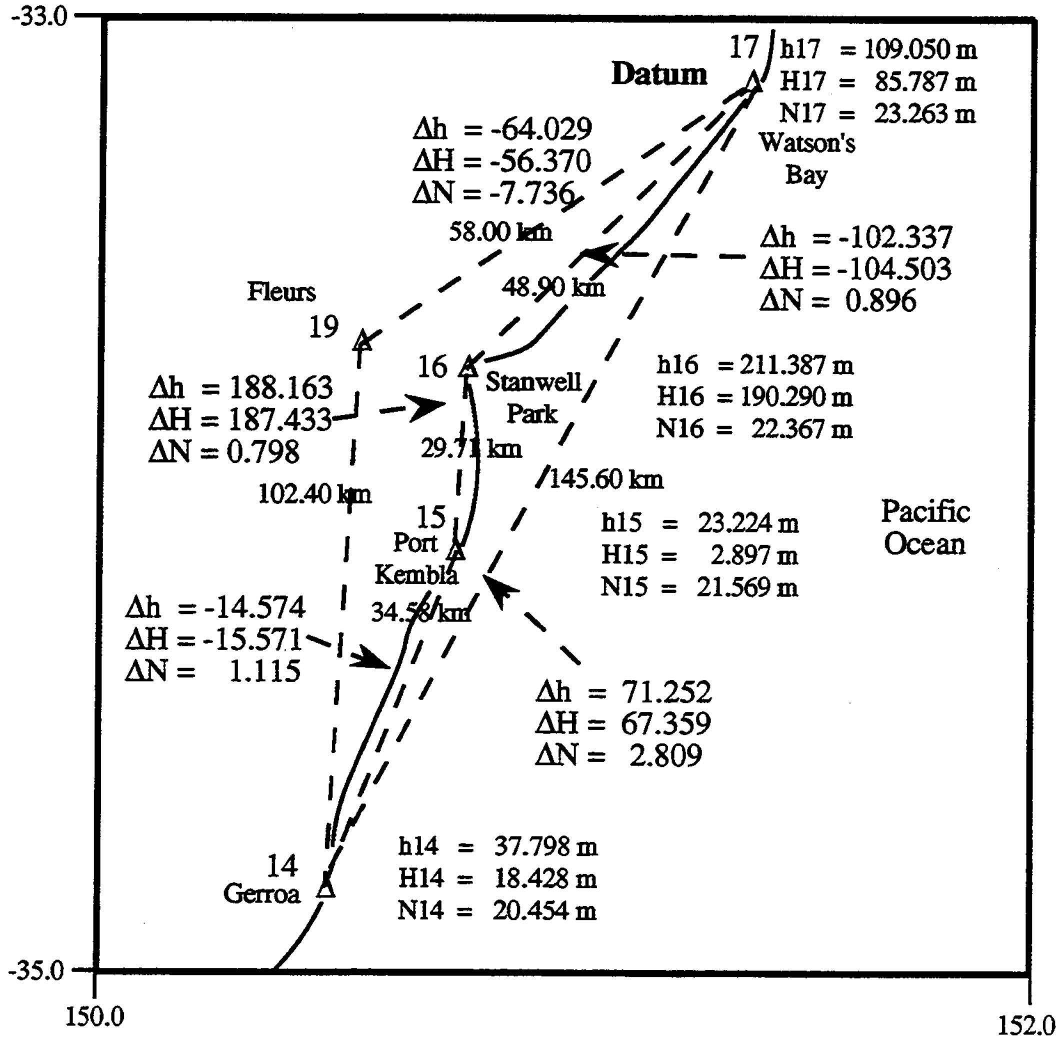

Figure 5.2 : NSW Coast network diagram.

GPS lines have been observed over the coastal lines, and out to the VLBI dish at Fleurs.

The network was adjusted using H and N at Sydney to provide the datum for h.

Two adjustments were done. The first assumed the *a priori* estimates of h were poorly known and were given standard errors of ±10 m. The second assumed they were good to about ±5 cm. In both cases H and N were given error estimates of about ±0.1 to ±0.07 m (for H),

Case	Station#	A priori Values						Total Corrections			Adjusted Values					
		h(m)	Sh(m)	H(m)	SH(m)	N(m)	SN(m)	∂h	∂H	∂N	h(m)	sh(m)	H(m)	SH(m)	N(m)	SN(m)
1	14	37.798	10.000	18.428	0.065	20.454	0.260	0.628	-0.044	-0.412	38.426	0.08	18.384	0.05	20.042	0.08
	15	23.224	10.000	2.857	0.070	21.569	0.260	0.652	-0.096	-0.454	23.876	0.07	2.761	0.04	21.115	0.07
	16	211.387	10.000	190.290	0.100	22.367	0.260	0.629	-0.174	-0.467	212.016	0.07	190.116	0.05	21.900	0.06
	17	109.050	0.000	85.787	0.000	23.263	0.000	0.000	0.000	0.000	109.050	0.00	85.787	0.00	23.263	0.00
2	14	37.798	0.047	18.428	0.065	20.454	0.260	0.060	-0.123	-0.901	37.858	0.04	18.306	0.04	19.553	0.05
	15	23.224	0.048	2.857	0.070	21.569	0.260	0.094	-0.193	-0.915	23.318	0.03	2.664	0.04	20.654	0.05
	16	211.387	0.050	190.290	0.100	22.367	0.260	0.142	-0.274	-0.854	211.529	0.03	190.016	0.04	21.514	0.05
	17	109.050	0.000	85.787	0.000	23.263	0.000	0.000	0.000	0.000	109.050	0.00	85.787	0.00	23.263	0.00

Table 5.5 (a) : NSW Coast - Results of adjustment applying various accuracies to the parameters.

Line	At	To	Obs.	Case 1			Case 2		
Element			(m)	s	v	v/s	s	v	v/s
Δh	14	15	-14.570	0.07	-0.02	-0.35	0.07	-0.03	-0.49
ΔH	14	15	-15.570	0.07	0.05	0.74	0.07	0.07	0.99
ΔN	14	15	1.110	0.07	0.04	0.60	0.07	0.01	0.20
Δh	15	16	188.160	0.06	0.02	0.39	0.06	-0.05	-0.81
ΔH	15	16	187.430	0.07	0.08	1.19	0.07	0.08	1.25
ΔN	15	16	0.800	0.06	0.01	0.22	0.06	-0.06	-1.04
Δh	16	17	-102.340	0.10	0.63	6.49	0.10	0.14	1.46
ΔH	16	17	-104.500	0.08	-0.17	-2.07	0.08	-0.27	-3.27
ΔN	16	17	0.900	0.10	-0.47	-4.82	0.10	-0.85	-8.80
Δh	14	17	71.250	0.29	0.63	2.13	0.29	0.06	0.20
ΔH	14	17	67.360	0.15	-0.04	-0.30	0.15	-0.12	-0.84
ΔN	14	17	2.810	0.29	-0.41	-1.40	0.29	-0.90	-3.06

Table 5.5 (b) : NSW Coast - Details of corrections to the line elements.

and ±0.26 m (for N), respectively. The precisions of the line elements are estimated in Table 5.5(a). The corrections from the adjustment to the line elements are summarised in Table 5.5(b) and corrections to the parameters detailed in Table 5.5 (c). See Appendices 11 and 12 for the output of the adjustment results.

We can see from Table 5.5 (c) what a profound influence the input standard deviation of the ellipsoidal heights can have upon this network adjustment. Without applying the station constraints the results of the two adjustments are identical, effectively so because no corrections are applied, since all the 'observations' are differences of the point values and we have therefore, already achieved the ideal zero misclose for the loop. When station constraints are applied, the h values between Case 1 and 2 change by up to 0.6 m; the H values by up to 0.1 m; and the N values by about 0.4 m. The input standard deviations of the h values used in Cases 1 and 2 changes by over 2 orders of magnitude which is, by any standards, a large change.

In this, and most GPS networks, the ellipsoidal heights will be poorly known (compared to Δh), and Case 1 ($s_h = \pm$ 10 m) is probably a more accurate reflection of the truth than is Case 2 ($s_h = \pm$ 0.5 m).

The v/s values are larger for the Δh in Case 1 than 2, and in Case 2, v/s for Δh and ΔN are larger than for Case 1. As a result, the variance factor for Case 2 is larger than for Case 1. This is because in Case 2 the h values are more tightly controlled, and thus errors in the networks are pushed into the H and N parameters, and the ΔH and ΔN line elements. This shows the importance of using realistic estimates of the standard deviations for the parameters in the adjustment.

Case	**Station#**	**Δx before constraint**			**Δx after constraint**			**Total Corrections**		
		∂h	∂H	∂N	∂h	∂H	∂N	∂h	∂H	∂N
1	14	0.00	0.00	0.00	0.63	-0.04	-0.41	0.63	-0.04	-0.41
	15	0.00	0.00	0.00	0.65	-0.10	-0.45	0.65	-0.10	-0.45
	16	0.00	0.00	0.00	0.63	-0.17	-0.47	0.63	-0.17	-0.47
	17	0.00	0.00	0.00	0.00	0.00	0.00	0.00	0.00	0.00
2	14	0.00	0.00	0.00	0.06	-0.12	-0.90	0.06	-0.12	-0.90
	15	0.00	0.00	0.00	0.09	-0.19	-0.91	0.09	-0.19	-0.91
	16	0.00	0.00	0.00	0.14	-0.27	-0.85	0.14	-0.27	-0.85
	17	0.00	0.00	0.00	0.00	0.00	0.00	0.00	0.00	0.00

Table 5.5 (c) : NSW Coast - Results of adjustment on the corrections to the parameters.

5.4 South-East Luzon Network

This test network is shown in Figure 5.3, and its details are summarised in Tables 5.1 and 5.2. It is a small part of a Philippines-wide GPS/levelling project undertaken recently for the AIDAB-sponsored Land Management and Resources Development Project for this country. This segment is typical of the network as a whole, with rugged terrain, complex tectonics and inadequate gravity data hindering the evaluation of the geoid heights and with levelling of (sometimes) uncertain quality connecting onto tide gauges. The GPS survey, at least, is homogeneous and well distributed.

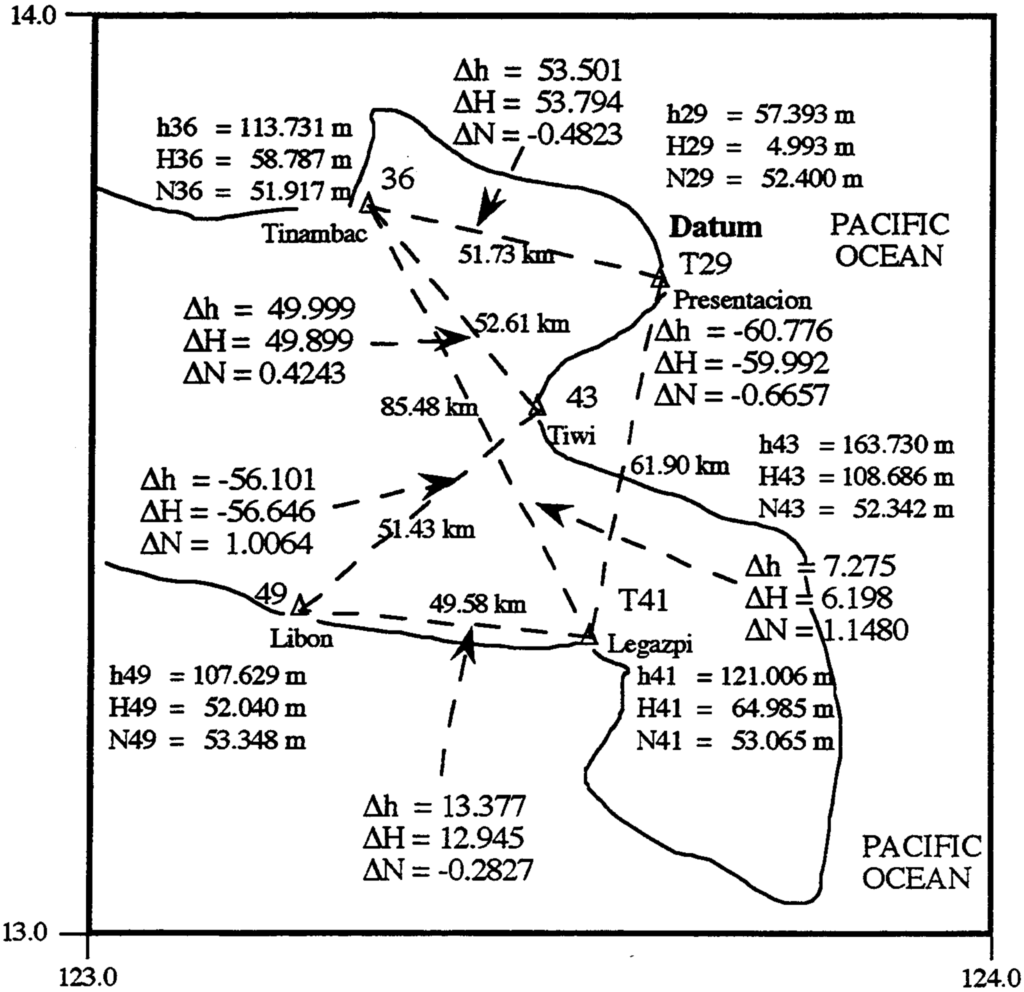

Figure 5.3 : South East Luzon network diagram.

The network was adjusted a number of ways, but always holding h, H and N for point T 29 (T-for tide gauge) fixed. The precisions of the line elements were derived as for Cases 1 and 2 of the South Australian Test. The input standard deviations of the parameter values, for Case 1, were all allowed to float i.e. were set to ±10 m. For Case 2, the input standard deviation of the tide gauge at Point T 41 was given as ±0.46 m; for Case 3, it was stated as ±0.05 m.

Case	Station#	A priori Values						Total Corrections			Adjusted Values					
		h(m)	Sh(m)	H(m)	SH(m)	N(m)	SN(m)	∂h	∂H	∂N	h(m)	sh(m)	H(m)	SH(m)	N(m)	SN(m)
1	T29	57.393	0.00	4.993	0.00	52.400	0.00	0.000	0.000	0.000	57.393	0.00	4.993	0.00	52.400	0.00
	36	113.731	10.00	58.787	10.00	51.917	10.00	-1.123	0.781	1.123	112.608	0.07	59.568	0.06	53.040	0.07
	T41	121.006	10.00	64.985	10.00	53.065	10.00	-1.092	0.772	1.092	119.914	0.06	65.757	0.06	54.157	0.06
	43	163.730	10.00	108.686	10.00	52.342	10.00	-1.003	0.696	1.003	162.727	0.10	109.382	0.09	53.345	0.10
	49	107.629	10.00	52.040	10.00	53.348	10.00	-0.821	0.599	0.821	106.808	0.09	52.639	0.08	54.169	0.09
2	T29	57.393	0.00	4.993	0.00	52.400	0.00	0.000	0.000	0.000	57.393	0.00	4.993	0.00	52.400	0.00
	36	113.731	10.00	58.787	10.00	51.917	10.00	-1.126	0.775	1.126	112.605	0.07	59.562	0.06	53.043	0.07
	T41	121.006	10.00	64.985	0.46	53.065	10.00	-1.098	0.760	1.098	119.908	0.06	65.745	0.06	54.163	0.06
	43	163.730	10.00	108.686	10.00	52.342	10.00	-1.007	0.688	1.007	162.723	0.10	109.374	0.09	53.349	0.10
	49	107.629	10.00	52.040	10.00	53.348	10.00	-0.827	0.588	0.827	106.803	0.09	52.628	0.08	54.175	0.09
3	T29	57.393	0.00	4.993	0.00	52.400	0.00	0.000	0.000	0.000	57.393	0.00	4.993	0.00	52.400	0.00
	36	113.731	10.00	58.787	10.00	51.917	10.00	-1.246	0.535	1.246	112.485	0.06	59.322	0.05	53.163	0.06
	T41	121.006	10.00	64.985	0.05	53.065	10.00	-1.315	0.326	1.315	119.691	0.06	65.311	0.04	54.380	0.06
	43	163.730	10.00	108.686	10.00	52.342	10.00	-1.157	0.389	1.157	162.573	0.10	109.075	0.08	53.498	0.10
	49	107.629	10.00	52.040	10.00	53.348	10.00	-1.019	0.203	1.019	106.610	0.09	52.243	0.07	54.367	0.09

Table 5.6 (a) : Luzon Coast - Results of adjustment applying various accuracies to the parameters

The results are summarised in Tables 5.6(a), 5.6(b) and 5.6(c). See Appendices 13, 14 and 15 for the output of the adjustment results.

Line Element	At	To	Obs. (m)	Case 1 s	Case 1 v	Case 1 v/s	Case 2 s	Case 2 v	Case 2 v/s	Case 3 s	Case 3 v	Case 3 v/s
Δh	T29	36	56.3384	0.10	1.12	10.90	0.10	1.13	10.93	0.10	1.25	12.10
ΔH	T29	36	53.7940	0.09	-0.78	-9.09	0.09	-0.77	-9.01	0.09	-0.53	-6.21
ΔN	T29	36	-0.4823	0.10	-1.12	-10.90	0.10	-1.13	-10.93	0.10	-1.25	-12.10
Δh	36	43	49.9990	0.12	-0.12	-0.97	0.12	-0.12	-0.97	0.12	-0.09	-0.73
ΔH	36	43	49.8990	0.09	0.09	0.91	0.09	0.09	0.92	0.09	0.15	1.55
ΔN	36	43	0.4243	0.12	0.12	0.97	0.12	0.12	0.97	0.12	0.09	0.73
Δh	43	49	-56.1010	0.17	-0.18	-1.07	0.17	-0.18	-1.06	0.17	-0.14	-0.81
ΔH	43	49	-56.6460	0.11	0.10	0.88	0.11	0.10	0.91	0.11	0.19	1.69
ΔN	43	49	1.0064	0.17	0.18	1.07	0.17	0.18	1.06	0.17	0.14	0.81
Δh	49	T41	13.3770	0.10	0.27	2.58	0.10	0.27	2.59	0.10	0.30	2.82
ΔH	49	T41	12.9450	0.09	-0.17	-1.99	0.09	-0.17	-1.97	0.09	-0.12	-1.41
ΔN	49	T41	-0.2827	0.10	-0.27	-2.58	0.10	-0.27	-2.59	0.10	-0.30	-2.82
Δh	T41	T29	63.6134	0.10	-1.09	-10.92	0.10	-1.10	-10.98	0.10	-1.31	-13.15
ΔH	T41	T29	-59.9920	0.08	0.77	9.19	0.80	0.76	9.04	0.80	0.33	3.88
ΔN	T41	T29	-0.6657	0.10	1.09	10.92	0.10	1.10	10.98	0.10	1.31	13.15
Δh	36	T41	7.2750	0.10	-0.03	-0.30	0.10	-0.03	-0.27	0.10	0.07	0.67
ΔH	36	T41	6.1980	0.09	0.01	0.11	0.90	0.02	0.18	0.90	0.21	2.42
ΔN	36	T41	1.1480	0.10	0.03	0.30	0.10	0.03	0.27	0.10	-0.07	-0.67

Table 5.6 (b) : Luzon Coast - Details of corrections to the line elements.

One problem existing in this network was the large discrepancy between datums. The ellipsoidal height values from GPS varied from those derived from H and N by up to 3 m in this region, and proved to be a major influence on the solutions of this network. The reduction of σ_H from ±10.0 m to ±0.5 m at point T41 had only a small impact on the results (compare Case 1 with Case 2 - Tables 5.6(b) and 5.6(c)). After applying the constraints, the corrections to the line elements, and to the parameters themselves, were up to 1 m or more in each of the H, h and N at some points, trying to resolve a large station misclose for both Cases 1 and 2. By reducing the input standard deviation of H at point T41 to ±0.05 m (Case 3) the corrections to all H and ΔH reduced significantly and the corrections to all h, N (and Δh, ΔN) increased accordingly.

It is obvious that, in a fully-observed network such as this, the inclusion of even just one accurate tide gauge height in the network has an effect well beyond the orthometric heights in the network. Nevertheless, the tide gauge value has still changed by 0.33 m (see Table 5.6(c), Case 3, Point 41), or about 6 times the stated accuracy. Clearly, in a real situation, the input standard deviation of the parameters must be estimated with care! For example, in this network, one would think it appropriate to give all N and H values higher accuracies (since both are known to about 0.5 to 1 m, at least) and let these parameters establish the datum for h, as was the case for the NSW Coast test. However it is suspected that gross errors exist in the ΔH observations, as shown by the large v/s values in Table 5.6(b) so more accurate values for H may not be justified.

Case	Station #	Δx before constraints			Δx before constraints			Total Corrections		
		∂h	∂H	∂N	∂h	∂H	∂N	∂h	∂H	∂N
1	T29	0.00	0.00	0.00	0.00	0.00	0.00	0.00	0.00	0.00
	36	0.00	0.00	0.00	-1.12	0.78	1.12	-1.12	0.78	1.12
	T41	0.00	0.00	0.00	-1.09	0.77	1.09	-1.09	0.77	1.09
	43	0.00	0.00	0.00	-1.00	0.70	1.00	-1.00	0.70	1.00
	49	0.00	0.00	0.00	-0.82	0.60	0.82	-0.82	0.60	0.82
2	T29	0.00	0.00	0.00	0.00	0.00	0.00	0.00	0.00	0.00
	36	0.00	0.00	0.00	-1.13	0.77	1.13	-1.13	0.77	1.13
	T41	0.00	0.00	0.00	-1.10	0.76	1.10	-1.10	0.76	1.10
	43	0.00	0.00	0.00	-1.01	0.69	1.01	-1.01	0.69	1.01
	49	0.00	0.00	0.00	-0.83	0.59	0.83	-0.83	0.59	0.83
3	T29	0.00	0.00	0.00	0.00	0.00	0.00	0.00	0.00	0.00
	36	0.00	0.00	0.00	-1.25	0.53	1.25	-1.25	0.53	1.25
	T41	0.00	0.00	0.00	-1.31	0.33	1.31	-1.31	0.33	1.31
	43	0.00	0.00	0.00	-1.16	0.39	1.16	-1.16	0.39	1.16
	49	0.00	0.00	0.00	-1.02	0.20	1.02	-1.02	0.20	1.02

Table 5.6 (c) : Luzon Coast - Results of the adjustment on the corrections to the parameters.

6 TREATMENT OF CORRELATIONS AND COVARIANCES IN THE ADJUSTMENT

The next stage of programming involves the use of correlation information between the stations in the network. This is significant especially when we are incorporating pre-computed information in the network. For example, unlike truly 'integrated' geodetic techniques (e.g.Milbert et al, 1992) which (at least in theory) start from the basic observation (gravity observation; staff measurement from levelling), we incorporate pre-computed (e.g. N from gravity), and even pre-adjusted (e.g. H from the AHD; Δh from GPS) into the network adjustment. It is important that reliable estimates of the variances and cross-correlations (or covariances) of the parameters be used, and this poses problems for us because many of these values are, at this early stage of our experience, 'guesstimations' at best. For example, the formal errors resulting from the internal error propagation for the h_{GPS}, or the N_{GRAV}, may be poor reflections of the true values. Only by carrying out investigations such as this, can we establish what values of the variances and covariances may be considered realistic.

Accurate information on the correlations is also vital, for example, in the estimation of geoid height **differences,** where the largest contribution to the error budget comes from the uncertainty in this estimation. Another aspect that we consider is the possibility of having different height elements fixed at different stations, depending on the accuracies of the elements. Currently, only one station could be held as datum, and consequently all three height elements at that particular station are held fixed.

6.1 VARIANCE COVARIANCE MATRIX FOR GEOID HEIGHTS

The geoid height, N, has both a long to medium wavelength component (N_L) and a short wavelength component (N_S), given by equation 6.1 below, whereas the propagation of error of N is outlined in equation 6.2. The difference in the geoid height between two stations takes the form of equation 6.3 and when the principles of propagation of errors are employed, we obtain equation 6.4, which gives the variance of the difference in geoid heights between two stations.

$$N = N_L + N_S \tag{6.1}$$

$$S_N^2 = S_{N_L}^2 + S_{N_S}^2 \tag{6.2}$$

$$\Delta N_{AB} = -\left(N_{L_A} + N_{S_A}\right) + \left(N_{L_B} + N_{S_B}\right) \tag{6.3}$$

$$S_{\Delta N_{AB}}^2 = S_{N_{LA}}^2 + S_{N_{LB}}^2 + S_{N_{SA}}^2 + S_{N_{SB}}^2 - 2S_{N_{LA}N_{LB}} - 2S_{N_{SA}N_{SB}} \tag{6.4}$$

The sample correlation coefficient r_{xy} between two random variables x and y can be calculated from two sets of observations using equation 6.5. Using this equation to get the correlation between two sites for both the long to medium wavelength component (N_{L_A} and N_{L_B}) and the short wavelength component (N_{S_A} and N_{S_B}), equation 6.6 is derived for both components, substituting in their respective variables. Putting equation 6.6 into equation 6.4, we obtain equation 6.7 below.

$$r_{xy} = \frac{S_{xy}}{S_x\, S_y} \tag{6.5}$$

$$S_{N_{LA}N_{LB}} = r_{N_{LA}N_{LB}}\, S_{N_{LA}}\ S_{N_{LB}} \tag{6.6}$$

$$S^2_{\Delta N_{AB}} = S^2_{N_{L_A}} + S^2_{N_{L_B}} + S^2_{N_{S_A}} + S^2_{N_{S_B}} - 2\, r_{N_{L_A}N_{L_B}} S_{N_{L_A}} S_{N_{L_B}} - 2\, r_{N_{S_A}N_{S_B}} S_{N_{S_A}} S_{N_{S_B}} \qquad (6.7)$$

Computations of the standard deviations of the geoid undulation from OSU89 (which contributes to the long to medium wavelength component) on a global 5° x 5° grid, is based on the error variance-covariance matrix of OSU89B for coefficients derived from GEM-T2 (Rapp and Pavlis, 1990). Referring to Figure 6.1, the standard deviations of geoid undulations from OSU89B range from 24 cm to 34 cm from the southern to northern Australia. For our sample of tested data which are in relatively small areas, the input standard deviation from the long to medium wavelength component (S_{N_L}) for the stations within any one test area would be very similar. Therefore, between stations A and B in, for example the Alcoa area in Western Australia, $S_{N_{L_A}}$ is approximately equal to $S_{N_{L_B}}$. The correlation in S_{N_L} between two stations in any of our test areas would be very high (close to unity) because

i. of the limited extent of the test regions (< 100 km), and

ii. of the high correlation of the errors in the gravity data 0.5° mean values which have been used to solve the coefficients of the OSU89 model.

The same general comments hold for other, more recent, high-order geopotential models, such as OSU91.

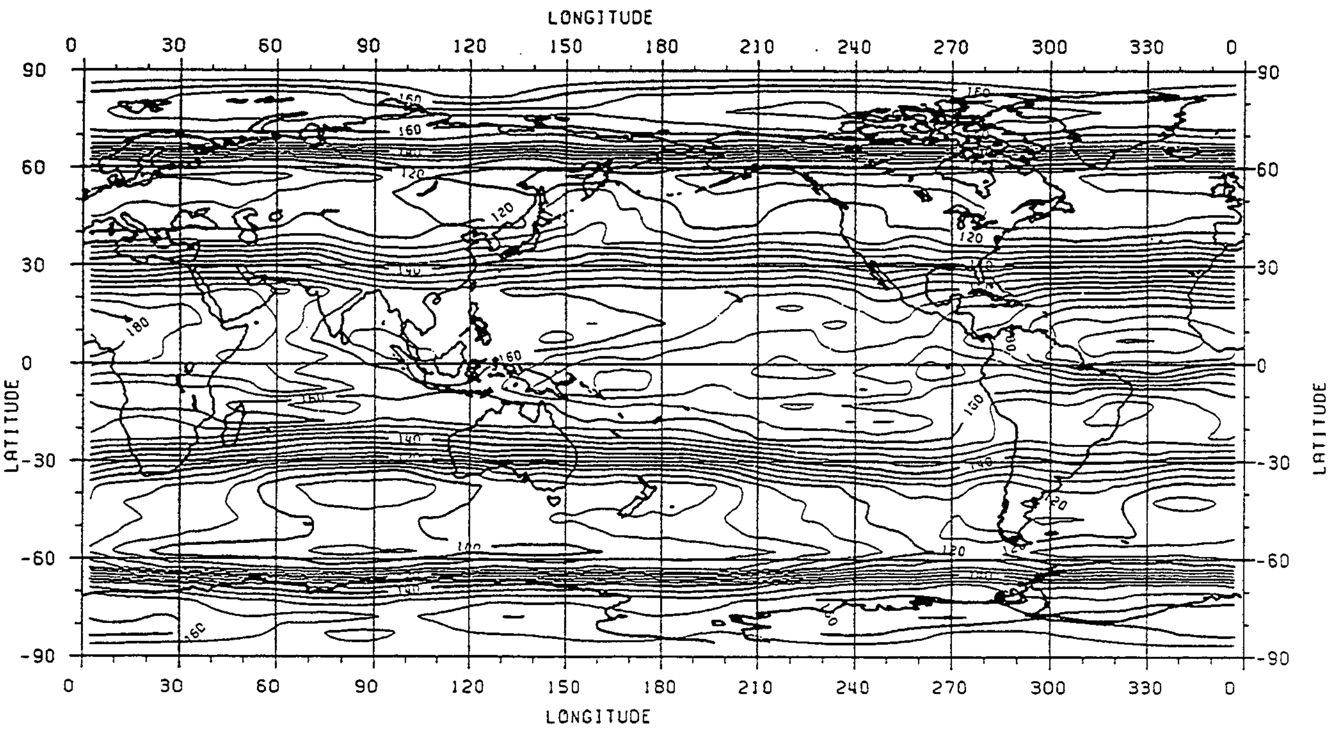

Fig. 6.1 : Geoid undulation standard deviations based on the error variance-covariance matrix of OSU89B for coefficients existing in GEM-T2 (see Rapp and Pavlis, 1990, p. 21 907)
(Contour interval is 2 cm)

From the contour pattern in Figure 6.1, we could also deduce that the associated standard deviations of the geoid undulation is latitude dependent. Thus the values of the standard deviation in the geoid undulations between Perth in Western Australia and Newcastle in New South Wales would be insignificantly small.

Taking the above assumptions into account, we obtain equation 6.8 which consists predominantly of the short wavelength components.

$$S^2_{\Delta N_{AB}} = S^2_{N_{S_A}} + S^2_{N_{S_B}} - 2\, r_{N_{S_A}N_{S_B}} S_{N_{S_A}} S_{N_{S_B}} \tag{6.8}$$

The correlation information in the short wavelength component between stations A and B is represented by equation 6.9. While both $S_{N_{S_A}}$ and $S_{N_{S_B}}$ results from the RINT integration and is based on such factors as the roughness of the gravity field or terrain, the proximity of gravity data to the RINT mid-compartment point and the area of the compartment (Kearsley, 1985 ; Kearsley, 1986), the $S_{\Delta N_{AB}}$ is assumed to be 2 ppm, when using the same RINT software (Kearsley, 1988), the equation of which is shown as 6.10. Finally, we could work out the covariance in the geoid height values between two stations, shown in equation 6.11, where the components contributing to this equation are obtained in the above discussion.

$$r_{N_{S_A}N_{S_B}} = \frac{S^2_{N_{S_A}} + S^2_{N_{S_B}} - S^2_{\Delta N_{AB}}}{2\, S_{N_{S_A}} S_{N_{S_B}}} \tag{6.9}$$

$$S_{\Delta N_{AB}} = \frac{\text{Distance}_{AB} \text{ x ppm}}{1000000} \tag{6.10}$$

$$S_{N_A N_B} = r_{N_A N_B}\, S_{N_A}\, S_{N_B} \tag{6.11}$$

6.2 DIFFERENTIAL ELLIPSOIDAL HEIGHTS AND VARIANCE COVARIANCE MATRIX FOR h

6.2.1 Data availability

The data from GPS surveys include the RAPX files which contain the geodetic coordinates (φ, λ, h) of the GPS stations, which can be used as the preliminary information on the coordinates. GPS observations in GEOLAB format are either in Code 41 (which gives the differences in cartesian coordinates, namely ΔX, ΔY and ΔZ) or in Code 92 (which gives the point positions of each observed station in cartesian coordinates X, Y and Z). Therefore, to get the 'observed' Δh using GPS, the processes followed are outlined as below.

i. Convert the preliminary geodetic coordinates (φ, λ, h) into cartesian coordinates (X,Y,Z), using the datum for which N was determined.

ii. Apply the corrections from GEOLAB output to get the corrected coordinates using

$$X' = X + \Delta X$$
$$Y' = Y + \Delta Y$$
$$Z' = Z + \Delta Z$$

where X', Y' and Z' are the corrected coordinates for one end of the baseline and X, Y and Z are the coordinates for the other end of the baseline.

iii. Convert the corrected cartesian coordinates into geodetic coordinates. The differences between stations, particularly Δh, are then calculated and used as the 'observed' difference in the ellipsoidal heights.

6.2.2 Theory and formula for forming VCV of Δh

From section 6.2.1, we have to accordingly account for two factors when calculating the error estimates of the differences in the ellipsoidal heights. These include using the internal accuracy supplied in the GEOLAB output of the associated standard deviation and the correlation information between the observed ΔX, ΔY and ΔZ, in the form of an upper triangular VCV matrix; and considering the process of conversion of the coordinates from the cartesian form into the geodetic form.

The variance covariance matrix for ΔX, ΔY and ΔZ is shown by 6.12. Using the relationship between the observed ΔX, ΔY and ΔZ, which is given by the correlation information between two variables of these parameters and the standard deviations of each variable as based on equation 6.5, we derived the covariance of two variables, reflected by equations 6.13, 6.14 and 6.15, for the covariance of ΔX and ΔY, ($S_{\Delta X\,\Delta Y}$); the covariance of ΔX and ΔZ ($S_{\Delta X\,\Delta Z}$); and the covariance of ΔY and ΔZ, ($S_{\Delta Y\,\Delta Z}$) respectively.

$$VCV_{\Delta X\,\Delta Y\,\Delta Z} = \begin{bmatrix} S^2_{\Delta X} & S_{\Delta X\,\Delta Y} & S_{\Delta X\,\Delta Z} \\ S_{\Delta X\,\Delta Y} & S^2_{\Delta Y} & S_{\Delta Y\,\Delta Z} \\ S_{\Delta X\,\Delta Z} & S_{\Delta Y\,\Delta Z} & S^2_{\Delta Z} \end{bmatrix} \tag{6.12}$$

$$S_{\Delta X \Delta Y} = r_{\Delta X \Delta Y} S_{\Delta X} \; S_{\Delta Y} \qquad (6.13)$$

$$S_{\Delta X \Delta Z} = r_{\Delta X \Delta Z} S_{\Delta X} \; S_{\Delta Z} \qquad (6.14)$$

$$S_{\Delta Y \Delta Z} = r_{\Delta Y \Delta Z} S_{\Delta Y} \; S_{\Delta Z} \qquad (6.15)$$

Given that Y = F(X), the variance-covariance matrix of Y is given as $\mathbf{VCV_Y = J \; VCV_X \; J^T}$ (**J** is the Jacobian matrix, given by 6.16), as based on the theory of conversion of variance covariance matrices and the propagation of variances (e.g. Mikhail, 1976).

$$\mathbf{J} = \frac{\partial Y}{\partial X} = \begin{bmatrix} \frac{\partial Y_1}{\partial X_1} & \frac{\partial Y_1}{\partial X_2} & \frac{\partial Y_1}{\partial X_3} & \\ \frac{\partial Y_2}{\partial X_1} & \frac{\partial Y_2}{\partial X_2} & \frac{\partial Y_2}{\partial X_3} & \cdots\cdot \\ \frac{\partial Y_3}{\partial X_1} & \frac{\partial Y_3}{\partial X_2} & \frac{\partial Y_3}{\partial X_3} & \\ \cdots & \cdots & \cdots & \text{etc} \end{bmatrix} \qquad (6.16)$$

The variance covariance matrix of $\Delta\varphi$, $\Delta\lambda$ and Δh therefore, is given by equation 6.17 below. (see Harvey, 1985; Harvey, 1991). The Jacobian matrix, **J** contains the differential of geodetic coordinates (φ, λ, h) in terms of their cartesian coordinates (X,Y,Z). Expanding 6.17 into its matrix form, we get 6.18, which will be used to estimate the associated standard deviation of the ellipsoidal height differences.

$$\mathrm{VCV}_{\Delta\varphi\,\Delta\lambda\,\Delta h} = \mathbf{J}\; \mathrm{VCV}_{\Delta X\,\Delta Y\,\Delta Z}\; \mathbf{J}^T \qquad (6.17)$$

$$\mathrm{VCV}_{\Delta\varphi\,\Delta\lambda\,\Delta h} = \begin{bmatrix} J_{11} & J_{12} & J_{13} \\ J_{21} & J_{22} & 0 \\ J_{31} & J_{32} & J_{33} \end{bmatrix} \begin{bmatrix} S^2_{\Delta X} & r_{\Delta X \Delta Y} S_{\Delta X} \; S_{\Delta Y} & r_{\Delta X \Delta Z} S_{\Delta X} \; S_{\Delta Z} \\ r_{\Delta X \Delta Y} S_{\Delta X} \; S_{\Delta Y} & S^2_{\Delta Y} & r_{\Delta Y \Delta Z} S_{\Delta Y} \; S_{\Delta Z} \\ r_{\Delta X \Delta Z} S_{\Delta X} \; S_{\Delta Z} & r_{\Delta Y \Delta Z} S_{\Delta Y} \; S_{\Delta Z} & S^2_{\Delta Z} \end{bmatrix} \mathbf{J}^T \qquad (6.18)$$

We could thus obtain the error estimate of the difference in the height element (Δh), the variance of which is given by equation 6.19, whose elements are constituted by equations 6.20 to 6.25 (Harvey, 1985). Note that the estimation of the Jacobian elements uses the values of the cartesian coordinates of the second station (the 'to' station). Hence,

$$s^2_{\Delta h} = \left(J(3,1)\, S^2_{\Delta X} + J(3,2)\ r_{\Delta X\,\Delta Y}\, S_{\Delta X}\ S_{\Delta Y} + J(3,3)\, r_{\Delta X\,\Delta Z}\, S_{\Delta X}\ S_{\Delta Z}\right)\ J(3,1) +$$
$$\left(J(3,1)\, r_{\Delta X\,\Delta Y}\, S_{\Delta X}\ S_{\Delta Y} + J(3,2)\ S^2_{\Delta Y} + J(3,3)\, r_{\Delta Y\,\Delta Z}\, S_{\Delta Y}\ S_{\Delta Z}\right)\ J(3,2) + \qquad (6.19)$$
$$\left(J(3,1)\, r_{\Delta X\,\Delta Z}\, S_{\Delta X}\ S_{\Delta Z} + J(3,2)\ r_{\Delta Y\,\Delta Z}\, S_{\Delta Y}\ S_{\Delta Z} + J(3,3)\ S^2_{\Delta Z}\right)\ J(3,3)$$

where

$$J(1,1) = \frac{X \tan\varphi}{R^2\left(e^2 - \sec^2\varphi\right)} \qquad (6.20)$$

$$J(3,1) = \left(\frac{X}{R\cos\varphi}\right) + J(1,1)\left[\left(\frac{R\sin\varphi}{\cos^2\varphi}\right) - \left(\frac{ve^2 \sin\varphi\cos\varphi}{1 - e^2\sin^2\varphi}\right)\right] \qquad (6.21)$$

$$J(1,2) = \frac{Y\, J(1,1)}{X} \qquad (6.22)$$

$$J(3,2) = \left(\frac{Y}{R\cos\varphi}\right) + J(1,2)\left[\left(\frac{R\sin\varphi}{\cos^2\varphi}\right) - \left(\frac{ve^2 \sin\varphi\cos\varphi}{1 - e^2\sin^2\varphi}\right)\right] \qquad (6.23)$$

$$J(1,3) = \frac{1}{\left[R\sec^2\varphi - e^2\, v\cos\varphi\right]} \qquad (6.24)$$

and

$$J(3,3) = J(1,3)\left[\left(\frac{R\sin\varphi}{\cos^2\varphi}\right) - \left(\frac{ve^2 \sin\varphi\cos\varphi}{1 - e^2\sin^2\varphi}\right)\right] \qquad (6.25)$$

6.3 ESTIMATION OF THE INPUT STANDARD DEVIATIONS FOR THE ORTHOMETRIC HEIGHTS

Values for the input standard deviations for the absolute values of the orthometric heights are taken from a posteriori information, such as the results of a national levelling adjustment. For instance, in the Australian example, the input standard deviations for the orthometric heights from the AHD are scaled from figure 6.2 (Roelse, Granger and Graham, 1975, Annex G), determined from a fixed adjustment by holding the thirty tide gauges as fixed, effectively fixing the sea level i.e. heights at the tide gauges are assumed as zero and errorless.

The levelling making up of the Australian Height Datum, AHD, consisted primarily of third order standard although some first order levelling was executed along the eastern of New South Wales, parts of Victoria and southern Western Australia. After its unconstrained adjustment, the levelling network was estimated to have an overall accuracy of $8.1\sqrt{k}$ mm and to have a maximum precision on the height difference at any tide gauge of 0.34 m from the centre of the continent (Granger, 1972; Mitchell, 1973; Roelse, Granger and Graham, 1975).

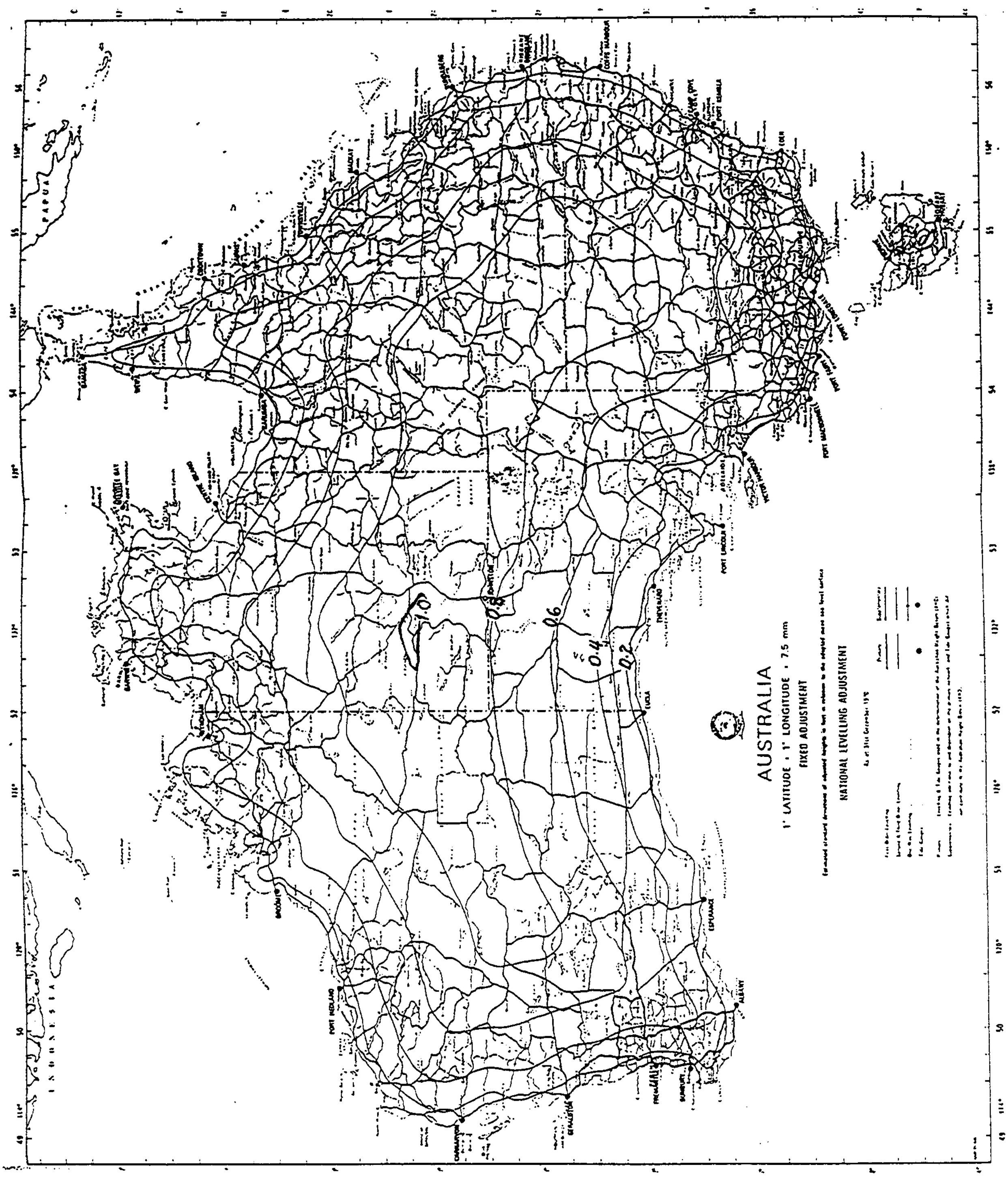

Fig. 6.2 : The estimated standard deviations of the adjusted height for the Australian Height Datum in feet in relation to the adopted mean sea level surface (see Roelse, Granger and Graham, 1995, Annex G) (Contour interval is 0.2 feet)

7 CONCLUSIONS

We have developed a technique to simultaneously adjust all the parameters involved in a complete height system - that is, ellipsoidal, orthometric and geoidal heights. We believe that by applying the appropriate accuracies and where required, the variance-covariances of observed parameters (e.g., heights at tide gauge stations) and post-adjustment elements, and the reliable input standard deviation to observed or derived line elements Δh, ΔH and ΔN, optimum values of <u>all</u> height parameters H, h and N are produced. This is achieved by simultaneously adjusting the observations and by applying the conditions which exists between the three parameters at each site. Thus the network conditions (e.g. loop misclose) ***and*** the station condition ($h = H + N$) are satisfied simultaneously, producing, we feel, the best possible values for ***all*** the parameters used in the heighting system because the weighted observations of H,h and N, as well as of ΔH, Δh and ΔN, are used in the adjustment.

This method should help to solve a number of the heighting problems which exist in this GPS age, as has been demonstrated in the three networks used to test the technique. Specifically, it provides a means by which

(i) GPS and geoid heights can be incorporated into existing levelling networks. This simultaneously benefits the existing levelling network and strengthens the local geoid information.

(ii) tide gauge information can also be incorporated into levelling networks as an observation and given an estimate of accuracy. This either improves the heights in the levelling network or where, the tide-gauge values are poorly determined (e.g. on the NW coast of Australia) will strengthen the information about mean sea level at the tide gauge.

(iii) gross errors can be identified and their effect eliminated. Because of the over-determined nature of the network (hitherto an independent evaluation of orthometric heights has not been available), we can improve aulty orthometric heights by giving them large standard deviations, thus down-weighting their impact on the adjustment.

(iv) the point values of H and N, with their covariances, can be entered as data, in preference to the line elements derived therefrom. This is of value where GPS observations are being incorporated into existing levelling network (which presumably, are already adjusted).

One point which emerges from the test networks is the need for realistic estimates of accuracy and precision for the observed and derived quantities. Some of these have yet to be properly established but, as experience with this adjustment grows, and as part of the analysis of the output produced by this method, our understanding of the precision estimators will improve. Once we have reliable input statistics then we can look for data errors and inconsistencies.

8 ACKNOWLEDGMENTS

This project was partly supported by a Faculty Research Grant from the Faculty of Engineering, UNSW and partly by the ICSM-sponsored study into the Australian Height Datum. The GPS data for the South Australian test was provided by Daniel Jacksa, South Australian Lands Department, for the NSW test by NSW Public Works Department, and for all data for the Philippines project came from SAGRIC as part of the AIDAB-sponsored Land Resources and Management Project for the Philippines.

9 BIBLIOGRAPHY

Bomford, G., 1980, ' *Geodesy* ', 4th Edition, Oxford University Press.

Cooper, M.A.R, 1987, ' *Control Surveys in Civil Engineering* ', Collins, London.

Cross, P.A., 1983, ' Advanced Least Squares Applied to Position Fixing ', *Working Papers, North East London Polytechnic*, Dept. of Land Surveying.

Eeg, J. and Krarup, T., 1973, 'Integrated Geodesy', *Intern. Rep. 7*, Dan. Geod. Inst., Copenhagen.

Fryer, J. G., 1971, 'The geoid in Australia - 1971', *Technical Report No. 13, Division of National Mapping*, Canberra.

Gere, J.M., 1965, ' *Matrix Algebra for Engineers* ', Van Nostrand Reinhol, New York.

Granger, H.W., 1972, ' The Australian Height Datum ', *The Australian Surveyor*, Vol. 24, No. 4, pp. 228-237

Harvey, B.R., 1985, '*The combination of VLBI and ground data for geodesy and geophysics*', Unisurv S-27, School of Surveying, UNSW, Kensington.

Harvey, B.R., 1987, ' Degrees of Freedom - Simplified', *Aust. J. Geod. Photogram.Surv.*, Nos. 46 and 47, pp. 57 - 68.

Harvey, B.R., 1991, ' *Practical Least Squares and Statistics for Surveyors* ', Monograph 13, School of Surveying, UNSW, Kensington.

Kääriäcnen, Erkki, 1966, ' The second levelling of Finland ', *Pub. Finnish Geodetic Inst.*, No. 42, 314 pp.

Kearsley, A. H. W., 1985,'Towards optimum evaluation of the inner zone contribution to the geoidal parameters', *Aust. J. Geod. Photogramm. Surv.*, 42, 75-98.

Kearsley, A. H. W., 1986,'The determination of precise geoid height differences using ring integration', *Boll. Geod. Sci. Affini.*, XLV(2), 151-174.

Kearsley, A. H. W., 1988,' Tests on the recovery of precise geoid height differences from gravimetry', *J. Geophys. Res.*, 93, 6559-6570.

Kearsley, A. H. W. and Ahmad, Z., 1992, ' *The evaluation of the geoid in the Philippines* ', Unisurv S-43, School of Surveying, UNSW, Kensington.

Kouba, J., 1970, ' *Generalised Sequential Least Squares Expressions and Matland Programming* '', M. Sc. Thesis, Dept. of Surveying Engineering, University of New Brunswick, Fredericton.

Krakiwsky, E.J., 1982, ' *A Synthesis of Recent Advances in the Method of Least Squares* ', Dept.Surv. Eng. Uni. of Calgary ,Canada.

Macleod, R.T., 1990, ' *The resolution of Mean Sea Level anomalies along the NSW coastline using the Global Positioning System* ', Unisurv S-41, School of Surveying, UNSW, Kensington.

Mikhail, E.M., 1976, ' *Observations and Least Squares* ', Dun-Donnelly, New York.

Milbert, D. G. and Dewhurst, W. T., 1992, ' The Yellowstone-Hebgen Lake geoid obtained through the integrated geodesy approach', *J. Geophys. Res.*, Vol. 97, 545-557.

Mitchell, H.L., 1973, '*Relations between mean sea level and geodetic levelling in Australia* ", Unisurv S-9, School of Surveying, UNSW, Kensington.

Mitchell, H.L. (Ed.), 1990, ' *GPS Heighting and the A.H.D.* ', Report, GPS Heighting Study Group, Aust. GPS Users Group.

Morgan, P., 1992, ' An Analysis of the Australian Height Datum: 1971', *The Australian Surveyor,* Vol. 37, No. 1, p. 46-63.

National Mapping Council of Australia., 1970, ' *Report on work completed during the period 1945-1970*", National Mapping Council of Australia.

National Mapping Council of Australia., 1981, ' *Standard Specifications and Recommended Practices for Horizontal and Vertical Control Surveys* ', Special Publication 1, 3rd Ed., Canberra, ACT.

Pelzer, H., 1986, ' Height Determination - Adjustment Models for Combined Data Sets', *Symposium on Height Determination and Recent Vertical Crustal Movements in Western Europe,* Hanover, September 15 - 19.

Rapp, R.H. and Pavlis, N.K., 1990, ' The Development and Analysis of Geopotential Models to Spherical Harmonic Degree 360 ', *J. Geoph. Res., 95, B13, 21 885 - 21 911.*

Roelse, A. , Granger, H.W. and Graham, J.W., 1975, ' *The adjustment of the Australian levelling survey 1970 - 1971* ', Department of National Development, Division of National Mapping, Technical Report 12, 2nd Edition, Canberra.

Vanicek, Petr and Kleusberg, Alfred, 1986, 'Towards a new combined geoid for Canada', *Boll. Geod. Sci. Affini,* Anno XLV, NO. 2, PP. 127-138.

Vanicek, P., and Krakiwsky, E.J., 1986, ' *Geodesy: The Concepts* ', Edition 2, Elsevier, Amsterdam, 697 pp.

Whalen, C.T. and Balazs, E, 1977, ' Test results of first -order class three levelling ', *NOAA Tech. Rep.* NOS68 NGS 4, 30 pp.

Zilkoski, D.B. and Hothem, L.D., 1988, ' GPS Satellite Surveys and Vertical Control ', *GPS-88 Engineering Application of GPS Satellite Surveying Technology* , Nashville, Tennessee, May 11 - 14.

Zilkoski, D.B., 1990,' Establishing Vertical Control Using GPS Satellite Surveys ', *FIG, June*.

Zilkoski, David B., Balazs, Emery I. and Bengston, Janice M., 1991,'Datum definition study for the North American Vertical Datum of 1988', *NGS Internal Report, NOAA*, Rockville.

10 APPENDICES

Appendix 1 : Example of input file for Baycon.

EXAMPLE INPUT FILE HGTH DATA

Code	Stn.#	h (m)	S_h (m)	H (m)	S_H (m)	N (m)	S_N (m)
1	2	125.474	0.80	117.940	0.20	7.573	0.30
1	3	71.290	0.70	58.186	0.30	12.871	0.25
1	17	145.260	0.75	148.678	0.40	-3.495	0.20
0	22	209.289	0.85	205.048	0.35	4.241	0.35
1	23	121.619	0.80	115.818	0.25	5.757	0.40

Code	AT	TO	Observations	Stn. Dev.
2	2	3	-54.284	0.310
3	2	3	-59.754	0.142
4	2	3	5.298	0.630
2	3	23	50.327	0.330
3	3	23	57.632	0.140
4	3	23	-7.114	0.650
2	17	23	-23.641	0.350
3	17	23	-32.860	0.135
4	17	23	9.252	0.700
2	22	2	-83.635	0.550
3	22	2	-87.108	0.108
4	22	2	3.332	1.100
2	22	17	-64.029	0.530
3	22	17	-56.370	0.110
4	22	17	-7.736	1.060
2	23	2	3.952	0.270
3	23	2	2.122	0.153
4	23	2	1.816	0.550
2	23	22	87.614	0.360
3	23	22	89.230	0.133
4	23	22	-1.516	0.720

Explanation for the codes used above.

0 Station used as datum

1 Other stations

2 Difference in the ellipsoidal heights

3 Difference in the orthometric heights

4 Difference in the geoid heights

Appendix 2 : Flow chart of programs for adjustment process

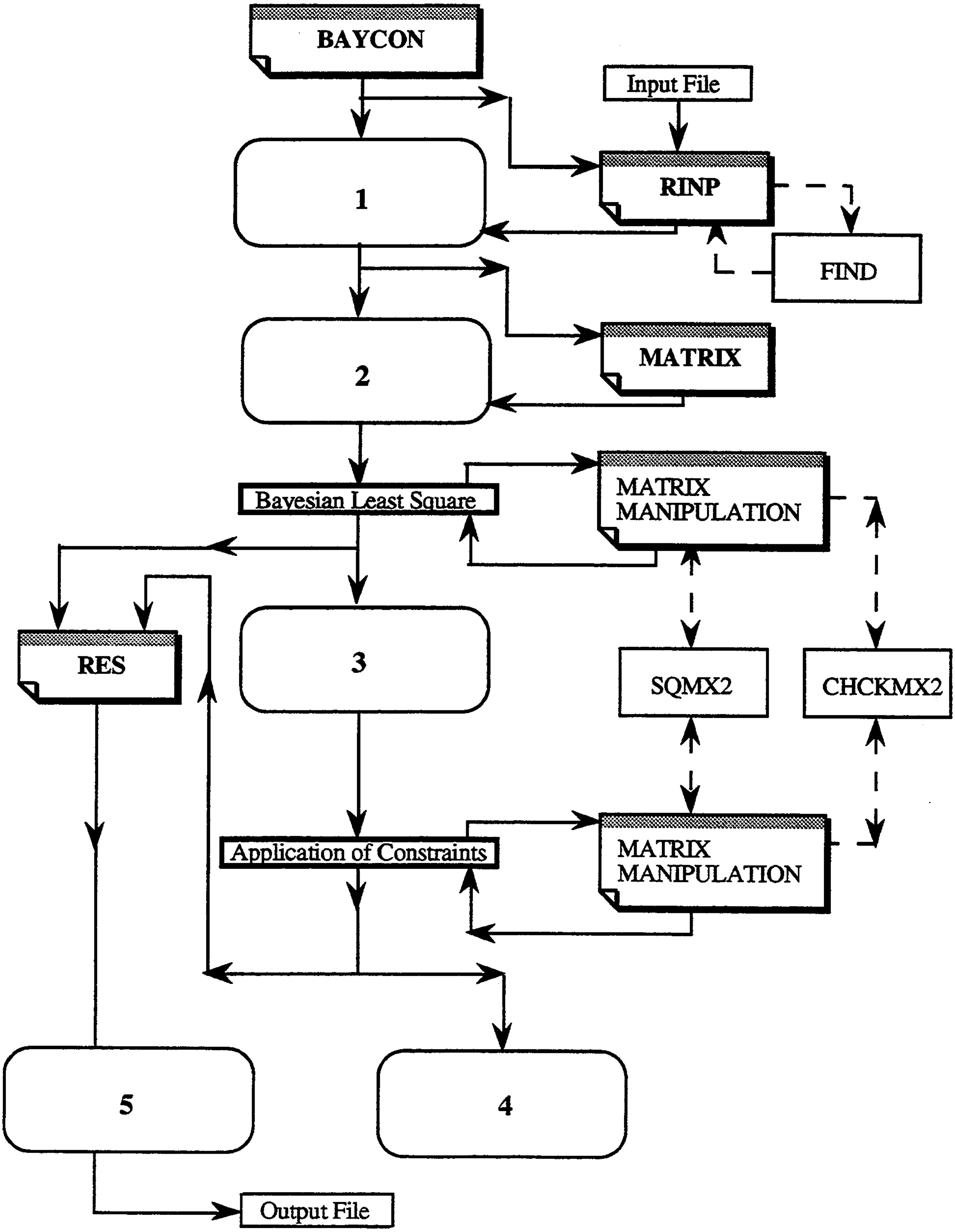

Appendix 3 : Description of the processing in the flow chart

1

- Reads in and store both observational elements and the a priori values of the parameters and the associated accuracies and precisions.
- Enforces an internal numbering system for the stations.

2

- Forms the relevant matrices for the adjustment.

3

- This step gives the results of adjustment using Bayesian Least Squares.
- The output include the corrections to the parameters and the VCV matrix to calculate the standard deviations of the corrected parameters.

4

- This step gives the results of adjustment after applying Constraints.
- The output include the corrections to the corrected parameters above and the VCV matrix for determining the standard deviations of the corrected parameters.

5

- This step apply corrections to the unknowns and compute the standard deviations. For storage, the height values are updated by the corrected values to be used for the next step.
- The output also include the residuals, errors and sum of errors.
- All these results are written into the output file.

Appendix 4 : Description of the subroutines.

1. *RINP . FOR*

This subroutine reads the input file which contains both the a priori values of the parameters namely the three height elements and their respective accuracies, and the observables with their precisions and line element information. It reads in the input file, count the number of stations, imposes an internal numbering system and store the heights and observed values. Subroutine *FIND* is used to get the internal station number.

2. *MATRIX . FOR*

The job that this subroutine has to implement is to form the matrices needed for the adjustment. This includes the ($\mathbf{A^TPA} + \mathbf{P_x}$) matrix; the RHS-matrix, ($\mathbf{A^TPb}$); matrix of constant term of the *a priori* values, $\mathbf{b_C}$; and the differentiation of the constraint equations with respect to the parameters matrix, **D**.

3. *RES . FOR*

In this subroutine, the corrections are applied to the parameters and the standard deviations are computed. The values stored are the corrected heights. Residuals from the observational elements, v/s and $\sum \left(\frac{v}{s}\right)^2$ (or more accurately, $\mathbf{v^TPv}$) are calculated. Ideally, we want to achieve the principle of least squares which is to have any changes to the observations to be as small as possible, where $\mathbf{v^TPv}$ is a minimum.

Appendix 5 : South Australia data set - Case 1

HEIGHT ADJUSTMENT PROGRAM
EXAMPLE INPUT FILE HGTH DATA

A PRIORI VALUES OF THE HEIGHT ELEMENTS:

CODE	STATION #	h m	Sh m	H m	SH m	N m	SN m
1	2	125.574	10.000	117.940	0.200	7.573	10.000
1	3	71.290	10.000	58.186	0.200	12.871	10.000
1	17	145.260	10.000	148.678	0.200	-3.495	10.000
0	22	209.289	0.000	205.048	0.000	4.241	0.000
1	23	121.619	10.000	115.818	0.200	5.757	10.000

CODE	FROM	TO	OBS	S (OBS)
2	2	3	-54.28 metre	0.63 metre
3	2	3	-59.75 metre	0.21 metre
4	2	3	5.30 metre	0.63 metre
2	3	23	50.33 metre	0.61 metre
3	3	23	57.63 metre	0.21 metre
4	3	23	-7.11 metre	0.61 metre
2	17	23	-23.64 metre	0.57 metre
3	17	23	-32.86 metre	0.20 metre
4	17	23	9.25 metre	0.57 metre
2	22	2	-83.63 metre	0.36 metre
3	22	2	-87.11 metre	0.16 metre
4	22	2	3.33 metre	0.36 metre
2	22	17	-64.03 metre	0.38 metre
3	22	17	-56.37 metre	0.17 metre
4	22	17	-7.74 metre	0.38 metre
2	23	2	3.95 metre	0.73 metre
3	23	2	2.12 metre	0.23 metre
4	23	2	1.82 metre	0.73 metre
2	23	22	87.61 metre	0.56 metre
3	23	22	89.23 metre	0.20 metre
4	23	22	-1.52 metre	0.56 metre

There are 5 stations, including 1 held fixed
and there are 21 observations and 12 params

PARAMETERS FROM BAYESIAN:

NO.	h OLD m	H OLD m	N OLD m	dh m	dH m	dN m	h NEW m	Sh m	H NEW m	SH m	N NEW m	SN m
2	125.5740	117.9400	7.5730	0.07	0.00	0.00	125.6440	0.32	117.9400	0.11	7.5730	0.32
3	71.2900	58.1860	12.8710	0.06	0.00	0.00	71.3493	0.52	58.1860	0.13	12.8710	0.52
17	145.2600	148.6780	-3.4950	0.01	0.00	0.00	145.2743	0.33	148.6780	0.11	-3.4950	0.33
22	209.2890	205.0480	4.2410	0.00	0.00	0.00	209.2890	0.00	205.0480	0.00	4.2410	0.00
23	121.6190	115.8180	5.7570	0.05	0.00	0.00	121.6665	0.36	115.8180	0.10	5.7570	0.36

NO.	TYPE	FROM	TO	MEASUREMENT	STND DEV	V	V/S
1	DELTA h	2	3	-54.2840 m	0.63 m	0.01 m	0.02
2	DELTA H	2	3	-59.7540 m	0.21 m	0.00 m	0.00
3	DELTA N	2	3	5.2980 m	0.63 m	0.00 m	0.00
4	DELTA h	3	23	50.3270 m	0.61 m	0.01 m	0.02
5	DELTA H	3	23	57.6320 m	0.21 m	0.00 m	0.00
6	DELTA N	3	23	-7.1140 m	0.61 m	0.00 m	0.00
7	DELTA h	17	23	-23.6410 m	0.57 m	-0.03 m	-0.06
8	DELTA H	17	23	-32.8600 m	0.20 m	0.00 m	0.00
9	DELTA N	17	23	9.2520 m	0.57 m	0.00 m	0.00
10	DELTA h	22	2	-83.6350 m	0.36 m	0.01 m	0.03
11	DELTA H	22	2	-87.1080 m	0.16 m	0.00 m	0.00
12	DELTA N	22	2	3.3320 m	0.36 m	0.00 m	0.00
13	DELTA h	22	17	-64.0290 m	0.38 m	-0.01 m	-0.04
14	DELTA H	22	17	-56.3700 m	0.17 m	0.00 m	0.00
15	DELTA N	22	17	-7.7360 m	0.38 m	0.00 m	0.00
16	DELTA h	23	2	3.9520 m	0.73 m	-0.03 m	-0.04
17	DELTA H	23	2	2.1220 m	0.23 m	0.00 m	0.00
18	DELTA N	23	2	1.8160 m	0.73 m	0.00 m	0.00
19	DELTA h	23	22	87.6140 m	0.56 m	-0.01 m	-0.02
20	DELTA H	23	22	89.2300 m	0.20 m	0.00 m	0.00
21	DELTA N	23	22	-1.5160 m	0.56 m	0.00 m	0.00

PARAMETERS AFTER CONSTRAINTS:

NO.	h OLD m	H OLD m	N OLD m	dh m	dH m	dN m	h NEW m	Sh m	H NEW m	SH m	N NEW m	SN m
2	125.6440	117.9400	7.5730	-0.06	0.01	0.06	125.5812	0.23	117.9453	0.10	7.6359	0.23
3	71.3493	58.1860	12.8710	-0.14	0.01	0.14	71.2076	0.37	58.1950	0.13	13.0127	0.37
17	145.2743	148.6780	-3.4950	-0.04	0.00	0.04	145.2307	0.24	148.6822	0.11	-3.4515	0.24
22	209.2890	205.0480	4.2410	0.00	0.00	0.00	209.2890	0.00	205.0480	0.00	4.2410	0.00
23	121.6665	115.8180	5.7570	-0.04	0.00	0.04	121.6219	0.26	115.8203	0.10	5.8016	0.26

NO.	TYPE	FROM	TO	MEASUREMENT	STND DEV	V	V/S
1	DELTA h	2	3	-54.2840 m	0.63 m	0.09 m	0.14
2	DELTA H	2	3	-59.7540 m	0.21 m	0.00 m	-0.02
3	DELTA N	2	3	5.2980 m	0.63 m	-0.08 m	-0.12
4	DELTA h	3	23	50.3270 m	0.61 m	-0.09 m	-0.14
5	DELTA H	3	23	57.6320 m	0.21 m	0.01 m	0.03
6	DELTA N	3	23	-7.1140 m	0.61 m	0.10 m	0.16
7	DELTA h	17	23	-23.6410 m	0.57 m	-0.03 m	-0.06
8	DELTA H	17	23	-32.8600 m	0.20 m	0.00 m	0.01
9	DELTA N	17	23	9.2520 m	0.57 m	0.00 m	0.00
10	DELTA h	22	2	-83.6350 m	0.36 m	0.07 m	0.20
11	DELTA H	22	2	-87.1080 m	0.16 m	-0.01 m	-0.03
12	DELTA N	22	2	3.3320 m	0.36 m	-0.06 m	-0.17
13	DELTA h	22	17	-64.0290 m	0.38 m	0.03 m	0.08
14	DELTA H	22	17	-56.3700 m	0.17 m	0.00 m	-0.03
15	DELTA N	22	17	-7.7360 m	0.38 m	-0.04 m	-0.12
16	DELTA h	23	2	3.9520 m	0.73 m	-0.01 m	-0.01
17	DELTA H	23	2	2.1220 m	0.23 m	0.00 m	-0.01
18	DELTA N	23	2	1.8160 m	0.73 m	-0.02 m	-0.03
19	DELTA h	23	22	87.6140 m	0.56 m	-0.05 m	-0.10
20	DELTA H	23	22	89.2300 m	0.20 m	0.00 m	0.01
21	DELTA N	23	22	-1.5160 m	0.56 m	0.04 m	0.08

Appendix 6 : South Australia data set - Case 2

```
HEIGHT ADJUSTMENT PROGRAM
 EXAMPLE INPUT FILE     HGTH    DATA

 A PRIORI VALUES OF THE HEIGHT ELEMENTS:

CODE    STATION #       h   m       Sh  m      H  m         SH  m        N  m         SN  m
  1         2         125.574      0.800    117.940       0.200       7.573        0.300
  1         3          71.290      0.800     58.186       0.200      12.871        0.300
  1        17         145.260      0.800    148.678       0.200      -3.495        0.300
  0        22         209.289      0.800    205.048       0.200       4.241        0.300
  1        23         121.619      0.800    115.818       0.200       5.757        0.300

CODE     FROM    TO          OBS            S (OBS)
  2         2     3       -54.28 metre     0.63 metre
  3         2     3       -59.75 metre     0.21 metre
  4         2     3         5.30 metre     0.63 metre
  2         3    23        50.33 metre     0.61 metre
  3         3    23        57.63 metre     0.21 metre
  4         3    23        -7.11 metre     0.61 metre
  2        17    23       -23.64 metre     0.57 metre
  3        17    23       -32.86 metre     0.20 metre
  4        17    23         9.25 metre     0.57 metre
  2        22     2       -83.63 metre     0.36 metre
  3        22     2       -87.11 metre     0.16 metre
  4        22     2         3.33 metre     0.36 metre
  2        22    17       -64.03 metre     0.38 metre
  3        22    17       -56.37 metre     0.17 metre
  4        22    17        -7.74 metre     0.38 metre
  2        23     2         3.95 metre     0.73 metre
  3        23     2         2.12 metre     0.23 metre
  4        23     2         1.82 metre     0.73 metre
  2        23    22        87.61 metre     0.56 metre
  3        23    22        89.23 metre     0.20 metre
  4        23    22        -1.52 metre     0.56 metre

 There are    5 stations, including   1 held fixed
 and there are   21 observations and   12    params
```

PARAMETERS FROM BAYESIAN:

NO.	h OLD m	H OLD m	N OLD m	dh m	dH m	dN m	h NEW m	Sh m	H NEW m	SH m	N NEW m	SN m
2	125.5740	117.9400	7.5730	0.06	0.00	0.00	125.6293	0.29	117.9400	0.11	7.5730	0.21
3	71.2900	58.1860	12.8710	0.03	0.00	0.00	71.3241	0.43	58.1860	0.13	12.8710	0.25
17	145.2600	148.6780	-3.4950	0.01	0.00	0.00	145.2685	0.30	148.6780	0.11	-3.4950	0.22
22	209.2890	205.0480	4.2410	0.00	0.00	0.00	209.2890	0.00	205.0480	0.00	4.2410	0.00
23	121.6190	115.8180	5.7570	0.03	0.00	0.00	121.6515	0.32	115.8180	0.10	5.7570	0.22

NO.	TYPE	FROM	TO	MEASUREMENT	STND DEV	V	V/S
1	DELTA h	2	3	-54.2840 m	0.63 m	0.02 m	0.03
2	DELTA H	2	3	-59.7540 m	0.21 m	0.00 m	0.00
3	DELTA N	2	3	5.2980 m	0.63 m	0.00 m	0.00
4	DELTA h	3	23	50.3270 m	0.61 m	0.00 m	0.00
5	DELTA H	3	23	57.6320 m	0.21 m	0.00 m	0.00
6	DELTA N	3	23	-7.1140 m	0.61 m	0.00 m	0.00
7	DELTA h	17	23	-23.6410 m	0.57 m	-0.02 m	-0.04
8	DELTA H	17	23	-32.8600 m	0.20 m	0.00 m	0.00
9	DELTA N	17	23	9.2520 m	0.57 m	0.00 m	0.00
10	DELTA h	22	2	-83.6350 m	0.36 m	0.02 m	0.07
11	DELTA H	22	2	-87.1080 m	0.16 m	0.00 m	0.00
12	DELTA N	22	2	3.3320 m	0.36 m	0.00 m	0.00
13	DELTA h	22	17	-64.0290 m	0.38 m	-0.01 m	-0.02
14	DELTA H	22	17	-56.3700 m	0.17 m	0.00 m	0.00
15	DELTA N	22	17	-7.7360 m	0.38 m	0.00 m	0.00
16	DELTA h	23	2	3.9520 m	0.73 m	-0.03 m	-0.04
17	DELTA H	23	2	2.1220 m	0.23 m	0.00 m	0.00
18	DELTA N	23	2	1.8160 m	0.73 m	0.00 m	0.00
19	DELTA h	23	22	87.6140 m	0.56 m	-0.02 m	-0.04
20	DELTA H	23	22	89.2300 m	0.20 m	0.00 m	0.00
21	DELTA N	23	22	-1.5160 m	0.56 m	0.00 m	0.00

PARAMETERS AFTER CONSTRAINTS:

NO.	h OLD m	H OLD m	N OLD m	dh m	dH m	dN m	h NEW m	Sh m	H NEW m	SH m	N NEW m	SN m
2	125.6293	117.9400	7.5730	-0.08	0.01	0.03	125.5508	0.18	117.9495	0.10	7.6013	0.17
3	71.3241	58.1860	12.8710	-0.19	0.02	0.06	71.1364	0.24	58.2039	0.13	12.9325	0.22
17	145.2685	148.6780	-3.4950	-0.06	0.01	0.02	145.2132	0.19	148.6850	0.11	-3.4718	0.18
22	209.2890	205.0480	4.2410	0.00	0.00	0.00	209.2890	0.00	205.0480	0.00	4.2410	0.00
23	121.6515	115.8180	5.7570	-0.06	0.01	0.01	121.5910	0.19	115.8239	0.10	5.7670	0.18

NO.	TYPE	FROM	TO	MEASUREMENT	STND DEV	V	V/S
1	DELTA h	2	3	-54.2840 m	0.63 m	0.13 m	0.21
2	DELTA H	2	3	-59.7540 m	0.21 m	-0.01 m	-0.04
3	DELTA N	2	3	5.2980 m	0.63 m	-0.03 m	-0.05
4	DELTA h	3	23	50.3270 m	0.61 m	-0.13 m	-0.21
5	DELTA H	3	23	57.6320 m	0.21 m	0.01 m	0.06
6	DELTA N	3	23	-7.1140 m	0.61 m	0.05 m	0.08
7	DELTA h	17	23	-23.6410 m	0.57 m	-0.02 m	-0.03
8	DELTA H	17	23	-32.8600 m	0.20 m	0.00 m	0.01
9	DELTA N	17	23	9.2520 m	0.57 m	0.01 m	0.02
10	DELTA h	22	2	-83.6350 m	0.36 m	0.10 m	0.28
11	DELTA H	22	2	-87.1080 m	0.16 m	-0.01 m	-0.06
12	DELTA N	22	2	3.3320 m	0.36 m	-0.03 m	-0.08
13	DELTA h	22	17	-64.0290 m	0.38 m	0.05 m	0.12
14	DELTA H	22	17	-56.3700 m	0.17 m	-0.01 m	-0.04
15	DELTA N	22	17	-7.7360 m	0.38 m	-0.02 m	-0.06
16	DELTA h	23	2	3.9520 m	0.73 m	-0.01 m	-0.01
17	DELTA H	23	2	2.1220 m	0.23 m	0.00 m	-0.02
18	DELTA N	23	2	1.8160 m	0.73 m	-0.02 m	-0.03
19	DELTA h	23	22	87.6140 m	0.56 m	-0.08 m	-0.15
20	DELTA H	23	22	89.2300 m	0.20 m	0.01 m	0.03
21	DELTA N	23	22	-1.5160 m	0.56 m	0.01 m	0.02

Appendix 7 : South Australia data set - Case 3

HEIGHT ADJUSTMENT PROGRAM
EXAMPLE INPUT FILE HGTH DATA

A PRIORI VALUES OF THE HEIGHT ELEMENTS:

CODE	STATION #	h m	Sh m	H m	SH m	N m	SN m
1	2	125.574	10.000	117.940	0.200	7.573	10.000
1	3	71.290	10.000	58.186	0.200	12.871	10.000
1	17	145.260	10.000	148.678	0.200	-3.495	10.000
0	22	209.289	0.000	205.048	0.000	4.241	0.000
1	23	121.619	10.000	115.818	0.200	5.757	10.000

CODE	FROM	TO	OBS	S (OBS)
2	2	3	-54.28 metre	0.31 metre
3	2	3	-59.75 metre	0.14 metre
4	2	3	5.30 metre	0.63 metre
2	3	23	50.33 metre	0.33 metre
3	3	23	57.63 metre	0.14 metre
4	3	23	-7.11 metre	0.65 metre
2	17	23	-23.64 metre	0.35 metre
3	17	23	-32.86 metre	0.13 metre
4	17	23	9.25 metre	0.70 metre
2	22	2	-83.63 metre	0.55 metre
3	22	2	-87.11 metre	0.11 metre
4	22	2	3.33 metre	1.10 metre
2	22	17	-64.03 metre	0.53 metre
3	22	17	-56.37 metre	0.11 metre
4	22	17	-7.74 metre	1.06 metre
2	23	2	3.95 metre	0.27 metre
3	23	2	2.12 metre	0.15 metre
4	23	2	1.82 metre	0.55 metre
2	23	22	87.61 metre	0.36 metre
3	23	22	89.23 metre	0.13 metre
4	23	22	-1.52 metre	0.72 metre

There are 5 stations, including 1 held fixed
and there are 21 observations and 12 params

PARAMETERS FROM BAYESIAN:

NO.	h OLD m	H OLD m	N OLD m	dh m	dH m	dN m	h NEW m	Sh m	H NEW m	SH m	N NEW m	SN m
2	125.5740	117.9400	7.5730	0.05	0.00	0.00	125.6277	0.32	117.9400	0.08	7.5730	0.64
3	71.2900	58.1860	12.8710	0.05	0.00	0.00	71.3432	0.36	58.1860	0.10	12.8710	0.71
17	145.2600	148.6780	-3.4950	0.04	0.00	0.00	145.2953	0.35	148.6780	0.08	-3.4950	0.70
22	209.2890	205.0480	4.2410	0.00	0.00	0.00	209.2890	0.00	205.0480	0.00	4.2410	0.00
23	121.6190	115.8180	5.7570	0.05	0.00	0.00	121.6697	0.28	115.8180	0.08	5.7570	0.55

NO.	TYPE	FROM	TO	MEASUREMENT	STND DEV	V	V/S
1	DELTA h	2	3	-54.2840 m	0.31 m	0.00 m	0.00
2	DELTA H	2	3	-59.7540 m	0.14 m	0.00 m	0.00
3	DELTA N	2	3	5.2980 m	0.63 m	0.00 m	0.00
4	DELTA h	3	23	50.3270 m	0.33 m	0.00 m	0.00
5	DELTA H	3	23	57.6320 m	0.14 m	0.00 m	0.00
6	DELTA N	3	23	-7.1140 m	0.65 m	0.00 m	0.00
7	DELTA h	17	23	-23.6410 m	0.35 m	-0.02 m	-0.04
8	DELTA H	17	23	-32.8600 m	0.13 m	0.00 m	0.00
9	DELTA N	17	23	9.2520 m	0.70 m	0.00 m	0.00
10	DELTA h	22	2	-83.6350 m	0.55 m	0.03 m	0.05
11	DELTA H	22	2	-87.1080 m	0.11 m	0.00 m	0.00
12	DELTA N	22	2	3.3320 m	1.10 m	0.00 m	0.00
13	DELTA h	22	17	-64.0290 m	0.53 m	-0.04 m	-0.07
14	DELTA H	22	17	-56.3700 m	0.11 m	0.00 m	0.00
15	DELTA N	22	17	-7.7360 m	1.06 m	0.00 m	0.00
16	DELTA h	23	2	3.9520 m	0.27 m	-0.01 m	-0.02
17	DELTA H	23	2	2.1220 m	0.15 m	0.00 m	0.00
18	DELTA N	23	2	1.8160 m	0.55 m	0.00 m	0.00
19	DELTA h	23	22	87.6140 m	0.36 m	-0.01 m	-0.01
20	DELTA H	23	22	89.2300 m	0.13 m	0.00 m	0.00
21	DELTA N	23	22	-1.5160 m	0.72 m	0.00 m	0.00

PARAMETERS AFTER CONSTRAINTS:

NO.	h OLD m	H OLD m	N OLD m	dh m	dH m	dN m	h NEW m	Sh m	H NEW m	SH m	N NEW m	SN m
2	125.6277	117.9400	7.5730	-0.02	0.00	0.09	125.6044	0.28	117.9405	0.08	7.6639	0.29
3	71.3432	58.1860	12.8710	-0.06	0.01	0.22	71.2868	0.32	58.1918	0.10	13.0950	0.33
17	145.2953	148.6780	-3.4950	-0.02	0.00	0.09	145.2729	0.31	148.6788	0.08	-3.4059	0.32
22	209.2890	205.0480	4.2410	0.00	0.00	0.00	209.2890	0.00	205.0480	0.00	4.2410	0.00
23	121.6697	115.8180	5.7570	-0.02	0.00	0.08	121.6507	0.25	115.8183	0.08	5.8324	0.25

NO.	TYPE	FROM	TO	MEASUREMENT	STND DEV	V	V/S
1	DELTA h	2	3	-54.2840 m	0.31 m	0.03 m	0.11
2	DELTA H	2	3	-59.7540 m	0.14 m	-0.01 m	-0.04
3	DELTA N	2	3	5.2980 m	0.63 m	-0.13 m	-0.21
4	DELTA h	3	23	50.3270 m	0.33 m	-0.04 m	-0.11
5	DELTA H	3	23	57.6320 m	0.14 m	0.01 m	0.04
6	DELTA N	3	23	-7.1140 m	0.65 m	0.15 m	0.23
7	DELTA h	17	23	-23.6410 m	0.35 m	-0.02 m	-0.05
8	DELTA H	17	23	-32.8600 m	0.13 m	0.00 m	0.00
9	DELTA N	17	23	9.2520 m	0.70 m	0.01 m	0.02
10	DELTA h	22	2	-83.6350 m	0.55 m	0.05 m	0.09
11	DELTA H	22	2	-87.1080 m	0.11 m	0.00 m	0.00
12	DELTA N	22	2	3.3320 m	1.10 m	-0.09 m	-0.08
13	DELTA h	22	17	-64.0290 m	0.53 m	-0.01 m	-0.02
14	DELTA H	22	17	-56.3700 m	0.11 m	0.00 m	-0.01
15	DELTA N	22	17	-7.7360 m	1.06 m	-0.09 m	-0.08
16	DELTA h	23	2	3.9520 m	0.27 m	0.00 m	-0.01
17	DELTA H	23	2	2.1220 m	0.15 m	0.00 m	0.00
18	DELTA N	23	2	1.8160 m	0.55 m	-0.02 m	-0.03
19	DELTA h	23	22	87.6140 m	0.36 m	-0.02 m	-0.07
20	DELTA H	23	22	89.2300 m	0.13 m	0.00 m	0.00
21	DELTA N	23	22	-1.5160 m	0.72 m	0.08 m	0.10

Appendix 8 : South Australia data set - Case 4

HEIGHT ADJUSTMENT PROGRAM
EXAMPLE INPUT FILE HGTH DATA

A PRIORI VALUES OF THE HEIGHT ELEMENTS:

CODE	STATION #	h m	Sh m	H m	SH m	N m	SN m
1	2	125.574	0.800	117.940	0.200	7.573	0.300
1	3	71.290	0.800	58.186	0.200	12.871	0.300
1	17	145.260	0.800	148.678	0.200	-3.495	0.300
0	22	209.289	0.000	205.048	0.000	4.241	0.000
1	23	121.619	0.800	115.818	0.200	5.757	0.300

CODE	FROM	TO	OBS	S (OBS)
2	2	3	-54.28 metre	0.31 metre
3	2	3	-59.75 metre	0.14 metre
4	2	3	5.30 metre	0.63 metre
2	3	23	50.33 metre	0.33 metre
3	3	23	57.63 metre	0.14 metre
4	3	23	-7.11 metre	0.65 metre
2	17	23	-23.64 metre	0.35 metre
3	17	23	-32.86 metre	0.13 metre
4	17	23	9.25 metre	0.70 metre
2	22	2	-83.63 metre	0.55 metre
3	22	2	-87.11 metre	0.11 metre
4	22	2	3.33 metre	1.10 metre
2	22	17	-64.03 metre	0.53 metre
3	22	17	-56.37 metre	0.11 metre
4	22	17	-7.74 metre	1.06 metre
2	23	2	3.95 metre	0.27 metre
3	23	2	2.12 metre	0.15 metre
4	23	2	1.82 metre	0.55 metre
2	23	22	87.61 metre	0.36 metre
3	23	22	89.23 metre	0.13 metre
4	23	22	-1.52 metre	0.72 metre

There are 5 stations, including 1 held fixed
and there are 21 observations and 12 params

PARAMETERS FROM BAYESIAN:

NO.	h OLD m	H OLD m	N OLD m	dh m	dH m	dN m	h NEW m	Sh m	H NEW m	SH m	N NEW m	SN m
2	125.5740	117.9400	7.5730	0.04	0.00	0.00	125.6118	0.27	117.9400	0.08	7.5730	0.24
3	71.2900	58.1860	12.8710	0.04	0.00	0.00	71.3254	0.31	58.1860	0.10	12.8710	0.26
17	145.2600	148.6780	-3.4950	0.02	0.00	0.00	145.2826	0.31	148.6780	0.08	-3.4950	0.27
22	209.2890	205.0480	4.2410	0.00	0.00	0.00	209.2890	0.00	205.0480	0.00	4.2410	0.00
23	121.6190	115.8180	5.7570	0.04	0.00	0.00	121.6558	0.24	115.8180	0.08	5.7570	0.23

NO.	TYPE	FROM	TO	MEASUREMENT	STND DEV	V	V/S
1	DELTA h	2	3	-54.2840 m	0.31 m	0.00 m	0.01
2	DELTA H	2	3	-59.7540 m	0.14 m	0.00 m	0.00
3	DELTA N	2	3	5.2980 m	0.63 m	0.00 m	0.00
4	DELTA h	3	23	50.3270 m	0.33 m	0.00 m	-0.01
5	DELTA H	3	23	57.6320 m	0.14 m	0.00 m	0.00
6	DELTA N	3	23	-7.1140 m	0.65 m	0.00 m	0.00
7	DELTA h	17	23	-23.6410 m	0.35 m	-0.01 m	-0.04
8	DELTA H	17	23	-32.8600 m	0.13 m	0.00 m	0.00
9	DELTA N	17	23	9.2520 m	0.70 m	0.00 m	0.00
10	DELTA h	22	2	-83.6350 m	0.55 m	0.04 m	0.08
11	DELTA H	22	2	-87.1080 m	0.11 m	0.00 m	0.00
12	DELTA N	22	2	3.3320 m	1.10 m	0.00 m	0.00
13	DELTA h	22	17	-64.0290 m	0.53 m	-0.02 m	-0.04
14	DELTA H	22	17	-56.3700 m	0.11 m	0.00 m	0.00
15	DELTA N	22	17	-7.7360 m	1.06 m	0.00 m	0.00
16	DELTA h	23	2	3.9520 m	0.27 m	0.00 m	-0.01
17	DELTA H	23	2	2.1220 m	0.15 m	0.00 m	0.00
18	DELTA N	23	2	1.8160 m	0.55 m	0.00 m	0.00
19	DELTA h	23	22	87.6140 m	0.36 m	-0.02 m	-0.05
20	DELTA H	23	22	89.2300 m	0.13 m	0.00 m	0.00
21	DELTA N	23	22	-1.5160 m	0.72 m	0.00 m	0.00

PARAMETERS AFTER CONSTRAINTS:

NO.	h OLD m	H OLD m	N OLD m	dh m	dH m	dN m	h NEW m	Sh m	H NEW m	SH m	N NEW m	SN m
2	125.6118	117.9400	7.5730	-0.08	0.00	0.01	125.5281	0.18	117.9445	0.08	7.5836	0.18
3	71.3254	58.1860	12.8710	-0.15	0.02	0.10	71.1770	0.20	58.2024	0.10	12.9745	0.19
17	145.2826	148.6780	-3.4950	-0.07	0.00	0.03	145.2125	0.21	148.6816	0.08	-3.4692	0.20
22	209.2890	205.0480	4.2410	0.00	0.00	0.00	209.2890	0.00	205.0480	0.00	4.2410	0.00
23	121.6558	115.8180	5.7570	-0.07	0.00	0.01	121.5848	0.16	115.8224	0.07	5.7624	0.16

NO.	TYPE	FROM	TO	MEASUREMENT	STND DEV	V	V/S
1	DELTA h	2	3	-54.2840 m	0.31 m	0.07 m	0.22
2	DELTA H	2	3	-59.7540 m	0.14 m	-0.01 m	-0.08
3	DELTA N	2	3	5.2980 m	0.63 m	-0.09 m	-0.15
4	DELTA h	3	23	50.3270 m	0.33 m	-0.08 m	-0.24
5	DELTA H	3	23	57.6320 m	0.14 m	0.01 m	0.09
6	DELTA N	3	23	-7.1140 m	0.65 m	0.10 m	0.15
7	DELTA h	17	23	-23.6410 m	0.35 m	-0.01 m	-0.04
8	DELTA H	17	23	-32.8600 m	0.13 m	0.00 m	-0.01
9	DELTA N	17	23	9.2520 m	0.70 m	0.02 m	0.03
10	DELTA h	22	2	-83.6350 m	0.55 m	0.13 m	0.23
11	DELTA H	22	2	-87.1080 m	0.11 m	0.00 m	-0.04
12	DELTA N	22	2	3.3320 m	0.10 m	-0.01 m	-0.01
13	DELTA h	22	17	-64.0290 m	0.53 m	0.05 m	0.09
14	DELTA H	22	17	-56.3700 m	0.11 m	0.00 m	-0.03
15	DELTA N	22	17	-7.7360 m	1.06 m	-0.03 m	-0.02
16	DELTA h	23	2	3.9520 m	0.27 m	0.01 m	0.03
17	DELTA H	23	2	2.1220 m	0.15 m	0.00 m	0.00
18	DELTA N	23	2	1.8160 m	0.55 m	-0.01 m	-0.01
19	DELTA h	23	22	87.6140 m	0.36 m	-0.09 m	-0.25
20	DELTA H	23	22	89.2300 m	0.13 m	0.00 m	0.03
21	DELTA N	23	22	-1.5160 m	0.72 m	0.01 m	0.01

Appendix 9 : South Australia data set - Case 5

HEIGHT ADJUSTMENT PROGRAM
EXAMPLE INPUT FILE HGTH DATA

A PRIORI VALUES OF THE HEIGHT ELEMENTS:

CODE	STATION #	h m	Sh m	H m	SH m	N m	SN m
1	2	125.574	0.800	117.940	0.200	7.573	0.300
1	3	71.290	0.700	58.186	0.300	12.871	0.250
1	17	145.260	0.750	148.678	0.400	-3.495	0.200
0	22	209.289	0.000	205.048	0.000	4.241	0.000
1	23	121.619	0.800	115.818	0.250	5.757	0.400

CODE	FROM	TO	OBS	S (OBS)
2	2	3	-54.28 metre	0.31 metre
3	2	3	-59.75 metre	0.14 metre
4	2	3	5.30 metre	0.63 metre
2	3	23	50.33 metre	0.33 metre
3	3	23	57.63 metre	0.14 metre
4	3	23	-7.11 metre	0.65 metre
2	17	23	-23.64 metre	0.35 metre
3	17	23	-32.86 metre	0.13 metre
4	17	23	9.25 metre	0.70 metre
2	22	2	-83.63 metre	0.55 metre
3	22	2	-87.11 metre	0.11 metre
4	22	2	3.33 metre	1.10 metre
2	22	17	-64.03 metre	0.53 metre
3	22	17	-56.37 metre	0.11 metre
4	22	17	-7.74 metre	1.06 metre
2	23	2	3.95 metre	0.27 metre
3	23	2	2.12 metre	0.15 metre
4	23	2	1.82 metre	0.55 metre
2	23	22	87.61 metre	0.36 metre
3	23	22	89.23 metre	0.13 metre
4	23	22	-1.52 metre	0.72 metre

There are 5 stations, including 1 held fixed
and there are 21 observations and 12 params

PARAMETERS FROM BAYESIAN:

NO.	h OLD m	H OLD m	N OLD m	dh m	dH m	dN m	h NEW m	Sh m	H NEW m	SH m	N NEW m	SN m
2	125.5740	117.9400	7.5730	0.04	0.00	0.00	125.6108	0.27	117.9400	0.08	7.5730	0.25
3	71.2900	58.1860	12.8710	0.03	0.00	0.00	71.3238	0.30	58.1860	0.11	12.8710	0.22
17	145.2600	148.6780	-3.4950	0.02	0.00	0.00	145.2817	0.31	148.6780	0.09	-3.4950	0.19
22	209.2890	205.0480	4.2410	0.00	0.00	0.00	209.2890	0.00	205.0480	0.00	4.2410	0.00
23	121.6190	115.8180	5.7570	0.04	0.00	0.00	121.6549	0.24	115.8180	0.08	5.7570	0.26

NO.	TYPE	FROM	TO	MEASUREMENT	STND DEV	V	V/S
1	DELTA h	2	3	-54.2840 m	0.31 m	0.00 m	0.01
2	DELTA H	2	3	-59.7540 m	0.14 m	0.00 m	0.00
3	DELTA N	2	3	5.2980 m	0.63 m	0.00 m	0.00
4	DELTA h	3	23	50.3270 m	0.33 m	0.00 m	-0.01
5	DELTA H	3	23	57.6320 m	0.14 m	0.00 m	0.00
6	DELTA N	3	23	-7.1140 m	0.65 m	0.00 m	0.00
7	DELTA h	17	23	-23.6410 m	0.35 m	-0.01 m	-0.04
8	DELTA H	17	23	-32.8600 m	0.13 m	0.00 m	0.00
9	DELTA N	17	23	9.2520 m	0.70 m	0.00 m	0.00
10	DELTA h	22	2	-83.6350 m	0.55 m	0.04 m	0.08
11	DELTA H	22	2	-87.1080 m	0.11 m	0.00 m	0.00
12	DELTA N	22	2	3.3320 m	1.10 m	0.00 m	0.00
13	DELTA h	22	17	-64.0290 m	0.53 m	-0.02 m	-0.04
14	DELTA H	22	17	-56.3700 m	0.11 m	0.00 m	0.00
15	DELTA N	22	17	-7.7360 m	1.06 m	0.00 m	0.00
16	DELTA h	23	2	3.9520 m	0.27 m	0.00 m	-0.01
17	DELTA H	23	2	2.1220 m	0.15 m	0.00 m	0.00
18	DELTA N	23	2	1.8160 m	0.55 m	0.00 m	0.00
19	DELTA h	23	22	87.6140 m	0.36 m	-0.02 m	-0.06
20	DELTA H	23	22	89.2300 m	0.13 m	0.00 m	0.00
21	DELTA N	23	22	-1.5160 m	0.72 m	0.00 m	0.00

PARAMETERS AFTER CONSTRAINTS:

NO.	h OLD m	H OLD m	N OLD m	dh m	dH m	dN m	h NEW m	Sh m	H NEW m	SH m	N NEW m	SN m
2	125.6108	117.9400	7.5730	-0.09	0.01	0.00	125.5236	0.18	117.9460	0.08	7.5776	0.17
3	71.3238	58.1860	12.8710	-0.16	0.02	0.09	71.1662	0.19	58.2078	0.11	12.9584	0.18
17	145.2817	148.6780	-3.4950	-0.08	0.01	0.02	145.2041	0.17	148.6835	0.09	-3.4794	0.16
22	209.2890	205.0480	4.2410	0.00	0.00	0.00	209.2890	0.00	205.0480	0.00	4.2410	0.00
23	121.6549	115.8180	5.7570	-0.07	0.01	0.00	121.5804	0.16	115.8243	0.08	5.7560	0.16

NO.	TYPE	FROM	TO	MEASUREMENT	STND DEV	V	V/S
1	DELTA h	2	3	-54.2840 m	0.31 m	0.07 m	0.24
2	DELTA H	2	3	-59.7540 m	0.14 m	-0.02 m	-0.11
3	DELTA N	2	3	5.2980 m	0.63 m	-0.08 m	-0.13
4	DELTA h	3	23	50.3270 m	0.33 m	-0.09 m	-0.26
5	DELTA H	3	23	57.6320 m	0.14 m	0.02 m	0.11
6	DELTA N	3	23	-7.1140 m	0.65 m	0.09 m	0.14
7	DELTA h	17	23	-23.6410 m	0.35 m	-0.02 m	-0.05
8	DELTA H	17	23	-32.8600 m	0.13 m	0.00 m	-0.01
9	DELTA N	17	23	9.2520 m	0.70 m	0.02 m	0.02
10	DELTA h	22	2	-83.6350 m	0.55 m	0.13 m	0.24
11	DELTA H	22	2	-87.1080 m	0.11 m	-0.01 m	-0.06
12	DELTA N	22	2	3.3320 m	1.10 m	0.00 m	0.00
13	DELTA h	22	17	-64.0290 m	0.53 m	0.06 m	0.11
14	DELTA H	22	17	-56.3700 m	0.11 m	-0.01 m	-0.05
15	DELTA N	22	17	-7.7360 m	1.06 m	-0.02 m	-0.01
16	DELTA h	23	2	3.9520 m	0.27 m	0.01 m	0.03
17	DELTA H	23	2	2.1220 m	0.15 m	0.00 m	0.00
18	DELTA N	23	2	1.8160 m	0.55 m	-0.01 m	-0.01
19	DELTA h	23	22	87.6140 m	0.36 m	-0.09 m	-0.26
20	DELTA H	23	22	89.2300 m	0.13 m	0.01 m	0.05
21	DELTA N	23	22	-1.5160 m	0.72 m	0.00 m	0.00

Appendix 10 : South Australia data set - Case 6

HEIGHT ADJUSTMENT PROGRAM
EXAMPLE INPUT FILE HGTH DATA

A PRIORI VALUES OF THE HEIGHT ELEMENTS:

CODE	STATION #	h m	Sh m	H m	SH m	N m	SN m
1	2	125.574	10.000	117.940	0.200	7.573	0.300
1	3	71.290	10.000	58.186	0.200	12.871	0.300
1	17	145.260	10.000	148.678	0.200	-3.495	0.300
0	22	209.289	0.000	205.048	0.000	4.241	0.000
1	23	121.619	10.000	115.818	0.200	5.757	0.300

CODE	FROM	TO	OBS	S (OBS)
2	2	3	-54.28 metre	0.31 metre
3	2	3	-59.75 metre	0.14 metre
4	2	3	5.30 metre	0.63 metre
2	3	23	50.33 metre	0.33 metre
3	3	23	57.63 metre	0.14 metre
4	3	23	-7.11 metre	0.65 metre
2	17	23	-23.64 metre	0.35 metre
3	17	23	-32.86 metre	0.13 metre
4	17	23	9.25 metre	0.70 metre
2	22	2	-83.63 metre	0.55 metre
3	22	2	-87.11 metre	0.11 metre
4	22	2	3.33 metre	1.10 metre
2	22	17	-64.03 metre	0.53 metre
3	22	17	-56.37 metre	0.11 metre
4	22	17	-7.74 metre	1.06 metre
2	23	2	3.95 metre	0.27 metre
3	23	2	2.12 metre	0.15 metre
4	23	2	1.82 metre	0.55 metre
2	23	22	87.61 metre	0.36 metre
3	23	22	89.23 metre	0.13 metre
4	23	22	-1.52 metre	0.72 metre

There are 5 stations, including 1 held fixed
and there are 21 observations and 12 params

PARAMETERS FROM BAYESIAN:

NO.	h OLD m	H OLD m	N OLD m	dh m	dH m	dN m	h NEW m	Sh m	H NEW m	SH m	N NEW m	SN m
2	125.5740	117.9400	7.5730	0.05	0.00	0.00	125.6277	0.32	117.9400	0.08	7.5730	0.24
3	71.2900	58.1860	12.8710	0.05	0.00	0.00	71.3432	0.36	58.1860	0.10	12.8710	0.26
17	145.2600	148.6780	-3.4950	0.04	0.00	0.00	145.2953	0.35	148.6780	0.08	-3.4950	0.27
22	209.2890	205.0480	4.2410	0.00	0.00	0.00	209.2890	0.00	205.0480	0.00	4.2410	0.00
23	121.6190	115.8180	5.7570	0.05	0.00	0.00	121.6697	0.28	115.8180	0.08	5.7570	0.23

NO.	TYPE	FROM	TO	MEASUREMENT	STND DEV	V	V/S
1	DELTA h	2	3	-54.2840 m	0.31 m	0.00 m	0.00
2	DELTA H	2	3	-59.7540 m	0.14 m	0.00 m	0.00
3	DELTA N	2	3	5.2980 m	0.63 m	0.00 m	0.00
4	DELTA h	3	23	50.3270 m	0.33 m	0.00 m	0.00
5	DELTA H	3	23	57.6320 m	0.14 m	0.00 m	0.00
6	DELTA N	3	23	-7.1140 m	0.65 m	0.00 m	0.00
7	DELTA h	17	23	-23.6410 m	0.35 m	-0.02 m	-0.04
8	DELTA H	17	23	-32.8600 m	0.13 m	0.00 m	0.00
9	DELTA N	17	23	9.2520 m	0.70 m	0.00 m	0.00
10	DELTA h	22	2	-83.6350 m	0.55 m	0.03 m	0.05
11	DELTA H	22	2	-87.1080 m	0.11 m	0.00 m	0.00
12	DELTA N	22	2	3.3320 m	1.10 m	0.00 m	0.00
13	DELTA h	22	17	-64.0290 m	0.53 m	-0.04 m	-0.07
14	DELTA H	22	17	-56.3700 m	0.11 m	0.00 m	0.00
15	DELTA N	22	17	-7.7360 m	1.06 m	0.00 m	0.00
16	DELTA h	23	2	3.9520 m	0.27 m	-0.01 m	-0.02
17	DELTA H	23	2	2.1220 m	0.15 m	0.00 m	0.00
18	DELTA N	23	2	1.8160 m	0.55 m	0.00 m	0.00
19	DELTA h	23	22	87.6140 m	0.36 m	-0.01 m	-0.01
20	DELTA H	23	22	89.2300 m	0.13 m	0.00 m	0.00
21	DELTA N	23	22	-1.5160 m	0.72 m	0.00 m	0.00

PARAMETERS AFTER CONSTRAINTS:

NO.	h OLD m	H OLD m	N OLD m	dh m	dH m	dN m	h NEW m	Sh m	H NEW m	SH m	N NEW m	SN m
2	125.6277	117.9400	7.5730	-0.11	0.00	0.00	125.5212	0.18	117.9436	0.08	7.5777	0.18
3	71.3432	58.1860	12.8710	-0.18	0.01	0.10	71.1671	0.20	58.2008	0.10	12.9662	0.20
17	145.2953	148.6780	-3.4950	-0.09	0.00	0.02	145.2070	0.21	148.6810	0.08	-3.4740	0.21
22	209.2890	205.0480	4.2410	0.00	0.00	0.00	209.2890	0.00	205.0480	0.00	4.2410	0.00
23	121.6697	115.8180	5.7570	-0.09	0.00	0.00	121.5789	0.16	115.8215	0.08	5.7574	0.16

NO.	TYPE	FROM	TO	MEASUREMENT	STND DEV	V	V/S
1	DELTA h	2	3	-54.2840 m	0.31 m	0.07 m	0.23
2	DELTA H	2	3	-59.7540 m	0.14 m	-0.01 m	-0.08
3	DELTA N	2	3	5.2980 m	0.63 m	-0.09 m	-0.14
4	DELTA h	3	23	50.3270 m	0.33 m	-0.08 m	-0.26
5	DELTA H	3	23	57.6320 m	0.14 m	0.01 m	0.08
6	DELTA N	3	23	-7.1140 m	0.65 m	0.09 m	0.15
7	DELTA h	17	23	-23.6410 m	0.35 m	-0.01 m	-0.04
8	DELTA H	17	23	-32.8600 m	0.13 m	0.00 m	0.00
9	DELTA N	17	23	9.2520 m	0.70 m	0.02 m	0.03
10	DELTA h	22	2	-83.6350 m	0.55 m	0.13 m	0.24
11	DELTA H	22	2	-87.1080 m	0.11 m	0.00 m	-0.03
12	DELTA N	22	2	3.3320 m	1.10 m	0.00 m	0.00
13	DELTA h	22	17	-64.0290 m	0.53 m	0.05 m	0.10
14	DELTA H	22	17	-56.3700 m	0.11 m	0.00 m	-0.03
15	DELTA N	22	17	-7.7360 m	1.06 m	-0.02 m	-0.02
16	DELTA h	23	2	3.9520 m	0.27 m	0.01 m	0.04
17	DELTA H	23	2	2.1220 m	0.15 m	0.00 m	0.00
18	DELTA N	23	2	1.8160 m	0.55 m	0.00 m	-0.01
19	DELTA h	23	22	87.6140 m	0.36 m	-0.10 m	-0.27
20	DELTA H	23	22	89.2300 m	0.13 m	0.00 m	0.03
21	DELTA N	23	22	-1.5160 m	0.72 m	0.00 m	0.00

Appendix 11 : New South Wales Coast data set - Case 1

```
HEIGHT ADJUSTMENT PROGRAM
EXAMPLE INPUT FILE    HGTH   DATA


A PRIORI VALUES OF THE HEIGHT ELEMENTS:

CODE   STATION #      h  m      Sh m      H m       SH m      N m      SN m
 1        14        37.798    10.000    18.428     0.065    20.454    0.260
 1        15        23.224    10.000     2.857     0.070    21.569    0.260
 1        16       211.387    10.000   190.290     0.100    22.367    0.260
 0        17       109.050     0.000    85.787     0.025    23.263    0.260


CODE    FROM   TO        OBS            S (OBS)
 2       14    15     -14.57 metre    0.07 metre
 3       14    15     -15.57 metre    0.07 metre
 4       14    15       1.11 metre    0.07 metre
 2       15    16     188.16 metre    0.06 metre
 3       15    16     187.43 metre    0.07 metre
 4       15    16       0.80 metre    0.06 metre
 2       16    17    -102.34 metre    0.10 metre
 3       16    17    -104.50 metre    0.08 metre
 4       16    17       0.90 metre    0.10 metre
 2       14    17      71.25 metre    0.29 metre
 3       14    17      67.36 metre    0.15 metre
 4       14    17       2.81 metre    0.29 metre

 There are    4 stations, including   1 held fixed
 and there are   12 observations and    9    params
```

PARAMETERS FROM BAYESIAN:

NO.	h OLD m	H OLD m	N OLD m	dh m	dH m	dN m	h NEW m	Sh m	H NEW m	SH m	N NEW m	SN m
14	37.7980	18.4280	20.4540	0.00	0.00	0.00	37.7980	0.12	18.4280	0.05	20.4540	0.10
15	23.2240	2.8570	21.5690	0.00	0.00	0.00	23.2240	0.11	2.8570	0.05	21.5690	0.09
16	211.3870	190.2900	22.3670	0.00	0.00	0.00	211.3870	0.09	190.2900	0.05	22.3670	0.08
17	109.0500	85.7870	23.2630	0.00	0.00	0.00	109.0500	0.00	85.7870	0.00	23.2630	0.00

NO.	TYPE	FROM	TO	MEASUREMENT	STND DEV	V	V/S
1	DELTA h	14	15	-14.5740 m	0.07 m	0.00 m	0.00
2	DELTA H	14	15	-15.5710 m	0.07 m	0.00 m	0.00
3	DELTA N	14	15	1.1150 m	0.07 m	0.00 m	0.00
4	DELTA h	15	16	188.1630 m	0.06 m	0.00 m	0.00
5	DELTA H	15	16	187.4330 m	0.07 m	0.00 m	0.00
6	DELTA N	15	16	0.7980 m	0.06 m	0.00 m	0.00
7	DELTA h	16	17	-102.3370 m	0.10 m	0.00 m	0.00
8	DELTA H	16	17	-104.5030 m	0.08 m	0.00 m	0.00
9	DELTA N	16	17	0.8960 m	0.10 m	0.00 m	0.00
10	DELTA h	14	17	71.2520 m	0.29 m	0.00 m	0.00
11	DELTA H	14	17	67.3590 m	0.15 m	0.00 m	0.00
12	DELTA N	14	17	2.8090 m	0.29 m	0.00 m	0.00

PARAMETERS AFTER CONSTRAINTS:

NO.	h OLD m	H OLD m	N OLD m	dh m	dH m	dN m	h NEW m	Sh m	H NEW m	SH m	N NEW m	SN m
14	37.7980	18.4280	20.4540	0.63	-0.04	-0.41	38.4257	0.08	18.3841	0.05	20.0416	0.08
15	23.2240	2.8570	21.5690	0.65	-0.10	-0.45	23.8760	0.07	2.7608	0.04	21.1151	0.07
16	211.3870	190.2900	22.3670	0.63	-0.17	-0.47	212.0162	0.07	190.1163	0.05	21.8999	0.06
17	109.0500	85.7870	23.2630	0.00	0.00	0.00	109.0500	0.00	85.7870	0.00	23.2630	0.00

NO.	TYPE	FROM	TO	MEASUREMENT	STND DEV	V	V/S
1	DELTA h	14	15	-14.5740 m	0.07 m	-0.02 m	-0.35
2	DELTA H	14	15	-15.5710 m	0.07 m	0.05 m	0.74
3	DELTA N	14	15	1.1150 m	0.07 m	0.04 m	0.60
4	DELTA h	15	16	188.1630 m	0.06 m	0.02 m	0.39
5	DELTA H	15	16	187.4330 m	0.07 m	0.08 m	1.19
6	DELTA N	15	16	0.7980 m	0.06 m	0.01 m	0.22
7	DELTA h	16	17	-102.3370 m	0.10 m	0.63 m	6.49

8	DELTA H	16	17	-104.5030 m	0.08 m	-0.17 m	-2.07
9	DELTA N	16	17	0.8960 m	0.10 m	-0.47 m	-4.82
10	DELTA h	14	17	71.2520 m	0.29 m	0.63 m	2.13
11	DELTA H	14	17	67.3590 m	0.15 m	-0.04 m	-0.30
12	DELTA N	14	17	2.8090 m	0.29 m	-0.41 m	-1.40

Appendix 12 : New South Wales Coast data set - Case 2

HEIGHT ADJUSTMENT PROGRAM
EXAMPLE INPUT FILE HGTH DATA

A PRIORI VALUES OF THE HEIGHT ELEMENTS:

CODE	STATION #	h m	Sh m	H m	SH m	N m	SN m
1	14	37.798	0.047	18.428	0.065	20.454	0.260
1	15	23.224	0.048	2.857	0.070	21.569	0.260
1	16	211.387	0.050	190.290	0.100	22.367	0.260
0	17	109.050	0.000	85.787	0.025	23.263	0.260

CODE	FROM	TO	OBS	S (OBS)
2	14	15	-14.57 metre	0.07 metre
3	14	15	-15.57 metre	0.07 metre
4	14	15	1.11 metre	0.07 metre
2	15	16	188.16 metre	0.06 metre
3	15	16	187.43 metre	0.07 metre
4	15	16	0.80 metre	0.06 metre
2	16	17	-102.34 metre	0.10 metre
3	16	17	-104.50 metre	0.08 metre
4	16	17	0.90 metre	0.10 metre
2	14	17	71.25 metre	0.29 metre
3	14	17	67.36 metre	0.15 metre
4	14	17	2.81 metre	0.29 metre

There are 4 stations, including 1 held fixed
and there are 12 observations and 9 params

PARAMETERS FROM BAYESIAN:

NO.	h OLD m	H OLD m	N OLD m	dh m	dH m	dN m	h NEW m	Sh m	H NEW m	SH m	N NEW m	SN m
14	37.7980	18.4280	20.4540	0.00	0.00	0.00	37.7980	0.04	18.4280	0.05	20.4540	0.10
15	23.2240	2.8570	21.5690	0.00	0.00	0.00	23.2240	0.04	2.8570	0.05	21.5690	0.09
16	211.3870	190.2900	22.3670	0.00	0.00	0.00	211.3870	0.04	190.2900	0.05	22.3670	0.08
17	109.0500	85.7870	23.2630	0.00	0.00	0.00	109.0500	0.00	85.7870	0.00	23.2630	0.00

NO.	TYPE	FROM	TO	MEASUREMENT	STND DEV	V	V/S
1	DELTA h	14	15	-14.5740 m	0.07 m	0.00 m	0.00
2	DELTA H	14	15	-15.5710 m	0.07 m	0.00 m	0.00
3	DELTA N	14	15	1.1150 m	0.07 m	0.00 m	0.00
4	DELTA h	15	16	188.1630 m	0.06 m	0.00 m	0.00
5	DELTA H	15	16	187.4330 m	0.07 m	0.00 m	0.00
6	DELTA N	15	16	0.7980 m	0.06 m	0.00 m	0.00
7	DELTA h	16	17	-102.3370 m	0.10 m	0.00 m	0.00
8	DELTA H	16	17	-104.5030 m	0.08 m	0.00 m	0.00
9	DELTA N	16	17	0.8960 m	0.10 m	0.00 m	0.00
10	DELTA h	14	17	71.2520 m	0.29 m	0.00 m	0.00
11	DELTA H	14	17	67.3590 m	0.15 m	0.00 m	0.00
12	DELTA N	14	17	2.8090 m	0.29 m	0.00 m	0.00

PARAMETERS AFTER CONSTRAINTS:

NO.	h OLD m	H OLD m	N OLD m	dh m	dH m	dN m	h NEW m	Sh m	H NEW m	SH m	N NEW m	SN m
14	37.7980	18.4280	20.4540	0.06	-0.12	-0.90	37.8581	0.04	18.3055	0.04	19.5526	0.05
15	23.2240	2.8570	21.5690	0.09	-0.19	-0.92	23.3179	0.03	2.6640	0.04	20.6540	0.05
16	211.3870	190.2900	22.3670	0.14	-0.27	-0.85	211.5290	0.03	190.0155	0.04	21.5135	0.05
17	109.0500	85.7870	23.2630	0.00	0.00	0.00	109.0500	0.00	85.7870	0.00	23.2630	0.00

NO.	TYPE	FROM	TO	MEASUREMENT	STND DEV	V	V/S
1	DELTA h	14	15	-14.5740 m	0.07 m	-0.03 m	-0.49
2	DELTA H	14	15	-15.5710 m	0.07 m	0.07 m	0.99
3	DELTA N	14	15	1.1150 m	0.07 m	0.01 m	0.20
4	DELTA h	15	16	188.1630 m	0.06 m	-0.05 m	-0.81

5	DELTA H	15	16	187.4330 m	0.07 m	0.08 m	1.25
6	DELTA N	15	16	0.7980 m	0.06 m	-0.06 m	-1.04
7	DELTA h	16	17	-102.3370 m	0.10 m	0.14 m	1.46
8	DELTA H	16	17	-104.5030 m	0.08 m	-0.27 m	-3.27
9	DELTA N	16	17	0.8960 m	0.10 m	-0.85 m	-8.80
10	DELTA h	14	17	71.2520 m	0.29 m	0.06 m	0.20
11	DELTA H	14	17	67.3590 m	0.15 m	-0.12 m	-0.84
12	DELTA N	14	17	2.8090 m	0.29 m	-0.90 m	-3.06

Appendix 13 : South East Luzon data set - Case 1

HEIGHT ADJUSTMENT PROGRAM
EXAMPLE INPUT FILE HGTH DATA

A PRIORI VALUES OF THE HEIGHT ELEMENTS:

CODE	STATION #	h m	Sh m	H m	SH m	N m	SN m
0	29	57.393	0.000	4.993	0.000	52.400	0.000
1	36	113.731	10.000	58.787	10.000	51.917	10.000
1	41	121.006	10.000	64.985	10.000	53.065	10.000
1	43	163.730	10.000	108.686	10.000	52.342	10.000
1	49	107.629	10.000	52.040	10.000	53.348	10.000

CODE	FROM	TO	OBS	S (OBS)
2	29	36	56.34 metre	0.10 metre
3	29	36	53.79 metre	0.09 metre
4	29	36	-0.48 metre	0.10 metre
2	36	43	50.00 metre	0.12 metre
3	36	43	49.90 metre	0.09 metre
4	36	43	0.42 metre	0.12 metre
2	43	49	-56.10 metre	0.17 metre
3	43	49	-56.65 metre	0.11 metre
4	43	49	1.01 metre	0.17 metre
2	49	41	13.38 metre	0.10 metre
3	49	41	12.95 metre	0.09 metre
4	49	41	-0.28 metre	0.10 metre

2	41	29	-63.61 metre	0.10 metre
3	41	29	-59.99 metre	0.08 metre
4	41	29	-0.67 metre	0.10 metre
2	36	41	7.28 metre	0.10 metre
3	36	41	6.20 metre	0.09 metre
4	36	41	1.15 metre	0.10 metre

There are 5 stations, including 1 held fixed
and there are 18 observations and 12 params

PARAMETERS FROM BAYESIAN:

NO.	h OLD m	H OLD m	N OLD m	dh m	dH m	dN m	h NEW m	Sh m	H NEW m	SH m	N NEW m	SN m
29	57.3926	4.9930	52.3996	0.00	0.00	0.00	57.3926	0.00	4.9930	0.00	52.3996	0.00
36	113.7310	58.7870	51.9173	0.00	0.00	0.00	113.7310	0.08	58.7870	0.07	51.9173	0.08
41	121.0060	64.9850	53.0653	0.00	0.00	0.00	121.0060	0.08	64.9850	0.07	53.0653	0.08
43	163.7300	108.6860	52.3416	0.00	0.00	0.00	163.7300	0.13	108.6860	0.10	52.3416	0.13
49	107.6290	52.0400	53.3480	0.00	0.00	0.00	107.6290	0.12	52.0400	0.10	53.3480	0.12

NO.	TYPE	FROM	TO	MEASUREMENT	STND DEV	V	V/S
1	DELTA h	29	36	56.3384 m	0.10 m	0.00 m	0.00
2	DELTA H	29	36	53.7940 m	0.09 m	0.00 m	0.00
3	DELTA N	29	36	-0.4823 m	0.10 m	0.00 m	0.00
4	DELTA h	36	43	49.9990 m	0.12 m	0.00 m	0.00
5	DELTA H	36	43	49.8990 m	0.09 m	0.00 m	0.00
6	DELTA N	36	43	0.4243 m	0.12 m	0.00 m	0.00
7	DELTA h	43	49	-56.1010 m	0.17 m	0.00 m	0.00
8	DELTA H	43	49	-56.6460 m	0.11 m	0.00 m	0.00
9	DELTA N	43	49	1.0064 m	0.17 m	0.00 m	0.00
10	DELTA h	49	41	13.3770 m	0.10 m	0.00 m	0.00
11	DELTA H	49	41	12.9450 m	0.09 m	0.00 m	0.00
12	DELTA N	49	41	-0.2827 m	0.10 m	0.00 m	0.00
13	DELTA h	41	29	-63.6134 m	0.10 m	0.00 m	0.00
14	DELTA H	41	29	-59.9920 m	0.08 m	0.00 m	0.00
15	DELTA N	41	29	-0.6657 m	0.10 m	0.00 m	0.00
16	DELTA h	36	41	7.2750 m	0.10 m	0.00 m	0.00
17	DELTA H	36	41	6.1980 m	0.09 m	0.00 m	0.00
18	DELTA N	36	41	1.1480 m	0.10 m	0.00 m	0.00

PARAMETERS AFTER CONSTRAINTS:

NO.	h OLD m	H OLD m	N OLD m	dh m	dH m	dN m	h NEW m	Sh m	H NEW m	SH m	N NEW m	SN m
29	57.3926	4.9930	52.3996	0.00	0.00	0.00	57.3926	0.00	4.9930	0.00	52.3996	0.00
36	113.7310	58.7870	51.9173	-1.12	0.78	1.12	112.6084	0.07	59.5684	0.06	53.0399	0.07
41	121.0060	64.9850	53.0653	-1.09	0.77	1.09	119.9140	0.06	65.7567	0.06	54.1573	0.06
43	163.7300	108.6860	52.3416	-1.00	0.70	1.00	162.7269	0.10	109.3822	0.09	53.3447	0.10
49	107.6290	52.0400	53.3480	-0.82	0.60	0.82	106.8080	0.09	52.6389	0.08	54.1690	0.09

NO.	TYPE	FROM	TO	MEASUREMENT	STND DEV	V	V/S
1	DELTA h	29	36	56.3384 m	0.10 m	1.12 m	10.90
2	DELTA H	29	36	53.7940 m	0.09 m	-0.78 m	-9.09
3	DELTA N	29	36	-0.4823 m	0.10 m	-1.12 m	-10.90
4	DELTA h	36	43	49.9990 m	0.12 m	-0.12 m	-0.97
5	DELTA H	36	43	49.8990 m	0.09 m	0.09 m	0.91
6	DELTA N	36	43	0.4243 m	0.12 m	0.12 m	0.97
7	DELTA h	43	49	-56.1010 m	0.17 m	-0.18 m	-1.07
8	DELTA H	43	49	-56.6460 m	0.11 m	0.10 m	0.88
9	DELTA N	43	49	1.0064 m	0.17 m	0.18 m	1.07
10	DELTA h	49	41	13.3770 m	0.10 m	0.27 m	2.58
11	DELTA H	49	41	12.9450 m	0.09 m	-0.17 m	-1.99
12	DELTA N	49	41	-0.2827 m	0.10 m	-0.27 m	-2.58
13	DELTA h	41	29	-63.6134 m	0.10 m	-1.09 m	-10.92
14	DELTA H	41	29	-59.9920 m	0.08 m	0.77 m	9.19
15	DELTA N	41	29	-0.6657 m	0.10 m	1.09 m	10.92
16	DELTA h	36	41	7.2750 m	0.10 m	-0.03 m	-0.30
17	DELTA H	36	41	6.1980 m	0.09 m	0.01 m	0.11
18	DELTA N	36	41	1.1480 m	0.10 m	0.03 m	0.30

Appendix 14 : South East Luzon data set - Case 2

HEIGHT ADJUSTMENT PROGRAM
EXAMPLE INPUT FILE HGTH DATA

A PRIORI VALUES OF THE HEIGHT ELEMENTS:

CODE	STATION #	h m	Sh m	H m	SH m	N m	SN m
0	29	57.393	0.000	4.993	0.000	52.400	0.000
1	36	113.731	10.000	58.787	10.000	51.917	10.000
1	41	121.006	10.000	64.985	0.460	53.065	10.000
1	43	163.730	10.000	108.686	10.000	52.342	10.000
1	49	107.629	10.000	52.040	10.000	53.348	10.000

CODE	FROM	TO	OBS	S (OBS)
2	29	36	56.34 metre	0.10 metre
3	29	36	53.79 metre	0.09 metre
4	29	36	-0.48 metre	0.10 metre
2	36	43	50.00 metre	0.12 metre
3	36	43	49.90 metre	0.09 metre
4	36	43	0.42 metre	0.12 metre
2	43	49	-56.10 metre	0.17 metre
3	43	49	-56.65 metre	0.11 metre
4	43	49	1.01 metre	0.17 metre
2	49	41	13.38 metre	0.10 metre
3	49	41	12.95 metre	0.09 metre
4	49	41	-0.28 metre	0.10 metre
2	41	29	-63.61 metre	0.10 metre
3	41	29	-59.99 metre	0.08 metre
4	41	29	-0.67 metre	0.10 metre
2	36	41	7.28 metre	0.10 metre
3	36	41	6.20 metre	0.09 metre
4	36	41	1.15 metre	0.10 metre

There are 5 stations, including 1 held fixed
and there are 18 observations and 12 params

PARAMETERS FROM BAYESIAN:

NO.	h OLD m	H OLD m	N OLD m	dh m	dH m	dN m	h NEW m	Sh m	H NEW m	SH m	N NEW m	SN m
29	57.3926	4.9930	52.3996	0.00	0.00	0.00	57.3926	0.00	4.9930	0.00	52.3996	0.00
36	113.7310	58.7870	51.9173	0.00	0.00	0.00	113.7310	0.08	58.7870	0.07	51.9173	0.08
41	121.0060	64.9850	53.0653	0.00	0.00	0.00	121.0060	0.08	64.9850	0.07	53.0653	0.08
43	163.7300	108.6860	52.3416	0.00	0.00	0.00	163.7300	0.13	108.6860	0.10	52.3416	0.13
49	107.6290	52.0400	53.3480	0.00	0.00	0.00	107.6290	0.12	52.0400	0.10	53.3480	0.12

NO.	TYPE	FROM	TO	MEASUREMENT	STND DEV	V	V/S
1	DELTA h	29	36	56.3384 m	0.10 m	0.00 m	0.00
2	DELTA H	29	36	53.7940 m	0.09 m	0.00 m	0.00
3	DELTA N	29	36	-0.4823 m	0.10 m	0.00 m	0.00
4	DELTA h	36	43	49.9990 m	0.12 m	0.00 m	0.00
5	DELTA H	36	43	49.8990 m	0.09 m	0.00 m	0.00
6	DELTA N	36	43	0.4243 m	0.12 m	0.00 m	0.00
7	DELTA h	43	49	-56.1010 m	0.17 m	0.00 m	0.00
8	DELTA H	43	49	-56.6460 m	0.11 m	0.00 m	0.00
9	DELTA N	43	49	1.0064 m	0.17 m	0.00 m	0.00
10	DELTA h	49	41	13.3770 m	0.10 m	0.00 m	0.00
11	DELTA H	49	41	12.9450 m	0.09 m	0.00 m	0.00
12	DELTA N	49	41	-0.2827 m	0.10 m	0.00 m	0.00
13	DELTA h	41	29	-63.6134 m	0.10 m	0.00 m	0.00
14	DELTA H	41	29	-59.9920 m	0.08 m	0.00 m	0.00
15	DELTA N	41	29	-0.6657 m	0.10 m	0.00 m	0.00
16	DELTA h	36	41	7.2750 m	0.10 m	0.00 m	0.00
17	DELTA H	36	41	6.1980 m	0.09 m	0.00 m	0.00
18	DELTA N	36	41	1.1480 m	0.10 m	0.00 m	0.00

PARAMETERS AFTER CONSTRAINTS:

NO.	h OLD m	H OLD m	N OLD m	dh m	dH m	dN m	h NEW m	Sh m	H NEW m	SH m	N NEW m	SN m
29	57.3926	4.9930	52.3996	0.00	0.00	0.00	57.3926	0.00	4.9930	0.00	52.3996	0.00
36	113.7310	58.7870	51.9173	-1.13	0.77	1.13	112.6050	0.07	59.5617	0.06	53.0433	0.07
41	121.0060	64.9850	53.0653	-1.10	0.76	1.10	119.9079	0.06	65.7445	0.06	54.1634	0.06
43	163.7300	108.6860	52.3416	-1.01	0.69	1.01	162.7227	0.10	109.3738	0.09	53.3489	0.10
49	107.6290	52.0400	53.3480	-0.83	0.59	0.83	106.8025	0.09	52.6281	0.08	54.1745	0.09

NO.	TYPE	FROM	TO	MEASUREMENT	STND DEV	V	V/S
1	DELTA h	29	36	56.3384 m	0.10 m	1.13 m	10.93
2	DELTA H	29	36	53.7940 m	0.09 m	-0.77 m	-9.01
3	DELTA N	29	36	-0.4823 m	0.10 m	-1.13 m	-10.93
4	DELTA h	36	43	49.9990 m	0.12 m	-0.12 m	-0.97
5	DELTA H	36	43	49.8990 m	0.09 m	0.09 m	0.92
6	DELTA N	36	43	0.4243 m	0.12 m	0.12 m	0.97
7	DELTA h	43	49	-56.1010 m	0.17 m	-0.18 m	-1.06
8	DELTA H	43	49	-56.6460 m	0.11 m	0.10 m	0.91
9	DELTA N	43	49	1.0064 m	0.17 m	0.18 m	1.06
10	DELTA h	49	41	13.3770 m	0.10 m	0.27 m	2.59
11	DELTA H	49	41	12.9450 m	0.09 m	-0.17 m	-1.97
12	DELTA N	49	41	-0.2827 m	0.10 m	-0.27 m	-2.59
13	DELTA h	41	29	-63.6134 m	0.10 m	-1.10 m	-10.98
14	DELTA H	41	29	-59.9920 m	0.08 m	0.76 m	9.04
15	DELTA N	41	29	-0.6657 m	0.10 m	1.10 m	10.98
16	DELTA h	36	41	7.2750 m	0.10 m	-0.03 m	-0.27
17	DELTA H	36	41	6.1980 m	0.09 m	0.02 m	0.18
18	DELTA N	36	41	1.1480 m	0.10 m	0.03 m	0.27

Appendix 15 : South East Luzon data set - Case 3

HEIGHT ADJUSTMENT PROGRAM
EXAMPLE INPUT FILE HGTH DATA

A PRIORI VALUES OF THE HEIGHT ELEMENTS:

CODE	STATION #	h m	Sh m	H m	SH m	N m	SN m
0	29	57.393	0.000	4.993	0.000	52.400	0.000
1	36	113.731	10.000	58.787	10.000	51.917	10.000
1	41	121.006	10.000	64.985	0.050	53.065	10.000
1	43	163.730	10.000	108.686	10.000	52.342	10.000
1	49	107.629	10.000	52.040	10.000	53.348	10.000

CODE	FROM	TO	OBS	S (OBS)
2	29	36	56.34 metre	0.10 metre
3	29	36	53.79 metre	0.09 metre
4	29	36	-0.48 metre	0.10 metre
2	36	43	50.00 metre	0.12 metre
3	36	43	49.90 metre	0.09 metre
4	36	43	0.42 metre	0.12 metre
2	43	49	-56.10 metre	0.17 metre
3	43	49	-56.65 metre	0.11 metre
4	43	49	1.01 metre	0.17 metre
2	49	41	13.38 metre	0.10 metre
3	49	41	12.95 metre	0.09 metre
4	49	41	-0.28 metre	0.10 metre
2	41	29	-63.61 metre	0.10 metre
3	41	29	-59.99 metre	0.08 metre
4	41	29	-0.67 metre	0.10 metre
2	36	41	7.28 metre	0.10 metre
3	36	41	6.20 metre	0.09 metre
4	36	41	1.15 metre	0.10 metre

There are 5 stations, including 1 held fixed
and there are 18 observations and 12 params

PARAMETERS FROM BAYESIAN:

NO.	h OLD m	H OLD m	N OLD m	dh m	dH m	dN m	h NEW m	Sh m	H NEW m	SH m	N NEW m	SN m
29	57.3926	4.9930	52.3996	0.00	0.00	0.00	57.3926	0.00	4.9930	0.00	52.3996	0.00
36	113.7310	58.7870	51.9173	0.00	0.00	0.00	113.7310	0.08	58.7870	0.06	51.9173	0.08
41	121.0060	64.9850	53.0653	0.00	0.00	0.00	121.0060	0.08	64.9850	0.04	53.0653	0.08
43	163.7300	108.6860	52.3416	0.00	0.00	0.00	163.7300	0.13	108.6860	0.09	52.3416	0.13
49	107.6290	52.0400	53.3480	0.00	0.00	0.00	107.6290	0.12	52.0400	0.08	53.3480	0.12

NO.	TYPE	FROM	TO	MEASUREMENT	STND DEV	V	V/S
1	DELTA h	29	36	56.3384 m	0.10 m	0.00 m	0.00
2	DELTA H	29	36	53.7940 m	0.09 m	0.00 m	0.00
3	DELTA N	29	36	-0.4823 m	0.10 m	0.00 m	0.00
4	DELTA h	36	43	49.9990 m	0.12 m	0.00 m	0.00
5	DELTA H	36	43	49.8990 m	0.09 m	0.00 m	0.00

6	DELTA N	36	43	0.4243 m	0.12 m	0.00 m	0.00
7	DELTA h	43	49	-56.1010 m	0.17 m	0.00 m	0.00
8	DELTA H	43	49	-56.6460 m	0.11 m	0.00 m	0.00
9	DELTA N	43	49	1.0064 m	0.17 m	0.00 m	0.00
10	DELTA h	49	41	13.3770 m	0.10 m	0.00 m	0.00
11	DELTA H	49	41	12.9450 m	0.09 m	0.00 m	0.00
12	DELTA N	49	41	-0.2827 m	0.10 m	0.00 m	0.00
13	DELTA h	41	29	-63.6134 m	0.10 m	0.00 m	0.00
14	DELTA H	41	29	-59.9920 m	0.08 m	0.00 m	0.00
15	DELTA N	41	29	-0.6657 m	0.10 m	0.00 m	0.00
16	DELTA h	36	41	7.2750 m	0.10 m	0.00 m	0.00
17	DELTA H	36	41	6.1980 m	0.09 m	0.00 m	0.00
18	DELTA N	36	41	1.1480 m	0.10 m	0.00 m	0.00

PARAMETERS AFTER CONSTRAINTS:

NO.	h OLD m	H OLD m	N OLD m	dh m	dH m	dN m	h NEW m	Sh m	H NEW m	SH m	N NEW m	SN m
29	57.3926	4.9930	52.3996	0.00	0.00	0.00	57.3926	0.00	4.9930	0.00	52.3996	0.00
36	113.7310	58.7870	51.9173	-1.25	0.53	1.25	112.4849	0.06	59.3215	0.05	53.1634	0.06
41	121.0060	64.9850	53.0653	-1.31	0.33	1.31	119.6912	0.06	65.3112	0.04	54.3801	0.06
43	163.7300	108.6860	52.3416	-1.16	0.39	1.16	162.5732	0.10	109.0749	0.08	53.4984	0.10
49	107.6290	52.0400	53.3480	-1.02	0.20	1.02	106.6101	0.09	52.2432	0.07	54.3669	0.09

NO.	TYPE	FROM	TO	MEASUREMENT	STND DEV	V	V/S
1	DELTA h	29	36	56.3384 m	0.10 m	1.25 m	12.10
2	DELTA H	29	36	53.7940 m	0.09 m	-0.53 m	-6.21
3	DELTA N	29	36	-0.4823 m	0.10 m	-1.25 m	-12.10
4	DELTA h	36	43	49.9990 m	0.12 m	-0.09 m	-0.73
5	DELTA H	36	43	49.8990 m	0.09 m	0.15 m	1.55
6	DELTA N	36	43	0.4243 m	0.12 m	0.09 m	0.73
7	DELTA h	43	49	-56.1010 m	0.17 m	-0.14 m	-0.81
8	DELTA H	43	49	-56.6460 m	0.11 m	0.19 m	1.69
9	DELTA N	43	49	1.0064 m	0.17 m	0.14 m	0.81
10	DELTA h	49	41	13.3770 m	0.10 m	0.30 m	2.82
11	DELTA H	49	41	12.9450 m	0.09 m	-0.12 m	-1.41
12	DELTA N	49	41	-0.2827 m	0.10 m	-0.30 m	-2.82
13	DELTA h	41	29	-63.6134 m	0.10 m	-1.31 m	-13.15

14	DELTA H	41	29	-59.9920 m	0.08 m	0.33 m	3.88
15	DELTA N	41	29	-0.6657 m	0.10 m	1.31 m	13.15
16	DELTA h	36	41	7.2750 m	0.10 m	0.07 m	0.67
17	DELTA H	36	41	6.1980 m	0.09 m	0.21 m	2.42
18	DELTA N	36	41	1.1480 m	0.10 m	-0.07 m	-0.67

Publications from

THE SCHOOL OF SURVEYING, THE UNIVERSITY OF NEW SOUTH WALES.

All prices include postage by surface mail. Air mail rates on application. (Effective Oct. 1992)

To order, write to Publications Officer, School of Surveying, The University of New South Wales, P.O. Box 1, Kensington N.S.W., 2033 AUSTRALIA

NOTE: ALL ORDERS MUST BE PREPAID

UNISURV REPORTS - G SERIES

Price (including postage): $6.00

G14. A. Stolz, "The computation of three dimensional Cartesian coordinates of terrestrial networks by the use of local astronomic vector systems", Unisurv Rep. 18, 47 pp, 1970.

G16. R.S. Mather et al, "Communications from Australia to Section V, International Association of Geodesy, XV General Assembly, International Union of Geodesy and Geophysics, Moscow 1971", Unisurv Rep. 22, 72 pp, 1971.

G17. Papers by R.S. Mather, H.L. Mitchell & A. Stolz on the following topics:- Four-dimensional geodesy, Network adjustment and Sea surface topography, Unisurv G17, 73 pp, 1972.

G18. Papers by L. Berlin, G.J.F. Holden, P.V. Angus-Leppan, H.L. Mitchell & A.H. Campbell on the following topics:- Photogrammetry co-ordinate systems for surveying integration, Geopotential networks and Linear measurement, Unisurv G18, 80 pp, 1972.

G19. R.S. Mather, P.V. Angus-Leppan, A. Stolz & I. Lloyd, "Aspects of four-dimensional geodesy", Unisurv G19, 100 pp, 1973.

G20. Papers by J.S. Allman, R.C. Lister, J.C. Trinder & R.S. Mather on the following topics:- Network adjustments, Photogrammetry, and 4-Dimensional geodesy, Unisurv G20, 133 pp, 1974.

G21. Papers by E. Grafarend, R.S. Mather & P.V. Angus-Leppan on the following topics:- Mathematical geodesy, Coastal geodesy and Refraction, Unisurv G21, 100 pp, 1974.

G22. Papers by R.S. Mather, J.R. Gilliland, F.K. Brunner, J.C. Trinder, K. Bretreger & G. Halsey on the following topics:- Gravity, Levelling, Refraction, ERTS imagery, Tidal effects on satellite orbits and Photogrammetry, Unisurv G22, 96 pp, 1975.

G23. Papers by R.S. Mather, E.G. Anderson, C. Rizos, K. Bretreger, K. Leppert, B.V. Hamon & P.V. Angus-Leppan on the following topics:- Earth tides, Sea surface topography, Atmospheric effects in physical geodesy, Mean sea level and Systematic errors in levelling, Unisurv G23, 96 pp, 1975.

G24. Papers by R.C. Patterson, R.S. Mather, R. Coleman, O.L. Colombo, J.C. Trinder, S.U. Nasca, T.L. Duyet & K. Bretreger on the following topics:- Adjustment theory, Sea surface topography determinations, Applications of LANDSAT imagery, Ocean loading of Earth tides, Physical geodesy, Photogrammetry and Oceanographic applications of satellites, Unisurv G24, 151 pp, 1976.

G25. Papers by S.M. Nakiboglu, B. Ducarme, P. Melchior, R.S. Mather, B.C. Barlow, C. Rizos, B. Hirsch, K. Bretreger, F.K. Brunner & P.V. Angus-Leppan on the following topics:- Hydrostatic equilibrium figures of the Earth, Earth tides, Gravity anomaly data banks for Australia, Recovery of tidal signals from satellite altimetry, Meteorological parameters for modelling terrestrial refraction and Crustal motion studies in Australia, Unisurv G25, 124 pp, 1976.

G26. Papers by R.S. Mather, E.G. Masters, R. Coleman, C. Rizos, B. Hirsch, C.S. Fraser, F.K. Brunner, P.V. Angus-Leppan, A.J. McCarthy & C. Wardrop on the following topics:- Four-dimensional geodesy, GEOS-3 altimetry data analysis, analysis of meteorological measurements for microwave EDM and Meteorological data logging system for geodetic refraction research, Unisurv G26, 113 pp, 1977.

G27. Papers by F.K. Brunner, C.S. Fraser, S.U. Nasca, J.C. Trinder, L. Berlin, R.S. Mather, O.L. Colombo & P.V. Angus-Leppan on the following topics:- Micrometeorology in geodetic refraction, LANDSAT imagery in topographic mapping, adjustment of large systems, GEOS-3 data analysis, Kernel functions and EDM reductions over sea, Unisurv G27, 101 pp, 1977.

G29. Papers by F.L. Clarke, R.S. Mather, D.R. Larden & J.R. Gilliland on the following topics:- Three dimensional network adjustment incorporating ξ, η and N, Geoid determinations with satellite altimetry, Geodynamic information from secular gravity changes and Height and free-air anomaly correlation, Unisurv G29, 87 pp, 1978.

From June 1979 Unisurv G's name was changed to Australian Journal of Geodesy, Photogrammetry and Surveying. These can be ordered from The Managing Editor, Australian Journal of Geodesy, Photogrammetry and Surveying, Institution of Surveyors - Australia, Nos 27 - 29 Napier Close, Deakin, ACT 2600, AUSTRALIA.

UNISURV REPORTS - S SERIES

S8 - S20	Price (including postage):		$10.00
S27 onwards	Price (including postage):	Individuals	$25.00
		Institutions	$30.00

S8 A. Stolz, "Three-D Cartesian co-ordinates of part of the Australian geodetic network by the use of local astronomic vector systems", Unisurv Rep. S 8, 182 pp, 1972.

S10 A.J. Robinson, "Study of zero error & ground swing of the model MRA101 tellurometer", Unisurv Rep. S 10, 200 pp, 1973.

S12. G.J.F. Holden, "An evaluation of orthophotography in an integrated mapping system", Unisurv Rep. S 12, 232 pp, 1974.

S14. Edward G. Anderson, "The Effect of Topography on Solutions of Stokes' Problem", Unisurv Rep. S 14, 252 pp, 1976.

S16. K. Bretreger, "Earth Tide Effects on Geodetic Observations", Unisurv S 16, 173 pp, 1978.

S17. C. Rizos, "The role of the gravity field in sea surface topography studies", Unisurv S 17, 299 pp, 1980.

S18. B.C. Forster, "Some measures of urban residential quality from LANDSAT multi-spectral data", Unisurv S 18, 223 pp, 1981.

S19. Richard Coleman, "A Geodetic Basis for recovering Ocean Dynamic Information from Satellite Altimetry", Unisurv S 19,332 pp, 1981.

S20. Douglas R. Larden, "Monitoring the Earth's Rotation by Lunar Laser Ranging", Unisurv Report S 20, 280 pp, 1982.

S27. Bruce R. Harvey, "The Combination of VLBI and Ground Data for Geodesy and Geophysics", Unisurv Report S27, 239 pp, 1985.

S29. Gary S. Chisholm, "Integration of GPS into hydrographic survey operations", Unisurv S29, 190 pp, 1987.

S30. Gary Alan Jeffress, "An investigation of Doppler satellite positioning multi-station software", Unisurv S30, 118 pp, 1987.

S31. Jahja Soetandi, "A model for a cadastral land information system for Indonesia", Unisurv S31, 168 pp, 1988.

S32. D. B. Grant, "Combination of terrestrial and GPS data for earth deformation studies" Unisurv S32, 285 pp, 1990.

S33. R. D. Holloway, "The integration of GPS heights into the Australian Height Datum", Unisurv S33, 151 pp.,1988.

S34. Robin C. Mullin, "Data update in a Land Information Network", Unisurv S34, 168 pp. 1988.

S35. Bertrand Merminod, "The use of Kalman filters in GPS Navigation", Unisurv S35, 203 pp., 1989.

S36. Andrew R. Marshall, "Network design and optimisation in close range Photogrammetry", Unisurv S36, 249 pp., 1989.

S37. Wattana Jaroondhampinij, "A model of Computerised parcel-based Land Information System for the Department of Lands, Thailand," Unisurv S37, 281 pp., 1989.

S38. C. Rizos (Ed.), D.B. Grant, A. Stolz, B. Merminod, C.C. Mazur "Contributions to GPS Studies", Unisurv S38, 204 pp., 1990.

S39. C. Bosloper, "Multipath and GPS short periodic components of the time variation of the differential dispersive delay", Unisurv S39, 214 pp., 1990.

S40. John Michael Nolan, "Development of a Navigational System utilizing the Global Positioning System in a real time, differential mode", Unisurv S40, 163 pp., 1990.

S41. Roderick T. Macleod, "The resolution of Mean Sea Level anomalies along the NSW coastline using the Global Positioning System", 278 pp., 1990.

S42. Douglas A. Kinlyside, "Densification Surveys in New South Wales - coping with distortions", 209 pp., 1992.

S43. A. H. W. Kearsley (ed.), Z. Ahmad, B. R. Harvey and Adolfientje Kasenda, "Contributions to Geoid Evaluations and GPS Heighting", 209 pp. + xii, 1993.

PROCEEDINGS

Prices include postage by surface mail

P1. P.V. Angus-Leppan (Editor), "Proceedings of conference on refraction effects in geodesy & electronic distance measurement", 264 pp., 1968. Price: $10.00

P2. R.S. Mather & P.V. Angus-Leppan (Eds), "Australian Academy of Science/International Association of Geodesy Symposium on Earth's Gravitational Field & Secular Variations in Position", 740 pp., 1973. Price $15.00

SPECIAL GPSCO PUBLICATION

Price includes postage by surface mail

GPSCO 1. Simon McElroy, Ewan Masters, Glenn Jones, Douglas Kinlyside, Chris Rizos, Adrian Siversten, Patrick Brown, Owen Moss, Greg Dickson, "Getting Started with GPS Surveying", 186 pp, Approx 90 diagrams, 1992. Price $30.00

MONOGRAPHS

Prices include postage by surface mail

M1.	R.S. Mather, "The theory and geodetic use of some common projections", (2nd edition), 125 pp., 1978.	Price	$15.00
M2.	R.S. Mather, "The analysis of the earth's gravity field", 172 pp., 1971.	Price	$8.00
M3.	G.G. Bennett, "Tables for prediction of daylight stars", 24 pp.,1974.	Price	$5.00
M4.	G.G. Bennett, J.G. Freislich & M. Maughan, "Star prediction tables for the fixing of position", 200 pp., 1974.	Price	$8.00
M8.	A.H.W. Kearsley, "Geodetic Surveying", 77 pp., 1988.	Price	$12.00
M.9	R.W. King, et al, "Surveying with GPS", 133 pp., 1985.	Price	$20.00
M10.	W. Faig, "Aerial Triangulation and Digital Mapping", 102 pp., 1986.	Price	$16.00
M11.	W.F. Caspary, "Concepts of Network and Deformation Analysis", 183 pp., 1988.	Price	$25.00
M12.	F.K. Brunner, "Atmospheric Effects on Geodetic Space Measurements", 110 pp., 1988.	Price	$16.00
M13.	Bruce R. Harvey, "Practical Least Squares and Statistics for Surveyors", 229 pp., 1990.	Price	$25.00
M14.	Ewan G. Masters & John R. Pollard (Ed.), "Land Information Management", 269 pp., 1991. (Proceedings LIM Conference, July 1991).	Price	$50.00